



Modular Float Glass Systems Designed for Reuse

Novel Connections Designed for Reusability &
Sustainability of Laminated Glass

By

Minoo Motedayen

6020631

In partial fulfillment of the requirements for the Degree of
Master Thesis

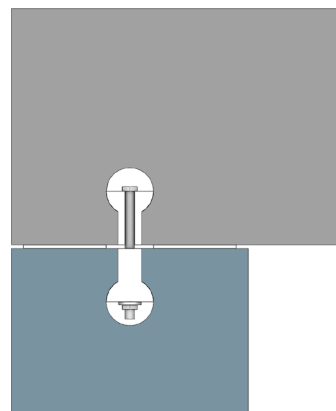
In Architecture, Urbanism and Building Science
Building Technology Track

Mentors:

Prof. James O'Callaghan

Dr. ing. Marcel Bilow

2025



Abstract

Key words: Modular glass systems, Design glass systems for reuse, Interlocking/demountable connections for glass, Glass reciprocal structures, modular glass pavilion, reusable glass Units

This research investigates the design and implementation of modular float glass systems that prioritize reusability and sustainability. The project addresses a significant gap in architectural practices involving glass by developing modular, demountable glass systems that can be disassembled and reused, challenging the traditional, single-use paradigm of glass in construction. Through a comprehensive review of existing glass systems and the exploration of novel connection designs, this master thesis aims to create a modular glass system as pavilion that exemplifies sustainability in architecture. The key focus is on innovating connections that allow for easy assembly and disassembly without compromising structural integrity or aesthetic values. Preliminary findings suggest this specific interlocking connection designs can enhance the life cycle and functionality of glass structures, thereby reducing their environmental impact.

Table of content:

1. Background	7
2. Problem Statement	9
• Sub-Problems	
3. Objectives	10
• Sub-Objectives	
• Final Products	
• Aim	
• Boundary Conditions	
4. Research Question	13
• Sub-Questions	
5. Methodology	13
5.1. Literature Review and Theoretical Foundation	
5.2. Concept Development and Analytical Modeling	
5.3. Prototyping and Experimental Validation	
5.4. Life cycle and Sustainability Assessment	
5.5. Iterative Refinement	
6. Planning and Organization	17
• Timeline	
7. Literature Survey	19
7.1.1 Glass Properties and Connection Types	
7.1.2 Novel Connections in Glass Structures	
7.2. Modular Systems with Dry Connections in Other Materials	
7.3. History of Modular Glass Systems	
7.4. Intermediate Materials for Glass-to-Glass Contact	
7.5. Testing Methods for Modular Systems	

8. **Research Through Design**76

8.1. Design Thinking Process

8.1.1. Connection to System

8.1.2. System-to-Connection Approach

8.2. Structural Analysis

8.2.1. Preliminarily sizing and calculations(Module)

8.2.2. Detailed analysis and calculations (Connection)

8.2.3. System analysis (Karamba)

8.2.4. Ansys Simulations(FEM)

8.3. Prototyping & Experiment

8.3.1. Test 1: Preliminary Prototype Testing (Plexiglas and Meranti)

8.3.2. Test 2: Parallel to grain test

8.3.3. Test 3: Perpendicular to grain test

9. **Final Products**195

9.1. Final Design

9.2. Assembly Sequence

9.3. End of life Scenarios

10.	Reflection	207
11.	Conclusion	212
12.	Reference	213

1 Background

Glass is one of the most striking materials used in architecture, admired for its transparency, elegance, and ability to transform spaces. Yet, when it comes to sustainability and adaptability, glass systems have fallen behind. Glass structures work well for a single purpose but make it nearly impossible to reuse or adapt components once their initial purpose is fulfilled. This single-use approach wastes the potential of glass as a versatile material and limits its contribution to sustainable construction. The movement towards sustainable building materials is gaining momentum globally, driven by environmental concerns and the need for more resource-efficient construction practices. (Bristogianni & Oikonomopoulou, 2023; Hartwell & Overend, 2019). However, the challenge of sustainability in glass use, especially laminated glass, remains prominent due to its complex recycling process. Laminated glass is notoriously difficult to recycle because of its layered materials, which require separation for elective recycling—a process that is both costly and environmentally taxing (Bristogianni & Oikonomopoulou, 2023). This highlights a critical need for alternative approaches to glass sustainability, emphasizing the reduction of waste and enhancement of lifecycle management.



Glass process	Recyclable to float line?	Notes
Annealed glass	Yes	Readily recyclable
Cutting and edge processing	Yes	No effect on recyclability
Laminating	Limited	Current methodology for delaminating reduces quality. Requires improved delamination processes to ensure stays in closed cycle level. Current methodology means laminated glass goes to container glass or mineral wool.
Heat strengthen	Yes	No effect on recyclability
Toughened (or tempered)	Yes	No effect on recyclability
Heat soak tested	Yes	No effect on recyclability
Glass coating (hard and soft)	Yes	No effect on recyclability
Ceramic printing and fritting	No	Current methodology does not allow for recycling of ceramic printed glass
Insulated glass units	Yes	Requires removal of the spacer bars and edge seals, limitations on processing of individual panes as noted above
Low iron glass	Yes	Specifying low iron glass may require float manufacturers to reduce the recycled glass content to ensure a clear product is achieved. Further discussion with glass supplier on a project basis is required.

Figure 1: A summary of typical glass processes and their effect on the recyclability of the glass for consideration during the design process project. Source: Glass on Web. (n.d.). Rethinking the life cycle of architectural glass. Retrieved from <https://www.glassonweb.com/article/rethinking-life->

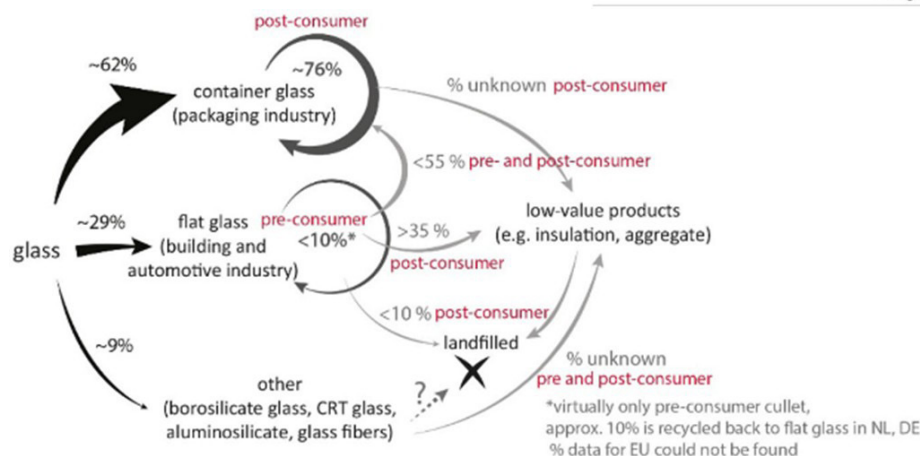


Figure 2: Illustration of the production and recycling of glass cullet in EU28 in 2017 based on approximate numbers as provided by (Rose and Nothacker 2019; Hestin et al. 2016)

Traditionally, glass systems have been designed for a single life cycle, with no consideration for disassembly or reuse. Typically, at the end of their service life, these materials are either discarded or down cycled, which fails to recover their full value and further exacerbates waste issues (Hartwell & Overend, 2019). In contrast to other materials like wood, glass has not been designed with the idea of modularity or disassembly in mind, which significantly limits its potential for reuse in new constructions or applications (Chong et al., 2019).



Figure 3/4: Sample of modular timber pavilion, Calton Hill Outdoor Learning Pavilion. Source: O'Donnell Brown. (n.d.). Calton Hill Pavilion. Retrieved from <https://www.odonnellbrown.com/caltonhillpavilion>

The absence of modular design principles in the creation of glass structures means that once their initial use is concluded, they cannot be efficiently repurposed or reconfigured, missing opportunities for extending their usability, lifetime, and contributing to sustainability. This approach not only limits the lifecycle of glass products but also fails to tap into the benefits of adaptable and reusable building materials. This missed opportunity—a modular glass system designed for easy assembly, disassembly, and reuse—is the main problem this research aims to tackle. By developing standardized, modular glass systems that are adaptable, we can significantly enhance their reuse across various architectural applications without the need for disassembly or traditional recycling. Such systems should be designed to be easily demountable and capable of reconfiguration, meeting diverse architectural demands while reducing the ecological footprint (Bristogianni & Oikonomopoulou, 2023). The connections and sizing of these modular components must be devised to accommodate easy assembly and reassembly, ensuring they meet practical and environmental criteria without compromising safety and aesthetic integrity (Gugger et al., 2020).

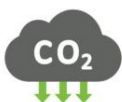
Sustainability Advantages of Modular Construction



Significant
Waste
Reduction



Relocate,
Renovate,
and Repurpose



Lower
Carbon
Footprint



Greater
Energy
Efficiency

Figure 5: Benefits of modularity on sustainability.

Source: NRB Modular. (n.d.). The sustainable benefits of modular construction.

Retrieved from <https://nrb-modular.com/blog/the-sustainable-benefits-of-modular-construction>

2 Problem statement

Achieving a modular and reusable glass system is a challenging but essential task. Glass, due to its brittle nature, relies heavily on permanent or customized connections that are tailored to specific loads and conditions. While effective for one-time use, these connections make glass structures rigid, inflexible, and difficult to adapt or re-use. In contrast, modular systems, composed of standardized components, allow for flexibility in design. They enable parts to be easily connected, disassembled, and re-used in different configurations, offering a more sustainable approach to construction. Adopting a modular approach for glass systems would not only enhance adaptability but also promote circular construction practices by significantly extending the lifecycle of glass components.

Overcoming these challenges requires innovative solutions that balance structural integrity, ease of assembly, and environmental sustainability.

"How might we achieve a modular glass structure that allows for easy disassembly and reuse of its components with minimal use of other materials?"

- **Sub-Problems:**

1. Designing Reusable Connections:

In opposite to conventional connection types in glass, modular glass systems must focus on innovative, standardized connections that are strong, non-invasive, and reusable. What types of non-invasive mechanisms can securely connect float glass elements while enabling disassembly?

2. Simplifying Assembly for Accessibility:

Glass systems are often viewed as requiring specialized skills for handling and installation. To make modular systems more practical, the focus should be on intuitive designs that allow components to "click" or "lock" into place without extensive training.

3. Life cycle and Sustainability

Recycling laminated glass is resource-intensive, and focusing solely on reuse may not address all environmental concerns. How might we incorporate life cycle thinking into modular systems—ensuring that components can be reused, re-purposed, and eventually recycled?

3 Objectives

To develop a modular, reusable float glass system, exemplified through a pavilion for exhibitions, that allows for easy assembly and disassembly, adaptable to various forms and arrangements, enhancing the potential for sustainability, re-usability, and adaptability in glass structures.

- **Sub-Objectives:**

1. Innovative Connections:

Create standardized, interlocking connections for float glass elements that eliminate bonding and enable modularity.

2. Validation:

Design two pavilions as test cases to evaluate connections, assembly, and adaptability.

3. Simplified Assembly:

Develop an IKEA-style guide with clear mapping for intuitive assembly by non-specialists.

4. Life cycle Integration:

Establish end-of-life strategies to ensure glass components can be reused, repaired, or recycled effectively.

- **Final Products:**

1. Real-Scale Component Assembly (Part of Pavilion design)

Design a case study of a pavilion which evaluates the connection concepts performance and adaptability. This includes a physical model highlighting the inter-unit connections, demonstrating the practical application and effectiveness of the joints and modular system. Here some scenarios of indoor pavilion are mentioned:



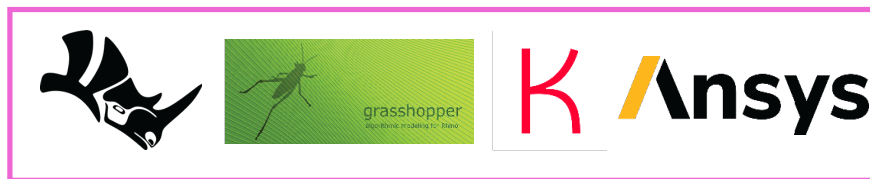
Figure 6,7: Sample of indoor pavilion, "Reporting from the Front" Arsenale Exhibition. Source: ArchDaily. (2016, May 28). First look: Reporting from the front - Arsenale exhibition. Retrieved from <https://www.archdaily.com/788285/first-look-reporting-from-the-front-arsenale-exhibition>



Figure 8,9: Two Glass pavilions, Glasstec Düsseldorf 2024, Eckersley O'Callaghan, in collaboration with NorthGlass

2. Software tools:

3D Model in Rhino, as showcase of adapting the glass system design to various forms and configurations, Grasshopper and Karamba script for Systems structural analysis, and ANSYS simulations employed to validate structural integrity and performance.



- **Aim:**

Introduce a novel connection type/language for enabling modular, reusable glass structures and adaptation in various forms.

- **Boundary Conditions:**

The research and design for this modular glass system are centered on creating a versatile pavilion for exhibitions. This pavilion serves as a demonstration of how modular glass systems can adapt to varied environments, scales, and forms while maintaining structural integrity and ease of use. The following boundary conditions define the scope and focus of the project.

Pavilion Scenario: Versatility in Use

1. Indoor Pavilion Applications of Two different forms

To demonstrate the versatility and reusability of the system, at least two pavilion configurations with different forms are to be designed. The concept follows a realistic scenario in which the pavilion is first assembled at the Glasstec exhibition in Düsseldorf, then disassembled, transported, and reconfigured into a new form for installation at the Turbine Hall of Tate Modern in London. This transition between two

distinct venues allows the system to be tested not only for structural performance but also for adaptability in form, assembly logic, and logistical feasibility. The design must withstand typical loading conditions, including **self-weight, light dead loads, and operational and maintenance loads**, ensuring consistent and safe behavior in both contexts. Although not intended for harsh outdoor exposure, the system is expected to remain stable and secure under moderate environmental conditions, reinforcing its potential for real-world application in varied exhibition settings.

2. Flexibility in Form and Scale:

The pavilion is designed not only to support varied forms and configurations, but also to offer **a flexible spectrum of scale and span**. The overall **size** of the structure is determined by the **number and arrangement of modules**, enabling both compact installations and more expansive architectural compositions. This adaptability allows the system to **respond to different spatial constraints** and functional requirements, making it **suitable for a range** of settings—from indoor exhibitions to a outdoor Pergola or larger-scale temporary structures.

Constraints and Practical Considerations

1. Portability and Size of Modules:

To ensure the system is practical, individual modules will adhere to **standard size limits** that make them easy to handle. Each module must be lightweight and portable enough to be carried and assembled by **two to three people** without requiring heavy equipment or tools but at the same time the size of the units is a parameter affected by scenario which the pavilion is designed for to be able to offer different loading cases.

2. Safety in Assembly and Use:

Safety will be prioritized both **during construction** and **throughout the pavilion's use**. This includes:

- Using **edge treatments** to reduce the risk of injury during handling.
- Selecting glass types and treatments (e.g., laminated tempered glass) to ensure **strength** and **minimize hazards** in case of breakage and reducing the risk of errors during assembly or disassembly.

3. Ease of Assembly:

The connection system will be **intuitive and simple**, allowing workers with **minimal training** to assemble the pavilion efficiently.

Structural and Environmental Considerations

1. Loads and Performance:

The pavilion will be designed to handle **typical structural loads**, including self-weight, Dead loads, Maintenance, and light exhibition setups. The system must maintain its stability and structural performance across various configurations, whether as a small-scale structure or a more expansive pavilion. Future in process also wind load and snow load was added, and system was validated for those as well.

2. Durability and Lifecycle Thinking:

The pavilion must be designed for **repeated assembly and disassembly** without damaging the modules or connections.

The system will emphasize **reuse over recycling**, ensuring that modules can be **re-configured or repurposed beyond the pavilion's initial use**. At the end of its lifecycle, the components should be easy to dismantle, and the materials should remain recyclable or reusable.

4 Research Questions

Main Research Question:

" How can novel connection with minimal use of other materials, be designed to maximize adaptability and reusability of modular float glass systems? "

Sub-Questions:

Design Feasibility:

What types of interlocking mechanisms or intermediate material (glass-to-glass connection) can securely and reusable connection between glass elements without permanent bonding?

Are the interlocking connections scalable or repeatable for different use-cases?

Structural impact:

How do modular connections impact the structural integrity of float glass under different loads?

What testing methods are needed to validate performance under repeated assembly/disassembly cycles?

Background Questions:

What are the existing examples of modular and demountable systems in other material systems, and how can these principles be adapted for glass?

What is the existing state of modular glass structures in architecture?

How in modular systems, size and form of a module is defined?

5 Methodology

This research employs a cyclical approach, integrating conceptual development, design iterations, and experimental validation to create a modular glass pavilion system. The methodology prioritizes adaptability, reusability, and sustainability, with each phase informing and refining the next. Here is the research design diagram showing the step-by-step approach:

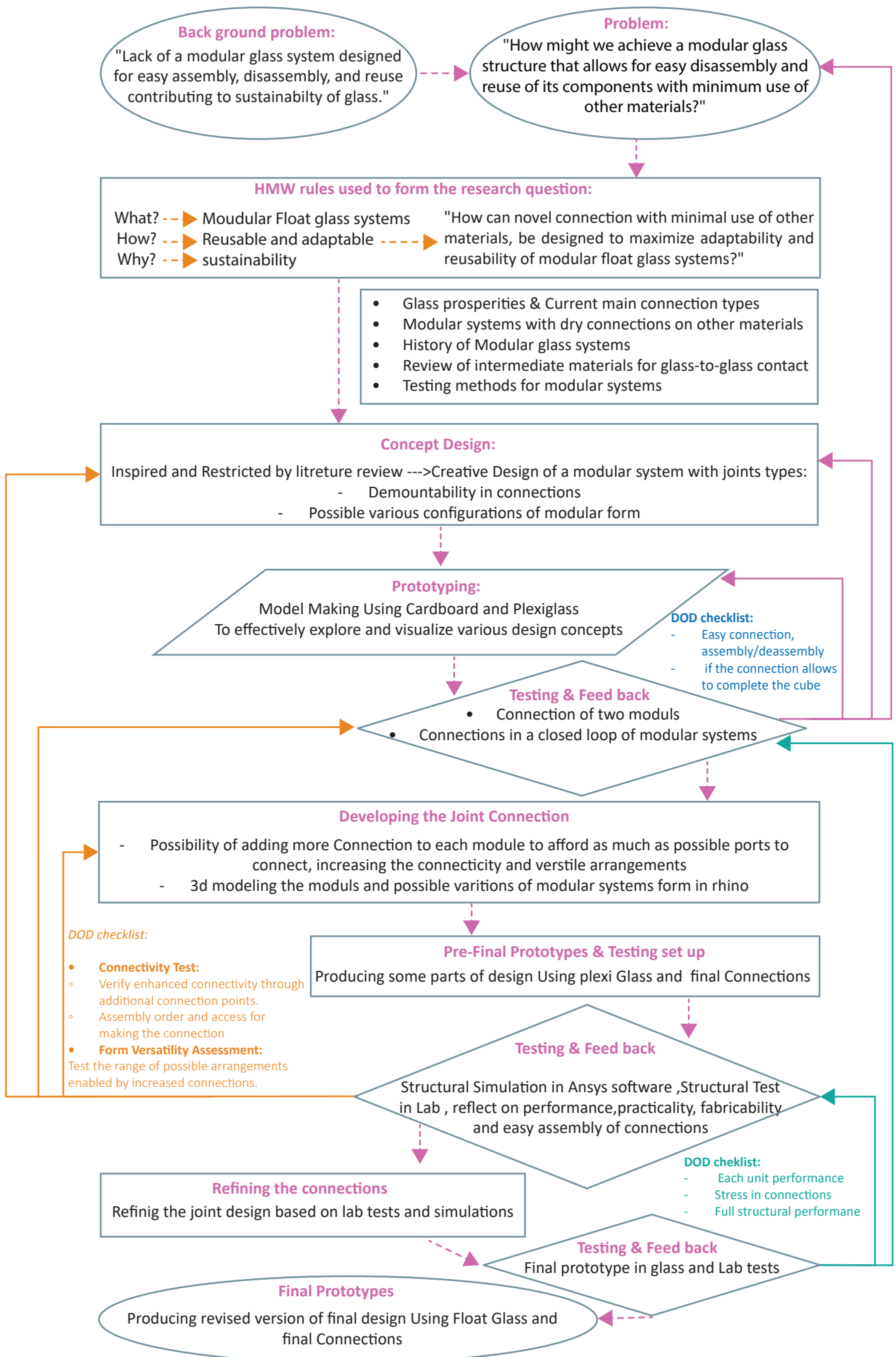


Figure 10: Research design Diagram illustrating logical process of graduation project

1. Literature Review and Theoretical Foundation

The study begins with a thematic review of existing research to establish a robust foundation for the modular system's development.

1.1 Glass Properties and Connection Types

Fundamental knowledge of structural glass, including manufacturing, treatments, strength, lamination, and safety in design.

Overview of connection types (adhesives, embedded, bolted) to establish a foundation of existing methods, assess performance, identify limitations, and determine gaps. This analysis will help set boundary conditions and module sizes and explore the feasibility of glass-to-glass connections.

1.2 Modular systems with dry connections on other materials

Examination of interlocking, dry, and demountable connection systems used in modular projects of other materials like wood, specially on brittle materials like, marble, stone, concrete.

Identification of requirements and parameters for designing the size and shape of units/modules.

1.3 History of Modular Glass Systems

Review previous modular glass applications to identify gaps, successes, and lessons that inform the novel aspects of this system.

1.4 Intermediate Materials for Glass-to-Glass Contact

Investigate materials like silicones, gaskets, and hybrid elastomers for reducing stress during assembly/disassembly and maintaining aesthetic harmony.

1.5 Testing Methods for Modular Systems

Review structural testing criteria, including cyclic, static, and dynamic loads, to develop validation frameworks for the proposed modular glass system.

2. Concept Development and Analytical Modeling

2.1 Connection Mechanism Design

The system's modularity depends on innovative, non-invasive connections that are secure, reusable, and adaptable. Initial designs will draw on the insights from dry connections and reusable systems in other materials.

Focus:

Enable configurations that balance ease of assembly with structural performance, considering factors like edge treatment, stress distribution, and modular scalability.

2.2 Pavilion Design

The pavilion serves as the testbed for the modular system, showcasing its versatility in form and adaptability for both indoor and outdoor use.

2.3 Digital Modeling and Simulation

Use Rhino and Grasshopper to develop 3D models for the pavilion, enabling iterative exploration of module scalability and connection behavior.

Validate structural integrity through ANSYS simulations, focusing on load distribution, joint performance, and stress points.

3. Prototyping and Experimental Validation**3.1 Prototype Development**

Fabricate glass modules and connections, incorporating intermediate materials where applicable.

3.2 Structural Testing

Conduct physical tests to validate the modular system's performance:

- **Static Loads:** Evaluate the system's ability to support self-weight and light operational loads.

4. Lifecycle and Sustainability Assessment

The lifecycle analysis evaluates the system's environmental performance:

Reuse and Recycling: Explore end-of-life scenarios to maximize component reuse and material recovery.

Durability Over Time: Assess long-term performance under repeated use and varying environmental conditions.

5. Iterative Refinement

This stage involves a cyclical process that begins with the literature review, progresses through design development, and continues through prototyping and testing. This iterative test and feedback loop ensures that if the design does not initially meet all the project requirements, aims, or boundaries, it is reprocessed and rethought until it satisfies all criteria. This method allows for continuous refinement and enhancement of the design, ensuring that each iteration brings the project closer to meeting its objectives comprehensively.

6 Planning and Organization

Timeline:

1. Concept Design Phase (P3:Mid-February 2025):

Initial sketching and conceptualization of joint designs, Module design, Size, Type of structural glass, interlayer material, creative design of interlocking joints, focusing on demount-ability and modular form configurations.

2. Computational Tool (March 2025):

3D modeling of modules in Rhino and scripting possible arrangements in Grasshopper. Simple loading and structural analysis on Karamba to define the loads on each module and joint.

Structural simulations in ANSYS, Refining and optimizing the joint connections based on structural performance and manufacturing feedback.

3. Prototyping Phase (April 2025):

Model making using cardboard and Plexiglass or acrylic sheets, to visualize various design concepts and evolving development of initial joint designs and prototype modules.

4. Pre-Final Prototyping and Development (April 2025):

Production or ordering glass modules using 2 layer or more laminated float glass with finalized connections.

5. Testing and Feedback I (April 2025)

Connection tests on two modules and in closed for like a simple cube or stable shell shape. Feedback collection and initial adjustments to designs.

6. Testing and Feedback II (May 2025)

Physical Structural testing in the lab to assess fabricability and performance.

Refinement of joint connections based on structural performance and fabricability feedback.

7. Final Design and Documentation (May-June)

Final adjustments to the design based on all feedback and test results.

Compilation and writing of the final report, detailing the research process, design development, testing methodology, and final designs.

Research Team:

Lead Researchers: Minoo Motedayen, supervised by James O'Callaghan & Marcel Bi-low.

Support Team: Test and experiment supervisor Fred Veer, MSE Lab Mechanical engineering faculty, upon the main mentors' recommendations, offering expert guidance and support from TU Delft professors and expertise.

Resources Required:

Laboratory space and facilities like water jet for cutting glass and laminating glass for structural testing.

Sponsor for making the connection or providing intermediate material.

Milestones:

Milestone 1: Completion of the concept design and initial prototypes First round of testing and feedback integration

Milestone 2: Computational Tool development and Structural simulations.

Milestone 3: Completion of at least 2 iterations of prototypes and testing.

Milestone 4: Submission of the final report and presentation of findings.

Risk Assessment and Mitigation:

Design Risks: Potential design flaws in joint connections. Mitigation by iterative prototyping and testing.

Material Risks: Unavailability of specified materials. Mitigation by identifying alternative materials early in the project.

Technical Risks: Lack of skill and knowledge in using Ansys as it is complicated and heavy for normal systems.

7 Literature Survey

This review delves into the multifaceted aspects of modular glass systems by exploring the interplay between glass properties, innovative connection techniques, material compatibility, and validation methods. This review seeks to answer the following questions and below each one of the categories the aim of literature review has been mentioned:

1. How can glass properties and connection types of support modularity in architectural systems?

Fundamental knowledge of structural glass, including manufacturing, treatments, strength, lamination, and safety in design.

Overview of connection types (adhesives, embedded, bolted) to establish a foundation of existing methods, assess performance, identify limitations, and determine gaps. This analysis will help set boundary conditions and module sizes and explore the feasibility of glass-to-glass connections.

2. What lessons from other materials and industries can inform modular glass design?

Examination of interlocking, dry, and demountable connection systems used in modular projects.

Identification of requirements and parameters for designing the size and shape of units/modules.

3. What historical insights into modular glass systems can guide innovation?

Review of case studies and reference projects in the field of modular glass systems.

4. How can intermediate materials enhance glass-to-glass connections?

Research on materials like silicones, gaskets, or hybrid elastomers for glass-to-glass contact may provide insights into reducing stress during assembly and disassembly. Considering exploring transparent materials for aesthetic harmony.

By synthesizing findings from a wide array of studies, this literature review aims to provide a comprehensive framework for understanding and advancing modular glass technologies. Also, testing and validation methods will be detailed in reviewing in each literature and having deep sight on how each project or research has been tested or analyzed.

7.1.1. Glass Properties and Connection Types

1. The Evolution and Structural Application of Glass

Glass, a material with centuries of evolution beginning in Roman times, has transitioned from basic utilitarian uses to a crucial element in modern architecture (Overend, 2008). Initially limited to small, non-load bearing applications like windows, technological advancements over the past few decades have enabled its use in larger and structurally significant roles such as floors, beams, and entire façades. Glass exhibits significant strength under compression but is notably weaker in tension, a property that defines its use in structural applications. Its brittle nature demands that glass be processed further to enhance its tensile strength and resistance to environmental stresses such as thermal shock (Cobb, n.d.).

2. Advanced Processing Techniques for Structural Glass

To address its inherent weaknesses, especially in tension, glass undergoes various post-manufacturing treatments aimed at enhancing its mechanical properties. Annealing, a critical process, involves slow cooling of glass after it is formed, relieving internal stresses and reducing its brittleness (Haldimann, Luible, & Overend, 2008). This treatment makes glass more durable and safer for use in structural applications.

Further advancements include toughening and lamination techniques, which significantly improve the performance of glass under various loading conditions. Heat-strengthened and thermally toughened glasses are made by rapidly cooling the heated glass, introducing compression at the surface while tension is retained at the core, thus increasing its overall strength and impact resistance. These processes result in a material that can better withstand thermal stresses and loading from environmental conditions, reducing the risk of failure (The Institution of Structural Engineers, 2014).

3. Laminated Glass and Interlayer

Laminated glass represents a significant advancement in structural glass technology. By bonding two or more layers of glass with a tough polymer interlayer, typically polyvinyl butyral (PVB), this composite material offers enhanced safety and performance characteristics. The interlayer holds the glass shards upon impact or breakage, preventing them from causing injury or falling, a crucial safety feature in overhead and high-traffic areas (Haldimann, Luible, & Overend, 2008).

Moreover, interlayers play a pivotal role in the structural integrity of laminated glass. They provide additional resistance to penetration and allow the glass to bear greater loads, thereby enhancing its structural capacity. This makes laminated glass ideal for use in balustrades, floors, and facade panels where load bearing and impact resistance are critical. Other interlayers include:

SentryGlas® (SGP): Offers greater strength and stiffness than PVB, improving safety and enabling larger pane sizes due to its higher load-bearing capacity (The Institution

of Structural Engineers, 2014).

Ethylene-vinyl acetate (EVA): Offers greater elasticity and resistance to moisture and UV rays, suitable for outdoor applications (Overend, 2008).

Thermoplastic polyurethane (TPU): Known for high impact resistance and durability under temperature variations (FprCEN/TS 19100, 2021).

Ionoplast interlayers: Provide enhanced structural support and impact resistance, useful in security applications and severe weather conditions (Cobb, n.d.).

Polyethylene terephthalate (PET): Used for its high tensile strength and acoustic insulation properties, often in security and bulletproof applications (The Institution of Structural Engineers, 2014).

Silicone interlayers: Offer increased elasticity and thermal stability, ideal for high-temperature applications (The Institution of Structural Engineers, 2014).

Comparison of Interlayers: Interlayers are chosen based on specific project requirements including impact resistance, safety, UV durability, and acoustic performance:

Strength and Stiffness: SGP offers the highest strength and stiffness, facilitating larger spans and enhanced structural integrity.

Impact Resistance: TPU and PET are superior in impact resistance, suitable for security and safety-critical applications.

Weather and UV Resistance: EVA excels in environments with high exposure to moisture and ultraviolet light.

Safety and Post-Breakage Behavior: SGP and PVB provide excellent shard retention, crucial for overhead glazing and areas where human safety is a priority.

Each type of interlayer brings distinct advantages to the laminated glass, allowing architects and engineers to tailor the glass properties to meet the stringent demands of modern architectural designs effectively. The selection of the appropriate interlayer is driven by the specific performance requirements of the project, ensuring optimal functionality and safety.

4. Connections

The transparency of glass necessitates that connections are designed with both structural integrity and minimal visual impact in mind, making the method of connection a critical component of glass architecture (Rammig, 2022).

To get a comprehensive overview of current methods for connecting glass components and how they are categorized, several sources have been considered. Here, one approach is reviewed from Rammig (2022), who explores advancing transparency by integrating heat bonding into glass connection design for structural applications.

- **Comprehensive Overview of Glass Connection Types**

General Categories:

Discrete Connections: These are point-fix connections where glass panels are typically joined at specific points, allowing for minimal interruption of the visual field.

Linear Connections: In contrast to discrete connections, linear connections involve continuous lines of connectivity, often used in scenarios where larger spans need support or reinforcement.

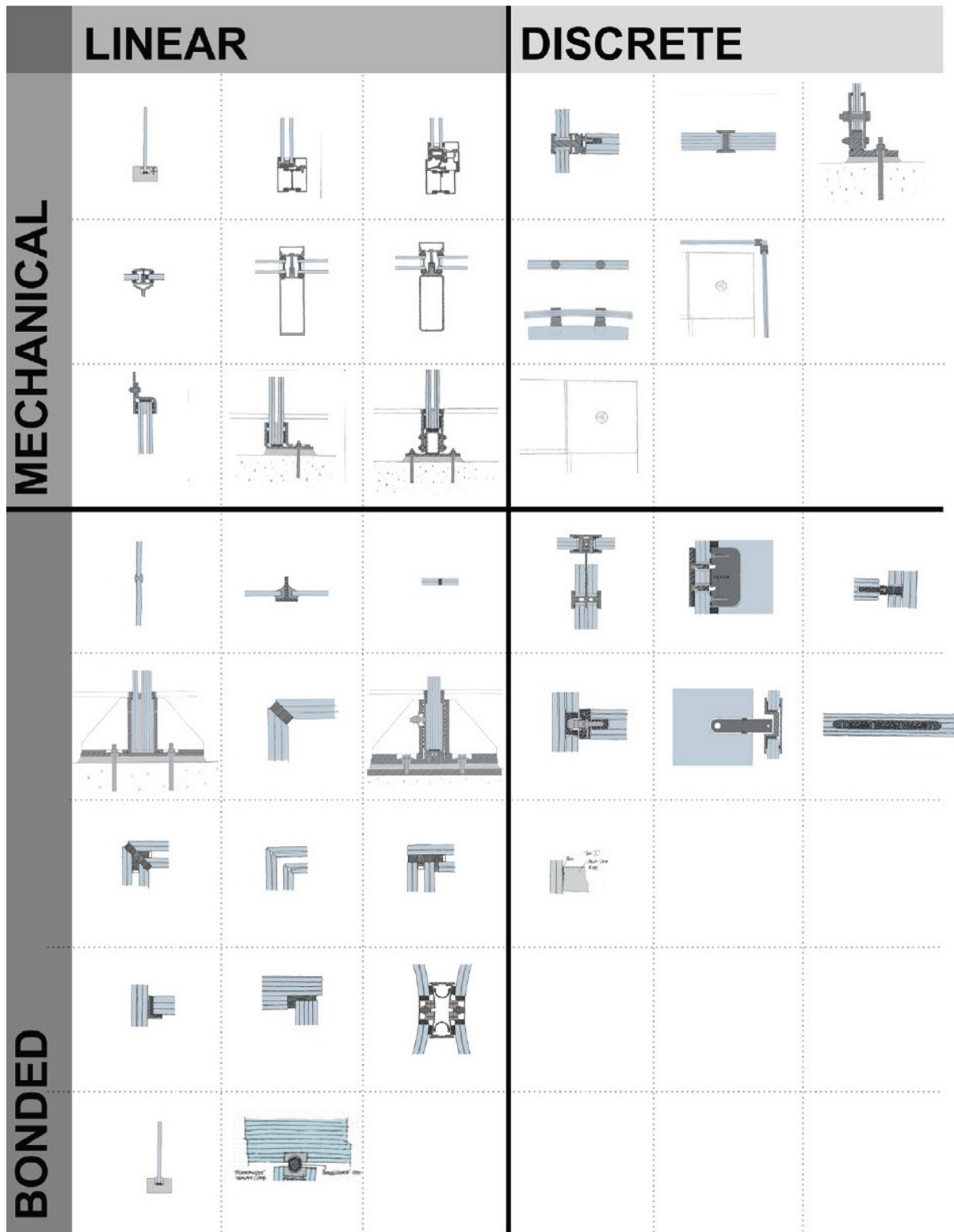


Figure 12: Geometry Glass connections. Source: Rammig, L. (2021). Advancing transparency, IOS, Delft. <https://doi.org/10.7480/abe.2022.09>

Specific Types of Connections:

- **Mechanical Connections:**

Bearing Connections: These involve direct support of glass by structural elements, providing stability and support where needed.

- **Clamped Connections:** Typically used for their non-intrusive installation, allowing glass panels to be held without permanent alterations
- **Bolted Connections:** These involve mechanically fastening glass panels through pre-drilled holes, which can introduce stress points but provide strong, durable joints.

Friction Connections: Utilize the friction between the glass and the support structure to maintain position without the need for permanent bonding.

- **Adhesive Connections:**

Bonded Connections: Employ adhesives to seamlessly bond glass panels to each other or to different structural elements, with TSSA being a prime example of achieving near-invisible bond lines. Various adhesives, including UV-curing types for glass-to-metal and two-part epoxies for glass-to-glass are also to be mentioned in this category.

5. Innovative Glass Connection Techniques

Dry Joints: Dry joints emulate traditional mortise-and-tenon woodworking techniques, eliminating metal bolts. While innovative, early experiments revealed challenges with cracking under load and movement due to the stiffness of the bond.

Transparent Structural Silicone Adhesive (TSSA): TSSA, a high-strength and optically clear silicone film, bonds glass to metal without visible support. Developed by Dow Corning, it offers enhanced load capacity and transparency compared to conventional structural silicones, making it ideal for discrete connections.

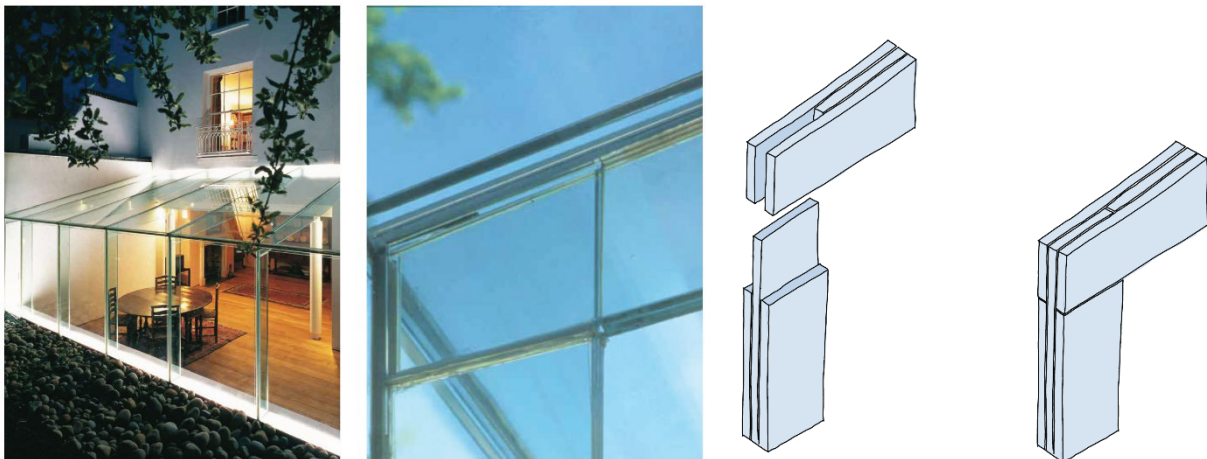


Figure 13: Keats Grove Extension, London, RMA/DMP. Source: Rammig, L. (2021). Advancing transparency, IOS, Delft.

Glass-to-Metal Connections: Originally intended for metal point fittings, TSSA enables cost effective production by reducing the need for titanium and precise machining. This innovation has expanded its feasibility for broader architectural use.

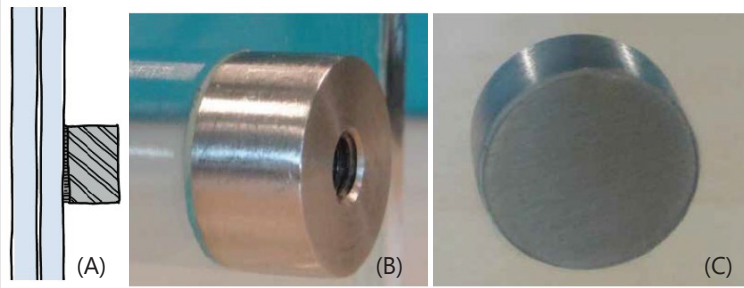


Figure 14: (A) Sketch detail Transparent Structural Silicone Lamine (TSSL) fitting. (B) Close up of Transparent Structural Silicone Lamine bonded point fitting (Sitte). (C) Closeup of Transparent Structural Silicone Lamine bonded point fitting through glass (Sitte). Source: Rammig, L. (2021). *Advancing transparency*, IOS, Delft.

Glass-to-Glass Connections: Using TSSA, transparent glass-to-glass bonds were achieved for the first time, showcased in installations like the Glass Technology Live exhibition. These connections demonstrated the potential for seamless, transparent assembly.

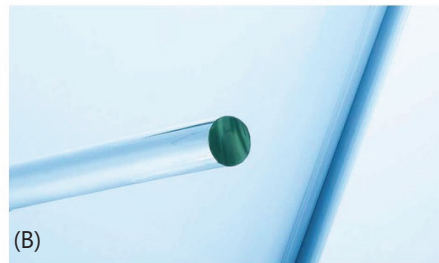
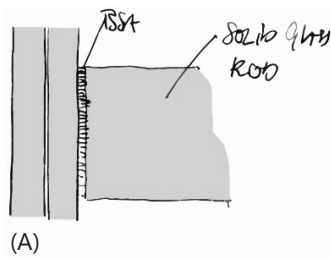


Figure 15: (A) Sketch detail TSSA tread connection. (B) Closeup of bonded glass tread connection. TSSA, Transparent structural silicone adhesive. Source: Rammig, L. (2021). *Advancing transparency*, IOS, Delft.

Glass Corners: Glass corners demand high transparency to preserve uninterrupted views. Innovative techniques, including the use of Sentry Glass laminates, have significantly improved corner transparency in projects like the ME Hotel in London.

- (A) Butt joined corner.
- (B) Stepped glass corner.
- (C) Stainless steel edge protection.
- (D) Image structural silicone mitred corner.
- (E) Sketch detail structural silicone mitred corner.
- (F) Sketch detail structural silicone mitred corner.

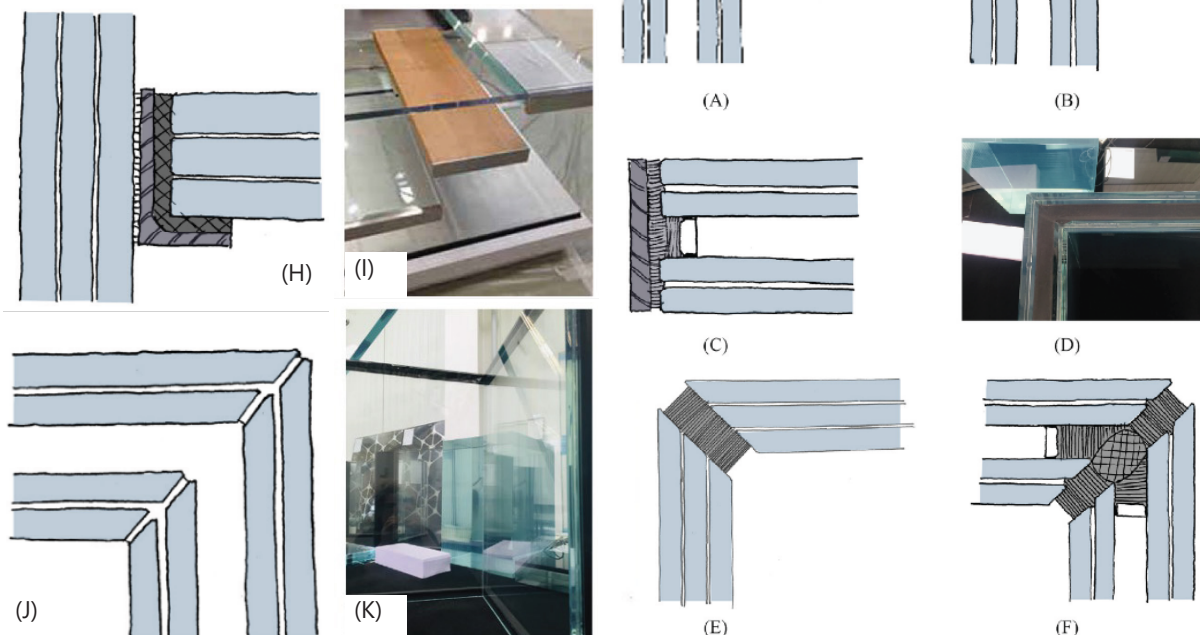


Figure 16: (H) Sketch detail TSSL tread connection. (I) Closeup of bonded TSSL metal to glass connection (Hayez, Kassnell-Henneberg). (J) SG-laminated corner—sketch detail. (K) SG-laminated corner inside (fabricated by Sedak). SG, Sentry glass. Source: Rammig, L. (2021). Advancing transparency, IOS, Delft.

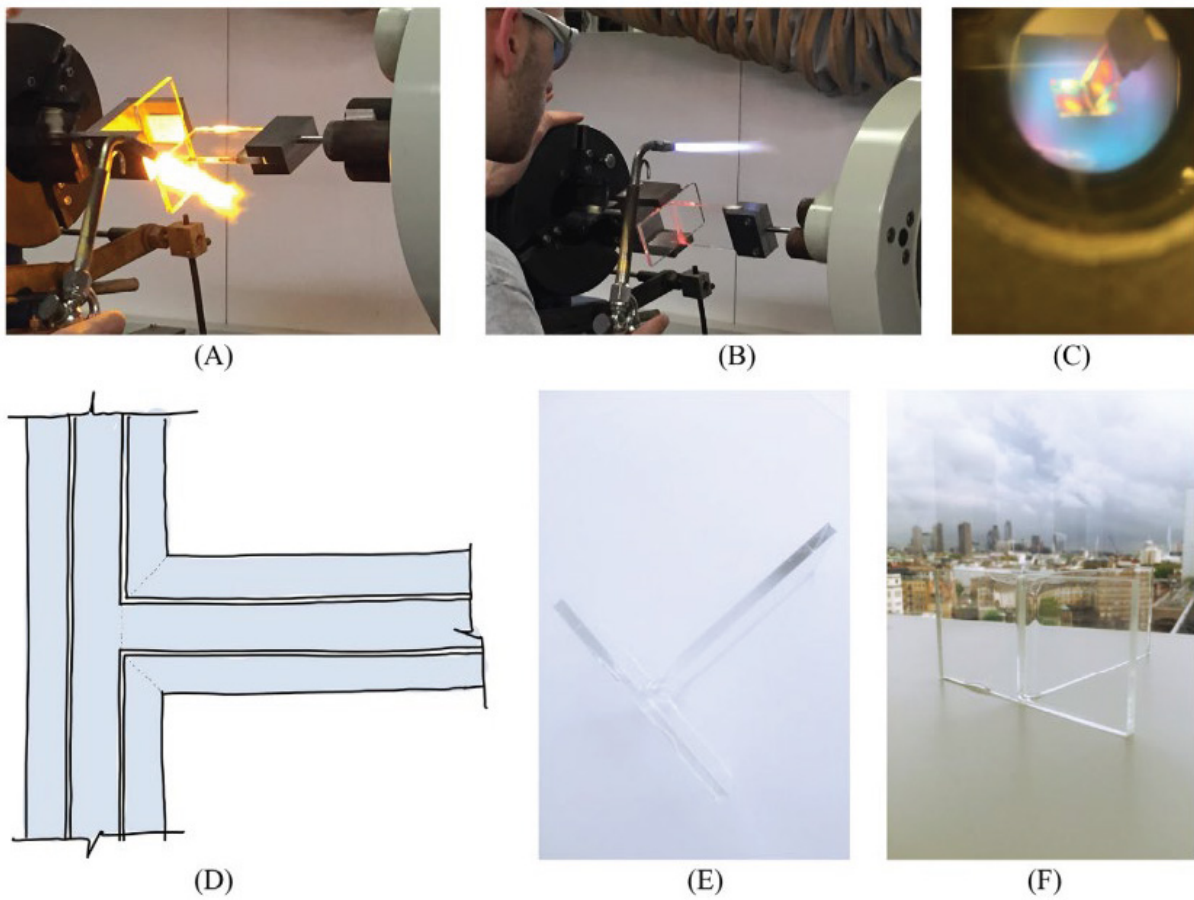


Figure 17: (A) large flame to heat up components in lathe. (B) Joint after bonding. (C) Visual stress visualized with polarization filter. (D) Detail heat-bonded glass fin connection. (E) Image HB T-joint. (F) Image HB T-joint. Source: Rammig, L. (2021). Advancing transparency, IOS, Delft.

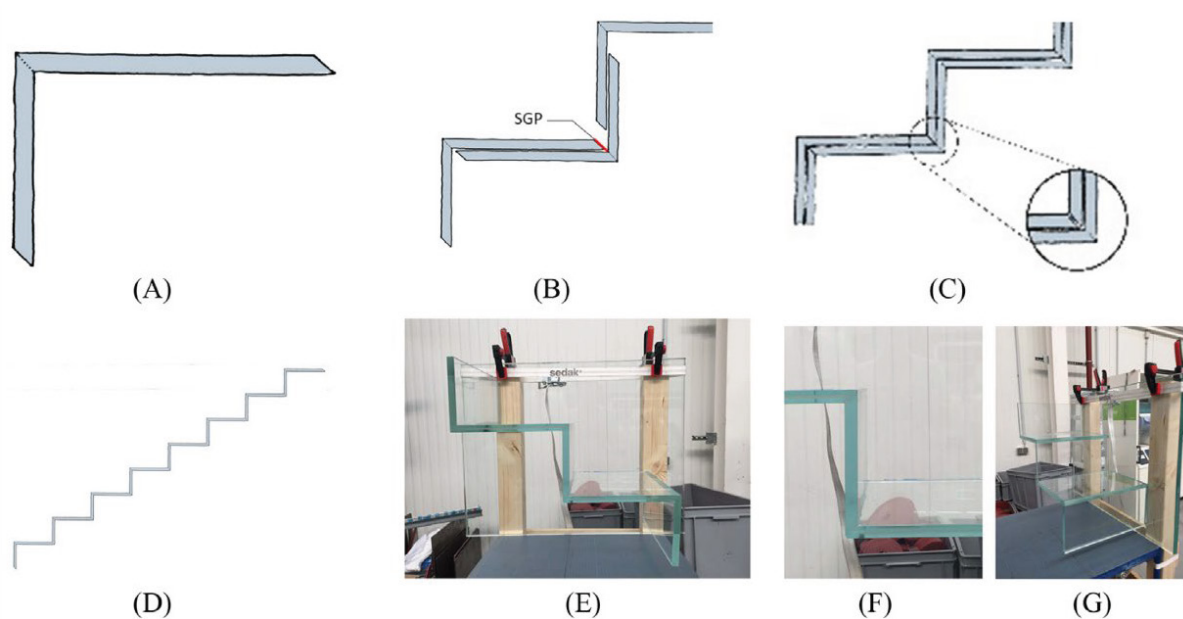


Figure 13: A_G Heatbonded corner concept w. SG stair tread lamination (Rammig,2021; laminated by Sedak). SG, Sentry glass. Source: Rammig, L. (2021). Advancing transparency, IOS, Delft.

3D-printed Glass Connections: Additive manufacturing techniques have been investigated for creating custom glass connections. While 3D printing enables intricate geometries, current limitations in optical clarity and resolution restrict its application in structural contexts.



Figure 14: 3D printed glass by TU Delft, Glass tech, Düsseldorf 2024. Source: Minoo Motedayen

To enhance our understanding of the structural performance and challenges associated with different types of glass connections, this review synthesizes findings from key research studies. Bedon, C., and Santarsiero, M. (2018) explore mechanical and adhesive connections, examining their robustness, tensile strength, and resilience against environmental stressors. Their rigorous testing assesses the efficacy of clamped, bolted, and friction connections as well as bonded and UV-cured adhesive methods, emphasizing their applicability in high-rise buildings and glass facades with safety-critical applications.

1. Performance of Glass Connection Types

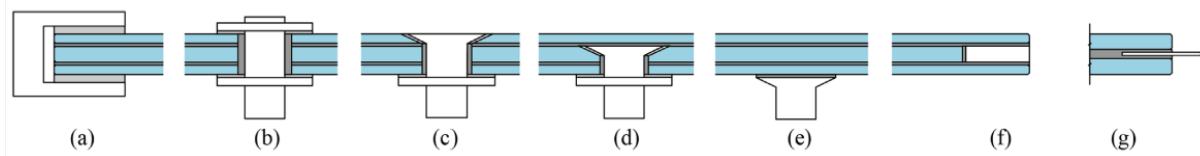


Figure 5: Scheme of connection typologies used in structural glass applications. a) Clamped; b) bolted; c) bolted with countersunk bolt; d) hybrid with countersunk bolt; e) adhesive; f) embedded with thick insert; g) embedded with thin insert. Source: Bedon, C., & Santarsiero, M. (2018). Transparency in structural glass systems via mechanical, adhesive, and laminated connections. <https://doi.org/10.1002/adem.201700815>

• Mechanical Connections:

Clamped Connections: Typically used where high strength is required. Test results often show that clamped connections provide robust support, distributing stress evenly across the glass surface, which minimizes the risk of breakage under normal loads.

Bolted Connections: Known for their high tensile strength, bolted connections are tested for both shear and tension. They are particularly effective in exterior applications where wind and gravitational loads are a concern. The performance tests indicate that these connections maintain structural integrity even under high stress, making them suitable for high-rise installations.

Friction Connections: Employed in settings where minimal visual disruption is desired. The strength tests focus on the slip resistance under various load conditions, showing that while effective, they require precise engineering to ensure stability.

- **Adhesive Connections:**

Bonded Connections: These connections are tested for long-term durability and loadbearing capacity. Using adhesives like structural silicone, the tests typically evaluate the cohesive and adhesive failure modes under cyclic loading to simulate real-world environmental stressors.

UV-Cured Connections: Notable for their rapid curing time and strong bond formation, these adhesive connections undergo rigorous testing to assess their transparency and bond integrity over time. The strength tests reveal that UV-cured adhesives provide excellent resistance to UV degradation and thermal expansion mismatches, making them ideal for glass facades.

1. Types of Glass and Connection Applications

Tempered Glass: Often used in both mechanical and adhesive connections due to its high strength-to-weight ratio. Strength tests for tempered glass in bolted connections highlight its ability to withstand significant force without compromising the structural safety.

Laminated Glass: Preferred in bonded connections for its post-breakage safety characteristics. Test results demonstrate that laminated glass maintains its integrity even when cracked, which is crucial for overhead and safety-critical applications.

Additionally, another pivotal study by Overend, M., Nhamoinesu, S., & Watson, J. (2013) in the *Journal of Structural Engineering*, focuses on the structural performance of bolted connections and adhesively bonded joints within frameless glazing systems. This research critically evaluates how these connections perform under various loading conditions, aiming to delineate their effectiveness and suitability for use in architectural glass applications.

1. Analysis of Structural Performance

Stress Distribution: The paper details how the type of connection impacts the stress distribution within the glass, which is crucial for preventing failure. Bolted connections often concentrate stress around the hole, while adhesive bonds provide a more uniform stress distribution.

Load-bearing Capacity: Tests reveal that adhesively bonded connections can achieve higher load-bearing capacities compared to bolted connections, due to their more favorable stress distribution and the inherent properties of the adhesives used.

Failure Modes: Observations indicate that while bolted connections fail due to stress concentration around the holes, adhesive connections tend to fail less catastrophically, with potential for gradual failure which provides better safety in structural applications.

7.1.2. Novel Connections in Glass Structures

1. Kinematics of Folded Glass Plate Structures

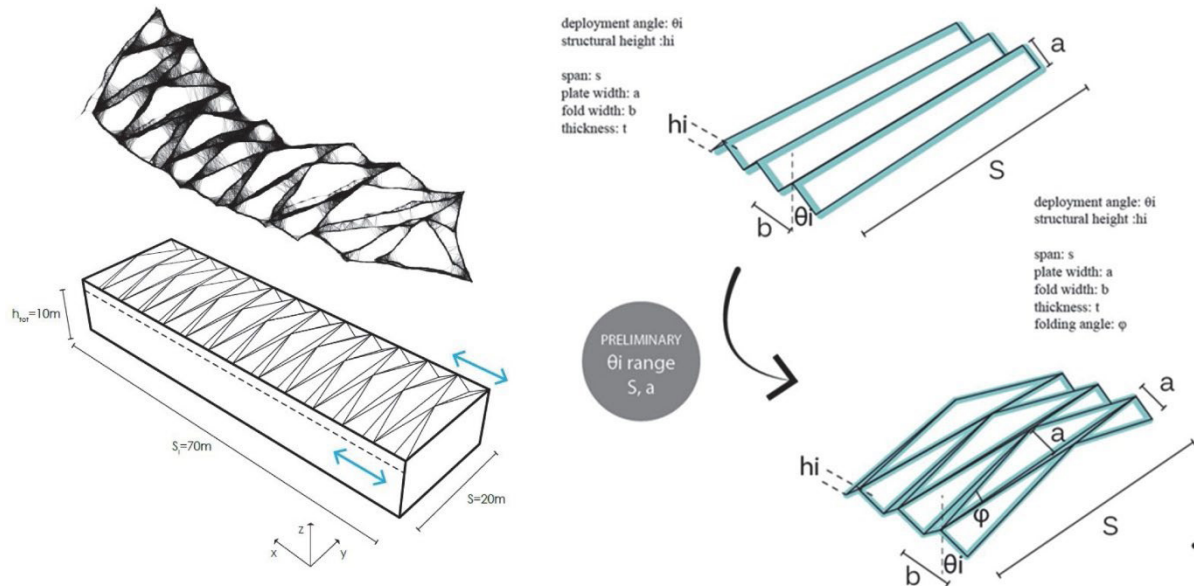


Figure 6: Geometry boundaries for design developments and parameter description. Source: Krousti, A., Snijder, A., & Turrin, M. (2018). Kinematics of folded glass plate structures: Study of a deployable roof system. *Challenging Glass 6*, Delft University of Technology. <https://doi.org/10.7480/cgc.6.2117>

Among the innovative projects explored in recent research, "Kinematics of Folded Glass Plate Structures: Study of a Deployable Roof System" by Alkistis Krousti et al. Stands out. This project introduces a novel approach to glass architecture by designing a deployable origami-shaped glass roof, intended as a dynamic shelter over a pool. The design leverages the aesthetic and functional benefits of glass, combined with the principles of origami to create a structure that is not only visually striking but also mechanically functional.

• Connection Details

Connection Type: The connections used in this deployable glass roof system are primarily hinged connections that facilitate movement and deployment without compromising the structure's stability. The connections are designed to be discrete to maximize transparency

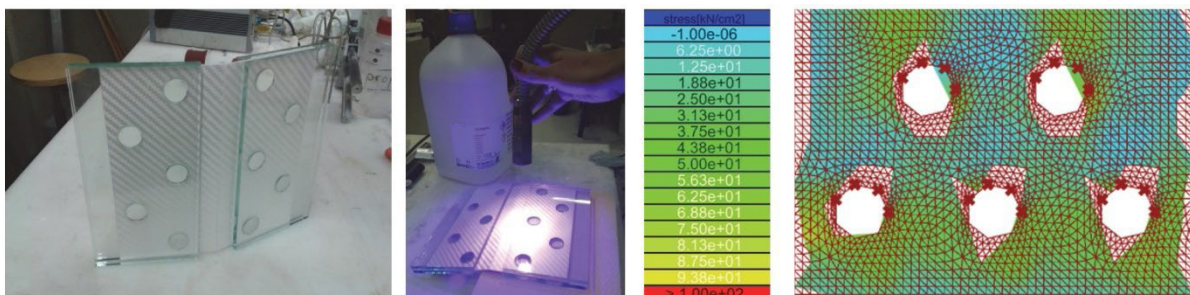


Figure 7: Mock up preparation and digital optimization of the hinged connection. Source: Krousti, A., Snijder, A., & Turrin, M. (2018). Kinematics of folded glass plate structures.

and include tolerance in both x and y directions, ensuring waterproofing and ease of repair.

Materials and Fabrication: The connections utilize PURE® composite sheets, which are flexible and strong polypropylene composites with a 70% fiber composition. This material choice supports the structure's kinematic behavior while maintaining a high architectural quality.

Performance and Durability: The hinged connections are experimentally tested for their mechanical properties, including their ability to handle shear stress and their fatigue resistance. These tests ensure that the connections can withstand the operational demands of a deployable roof without failure.

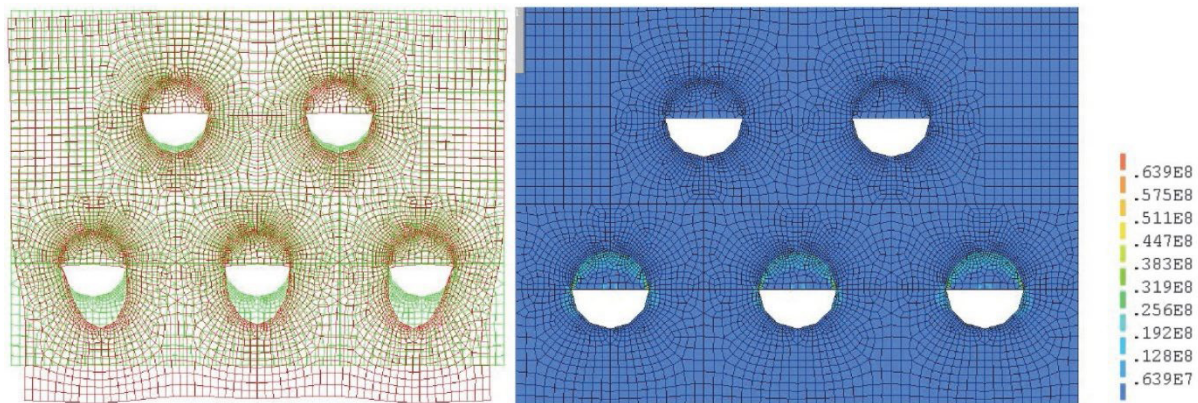


Figure 8: Graphic representation of the 2D model of connection element of perforated sheet of PURE composite and the stress results of finite element analysis. Source: Krousti, A., Snijder, A., & Turrin, M. (2018). Kinematics of folded glass plate structures.

- **Performance Characteristics**

Structural Integrity: The structural analysis shows that the connections effectively transfer out-of plane forces into the plane, leveraging the stiffness of folded structures. This behavior is critical in maintaining the integrity of the glass plates under various load conditions.

Deployment Mechanism: The deployment mechanism, integral to the connection system, allows the roof to adjust to different configurations without additional support structures. This system's design uses directional rails, which are part of the connection assembly, facilitating the roof's expansion and contraction.

From technical sheet

MAX TENS. STRESS 200 Mpa

From fatigue testing

safe design stress for PURE composite: Unnotched

6500 N over area of 15mm x 40mm:
Max tensile stress 9.03E+07 [N/m2]
90.28 [Mpa]
MAX pricipal force 1.35E+05 [N/m]

Pull-Out testing

on a 40mm width

		N	to	N/m
SINGLE 1.5mm /1 DISK	Average force	2383.98	[N]	5.96E+04
	Max. shear stress	3.97E+07	[N/m2]	
		39.73	[Mpa]	
DOUBLE 1.5mm /2 DISK	Average force	4417.37	[N]	1.10E+05
	Max. shear stress	7.36E+07	[N/m2]	
		73.62	[Mpa]	



Figure 9: Comparative results concerning design stresses as occurring from fatigue and pullout testing. Source: Krousti, A., Snijder, A., & Turrin, M. (2018). Kinematics of folded glass plate structures.

- **Categorization of Connection Types**

Based on your description, the connections in this system could be categorized under several of your predefined types:

Adhesive Connections: The use of PURE® composite in conjunction with glass or steel disks bonded to glass panels resembles adhesive connections, albeit with a mechanical component.

Mechanical Connections: The overall deployment mechanism, including the use of hinged connections that incorporate mechanical components (e.g., glass or steel disks), aligns with mechanical connection types.

- **Permanence of Connections**

The connections are designed to be permanent in terms of their installation but allow for the modular and adjustable nature of the structure. They enable the glass panels to move as required but are not intended to be disassembled regularly. This system illustrates a novel approach to architectural challenges, leveraging both the material properties and the kinematic possibilities of modern engineering.

2. Novel liquid-laminated embedded connection

This research introduces an innovative liquid-laminated embedded connection tailored specifically for glass structures, featuring a steel insert encapsulated by a transparent resin. This connection is particularly notable for its application in situations where traditional bolted connections may fall short due to stress concentrations and aesthetic limitations. (Volakos et al., 2022).

- **Detailed Connection Overview**

Connection Type and Implementation: The innovative connection utilizes an embedded steel insert combined with a cold-poured resin. This combination allows for a strong bond that maintains clarity and reduces the visibility of the connection points, aligning with modern architectural demands for sleek, unobtrusive designs.

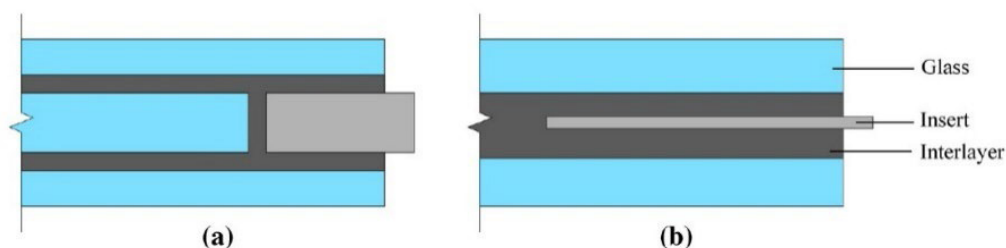


Figure 10: Scheme of embedded laminated connections with thick (a) and thin insert (b). Source: Volakos, E., Davis, C., Teich, M., Lenk, P., & Overend, M. (2021). Structural performance of a novel liquid-laminated embedded connection for glass. *Glass Structures & Engineering*, 6(4), 487–510. <https://doi:10.1007/s40940-021-00162-w>

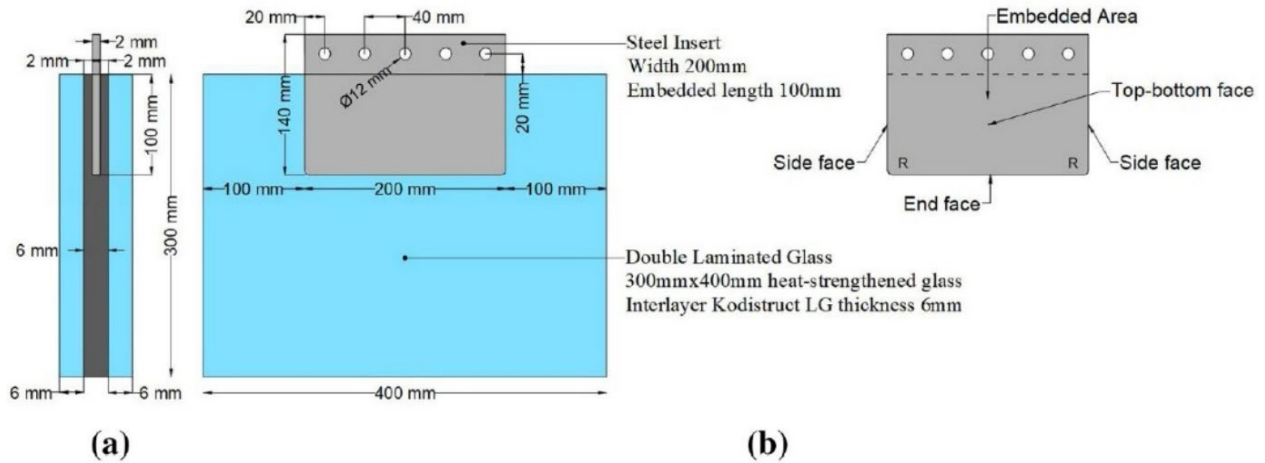


Figure 11: Pullout specimen; section (a) and top view (b). Source: Volakos, E., Davis, C., Teich, M., Lenk, P., & Overend, M. (2021). Structural performance of a novel liquid-laminated embedded connection for glass.

Materials and Fabrication: The steel insert is encapsulated by a transparent resin, chosen for its high stiffness and excellent adhesion qualities. This method eliminates the unfavorable residual stresses typically associated with different thermal expansion rates in conventional lamination processes.

- **Performance and Durability Analysis**

Mechanical Properties:

The study meticulously examines the axial tensile mechanical response of the connection through both numerical analyses and destructive pull-out tests. These tests assess how the connection behaves under different strain rates, providing insights into its mechanical resilience and reliability. The results indicated that the connection could sustain significant axial load without structural failure, showcasing its robustness.

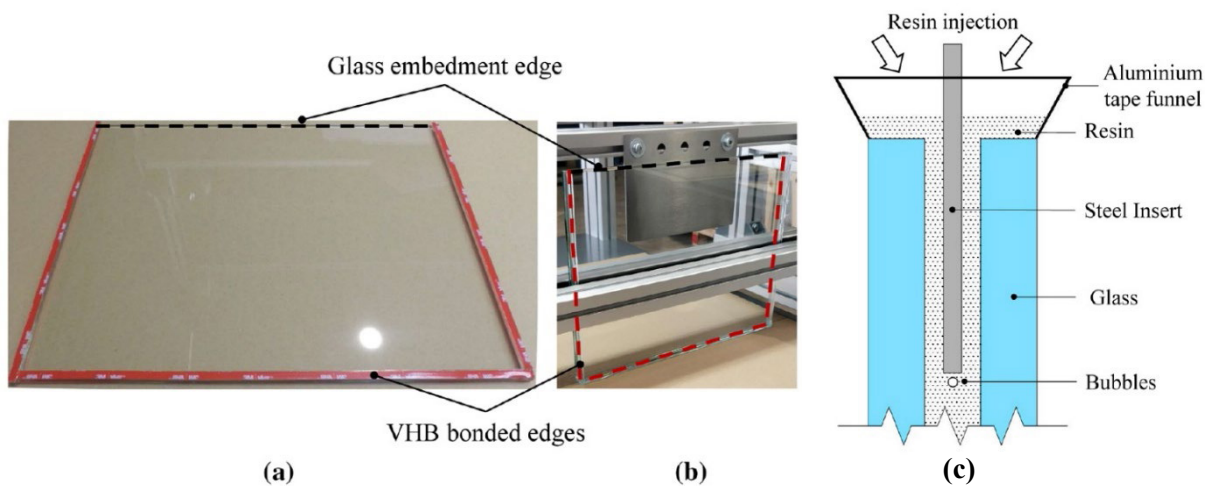


Figure 12: Glass ply with VHB tape (a) and glass assembly (b) and scheme of resin injection (c). Source: Volakos, E., Davis, C., Teich, M., Lenk, P., & Overend, M. (2021). Structural performance of a novel liquid-laminated embedded connection for glass.

Load-bearing Capacity:

The connection exhibits high load-bearing capabilities, with the resin playing a crucial role in distributing stresses evenly and maintaining the structural integrity of the glass components. The innovative use of cold-poured resin overcomes the limitations of traditional adhesives by accommodating fabrication tolerances and reducing production costs. Specific test results showed that this connection type could handle increased load capacities up to 20% more than conventional adhesive systems, without any degradation in performance or aesthetics.

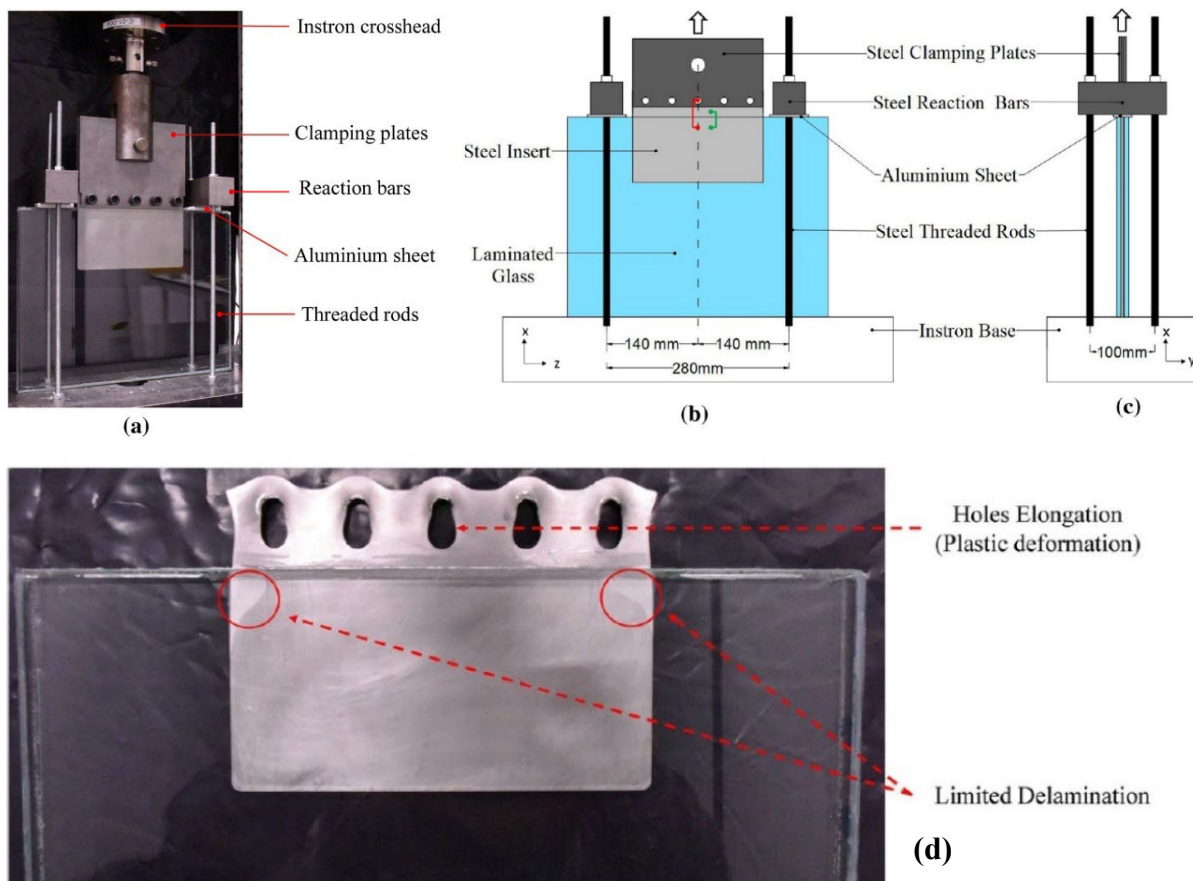


Figure 13: Scheme of the test setup; photo (a), frontal View (b) and lateral view (c) Steel failure at 10 mm/min tested specimens (d). Source: Volakos, E., Davis, C., Teich, M., Lenk, P., & Overend, M. (2021). Structural performance of a novel liquid-laminated embedded connection for glass.

- **Categorization and Permanence of Connections**

Categorization:

Adhesive Connections: This connection represents an advanced form of adhesive connections where the bond is achieved through a resin that provides both transparency and strength.

Embedded Connections: The steel insert embedded within the laminated glass categorizes this as an embedded connection, a method that enhances load-bearing capacities and integrates seamlessly with the glass.

Comparison with Traditional Connections

Compared to traditional **adhesive connections**, the novel connection offers enhanced load-bearing capabilities and greater durability due to the integration of resin and steel, which distributes stresses more effectively. Unlike typical **embedded connections**, which can visually disrupt the glass, this method maintains the transparency and aesthetic appeal of glass structures by minimizing the visibility of the connection points.

Permanence:

The connections are designed to be permanent, providing durable and stable joins without the need for frequent maintenance or adjustments. They are particularly suited for applications where longterm reliability and aesthetic cleanliness are critical.

3. Glass Connection in Folded Plate Structures

The study, "Folded plate structures made of glass laminates: a proposal for the structural assessment" by Marinitsch, Schranz, and Teich (2015), examines the structural integrity of glass laminates used in folded plate structures. This research introduces a novel connection design that not only enhances the load-bearing capacity but also integrates aesthetically, making it ideal for applications requiring expansive spans and minimal visual disruption.

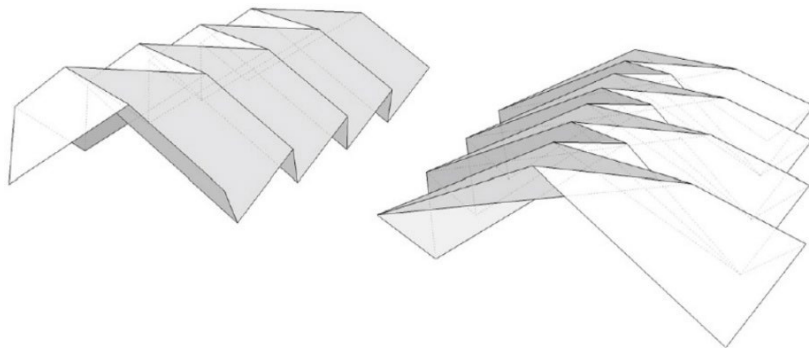


Figure 14: folded plate structures made of glass laminates using a new connection detail. Source: Marinitsch, S., Schranz, C., & Teich, M. (2016). Folded plate structures made of glass laminates: a proposal for the structural assessment. *Glass Structures & Engineering*, (2), 451–460. <https://doi:10.1007/s40940-01500021>

• Detailed Connection overview

This innovative connection integrates triple-laminated glass with metallic inserts. Initially, these inserts are connected using rivets through oversized holes to accommodate tolerances. This provisional setup allows for adjustments and alignment before final settings.

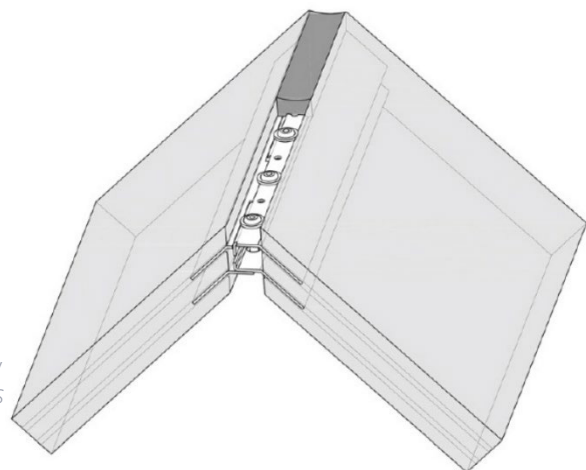


Figure 15: Connection detail AA. Source: Marinitsch, S., Schranz, C., & Teich, M. (2016). Folded plate structures made of glass laminates.

- **Materials and Fabrication:**

Following this initial assembly, the cavity around the protruding inserts is filled with epoxy-grout, converting the connection from relying on friction to a tight-fit assembly. This shift in load transfer mechanism ensures that compression forces are effectively transmitted through the grout and the inserts, while tension forces are managed through the shear interaction in the interlayer, from one side of the glass to the other.

Additionally, the design addresses shear forces by utilizing continuous serration with alternating shear dowels, formed by the folds of the metallic inserts and supported by the rivets. This setup helps to distribute shear loads evenly and effectively.

- **Performance and Durability Analysis:**

The axial tensile strength and response under various loading conditions were rigorously assessed through both numerical analyses and destructive pull-out tests. The connection design cleverly handles stress concentrations through the metal components rather than the glass itself, mitigating risks associated with the brittle nature of the glass. The weatherproofing of the connection is achieved by concealing the joint assembly between the outer glass plies, creating a flush surface and maintaining the aesthetic integrity of the glass facade. These evaluations demonstrate that the connection can withstand significant stresses without compromising the structural integrity of the glass, positioning it as a robust alternative to traditional connection methods (Marinitsch et al., 2015).

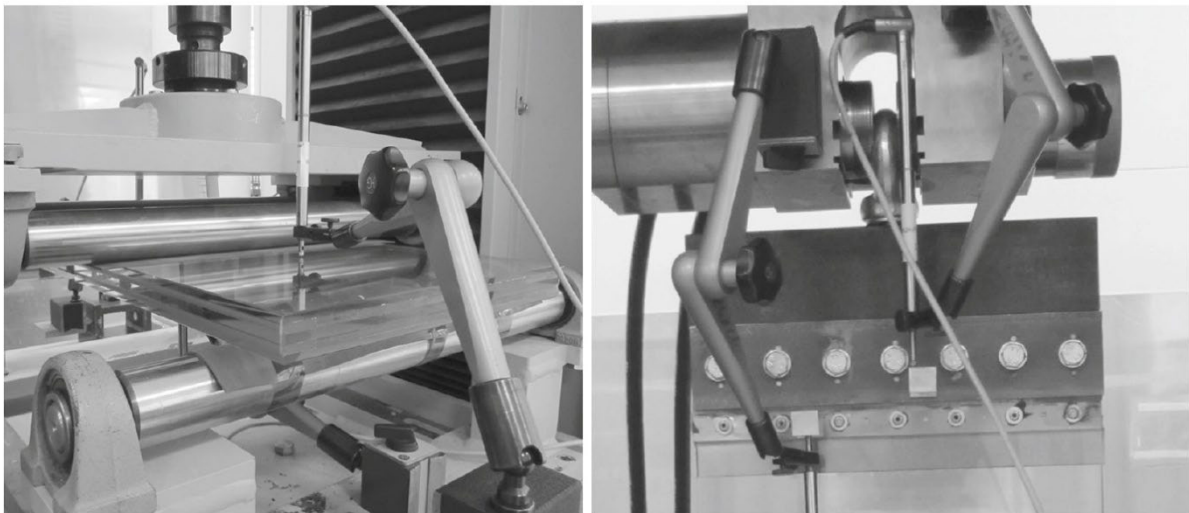


Figure 16: Fourpointbending test (left) and tension test (right). Source: Marinitsch, S., Schranz, C., & Teich, M. (2016). Folded plate structures made of glass laminates.

- **Comparison with Traditional Connections:**

Adhesive Connections: This novel method transcends the typical visual and distribution limitations of conventional adhesive connections, offering seamless integration.

Embedded Connections: Unlike traditional embedded connections that can disrupt the glass's aesthetic with visible hardware, this approach incorporates embedded elements more subtly, enhancing both functionality and appearance.

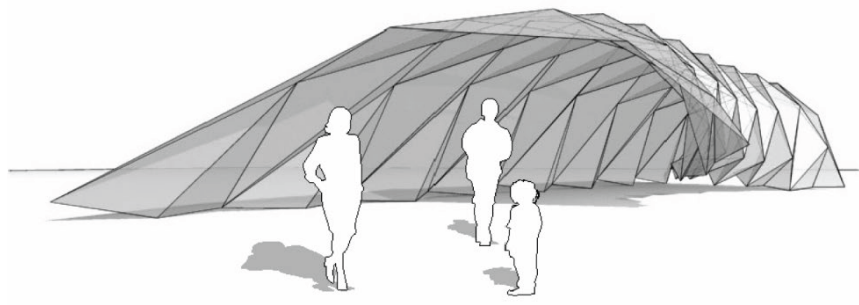
- **Permanence of Connections:**

Designed to be permanent, the connection requires minimal maintenance while providing long-term reliability and stability, making it highly suitable for architectural applications where durability and aesthetic cleanliness are paramount.

4. Glass Folded Plate Structures

In their 2006 study, Trometer and Krupna investigate innovative uses of glass in folded plate structures, particularly through the development of hinge-like connections. These connections are designed to mimic origami, allowing the glass plates to flex under load, which reduces bending stresses and maintains structural integrity.

Figure 17: Freeform model for conceptual design.
Source: Trometer, S., & Krupna, M. (2006). Development and design of glass folded plate structures. *Journal of the International Association for Shell and Spatial Structures*, 47(3), 152158.



- **Connection Details:**

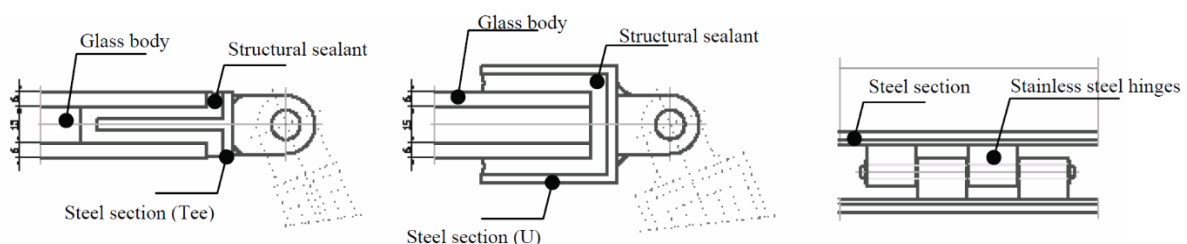
The engineered hinges act as pivot points that facilitate the glass's folding movements without compromising its strength. These hinges are integrated discreetly to preserve the aesthetic continuity of the glass surfaces.

- **Materials and Construction:**

The study uses durable materials for the hinges, capable of withstanding significant stress without degrading. Silicone adhesive bonds and structural sealants are applied to attach the glass panels to stainless steel hinges. These adhesives are chosen for their ability to evenly distribute stress and resist environmental factors like UV light and temperature fluctuations.

- **Structural Validation:**

Finite element modeling is used to validate the connection design, ensuring it can accommodate the differential thermal expansion often seen in structural glass applications. This method confirms the long-term viability and performance of the connections.



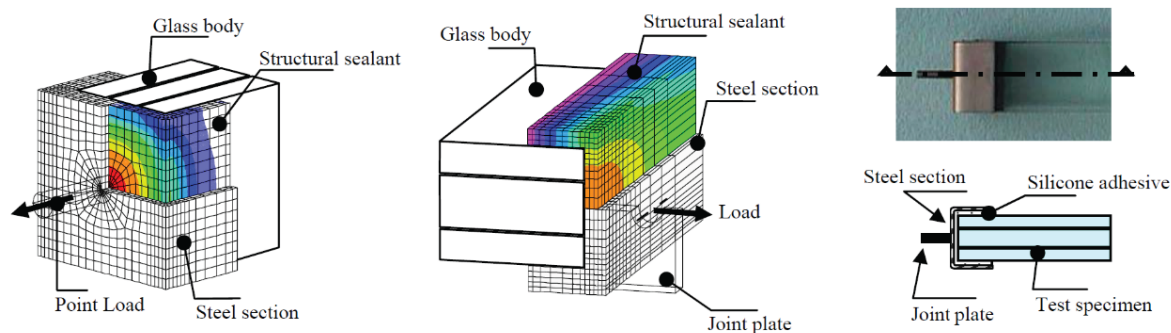


Figure 18: System section of structural sealant connection at the hinges(above), FE model with normal stress distribution in structural sealant and specimen(below). Source: Trometer, S., & Krupna, M. (2006). *Development and design of glass folded plate structures*

5. Integrated Connections for Glass-Plastic-Composite Panels

The innovative study by Hänig and Weller (2022) investigates the structural performance of glass-plastic-composite panels under tensile loading across varying temperatures. Their research is driven by the architectural demand for high transparency and lightweight structures in modern glass facades, which traditional glass systems with visually prominent fittings fail to address adequately.

• Glass-Plastic-Composite Panels

The composite panels developed in this study consist of a polymethylmethacrylate (PMMA) interlayer flanked by thin glass layers. This composition not only offers a significant reduction in weight—up to 44% compared to traditional glass—but also enhances the structural integrity and impact resistance of the panels. Such characteristics are crucial for applications requiring both aesthetic appeal and functional durability.

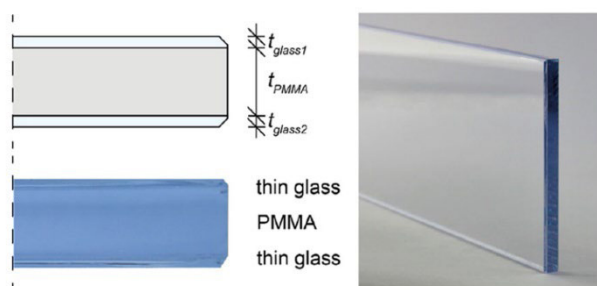


Figure 19: Glass-plastic composite panel build-up and edge view. Source: Hänig, J., & Weller, B. (2022). *Integrated connections for glass-plastic-composite panels*. <https://doi.org/10.1007/s40940022001740>

• Connection Designs

Hänig and Weller categorize the connections into two types: mechanical and adhesive. Mechanical connections utilize stainless steel blocks and fasteners, cleverly designed to minimize optical intrusion and stress concentration at the connection points. In contrast, adhesive connections employ various polymers such as epoxy, acrylate, and polyurethane, each selected for their distinct mechanical properties and performance under stress, which are pivotal for ensuring the long-term integrity of the panels.

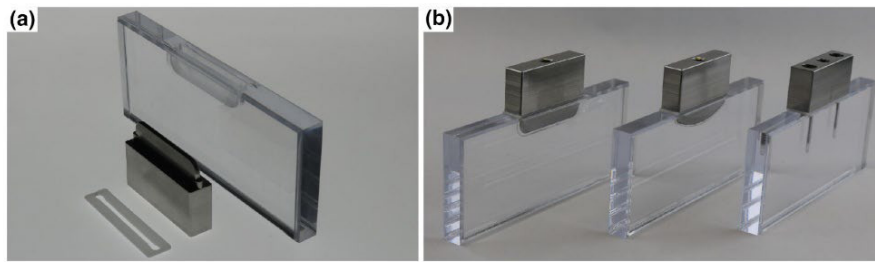


Figure 20: a CNC processed glass-plastic-composite specimen with connection components and b connection prototypes. Source: Hänig, J., & Weller, B. (2022). Integrated connections for glass-plastic-composite panels.

- **Experimental Study**

The experimental approach involved subjecting the specimens to tensile loading at temperatures of +23, +40, and +60 °C. The outcomes highlighted distinct failure mechanisms for each connection type. Mechanical connections displayed a nearly linear load-bearing behaviour, indicating robustness across the tested temperature range. Conversely, adhesive connections demonstrated variable stiffness and failure modes, heavily influenced by the thermal conditions and the properties of the adhesives used.

- **Key Findings**

The research revealed that:

Mechanical Connections exhibit consistent load-bearing behaviour with high durability under temperature variations. They are capable of sustaining significant post-fracture loads, indicating their suitability for dynamic structural applications.

Adhesive Connections vary in performance:

Epoxy Adhesives show high stiffness but are prone to early failure under high load due to their rigidity.

Acrylate Adhesives soften significantly at higher temperatures, leading to considerable displacement and eventual failure.

Polyurethane Adhesives were noted for their low stiffness and excluded from further tests due to inadequate performance.

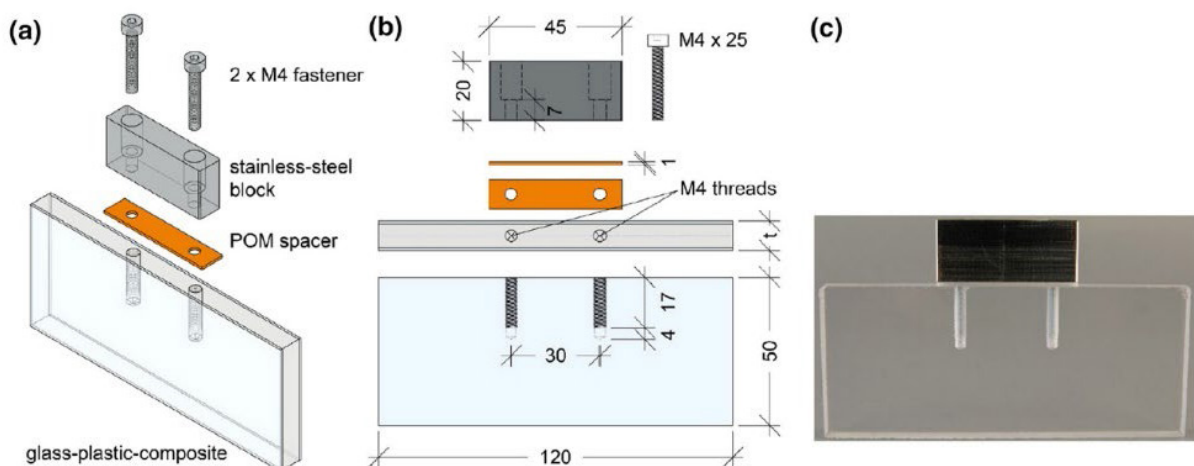


Figure 21: Components and dimensions of the mechanical connection: a isometric view of components, b associated dimensions and c front view of assembled specimen. Source: Hänig, J., & Weller, B. (2022). Integrated connections for glass-plastic-composite panels.

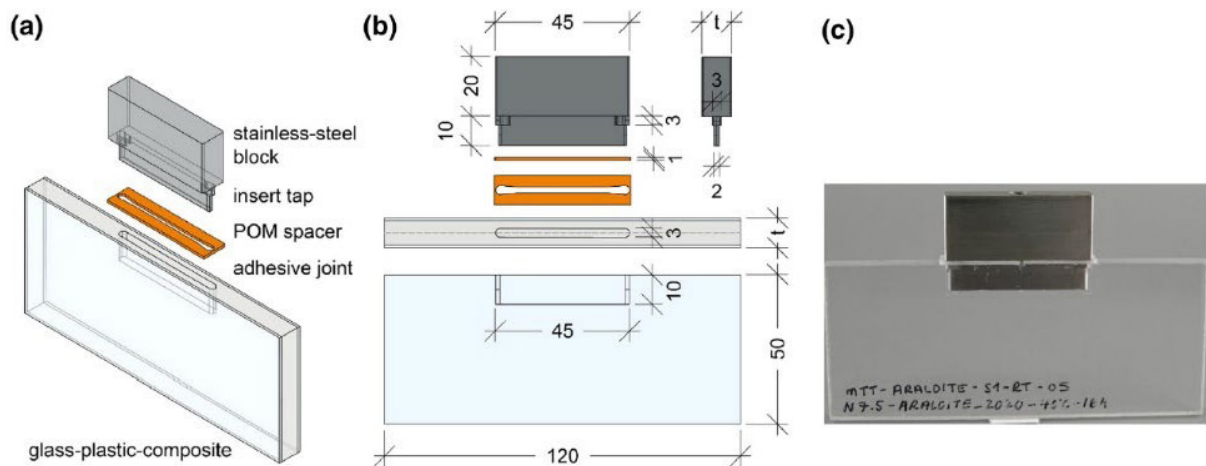


Figure 22: Components and dimensions of the adhesive connection: a isometric view of components, b associated dimensions and c front view of assembled specimen. Source: Hänig, J., & Weller, B. (2022). Integrated connections for glass– plasticcomposite panels.

7.2. Modular Systems with Dry Connections in Other Materials

Brittle materials such as glass share structural challenges with wood, stone, and concrete, particularly in stress management and adaptability. Interlocking systems in stone masonry, for example, demonstrate effective load distribution while maintaining ease of assembly and disassembly. These principles can be adapted to glass systems to enhance reusability and structural efficiency. Research into interlocking timber systems also offers insights into reducing material waste and improving precision through CNC machining (Oikonomopoulou et al., 2023).

1. Interlocking, Ribbing and Folding: Explorations in Parametric Constructions

The paper by Arturo Lyon and Rodrigo Garcia presents a compelling exploration into the realm of parametric constructions, utilizing digital manufacturing methods across three distinct architectural projects. The focus lies on the intricate balance between design creativity and technical execution, where historical influences like Gaudí and Calatrava resonate through modern computational techniques. This blend of past inspirations with contemporary digital tools sets the stage for a nuanced approach to architectural form and functionality.

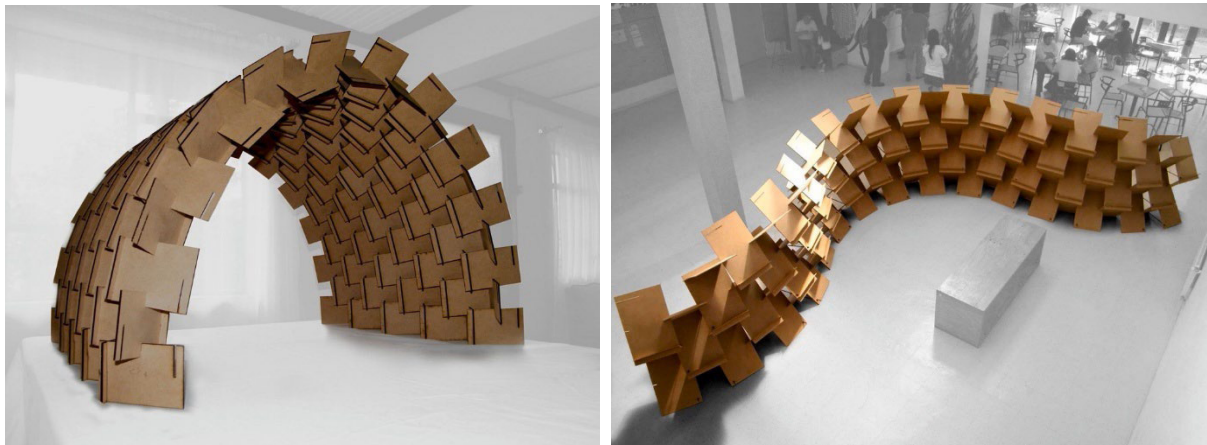


Figure 23: Modular interlocking platesPixelwall. Source: García Alvarado Rodrigo (2010).

- **Project 1: Pixel-Wall**

The Pixel-Wall project investigates the potential of modular, interlocking plates, utilizing medium density fiber board (MDF) crafted with precision through laser-cutting technology. These plates, designed to connect at right angles, form a self-supporting three-dimensional lattice that not only serves structural purposes but also achieves aesthetic expression through its pattern and openness. This system allows for versatile applications, from interior partitions to exterior facades, highlighting its adaptability and scalability. The integration of curvature enhances the structural integrity while introducing formal variety, which is parametrically programmed to achieve desired geometries and functionalities. Miotto, Bruscatto Underléa; García Alvarado Rodrigo (2010).



Figure 24: Various configurations of Modular interlocking plates Pixelwall. Source: García Alvarado Rodrigo (2010).

Materialization and Fabrication

The choice of MDF and the method of laser cutting are pivotal. The uniformity and precision provided by digital fabrication ensure that each component fits seamlessly within the larger structure, maintaining the integrity and strength of the overall assembly. The parametric software used, notably Rhinoceros with Grasshopper™, allows for an adaptive design process where changes in parameters dynamically influence the component shapes and their assembly logic.

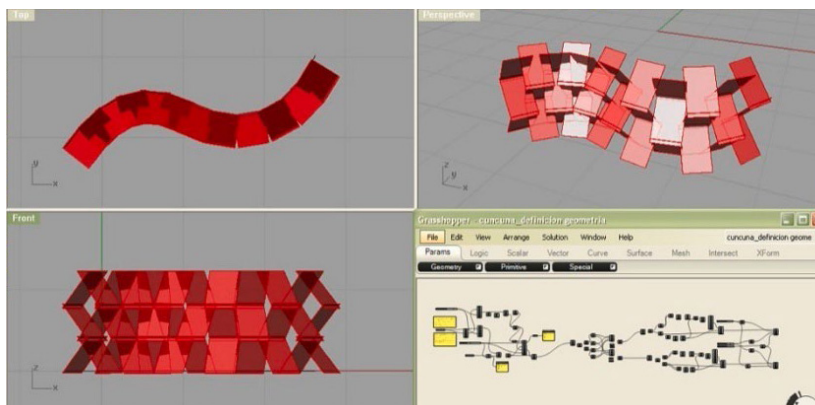


Figure 40: Computational tool used for parametric Modular interlocking plates Pixel-wall. Source: García Alvarado Rodrigo (2010).

Assembly Process

The assembly of the Pixel-Wall is designed to be straightforward, emphasizing ease and efficiency. The system's modularity supports quick assembly and disassembly, which is crucial for temporary installations or adaptive spatial solutions. This design approach significantly reduces the time and labor typically associated with traditional construction methods, offering a sustainable alternative that minimizes waste and resource use.

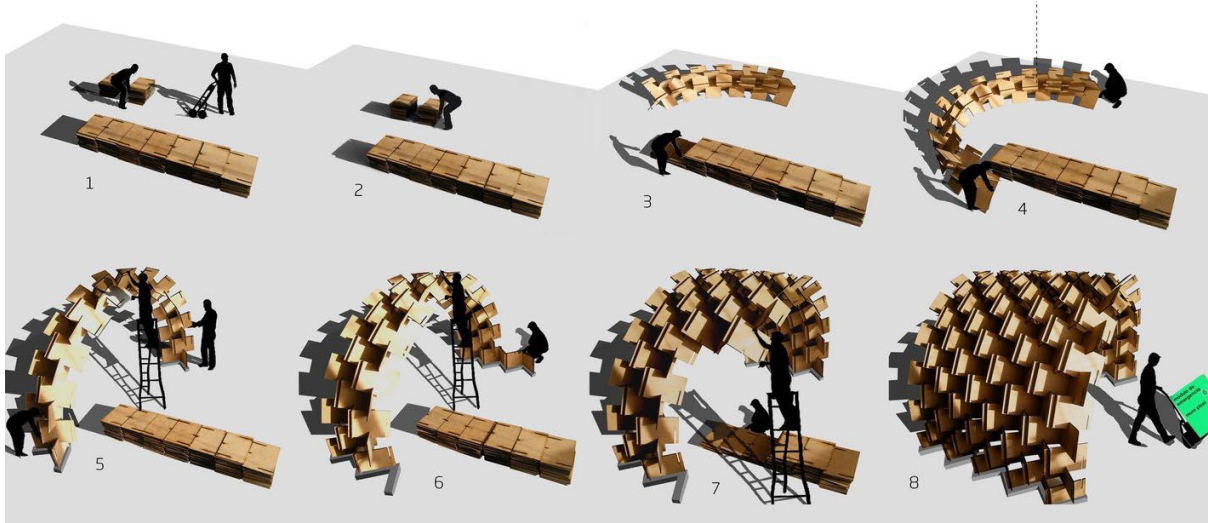


Figure 41: Assembly order of Modular interlocking plates Pixelwall. Source: García Alvarado Rodrigo (2010).

Structural Analysis

The structural analysis of the Pixel-Wall, although not detailed in granularity in the initial overview, would typically involve assessing the load-bearing capabilities of the interlocking system and the effects of various loads on its stability and durability. The use of curvature likely contributes to the overall strength, distributing stresses more evenly across the structure.

Conclusion and Future Work

Miotto and García Alvarado conclude that the "Pixel Wall" system holds significant potential for revolutionizing architectural design and construction. They advocate for further research and development to explore broader applications and to refine the system's capabilities, particularly in terms of scaling up the installations and enhancing material properties.

2. Populous Installation for the World Architecture Festival

The Populous installation for the World Architecture Festival (WAF) in London draws its conceptual inspiration from Charles and Ray Eames' iconic "House of Cards." This connection to the Eames' design philosophy is evident in the modular and inter connective aspects of the installation, which utilizes hundreds of super-sized 'W' shaped forms to create a dynamic, visually compelling centerpiece. This 7-meter-high installation not only serves as the focal point of the festival but also embodies the WAF's mission to highlight groundbreaking architectural achievements from around the globe.



Figure 42: House of Cards, pavilion in the World Architecture Festival (WAF) in London. Source: Populous. (2015) ArchDaily. Retrieved from <https://www.archdaily.com/769325/populous-creates-eames-inspired-installation-for-worldarchitecturefestivallondon>

- **Design and Execution**

Hosted by the University of Westminster in collaboration with the London Festival of Architecture, the WAF event is more than just an exhibition; it's a comprehensive showcase featuring talks, debates, and presentations from some of the most influential figures in the architectural world. The design by Populous cleverly utilizes every aspect of the venue's industrial space, integrating a magnetically suspended gallery that displays 350 shortlisted projects from renowned architects and designers worldwide. This innovative use of space and presentation underscores the festival's global reach and intellectual depth.



Figure 43: House of Cards, pavilion in the World Architecture Festival (WAF) in London. Source: Populous. (2015) Retrieved from ArchDaily.

- **Functionality and Global Relevance**

The design team at Populous was challenged not only with creating a striking installation but also with ensuring that the structure was functional and adaptable for global use. The installation was designed with modularity in mind, allowing it to be disassembled, shipped, and reassembled at various international locations. This adaptability speaks to the transient and expansive nature of modern architectural practices and exhibitions. According to Populous designer Aaron Richardson, the use of readily available industrial materials was a strategic choice, aligning with the budgetary and spatial constraints and enhancing the installation's fit within the rugged aesthetic of a former construction testing bunker.

3. Temporary Permanence Installation by Arup Associates

The "Temporary Permanence Installation" by Arup Associates, designed for the Urbanism & Architecture Biennale, exemplifies innovative approaches to temporary urban interventions. This installation was situated in Shanghai's Siping District, an area known for its vibrant street life and community engagement. The project aligns with themes of reuse and rethinking urban spaces, integrating seamlessly into the daily activities and cultural practices of the local community.



Figure 44: "Temporary Permanence Installation" by Arup Associates, designed for the Urbanism & Architecture Biennale, situated in Shanghai's Siping District. Source: ArchDaily. (2016). Temporary Permanence Installation / Arup Associates. Retrieved from <https://www.archdaily.com/786564/urban-public-spatial-installation-arup-as-associates>

- **Design Philosophy and Material Usage**

Arup Associates designed the installation using recycled off cuts of commercial polycarbonate sheeting, emphasizing sustainability and environmental consciousness. The choice of material reflects a commitment to reducing waste, while also ensuring that the structure is lightweight, durable, and adaptable to various uses and reconfigurations and the polycarbonate is laser-cut into precise shapes to facilitate the interlocking design.

- **Joints and Structural Design:**

The structural system of the installation is based on a simple repetitive cruciform module that slots together without the need for any fixings. This design choice supports ease of assembly and disassembly, enabling the structure to be adapted or reconfigured by commu-

nity members with minimal effort. The slot-connect technique also encourages participation from various age groups and user types, promoting community engagement through the construction process.



Figure 45: "Temporary Permanence Installation" by Arup Associates, designed for the Urbanism & Architecture Biennale, situated in Shanghai's Siping District. Source: ArchDaily. (2016).

- **Structural Design and Innovation**

The cruciform modules are designed to slot together without any fixings, allowing for rapid assembly and reconfiguration by people of all ages and abilities. This design not only reduces the time and technical skill required to modify the structure but also promotes inclusivity and community ownership of the space. The flexibility of the design enables it to be used for various purposes, including public gatherings, exhibitions, and recreational activities, adapting to the dynamic needs of the urban environment.



Figure 46: Close view of modules, made of recycled offcuts of commercial polycarbonate sheeting "Temporary Permanence Installation" by Arup Associates, Source: ArchDaily. (2016).

- **Community Impact and Interaction**

The installation's initial configuration was inspired by the local habit of playing chess, which typically attracts groups of spectators and fosters social interaction. This thoughtful consideration of local customs and activities enhances the installation's role as a communal space, where residents can not only engage in traditional pastimes but also experience new forms of communal interaction and cultural expression. The structure's adaptability allows it to morph organically according to community needs, serving as a living part of the urban landscape.

4. Optimal Segmentation of Glass Shell Structures

Glass shell structures offer a blend of aesthetic appeal and structural integrity, often used in modern architecture to create visually striking and naturally illuminated spaces. The design and engineering of glass shell structures pose unique challenges, particularly in achieving large spans with limited material sizes and handling the inherent brittleness of glass. The research by S. Goel at the University of Stuttgart addresses these challenges by exploring the segmentation of glass shells into smaller, manageable units that can be assembled to cover larger areas efficiently.

- **Previous Studies**

Historically, the use of segmented glass in architectural applications has been constrained by the available technology and material limitations. Early efforts, as noted by Veer et al. (2003) and Blandini (2005), focused on using flat glass segments for constructing domes and employing linear joint systems that allow for tolerances. These projects laid the groundwork for understanding the structural behavior of segmented glass shells but did not extensively explore the impact of segment shape and joint material on overall shell performance.

- **Current Research**

Goel's study advances this field by methodically analyzing the performance of segmented glass shells using different shapes and adhesive types. The research classifies shells based on their Gaussian curvature and employs a Reissner-Mindlin finite element approach to evaluate the structural behavior under various loading conditions. Shells are segmented into square, diamond, hexagon, and hexalock shapes, and joined with materials ranging from monolithic glass to softer adhesives like silicone and harder options like epoxy.

- **Findings**

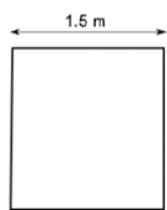
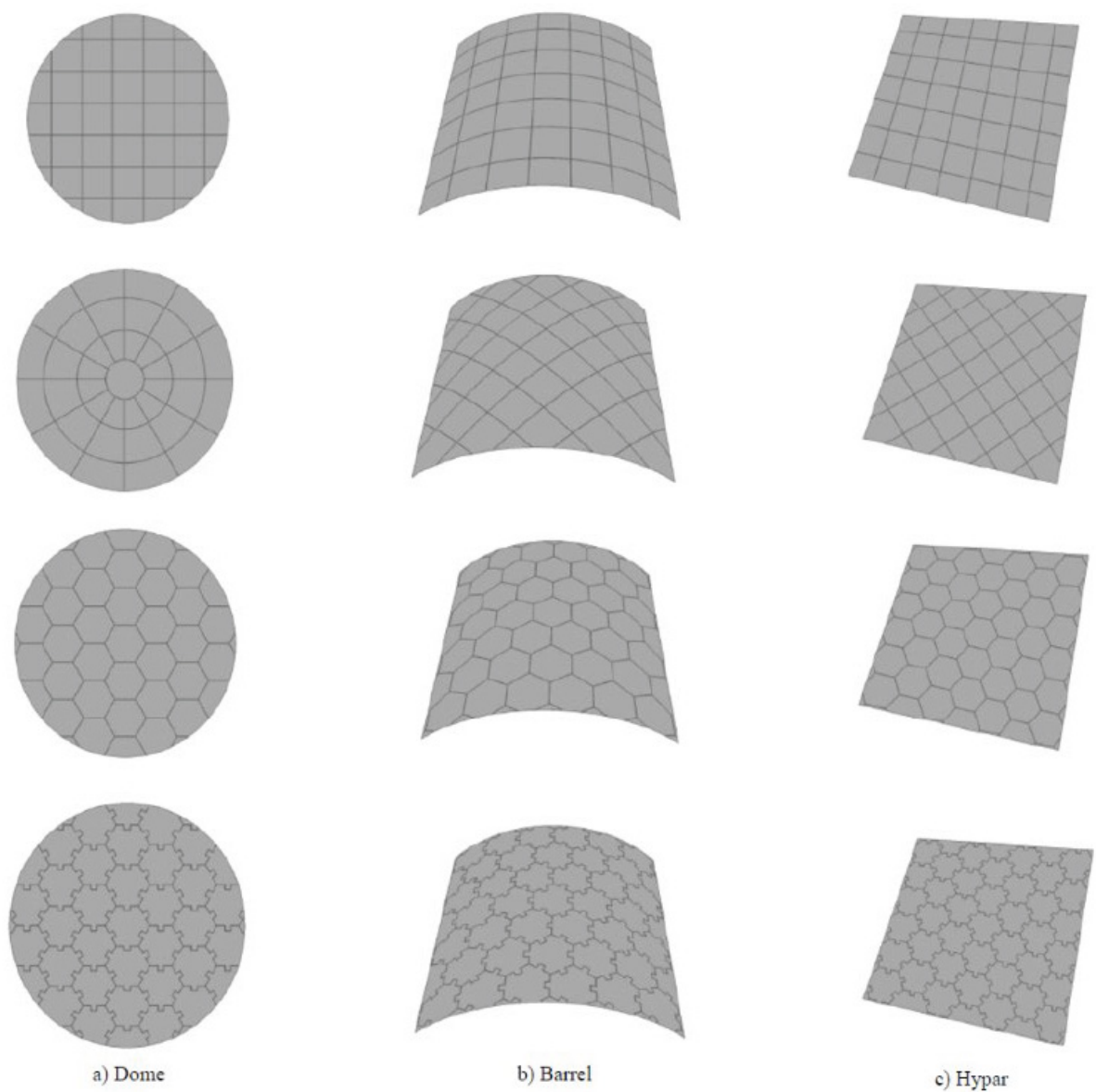
The findings reveal that the choice of segment shape and joint stiffness significantly influences the structural integrity and load-bearing capacity of glass shells. Optimal segment shapes are identified for different types of curvature:

Domes: Hexagonal segments minimize deflection and bending moments, suggesting an alignment with the natural form of doubly curved surfaces.

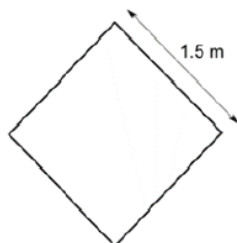
Cylindrical roofs (barrels): Square segments are found to be most effective, possibly due to their compatibility with the singly curved form of cylindrical structures.

Hyperbolic paraboloids (hypars): Diamond shapes provide the best performance, aligning with the complex curvature of hypars.

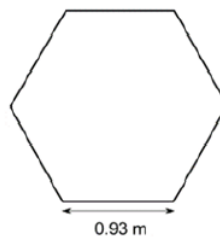
The study also underscores the superiority of hard adhesives like epoxy over softer options, attributing this to their ability to maintain rigidity and reduce deflection across all tested shapes and structures.



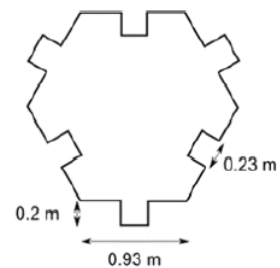
a) Square



b) Diamond



c) Hexagon



d) Hexalock

47: Segmented glass shell, Dome, Barrel and Hypar. Source: Goel, S. (2016). *Optimal Segmentation of Glass Shell Structures*. In *Challenging Glass 5 – Conference on Architectural and Structural Applications of Glass* (Belis, Bos & Louter, Eds.), Ghent University. ISBN 978-90-825-2680-6.

Arup Associates, Source: ArchDaily. (2016).

7.3. History of Modular Glass Systems

1. Laminated Glass Connection Details: Towards Homogeneous Material Joints in Glass

The article provides an in-depth exploration of the structural and architectural applications of laminated glass, particularly focusing on the development and implications of novel connection methodologies that avoid traditional steel elements. This study, conducted by Philipp Eversmann from the University of Kassel and André Ihde from TU München, investigates a modular glass system for potential small-scale architectural applications. The system employs a homogeneous glass joint, termed the Glass-dovetail (GD) connection, that leverages digital fabrication techniques. This approach reflects an ongoing architectural demand for transparent yet robust design solutions (Eversmann & Ihde, 2018).

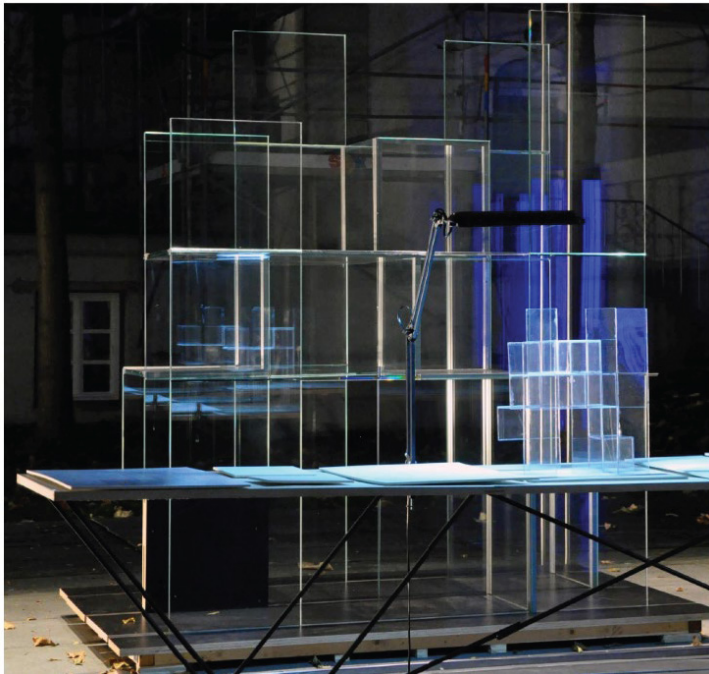


Figure 48: Exhibition of the final structure at the Bavarian Chamber of Architects BYAK in Munich. Source: Eversmann, P., & Ihde, A. (2018). Laminated Glass Connection Details: Towards Homogeneous Material Joints in Glass. Challenging Glass Conference Proceedings, Delft University of Technology, May 2018. <https://doi.org/10.7480/cgc.6.2158>

- **Connection Methodology: Glass-Dovetail (GD) Connection**

The innovative Glass-dovetail (GD) connection central to this research is a novel approach that eliminates the use of traditional steel elements within the joints of laminated glass structures. This connection is inspired by traditional dovetail joints commonly used in woodworking, which are renowned for their strength and simplicity. In the GD connection:

Design:

The GD connection involves glass elements with chamfered edges at 45 degrees. These chamfers are critical as they facilitate the interlocking mechanism, mimicking the locking nature of a dovetail joint. This method significantly reduces the need for additional adhesives or mechanical fasteners, promoting a cleaner aesthetic and reducing potential stress concentrations at the joint interfaces.

Integration:

The connection is integrated directly into the double-layer system of The innovative Glass-dovetail (GD) connection central to this research is a novel approach that eliminates the use of traditional steel elements within the joints of laminated glass structures. This connection is inspired by traditional dovetail joints commonly used in woodworking, which are renowned for their strength and simplicity. In the GD connection: the laminated glass, where each layer of glass is meticulously aligned to enhance the structural integrity and load-bearing capacity of the joint.

Advantages:

By employing this method, the design allows for the transmission of loads across the glass panels more evenly while maintaining transparency and visual continuity. This is particularly advantageous in architectural applications where aesthetics is paramount.



Figure 49: Exhibition of the prototype at TU Munich, detail of the glass joining method. Source: Eversmann, P., & Ihde, A. (2018). *Laminated Glass Connection Details: Towards Homogeneous Material Joints in Glass*.

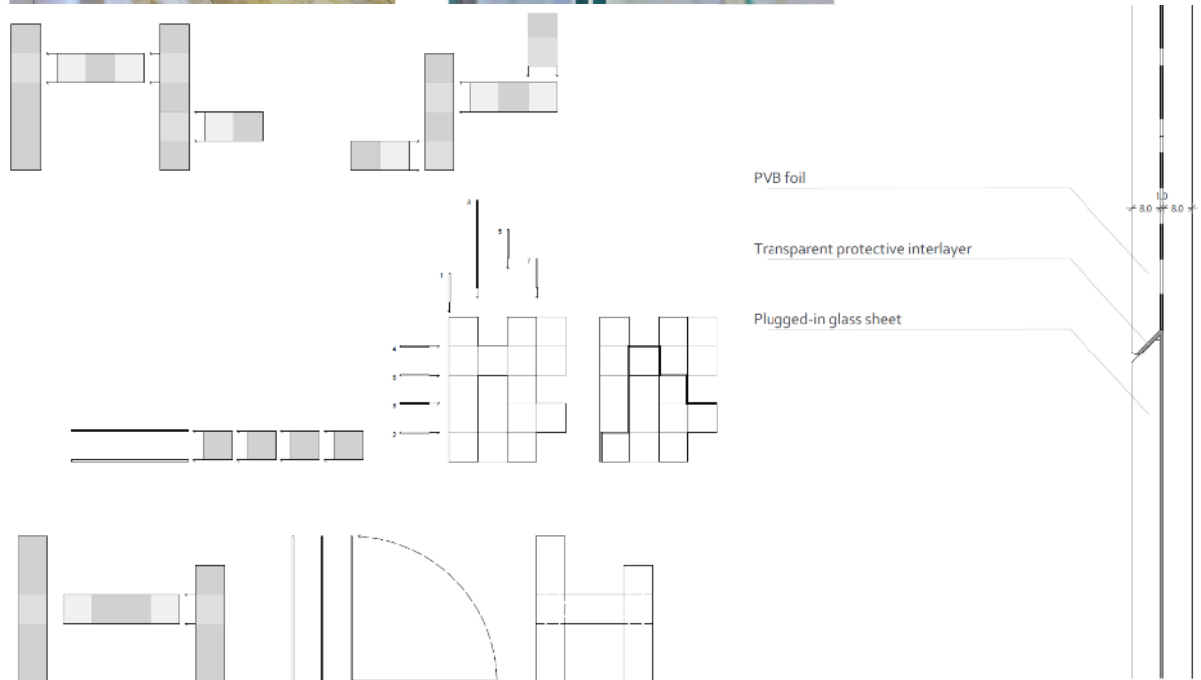


Figure 50: Assembly procedure and joint detail with 45° chamfers. Source: Eversmann, P., & Ihde, A. (2018). *Laminated Glass Connection Details: Towards Homogeneous Material Joints in Glass*.

- **Intermediate Materials Used**

In the research, two types of intermediate materials were mentioned: Polyvinyl Butyral (PVB) and acrylic sheets. Each serves distinct purposes in the construction and assembly of the glass structure:

- **Polyvinyl Butyral (PVB):**

Function: PVB is a resin typically used as an interlayer in laminated glass due to its excellent adhesive and film-forming properties. It enhances the impact resistance of the glass and holds shards in place upon breakage.

Application in Research: In the GD connection system, PVB is used to bond multiple layers of glass, ensuring that even if the glass breaks, it remains intact and in place, thereby maintaining the structural integrity of the entire assembly. The PVB also plays a role in damping vibrations and reducing noise, which is beneficial for architectural applications where these factors are considerations.

- **Acrylic Sheets:**

Function: Acrylic sheets are used as distance elements in the assembly process of the glass structures. Their primary role is to prevent the glass edges from coming into direct contact with each other during and after the assembly process, which can lead to stress concentrations and potential breakage points.

Application in Research: The acrylic distance elements are placed at strategic locations where glass panels intersect or come into close proximity. These sheets allow for slight movements and adjustments during the assembly, ensuring that the glass edges do not touch. This method is crucial for maintaining the longevity and durability of the glass structure, especially in environments where thermal expansion or other dynamic conditions may cause glass panels to shift slightly.

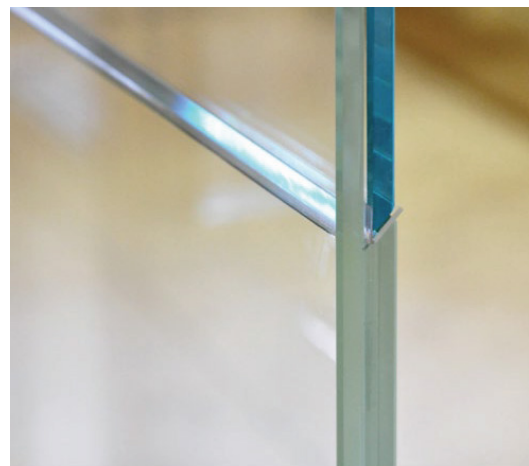
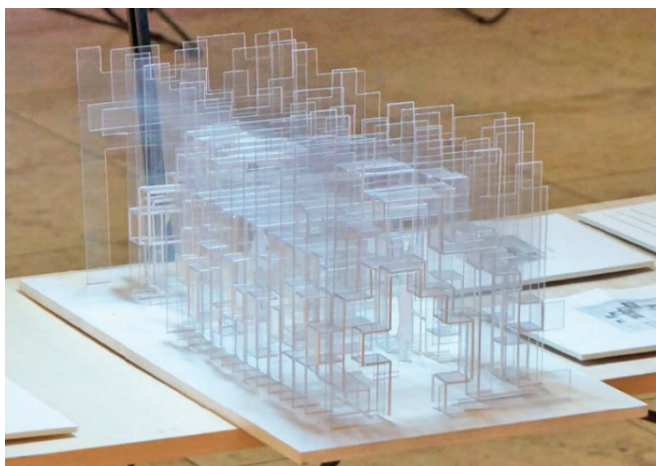


Figure 51 left, Model of Voxel structure of exhibition cuboids, right, Glassdovetail connection with thin acrylic sheets preventing edge-to-edge contact and allowing gliding during assembly. Source: Eversmann, P., & Ihde, A. (2018). *Laminated Glass Connection Details: Towards Homogeneous Material Joints in Glass*.

- **Computational and Structural Design**

The research primarily employs a voxel-based computational design method to simulate a cloud-like structure for an exhibition pavilion. This method enables the partial construction of voxels, optimizing material use and structural integrity, where complete voxels were initially considered but later adapted to only include necessary structural faces to save on material costs and weight.

- **Finite Element Analysis**

A critical aspect of the study is the Finite Element (FE) analysis, which utilizes Strand7 software to model the behavior of the GD connection under simulated load conditions, including wind loads. The FE models, refined through the integration of zero-gap elements and a mesh created via Rhino/Grasshopper, demonstrated that the GD connection could significantly reduce deflections and manage stress distribution more effectively than monolithic joint configurations (Eversmann & Ihde, 2018).

- **FE Analysis**

Presents detailed results from the FE analysis, highlighting the differences in structural behavior between models with zero-gap elements and those with fully linked glass panels. Zero-gap elements in finite element modeling allow for slight movements and contact under load between elements, simulating joints that aren't permanently bonded. In contrast, fully linked connections assume that elements are rigidly bonded with no relative movement, modeling them as a single continuous unit. The analysis showed that fully linked panels significantly reduced overall deflection and more evenly distributed stress across the structure.

- **Digital Fabrication and Assembly**

The practical application of this research was demonstrated through the construction of a 2 x 2 x 1m prototype, fabricated in collaboration with Bischoff Glastechnik. This prototype employed the GD connection details milled with CNC technology and showcased the feasibility of assembling such systems without direct glass contact, utilizing acrylic distance elements to prevent edge damage during assembly (Eversmann & Ihde, 2018).

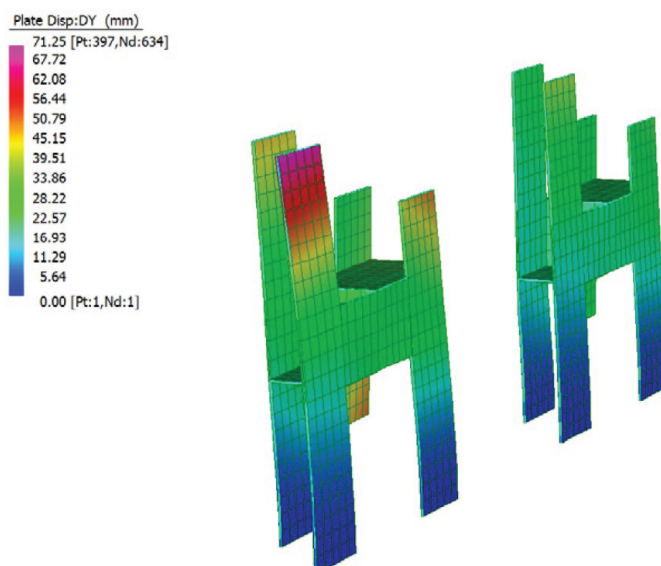


Figure 52 Displacements: Left structure with zero gap elements / right structure with monolithic linked glass panels. Source: Eversmann, P., & Ihde, A. (2018). Laminated Glass Connection Details: Towards Homogeneous Material Joints in Glass.

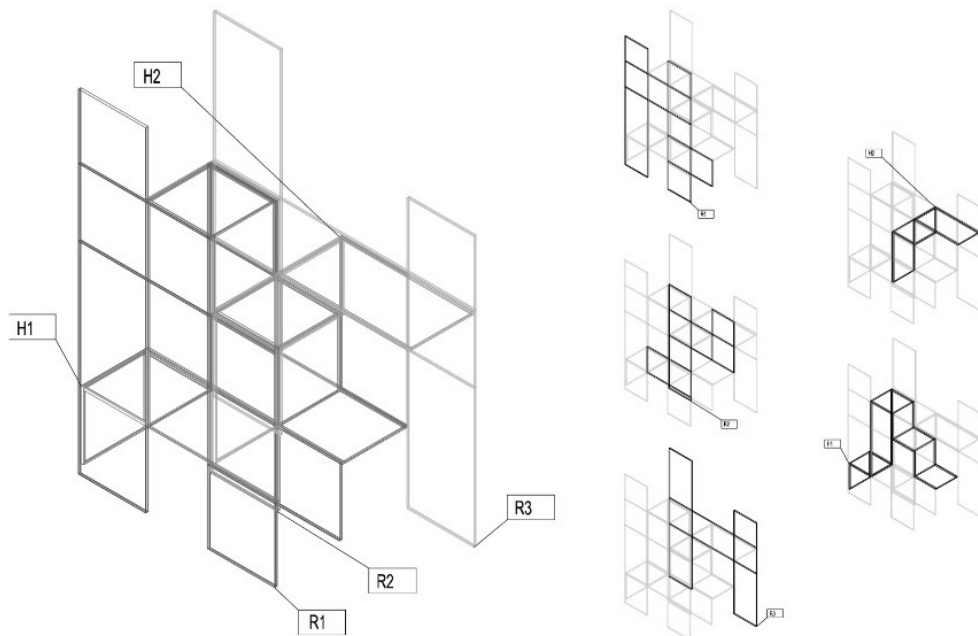


Figure 53 Components of the prototype. Source: Eversmann, P., & Ihde, A. (2018). *Laminated Glass Connection Details: Towards Homogeneous Material Joints in Glass*.

- **Additional Insights**

Sensitivity Analysis Using FEM:

The use of Finite Element Method (FEM) sensitivity analysis to evaluate the performance of the glass-dovetail connection under different scenarios. This analysis is crucial for understanding how small variations in the system's design can significantly impact its overall structural behavior.

Technical Challenges and Solutions:

The document outlines several technical challenges encountered during the design and fabrication processes, such as dealing with fabrication tolerances and the problematic excess of polyvinyl butyral (PVB) foil. Solutions such as the use of acrylic distance elements to prevent direct contact during glass insertion are elaborated upon, showing the iterative problem-solving process integral to the project's success.

Potential for Scalability:

While the conclusion discusses the need for further research for larger-scale applications, the article also subtly indicates the potential scalability challenges due to the weight and manoeuvrability of glass structures. These aspects hint at the practical limitations and considerations that need to be addressed to transition from prototype to full-scale applications.

- **Conclusion**

The Glass-dovetail connection, enhanced using PVB for bonding and acrylic sheets for protective distancing, represents a significant advancement in glass connection technology. This approach not only improves the structural performance of glass assemblies but also aligns with modern architectural demands for durability, safety, and aesthetic transparency. The integration of these materials into the connection design illustrates a deep understanding of material properties and their implications for structural design and application, making it a pioneering solution in the field of architectural glass.

2. Funicular Glass Bridge Prototype Design Optimization, Fabrication, and Assembly Challenges

In architectural design and engineering, graphical statics have progressed from basic 2D methods to more advanced 3D systems that can handle complex shapes and force distributions. This study investigates Polyhedral Graphic Statics (PGS) as an advanced method for designing funicular structures, using the flat shapes of polyhedral geometries to effectively use flat materials like glass in construction. The research builds on earlier efforts to combine architectural use with the structural capabilities of glass, focusing on modular hollow glass units (HGU) that are built for compression-only setups (Lu et al., 2022).

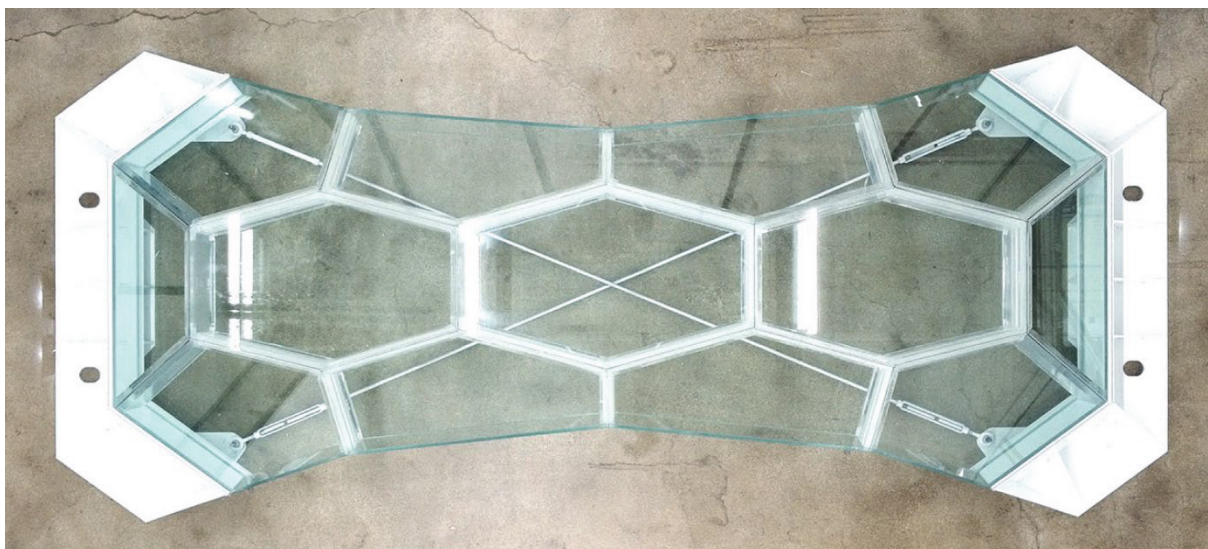


Figure 54: 3m-Span Modular Glass Pedestrian Bridge. Source: Lu, Y., Seyedahmadian, A., Chhadeh, P.A., Cregan, M., Bolhassani, M., Schneider, J., Yost, J.R., Brennan, G., & Akbarzadeh, M. (2022). Funicular glass bridge prototype: Design optimization, fabrication, and assembly challenges. *Glass Structures & Engineering*. <https://doi.org/10.1007/s40940-022-00177-x>.

- **Form-Finding Process:**

Initial Setup: The process starts with a 2D aggregation of polygonal faces that establishes the topology and load distribution of the bridge structure. This setup is fundamental for understanding how the forces will be distributed across the bridge.

3D Extrusion: These faces are extruded to a point, creating a set of 3D force polyhedrons that determine the spatial form of the bridge. The height of the extrusion influences the arch of the bridge and the internal force distribution, which is crucial for achieving a funicular form that naturally directs loads through compression.

Double-Layer Form Generation: A double-layer bridge form is derived by subdividing the force polyhedrons of the single-layer diagram. Each closed polyhedron cell in this model is destined to be fabricated as a hollow glass unit (HGU).

- **Optimization Techniques:**

Dimensional Adjustments: Modification to global dimensions and individual edge lengths are made to meet fabrication constraints and enhance practical assembly. Vertex and edge length constraints are strategically set to optimize the bridge's geometry.

Face Angle Adjustments: Face angles are tuned to maintain planarity and equilibrium, crucial for ensuring that the bridge's load paths are efficient and stable. This adjustment is facilitated by altering their dual elements in the force diagram.

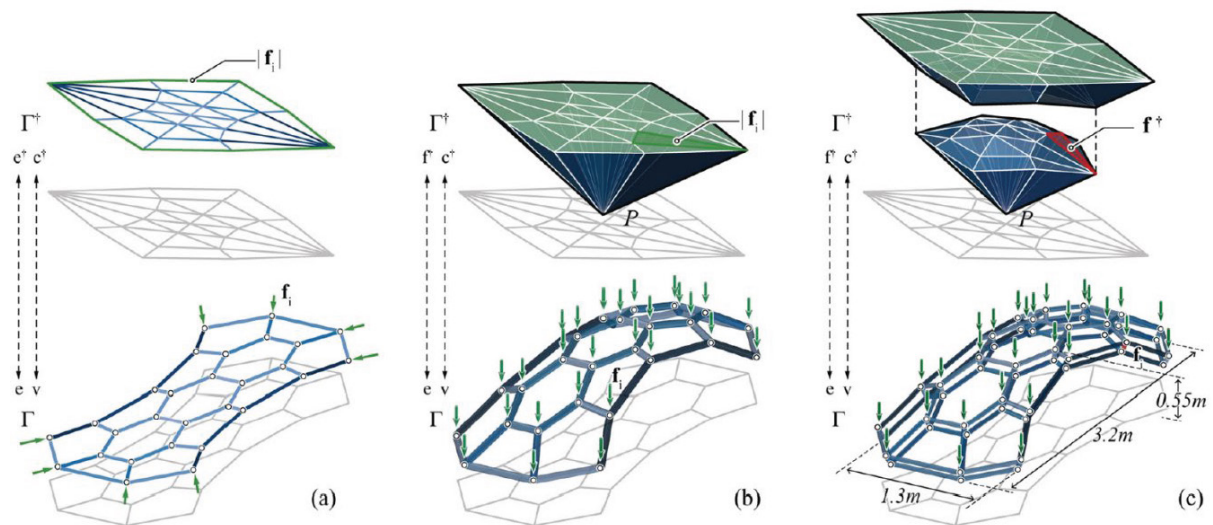


Figure 55: The form-finding process. a the 2D aggregation of polygons as force diagram and its reciprocal 2D form diagram; b the extruded polyhedrons as force diagram and its reciprocal 3D single-layer form diagram; c the further subdivided polyhedrons as force diagram and its reciprocal 3D double-layer form diagram. Source: Lu, Y., Seyedahmadian, et al. Funicular glass bridge prototype: Design optimization, fabrication, and assembly challenges. (2022)

- **Detailed Focus on Connections and Joints, Materialization Strategy and Fabrication**

The hybrid data structure of PolyFrame:

Utilizing this data management method facilitates complex geometrical modeling, crucial for translating design intent into manufacturer components.

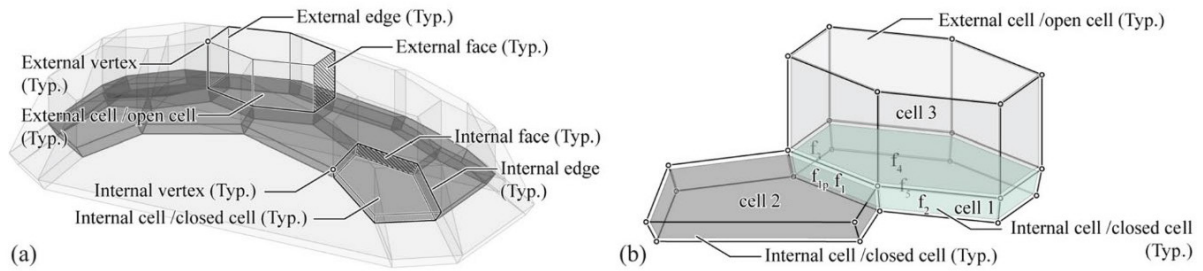


Figure 56: a The form diagram of the glass bridge that shows the four levels of geometrical and topological information, and only internal cells will be materialized as HGUs; b The geometrical information of face f_1 such as area, centroid, and plane can be computed based on its four corner coordinates. The topological information can also be easily queried, such as face pair (f_{1p}), all connected faces in the same cell (f_2, f_3, f_4, f_5)

Hollow Glass Units (HGUs):

Each HGU is crafted from annealed glass and acrylic, with top and bottom faces made from 9.5 mm glass, and side faces varying between glass and 21 mm acrylic depending on structural needs. The HGUs incorporate a butterfly locking mechanism to enhance stability by minimizing relative movements between units.

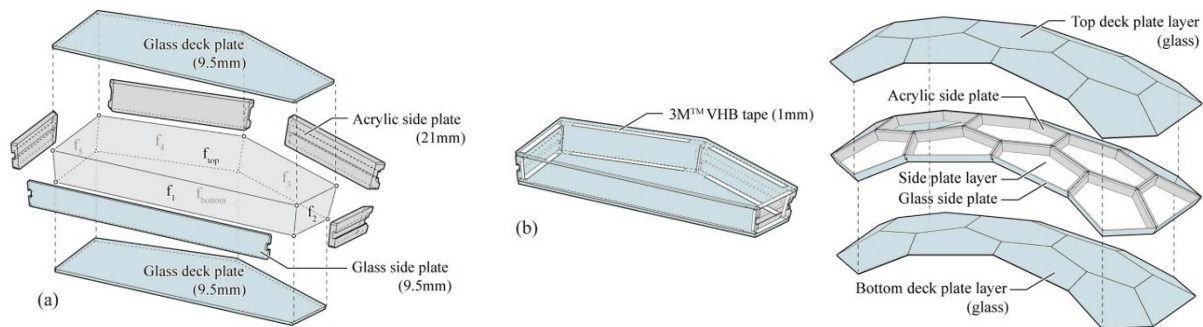


Figure 57: Left, A typical closed cell materialized as an HGU. a the top face top and bottom face bottom are materialized as deck plates; the "naked" side face f_1 is materialized as a glass side plate; all other faces are materialized as acrylic side plates; b All deck plates and side plates are bonded with 3 M™ VHB tape. Right, the top and bottom deck plates form two continuous layers and serve as the primary load transfer elements

Fabrication Techniques:

Advanced fabrication techniques, including 5-axis water jet cutting and CNC milling, are employed to achieve precision in shaping glass components, demonstrating the integration of traditional materials with modern manufacturing processes.

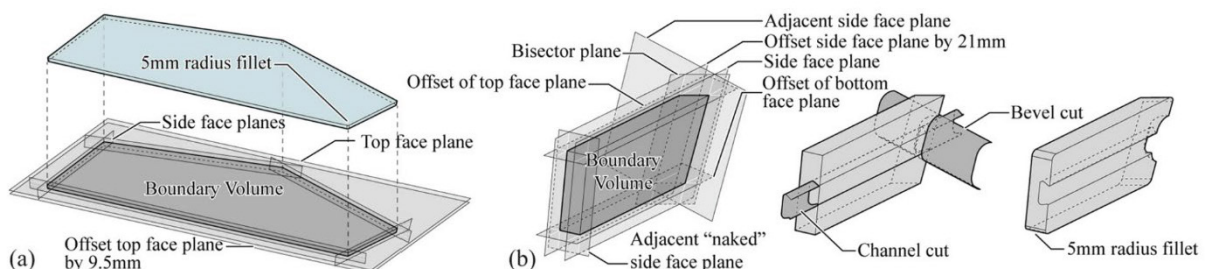


Figure 58: The geometries of deck plates and side plates are generated using planes. a The generation of a typical glass deck plate; b the generation of a typical acrylic side plate

Butterfly Locking Mechanism:

This specific joint design is crucial for maintaining the structural integrity of the bridge. The butterfly-shaped locking strip fits into pocket channels milled into the acrylic side plates of the HGUs. This design enhances the connection strength between units, effectively distributing loads and minimizing relative movements between them. The mechanism is designed to be robust enough to handle expected loads while also being simple enough to allow for easy assembly and disassembly.

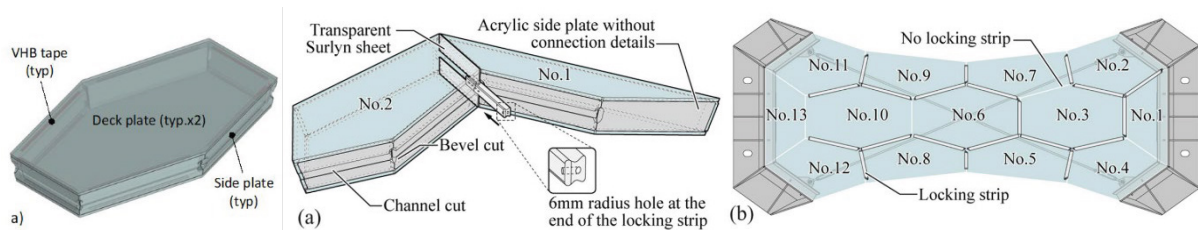


Figure 59: a A typical connection between two HGUs; b Assembly sequence and corresponding locations of the locking strips

Interface Materials:

The use of Surlyn sheets as interface materials between glass-to-glass and glass-to-other materials (like steel or acrylic) is a critical detail that prevents stress concentrations that could lead to cracking or breakage. These sheets act as soft, protective layers that absorb stresses and prevent direct contact, enhancing the durability and longevity of the glass units.



Figure 60: A locking strip is inserted into the channels of two neighbouring HGUs

• Structural Analysis

Finite Element Analysis:

Using ANSYS software, the structural integrity of the bridge under various load conditions is validated. This analysis is critical for testing the effectiveness of the butterfly locking mechanisms and ensuring the bridge's overall stability and safety under operational loads.

Results:

The analysis confirms that the bridge design can support its own weight with minimal deformation, validating the structural feasibility of using glass as a primary load-bearing material in modular construction.

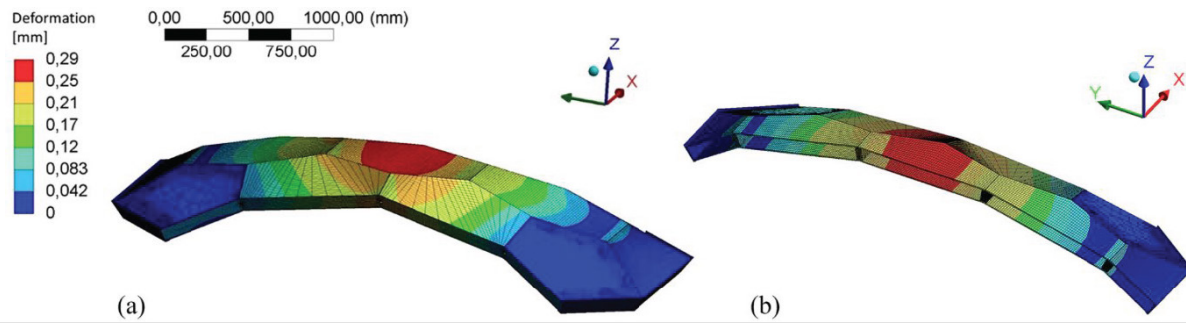


Figure 61: a the finite element model of the bridge under dead load with the total Deformation color-coded in [mm]. b the section view

• Assembly Process

Assembly Specifics:

The modular nature of the bridge is highlighted by the assembly process, where individual HGUs are precisely bonded using 3M™ VHB tape, a high-strength, doublesided adhesive that facilitates strong, durable, yet reversible connections. This choice of adhesive plays a significant role in the modular and temporary nature of the construction, allowing for future disassembly and reassembly if needed.

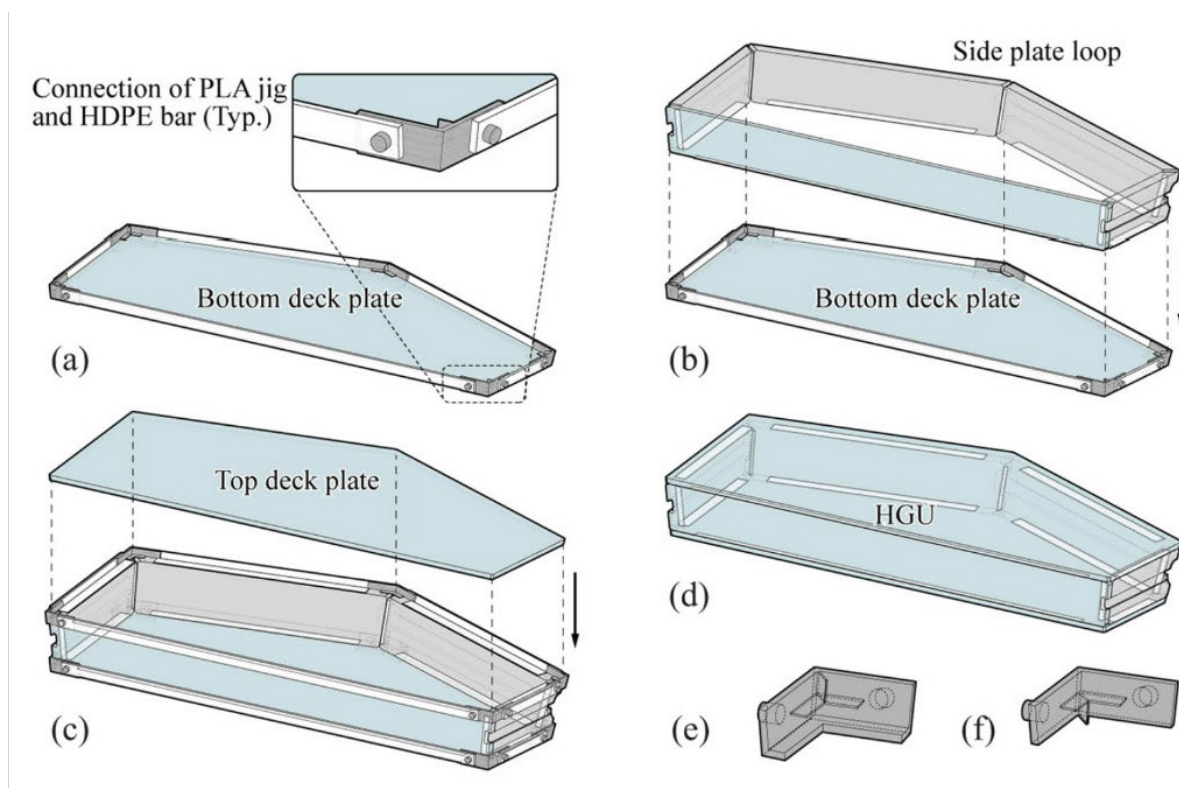


Figure 62: a The bottom deck plate and the bottom hoop of PLA jigs and HDPE bars; b all side plates are connected into a side-wall loop, then bonded to the bottom deck plate; c place the top hoop of PLA jigs and HDPE bars, and place the top deck plate into the hoop; d remove all PLA jigs and HDPE bars; e a typical bottom jig; f a typical top jig

Overall Bridge Assembly:

The bridge is assembled from individual HGUs, emphasizing the modular nature of the design. This modular approach facilitates single-person assembly without heavy machinery, showcasing an innovative construction method that can be easily replicated or adapted for other structures.

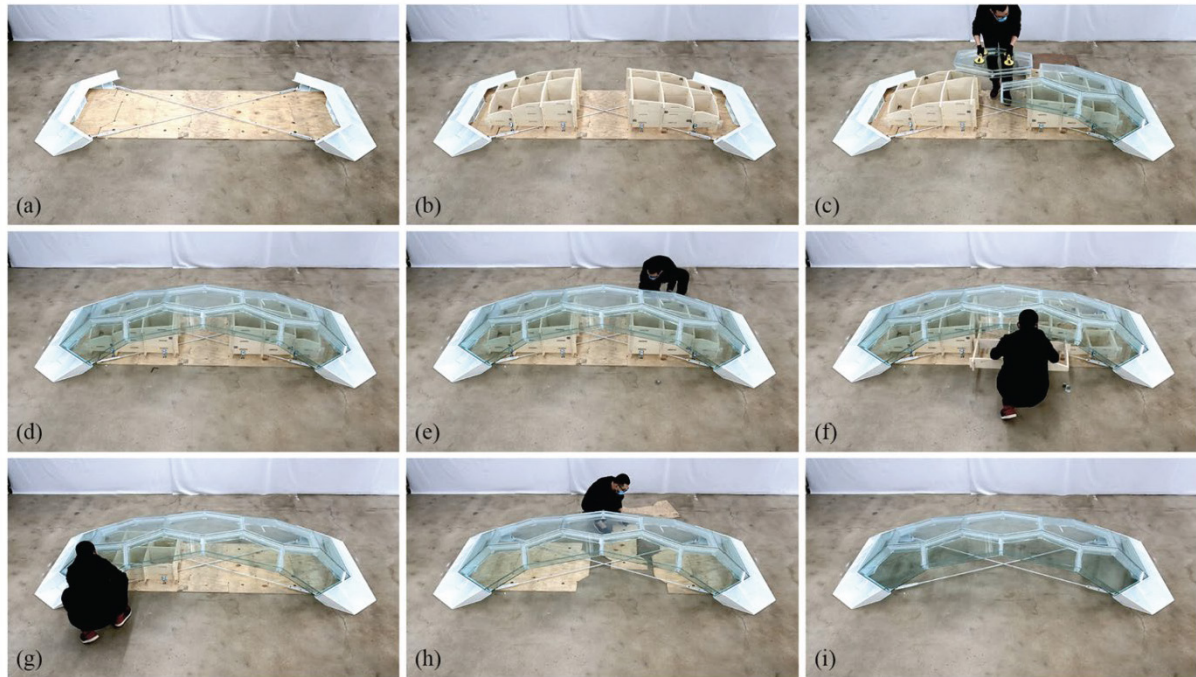


Figure 63: a Use plywood panels to locate the steel abutments; b place the falsework on the plywood panels; c, d put HGUs on the falsework; e turn the leveling feet and lower the falsework; f remove the middle layer of the falsework; g remove the other parts of the falsework; h remove the plywood panels; i completed glass bridge the Pnite element model of the bridge under dead load with the total Deformation color-coded in [mm]. b the section view of the Pnite element model

3. Zaryadye Park Glass Grid Shell Roof

The study by Gennady Vasilchenko-Malishev and S. Chesnokov meticulously describes the design, detailing, testing, and construction processes of the structural glass beams that form the Zaryadye Park's glass grid shell roof in Moscow. This pioneering structure is situated near Red Square and integrates 72 structural glass beams into a main undulating steel grid shell, showcasing a novel approach to architectural design and engineering under challenging conditions.

- **Design and Material Fabrication**

The Zaryadye Park Glass Grid Shell Roof, as described in the studies and construction details, does utilize modular components, but these are not strictly uniform in size across the entire structure. The design includes 72 structural glass beams that are each laminated from layers of toughened glass and connect at stainless steel nodes to support triangular glass

panels. This modular approach allows for the construction and assembly of complex curved shapes that form the undulating roof structure.

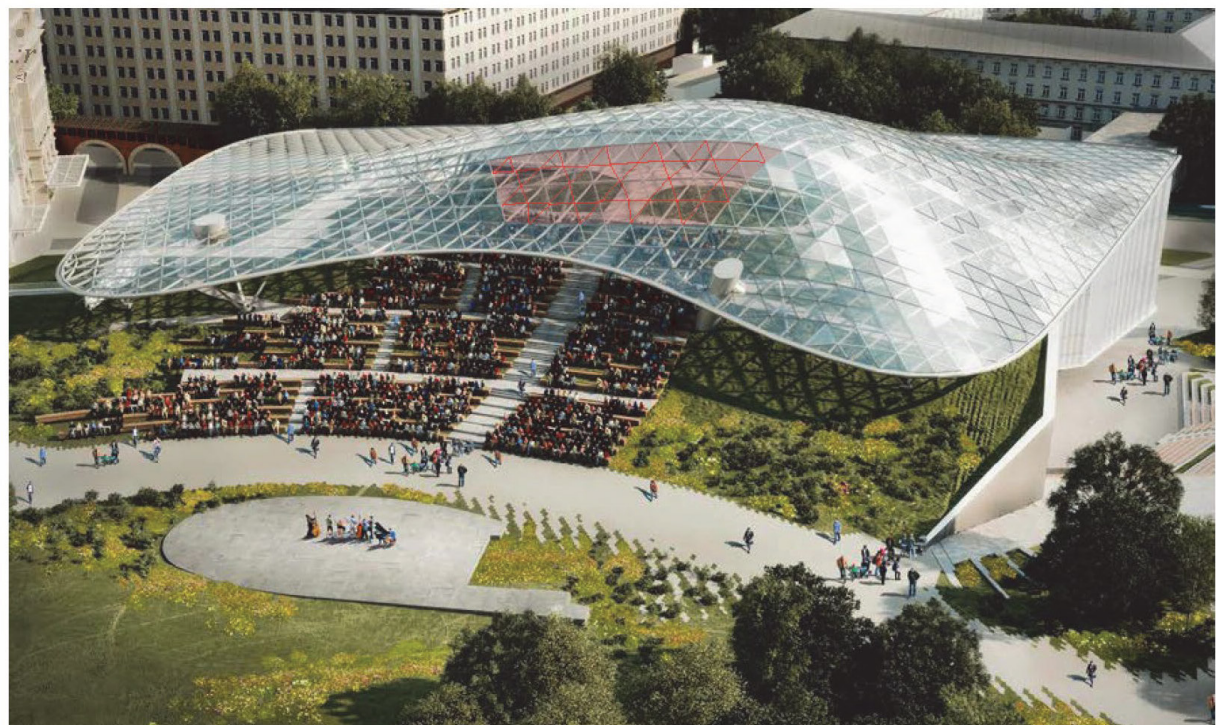
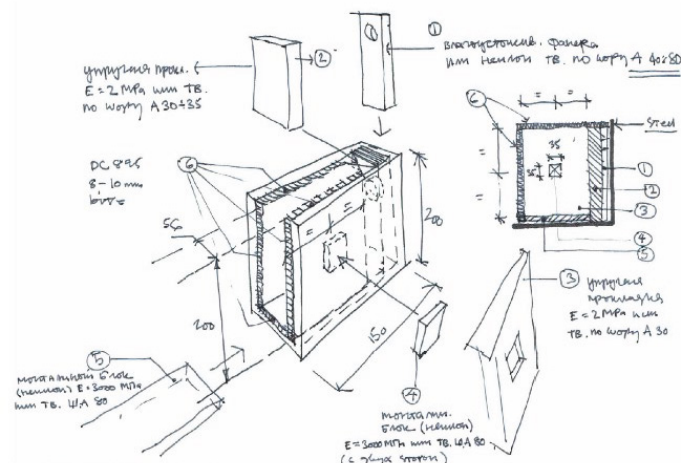


Figure 64: General view of the canopy with area in question highlighted in red. Source: Vasilchenko-Malishhev, G., & Chesnokov, S. (2018). Zaryadye Park Glass Grid Shell Roof. In *Challenging Glass 6 – Conference on Architectural and Structural Applications of Glass* (Louter, Bos, Belis, Veer, & Nijse, Eds.), Delft University of Technology. DOI: 10.7480/cgc.6.2196

The design of the glass grid shell roof was tailored to accommodate Moscow's harsh weather conditions, incorporating structural glass beams laminated from five layers of 10mm toughened glass with a 1.5mm Trosifol PVB interlayer for enhanced durability and stability. The beams, typically 3 meters in length and 0.2 meters deep, converge at custom-designed stainless-steel nodes, supporting triangular glass roof panels above.

While the basic concept involves repeating units—like the beams and nodes—the actual size and shape of the glass units may vary to accommodate the roof's complex geometry and the specific structural and aesthetic requirements of different sections of the roof. The design's modularity lies more in the concept of repeatable components and connection methods rather than in uniformity of size and shape across all units.

The adaptability of this modular system, with its reliance on sophisticated engineering and materials science, showcases how modern architecture can achieve visually striking results through the strategic use of modular components.



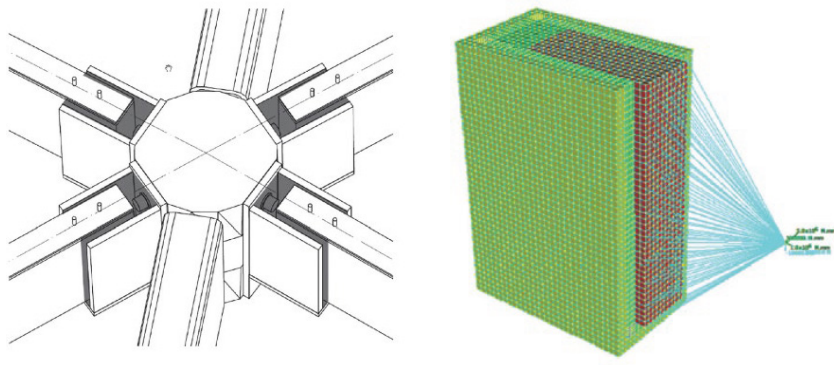


Figure 65: Detailing of the Silicone Connections, Typical joint detail (left), Brick Model of the Silicone Connections (Right). Source: Vasilchenko-Malishev, G., & Chesnokov, S. (2018). Zaryadye Park Glass Grid Shell Roof.

• Structural Analysis and Methodology

The analysis was complex due to the variable lengths of the beams and the intricate geometry of the shell. The team employed a sophisticated linear analysis approach involving over 150 load combinations to simulate the differential movements of the structure. This was crucial in refining the design of the nodal connections and ensuring the structure could withstand snow loads of up to 350 kg/m^2 without compromising on aesthetic integrity or visibility.

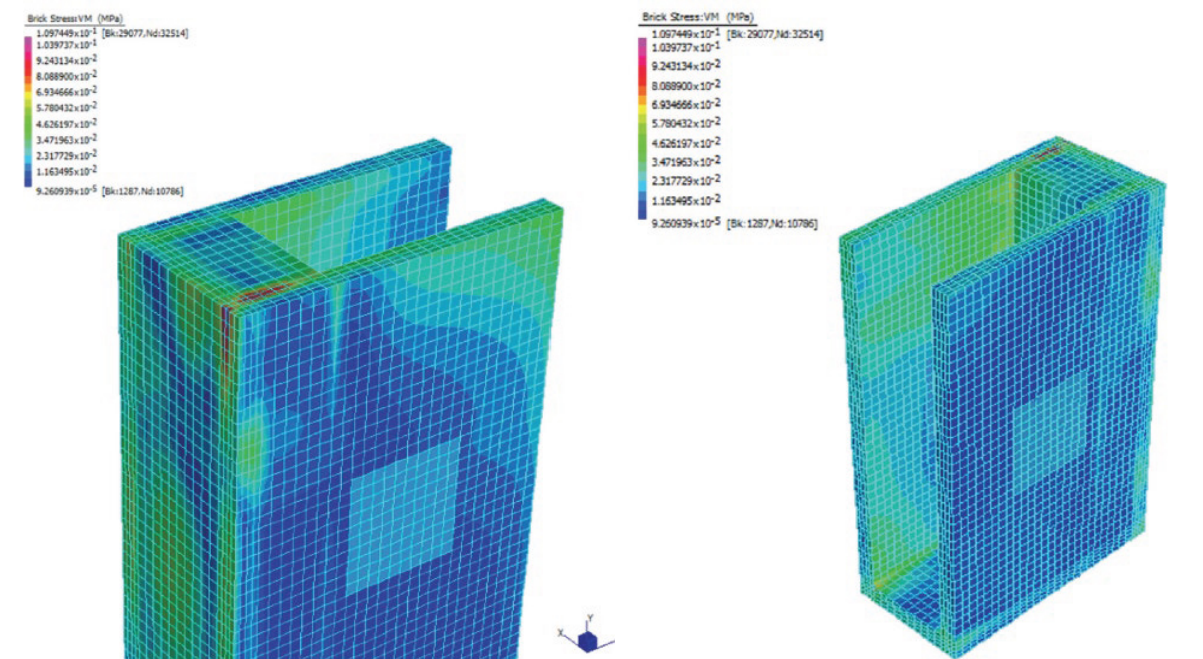


Figure 66: left, Stress in the silicone from the Connection Forces. Right, Peak Stresses in the Silicone. Source: Vasilchenko-Malishev, G., & Chesnokov, S. (2018). Zaryadye Park Glass Grid Shell Roof.

• Testing and Construction Challenges

One of the key challenges was the lack of existing legislation in Russia for structural glass. This gap necessitated the creation of a 'Special Technical Standard', which the team developed to address the technical specifications and performance criteria for the glass used. A full-scale mock-up of one roof panel was constructed and subjected to rigorous testing to validate the design before final construction, ensuring compliance with the newly established standards.

- **Connections and Joints**

The detailing of connections was particularly critical in this project. Originally designed to accommodate bolted connections, the final design required more flexibility to adapt to thermal expansion and structural movements. This led to the implementation of structural silicone (Dow Corning 895) for its flexibility and durability, which was essential for the connections between the glass beams and the steel nodes.



Figure 67: Zaryadye Park, Glass Grid Shell Roof. Source: Vasilchenko-Malishev, G., & Chesnokov, S. (2018). Zaryadye Park Glass Grid Shell Roof.

- **Local Analysis and Results**

The local analysis highlighted the need for silicone brick models to thoroughly understand the stress distributions within the connections. Finite Element Analysis (FEA) models were used to predict and optimize the performance of the silicone joints under various load cases, confirming that the stresses remained within safe limits under all scenarios, as stipulated by the Special Technical Standards.

4. Design Base for a Frameless Glass Structure Using Structural PVB Interlayers and StainlessSteel Fittings

This study by Stevels et al. (2022) addresses the challenge of increasing transparency in grid shell designs by minimizing or entirely eliminating metallic primary structures. By employing glass itself to bear loads, primarily through membrane forces, the study explores the structural potentials of glass in compression-only shell structures like domes and free-form shapes. This approach reduces tensile forces, crucial given glass's sensitivity to breakage under tension.

- **Methodology**

The research investigates modular glass structures that are structurally connected to address practical considerations such as safety, dimensions, weight, and assembly challenges. The study reviews various elements of modular glass construction, including joint patterns and load bearing behavior, through previous research by Blandini (2005), Bagger (2010), and Fildhuth et al. (2012a, b).



Figure 68: Photography of the assembled frameless glass structure. Source: Stevels, W., Fildhuth, T., Wüest, T., Haller, M., & Schieber, R. (2022). Design Base for a Frameless Glass Structure Using Structural PVB Interlayers and Stainless-Steel Fittings. Challenging Glass Conference Proceedings, 8, 369. <https://doi.org/10.47982/cgc.8.369>

- **Design Aspects, Connection and Joints**

Structural Interlayers: Discusses the use of structural interlayers in designing transparent glass structures where the mechanical properties of glass are maximized. A public demonstrator built with Saflex® Structural PVB interlayer is highlighted to show practical feasibility.

Stainless Steel Fittings: Connections are facilitated by stainless steel fittings embedded within the glass layers, structural PVB, focusing on their design to reduce stress peaks and provide rotational stiffness.

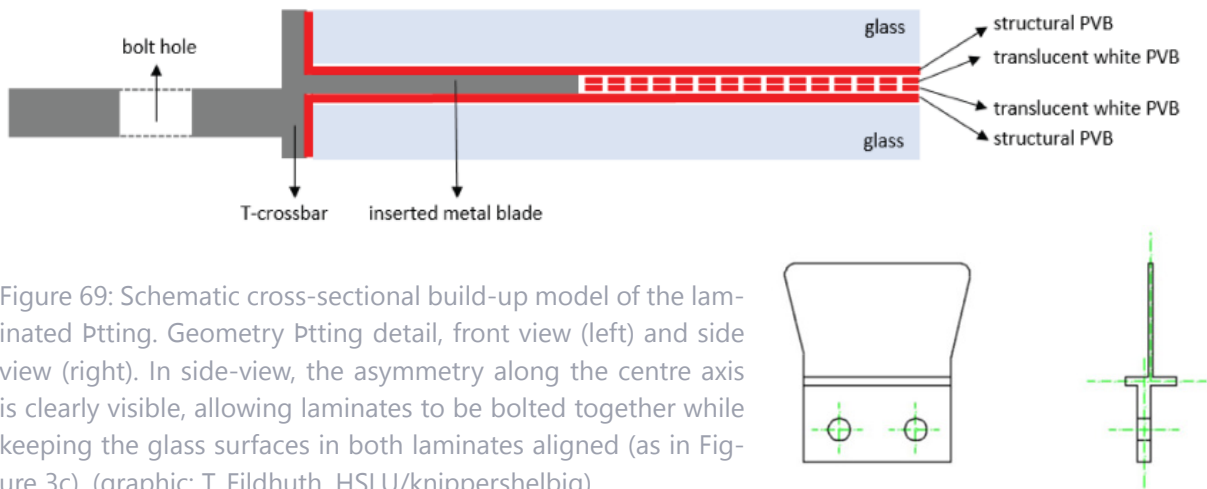


Figure 69: Schematic cross-sectional build-up model of the laminated Ptting. Geometry Ptting detail, front view (left) and side view (right). In side-view, the asymmetry along the centre axis is clearly visible, allowing laminates to be bolted together while keeping the glass surfaces in both laminates aligned (as in Figure 3c). (graphic: T. Fildhuth, HSLU/knippershelbig)

Design Challenges: The challenge in the connection design is ensuring that these joints can handle both the structural load and environmental factors without compromising the integrity of the glass or the clarity of the structure.

Fabrication Process: The glass is precision-cut and prepared for lamination in a controlled environment. The stainless-steel fittings are embedded within the glass layers during the lamination process, which involves careful alignment and bonding under heat and pressure to ensure complete integration.



Figure 70: Different views of the laminated Ptting: top view at angle (left), top view perpendicular (center) and side view (right) for specimen with Ptting on short edge.

• Assembly Process

Modular Design: The structure is designed in a modular fashion, allowing for on-site assembly with minimal heavy machinery. Each module is prefabricated and designed to interlock with adjacent modules, simplifying the overall construction process.

Handling and Installation: Special consideration is given to the handling and installation process to prevent any damage to the glass modules. Techniques for safe lifting, positioning, and securing of the glass panels are developed to ensure smooth on-site assembly.

- **Structural and Safety Concepts**

The frame less glass structure is conceptualized as a fully glass, **double-curved modular shell**. The design focuses on minimizing long-term tensile membrane forces, favoring compressive forces primarily due to dead loads, while addressing the discontinuities at joint gaps and the impact of asymmetric loads. The safety concept incorporates three pillars:

Compressive Membrane Forces: The structure supports permanent loads mainly via compressive forces, minimizing creep effects in the bond between interlayer and fittings under tensile load.

Ductile Fitting Behavior: The fittings exhibit ductile behavior before failure, showing significant non-linear deformation without complete failure, which adds to the safety.

Global Redundancy: The structure provides redundancy, allowing load redistribution among intact connections in case of joint failure.

- **Structural Analysis**

Finite Element Analysis (FEA): Advanced computational methods are used to simulate the structural behavior under various loading conditions. This analysis helps in refining the design by predicting how different components react to stress and identifying potential points of failure.

Load Testing: The fittings and joints undergo rigorous load testing to verify their capacity to sustain expected loads. These tests include tensile, compression, and shear tests, providing a comprehensive understanding of the structural integrity.

- **Results and Discussion**

Performance of PVB Interlayer: The structural analysis confirms that the PVB interlayers perform well under compression, significantly contributing to the structure's stability. The viscoelastic properties of the PVB ensure that it can handle long-term loads without significant deformation.

Adhesion and Mechanical Strength: Results from adhesion tests indicate excellent bonding between the glass and PVB, as well as between PVB and stainless-steel fittings. Mechanical tests demonstrate that the connections can withstand the applied loads without failure, providing a safe margin above the expected maximum loads.

Safety and Redundancy: The design incorporates several safety features, including redundancy in the connection design, allowing the structure to redistribute loads effectively in the event of a component failure. This redundancy is crucial for ensuring the safety and longevity of the structure.

- **Experimental Setup and Results**

Dynamic Mechanical Thermal Analysis (DMTA) Results:

Objective: To assess the viscoelastic properties of the PVB interlayer.

Findings: The experiments demonstrated that PVB's stiffness and damping characteristics change with temperature, confirming its suitability for use in varying climates due to its elastic and viscous behavior.

Adhesion Results from Compressive Shear Tests

Objective: To measure the adhesion between the structural PVB interlayers and the glass.

Findings: Tests showed high levels of consistent adhesion, crucial for the structural integrity and performance of the glass panels.

Mechanical Test Results on Laminated Fittings

Objective: To evaluate the structural performance of embedded fittings under tensile, bending, shear, and creep loads.

Findings:

- **Tensile and Bending:** Fittings withstood significant forces, essential for structural stability.
- **Shear Performance:** Demonstrated effective lateral resistance, important for joint integrity.
- **Creep Behavior:** Showed acceptable deformation over time, ensuring long-term durability.

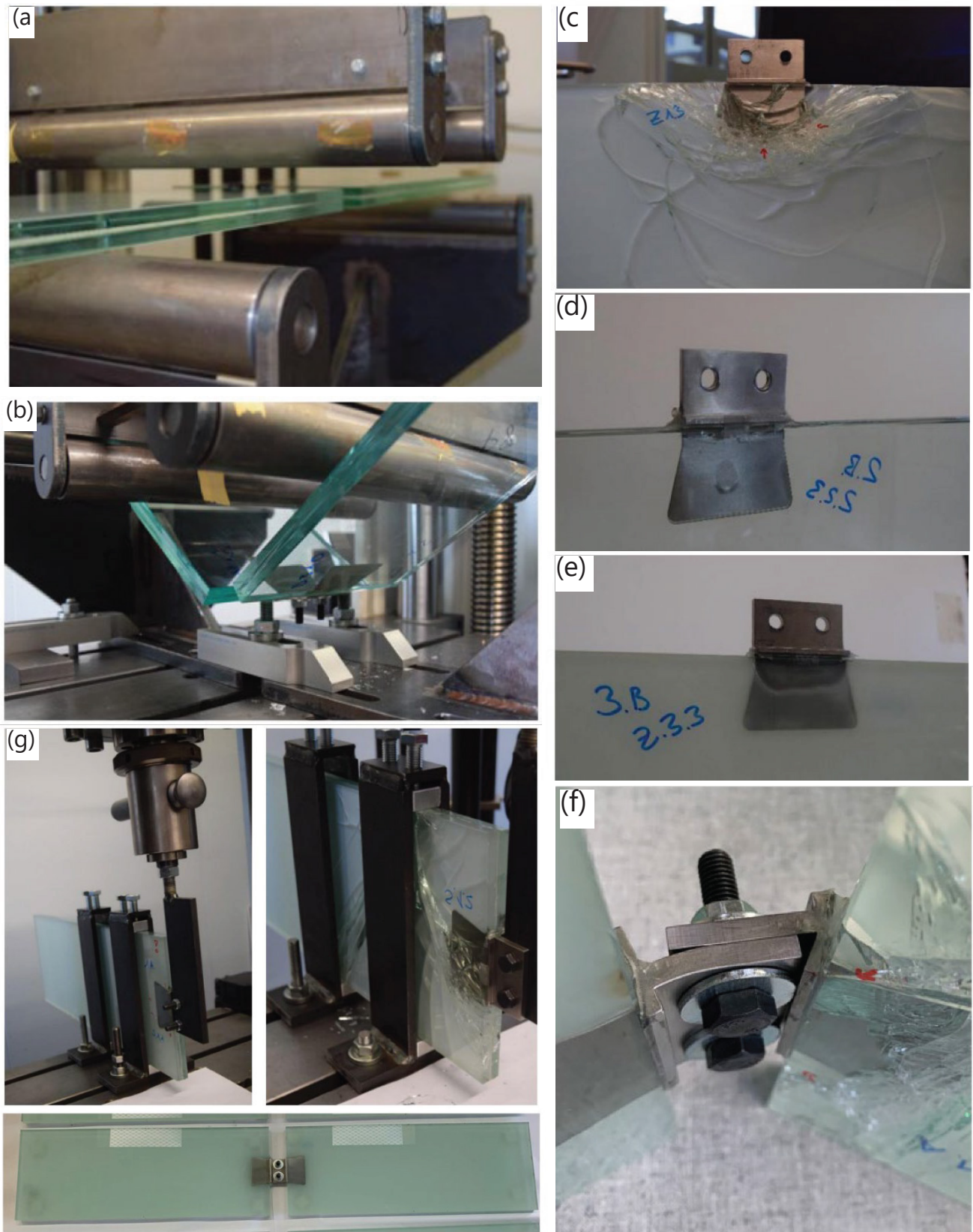


Figure 71: bottom left: assembled "butterfly-specimen" for bending test; a) planar specimen prior to test start in set-up; b) deformed specimen during test. Typical failure patterns for the three different interlayer configurations used c) glass breakage mixed stack; d) delamination in structural PVB at high force from cavitated origin; e) delamination front translucent white PVB interlayer f) Detail of failed specimen in bending mode post testing. Large deformation of the fitting occurred prior to glass breakage. G) Set-up of the shear test prior to displacement (left); failed configuration with typical crack pattern originating from glass edge.

5. Technoledge in Glass Structure course - TU Delft - "Glass Quarry Exhibit Hall"- Group project of this Author

The "Glass Quarry Exhibit Hall" project, spearheaded by Minoo Motedayen and team (Swornava Guha and June Choi), epitomizes the intersection of architectural ingenuity and engineering precision. The overarching concept of this project was inspired by dinosaur skin, translated architecturally into a triangular shell structure for a museum roof, melding transparency and visibility with structural integrity.

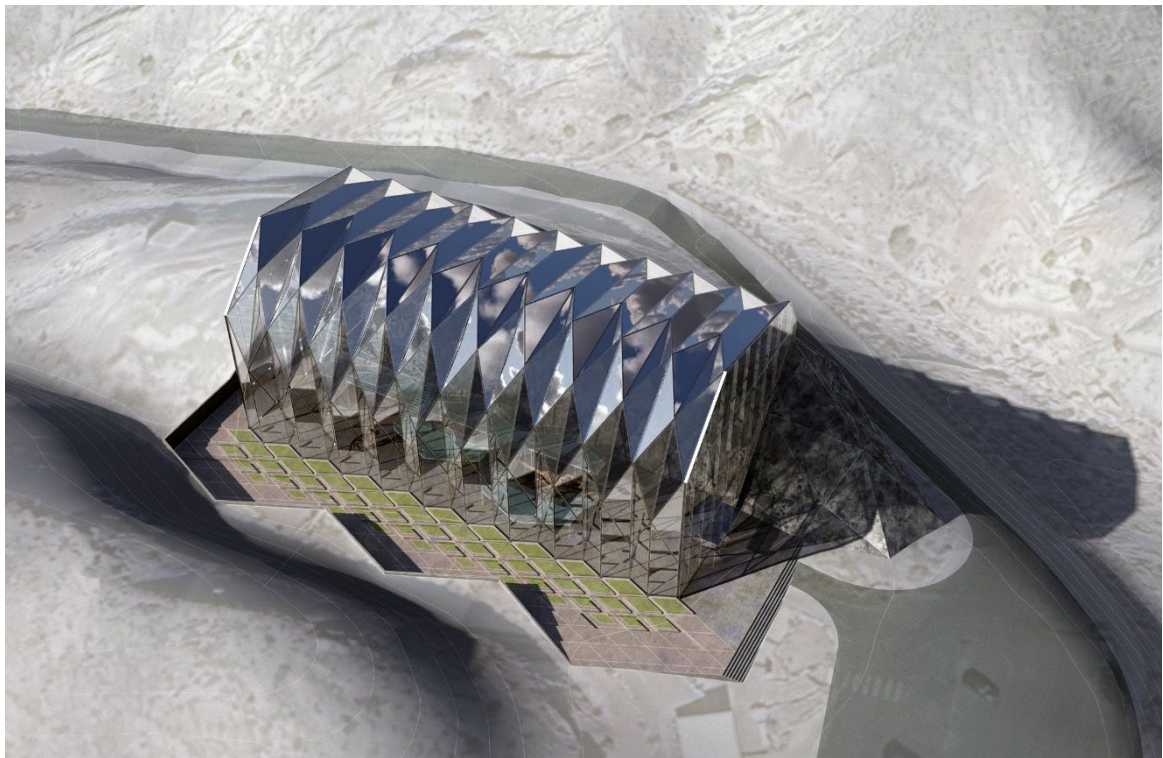


Figure 72: Render from the Technoledge in Glass Structure course - TU Delft - "Glass Quarry Exhibit Hall"-
Group project of this Author

- **Design Development**

Concept and Vision: The design germinates from an in-depth analysis of dinosaur skins, transformed into sketches that culminate in a triangular shell structure. The design aims for overwhelming transparency and visibility, echoing the textures and forms found in nature.

Evolution: The project leverages origami principles, particularly the Yoshimura pattern, known for its stability and capability to distribute stress uniformly. This stability is pivotal in supporting the structural integrity required for the museum's roof.

Drawings and Visualization: Detailed architectural drawings and visualizations are crafted to illustrate the proposed structure's aesthetic and functional attributes, providing a clear vision of the final construct.

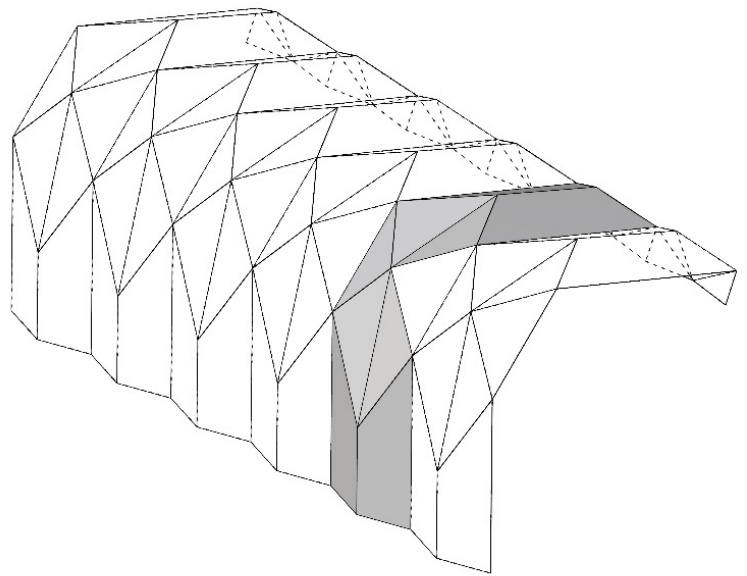
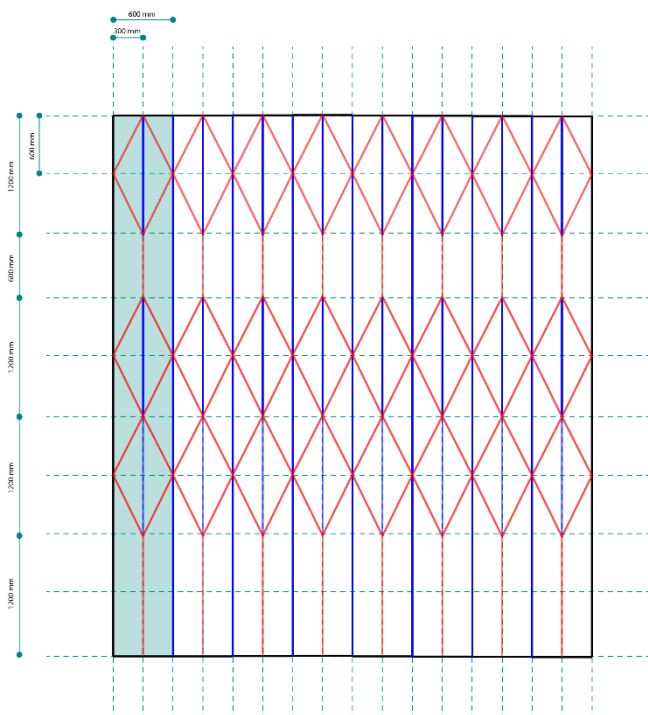


Figure 73: right, Full Yoshimura origami pattern.
Left, Crease of fold (Revised Yoshimura Pattern)

- **Component Size and Climate Adaptation**

Climate Analysis: A comprehensive climate analysis using EPW data and the Ladybug plugin in Grasshopper helps tailor the glass panels to the local environment, focusing on minimizing energy consumption while enhancing the structure's responsiveness to snow and wind loads.

Glass Sizing and Types: The project explores various glass types, settling on heat-strengthened glass for its superior load-bearing capabilities. Innovations like "Ipachrome" coating are integrated to adjust the glass tint dynamically, enhancing energy efficiency and occupant comfort.

- **Assembly and Structural Integration**

Connection Design:

The design includes innovative connections that facilitate the assembly and stability of the structure. The connections are engineered to support the structural loads efficiently while being aesthetically minimal. To reduce the size of the steel profile we flipped the hinge so it could be bolted to the glass. Furthermore, we revised the steel profile to T shape rather

than U shape to reduce the steel sticking out at the edge of glass panels. After assembling the hinge to the glass panels the aluminum capping is used to cover the edge. There are two rods in each hinge, one staying in place that hold two metals in place, and one movable rod that slides when the hinge moves. The center rods holds four metals in place and are bolted in site after finding the right angle. The place where six panels meet, there is a gap to protect the glasses from breaking and aluminum capping is used to cover the edges. The glasses are clamped in the foundation with L profile . And There is a vertical joint that connects two straight panels together since we have to split it in order to transfer.

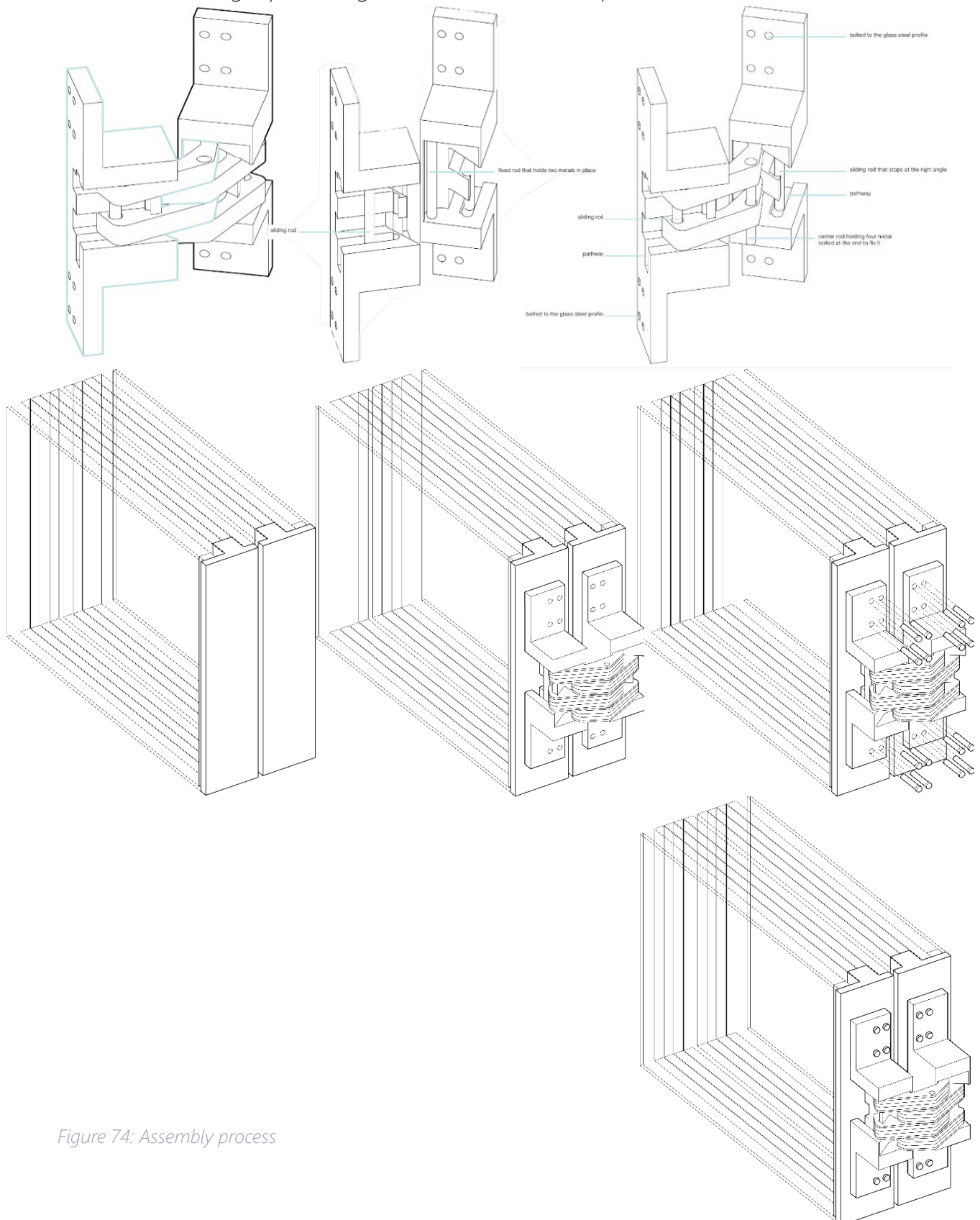


Figure 74: Assembly process

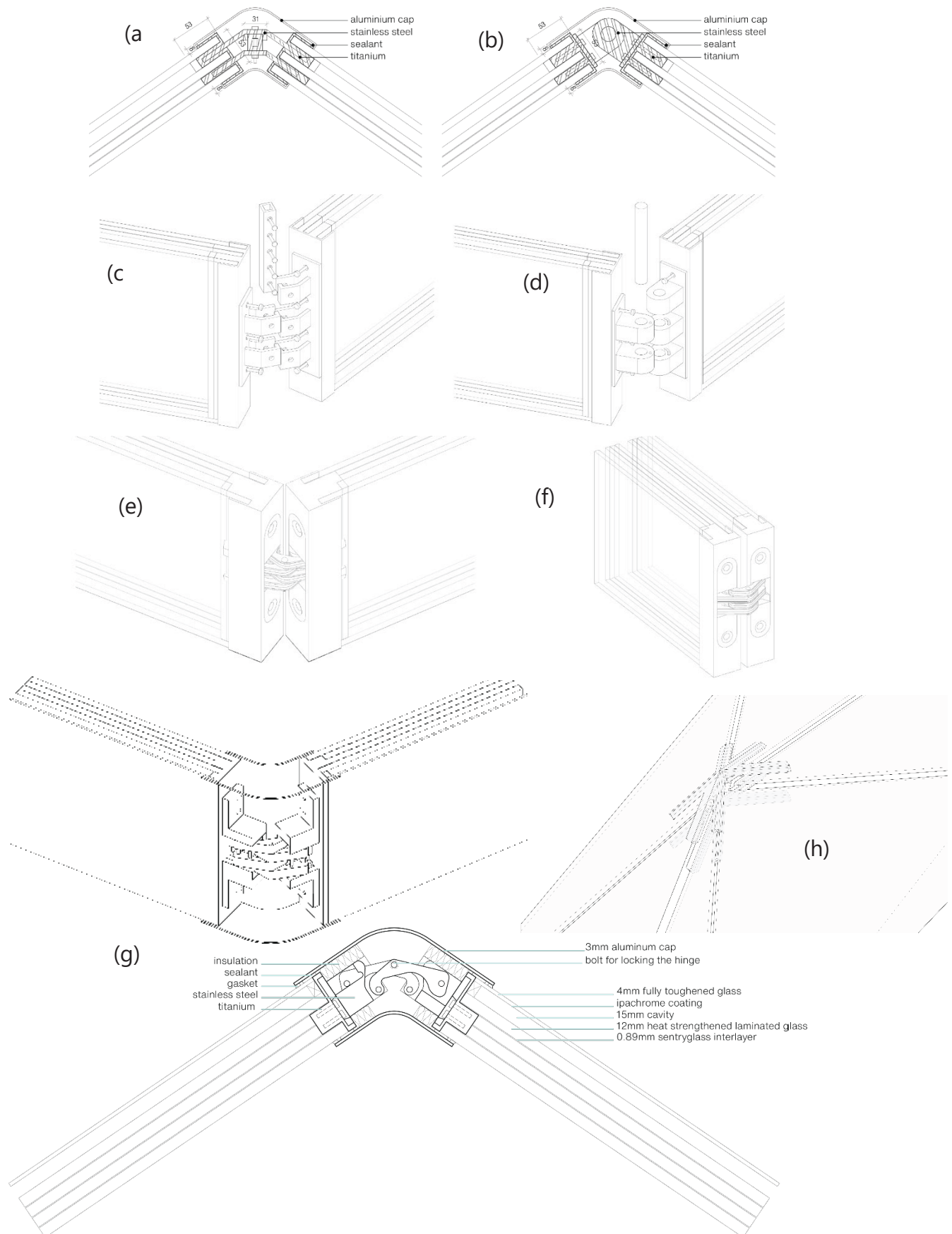


Figure 75: a) Initial fix connection, b) Initial fix connection in 3d, c) Second hinge connection when opened, d) 3D print of panel to panel connection, e) Initial hinge connection, f) Initial hinge connection in 3d, g) Open hinge connection with capping, h) Edge capping of vertexes where panels reach each other.

Assembly Order:

The structure's assembly is meticulously planned to ensure accuracy and efficiency. Panels are pre-manufactured and transported to the site where they are assembled using cranes and specialized hinges that allow for precise angle adjustments and robust structural connections.

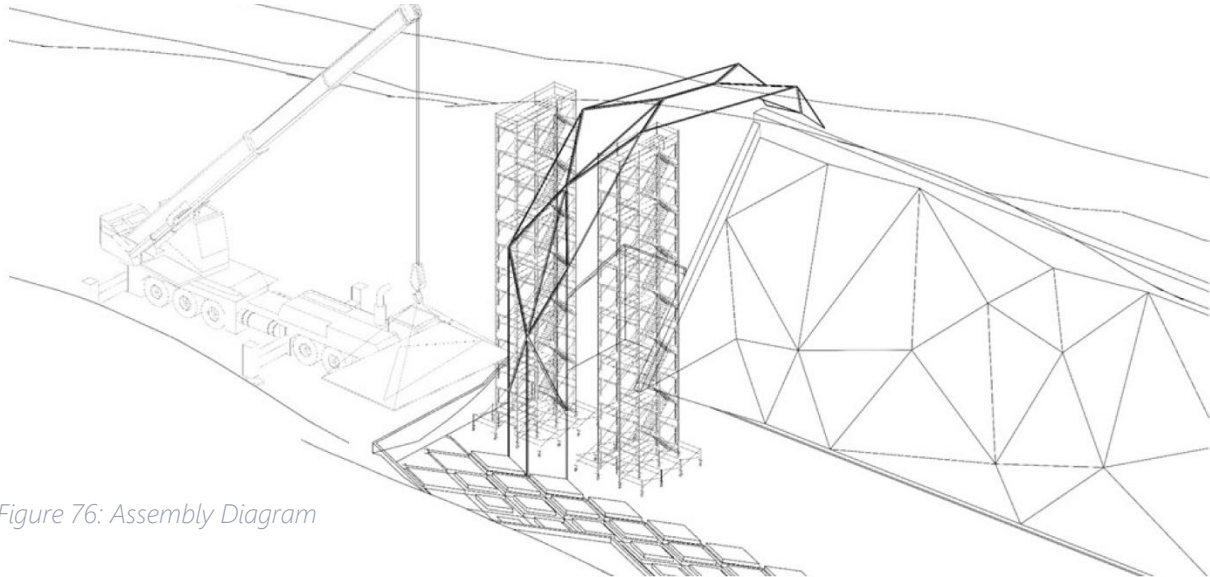


Figure 76: Assembly Diagram

- **Safety and Sustainability Analysis**

Risk Analysis: The project includes a detailed risk analysis considering potential environmental and physical impacts. Strategies are developed to mitigate these risks through design modification and physical measures.

Sustainability: Emphasis is placed on sustainability using thermally insulated glass units and low carbon construction methods. The structure aims to optimize energy usage and reduce environmental impact, reflecting modern sustainable design principles.

- **Structural Analysis and Optimization**

Load Path and Structural Analysis: Using Karamba, a thorough structural analysis is conducted to determine the load paths and optimize the structure's response to various forces. The analysis ensures that the structure can withstand predicted loads without significant deformation.

Karamba Optimization: Detailed parametric analysis and optimization are performed to finalize the structural dimensions and ensure maximum efficiency and safety. The final design effectively balances structural demands with architectural aesthetics.

- **Design Reflection:**

The team reflects on the design process, expressing satisfaction with the innovative approaches used and the final outcome. However, potential areas for improvement are identified, suggesting future exploration of alternative materials and more complex origami folds to enhance structural and thermal performance.

7.4. Intermediate Materials for Glass-to-Glass Contact

1. An Interlayer Material Study Towards Circular, Dry-Assembly, Interlocking Cast Glass Block Structures

This study by Dimas et al. (2022) investigates innovative approaches to interlocking cast glass block structures, focusing on transparency, reversibility, and sustainable material reuse. The research prioritizes evaluating various interlayer materials that facilitate both the assembly and disassembly processes, ensuring effective stress distribution across glass elements.

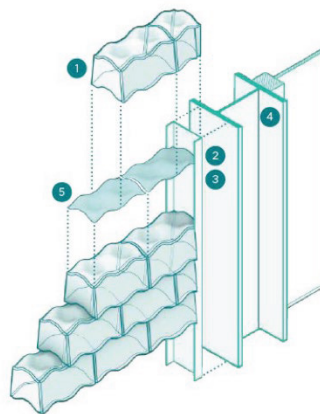
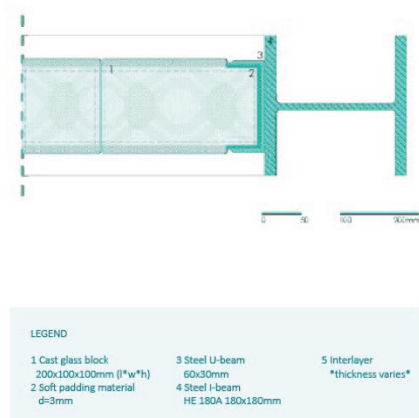


Figure 77: Side connection detail, plan and isometric. Source: Dimas, M., Oikonomopoulou, F., & Bilow, M. (2022). An Interlayer Material Study Towards Circular, Dry-Assembly, Interlocking Cast Glass Block Structures. *Challenging Glass Conference Proceedings*, 8. <https://doi.org/10.47982/cgc.8.416>

The researchers establish comprehensive criteria to assess the suitability of interlayer materials for use in interlocking cast glass block structures (Dimas, Oikonomopoulou, & Bilow, 2022). These criteria, derived from previous studies (Aurik, 2017; Oikonomopoulou, 2019b), are categorized into primary and secondary groups to ensure structural integrity and functional benefits:

- **Criteria for Material Selection**

Primary Criteria:

Ability to Be Shaped: Essential for materials to conform to the specific dimensions required by the design.

Compressive Strength: Must withstand structural loads without failure.

Stiffness: Optimally less stiff than glass to prevent system instability.

Creep Resistance: Critical to prevent deformation under prolonged stress.

Tear Strength: Necessary to maintain assembly integrity under mechanical stress.

Secondary Criteria:

Circularity and Recyclability: Supports the project's sustainability goals.

Optical Quality: Ensures materials do not compromise the required transparency.

Thermal Compatibility: Maintains similar expansion coefficients to glass.

Durability: Includes resistance to UV light, water, and fire.



Figure 78: Left: Typical Y breaking pattern, originating at the shortest section of the block during test under static load of 40 kN (14.2 MPa) by (Oikonomopoulou, 2019). Right: Possible explanation of the cause of failure of the specimens interleaved with PMC770 (70A) and Task16 (80A). Derived from (Oikonomopoulou, 2019b)

- Material Research and Evaluation**

Dimas et al. (2022) methodically assess various interlayer materials to meet the established criteria:

Polymers: Including PU and PETG, known for their formability and mechanical resilience.

Elastomers: Such as Neoprene, Silicone, and PTFE, valued for their flexibility and durability.

Metals: Aluminum and Lead are considered for their structural benefits and minimal visual impact.

Hybrids: Materials like Laminated PU and Soft-core Aluminum that offer a combination of properties from different material families.

	POLYMERS			ELASTOMERS			METALS			HYBRIDS	
	PU	PVC	VIVAK®	NEOPRENE	SILICONE	TEFLON	Aluminum	LEAD	METAL FOAM SANDWICH	LAMINATED PU	SOFT CORE Aluminum
PRIMARY	COMPRESSIVE STRENGTH $\geq 2\text{MPa}$	YES	YES	YES	YES	YES	YES	YES	YES	YES	YES
	CREEP RESISTANT	UNKNOWN	NO	UNKNOWN	NO	MAYBE	YES	YES	YES	MAYBE	YES
	SLIGHTLY LESS STIFF THAN GLASS	NO (MUCH LESS)	NO (MUCH LESS)	YES	NO (MUCH LESS)	MAYBE	YES	YES	YES	MAYBE	YES
	TEAR STRENGTH	DEPENDS ON THE HARDNESS	DEPENDS ON THE HARDNESS	SATISFACTORY	SATISFACTORY	SATISFACTORY	HIGH	HIGH	HIGH	HIGH	HIGH
	ABILITY TO BE SHAPED IN FINAL GEOMETRY & THICKNESS	YES INJECTION MOLDING	YES INJECTION MOLDING	YES VACUUM FORMING	NO N/A	YES INJECTION MOLDING	MAYBE/ NO MILLING	YES PRESS FORMING	YES PRESS FORMING	MAYBE/ NO *COMBINATION*	MAYBE *COMBINATION*
SECONDARY	ENABLES CIRCULARITY	YES	YES	YES	YES	NO	MAYBE	YES	NO	MAYBE/ NO	MAYBE/ NO
	OPTICAL QUALITY	TRANSPARENT/ TRANSLUCENT	TRANSPARENT/ TRANSLUCENT	TRANSPARENT/ TRANSLUCENT	OPAQUE WHITE	TRANSLUCENT	TRANSLUCENT	REFLECTIVE SILVER	OPAQUE ASH GRAY	REFLECTIVE	TRANSLUCENT/ OPAQUE
	THERMAL EXPANSION COEFFICIENT* GLASS: 4-10 MSTRAIN/ ° C	90-92	45-180	120-130	110-240	250-300	120-180	18-26	18-30	UNKNOWN	UNKNOWN
	DURABILITY: WATER, FIRE & UV	YES	YES	YES	YES	WATERTIGHT FOR APPROX. 20 YEARS YES YES	YES	YES	YES	MAYBE *CONSIDER THE EDGES*	YES

Figure 79: Overview of selected materials and qualitative assessment according to their performance on the established primary and secondary criteria. Source: Dimas, M., Oikonomopoulou, F., & Bilow, M. (2022). An Interlayer Material Study Towards Circular, Dry-Assembly, Interlocking Cast Glass Block Structures.

- **Testing Protocols and Evaluation**

The study involves extensive testing to validate each material against the primary criteria:

Formability Tests: Assessing the capability of materials to be molded into precise geometrical configurations required for the design.

Creep Performance: Evaluating materials like PU and PVC for their behavior under sustained loads.

Mechanical Tests: Measuring compressive and tear strengths to confirm durability and load bearing capacity.

Environmental Durability Tests: Analyzing how materials withstand environmental factors such as UV exposure, moisture, and temperature fluctuations.

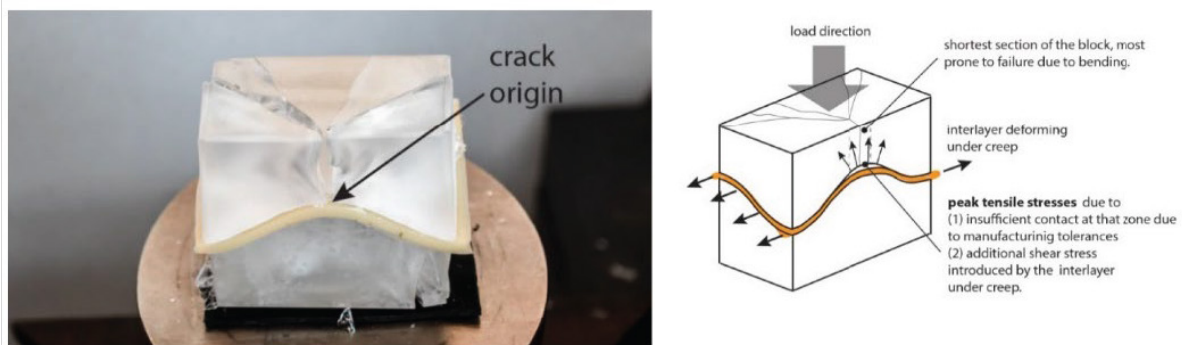


Figure 80: left, previously cast Polyurethane interlayer at TU Delft. Right, Interlocking cast glass block developed by (Jacobs, 2017) and used as the interlocking glass block reference in this research. Source: Dimas, M., Oikonomopoulou, F., & Bilow, M. (2022). *An Interlayer Material Study Towards Circular, Dry-Assembly, Interlocking Cast Glass Block Structures*.

- **Material Testing Results**

Polyurethane (PU) and Polyvinyl Chloride (PVC): Re-evaluated for creep behavior and stress adaptability.

PETG Sheets (Vivak®): Noted for excellent formability and stress distribution, aiding in micro-asperity accommodation.

Neoprene: Assessed for flexibility, durability, and its common use in sealing applications.

Aluminum: Reviewed for its structural advantages and challenges related to stress concentrations.

Laminated Polyurethane: Explored for its enhanced flexibility and complex fabrication needs.

Soft-core Aluminum: Evaluated for its hybrid structure providing both rigidity and adaptability.

- **Conclusion**

The findings from Dimas et al. (2022) are pivotal for choosing suitable materials that meet specific architectural requirements, such as transparency and sustainability. This comprehensive assessment aids in understanding material behaviours under operational stresses and their long-term viability in architectural applications.

7.5. Testing Methods for Modular Systems

Overview

When developing modular systems, especially those involving innovative materials and connections, setting up a rigid testing methodology before the final design is solidified isn't practical. However, a flexible approach based on the current literature and the resources available at our facility can provide a solid foundation for preliminary testing. This method allows me to adjust as the design evolves while ensuring that the prototypes meet essential performance criteria.

- **Software-Assisted Testing**

After designing a connection type and laminated glass modules, which would be the result of iterative loops making sure all the requirements of the project are observed, the structural and performance testing will begin. To stay within the scope of the project, future testing phases will utilize software exclusively. I will employ a rhino model to generate the forms and configurations of the modules. Utilizing Karamba, I will define the forces and their magnitudes acting on the modules. Further analysis will be conducted using ANSYS to test a single module and the connection of two modules under applied forces. This will help determine the capacity of the connections and the module corresponding to the optimized shape, thickness, and materials used in connections of the glass units. Ultimately, a guideline outlining which forces can be handled by which units will be developed, providing a comprehensive framework for the structural capabilities of the modular system.

- **Prototype Development**

The first step in my testing approach is to create small-scale prototypes. These models are crucial for visualizing the design and testing assembly mechanisms. I plan to use materials such as acrylic or plexiglass sheets to construct at least two different configurations of the design. This stage is vital for comparing variations and refining the modular connections and overall aesthetic.

- **Fabrication and Material Testing**

Moving from the design phase to real-world application, I plan to approach companies interested in supporting academic research projects to produce the required glass modules. These modules will consist of one or two layers of laminated glass, precisely fabricated according to my design specifications. Integrating a specially engineered connection system within these modules is crucial. This practical step will enable me to evaluate how effectively the theoretical design translates into durable, real-world components and rigorously test the performance and reliability of the connections under realistic conditions.

- **Structural Integrity Testing**

For the structural testing of the modules, there are possible methods to be applied:

- **Bending:** This test will determine how well the module withstands loads that could cause bending. I'm looking to see how the module holds up under stress without permanently deforming or failing.
- **Shear:** This testing will help me understand the module's resistance to connection behavior and internal shear stress in glass, which is crucial for ensuring the stability of the joints and the structural integrity of the entire module.
- **Tension:** Testing for tension/compression is important to evaluate how the module responds to stretching/compacting forces. This test will also assess the strength of connection agents and the glass itself and how they behave together.

But only after design is fixed and facilities in university are known I can decide on the testing scope of my project.

This proposed methodology blends both software simulations and physical testing to provide a comprehensive analysis of the modular system's performance. Starting with digital simulations allows for initial optimization and problem-solving, which streamlines the subsequent stages of prototype development and material testing. This phased approach not only enhances the feasibility and durability of the designs but also ensures that the research remains grounded in practical experimentation, paving the way for informed developments as the project progresses.

8. Research Through Design

8.1. Design Thinking Process

Reciprocal Roof Structure as the Basis for Design

To design a modular structural glass pavilion with demountable connections, inspiration was drawn from reciprocal structures, which are inherently modular in nature. In these systems, each element plays an active structural role, making this a promising direction for developing a self-supporting glass system.

Reciprocal structures are self-supporting systems composed of mutually supporting elements arranged in a closed circuit, where each component both supports and is supported by its neighbors. This creates a stable, interdependent network without the need for continuous linear supports spanning the entire structure. Traditionally used in timber construction and seen in historical examples such as Leonardo da Vinci's bridge designs, reciprocal systems allow for wide spans and complex geometries using relatively simple elements. Their modular and repetitive nature makes them adaptable to different materials and scales, offering significant potential for prefabrication and ease of assembly. In modern applications, reciprocal structures are increasingly explored for their aesthetic qualities and structural efficiency, especially in projects aiming for material optimization and lightweight design.



Considering these features, it became clear that simplicity in the shape of the modules is essential, ensuring that assembly remains practical and efficient. At the same time, stability must be derived either from the inherent geometry of the modules or from the connection type itself. Achieving a balance between structural performance, modular repetition, and ease of construction required careful evaluation of the module design and its interaction with the overall system.

8.1.1. Connection to System

The design process began with an approach that differed from the one which ultimately shaped the final outcome. The initial focus was placed on developing the connection, using it as a foundation for defining the overall system. Instead of starting with a complete structural concept, the boundaries of the system were derived from the constraints and possibilities introduced by the connection itself. At this early stage, only the idea of the connection and a basic module shape were in place. Through further exploration of geometric variations, the connection was tested and refined, gradually informing the development of the system as a whole.

8.1.2. System-to-Connection Approach

In this phase, the process was approached differently by first establishing a clear definition of the modules. A systematic design for the overall structure was then developed, followed by an exploration of suitable connection concepts. Rather than starting with the connection itself, the focus was placed on defining the system's requirements and goals, allowing the connections to be designed in direct response to the identified needs. This method ensured that the connections were fully aligned with the broader objectives of the project, resulting in a more coherent and integrated design.

To design a reciprocal structure as a pavilion, it is necessary first to define the modules and then develop the connections that allow for disassembly and demountability. Two main starting points were identified for this process: a connection-to-system approach, where the connection concept is developed first and the system is shaped around it, and a system-to-connection approach, where the overall system is designed first, and the connections are developed in response to its requirements.

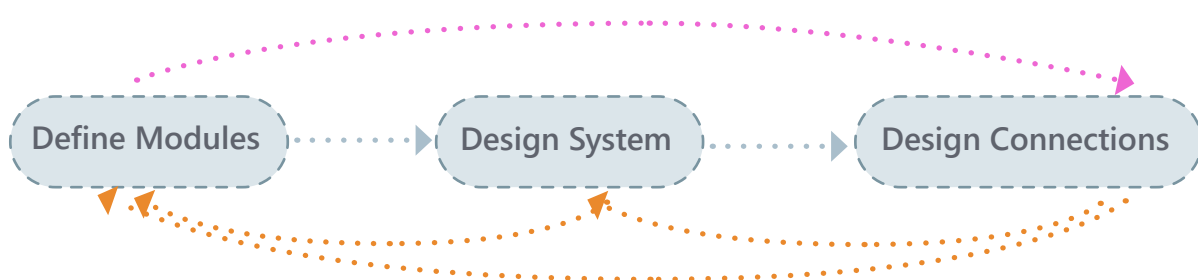


Figure 8.2.1, Design Process diagram, Source: Author's own

Process of Defining Modules Geometry:

At this stage, defining the geometry for the system became an iterative process, moving back and forth between form exploration and considerations of how the modules could be connected efficiently, such as through slot joints. The focus was on testing how different geometries and their placement within the design could influence the overall system and form. This exploration was supported by prototyping, using plexiglass and laser cutting to quickly test ideas in physical form. Through this hands-on process, it became clear that the simpler and more familiar the module design, the greater the potential for variation and formal flexibility. Such modules also proved to be more practical, as they could be easily integrated into existing construction practices, making them a more viable solution for real-world applications.

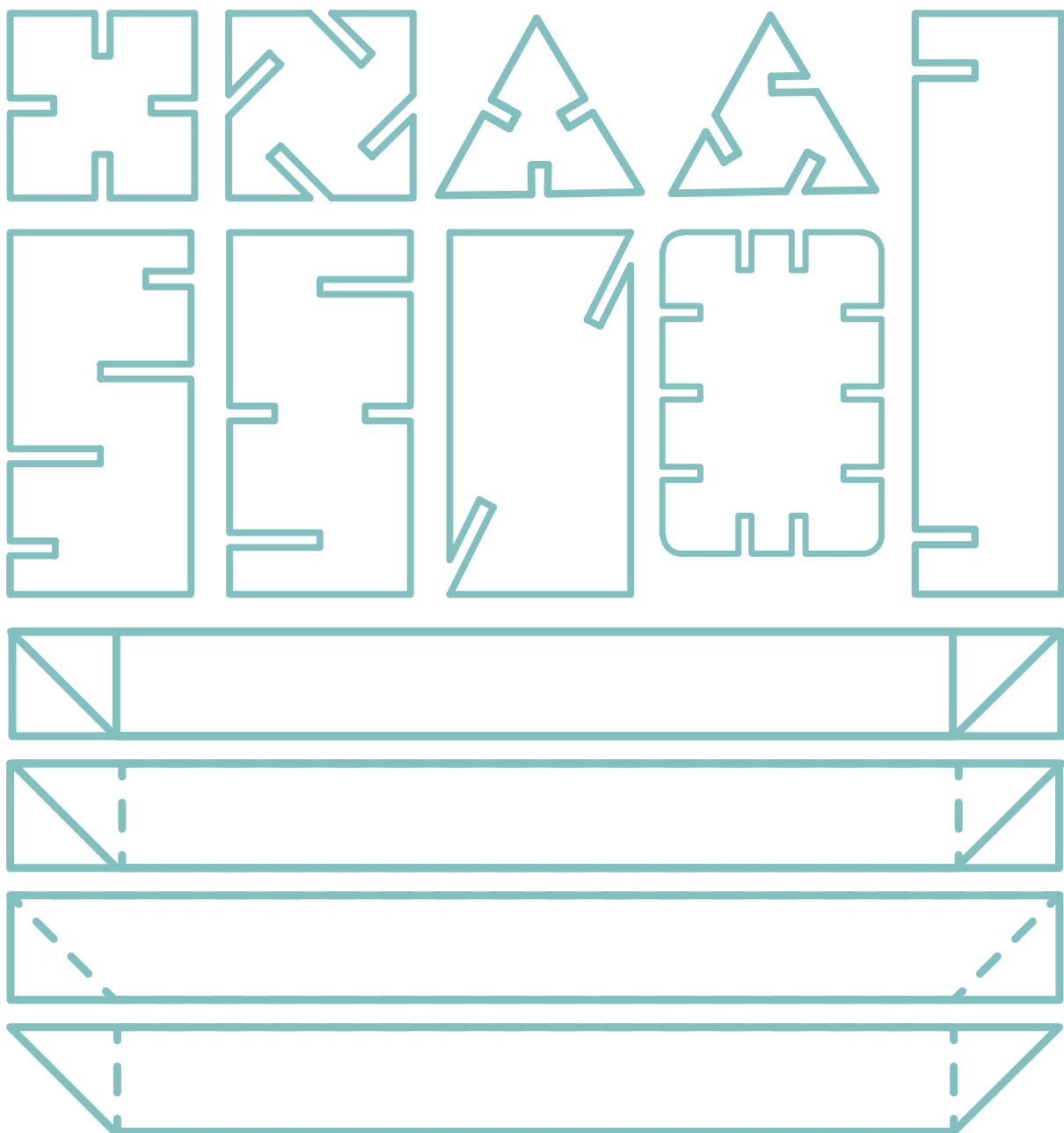


Figure 8.2.2, Modules Geometry variation diagram, Source: Author's own

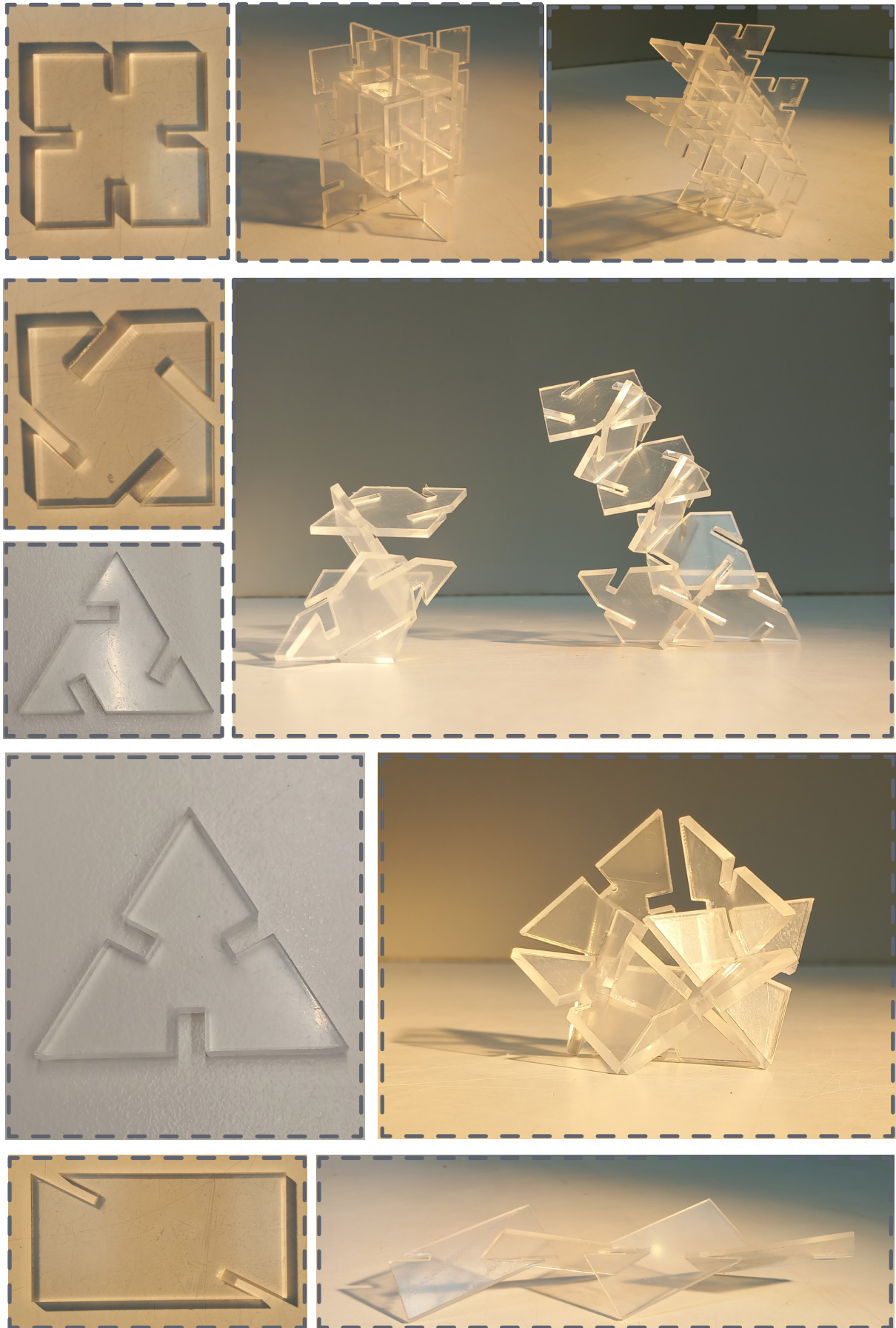


Figure 8.2.3 to 11, Modules Geometry variation prototypes and forms, Source: Author's own

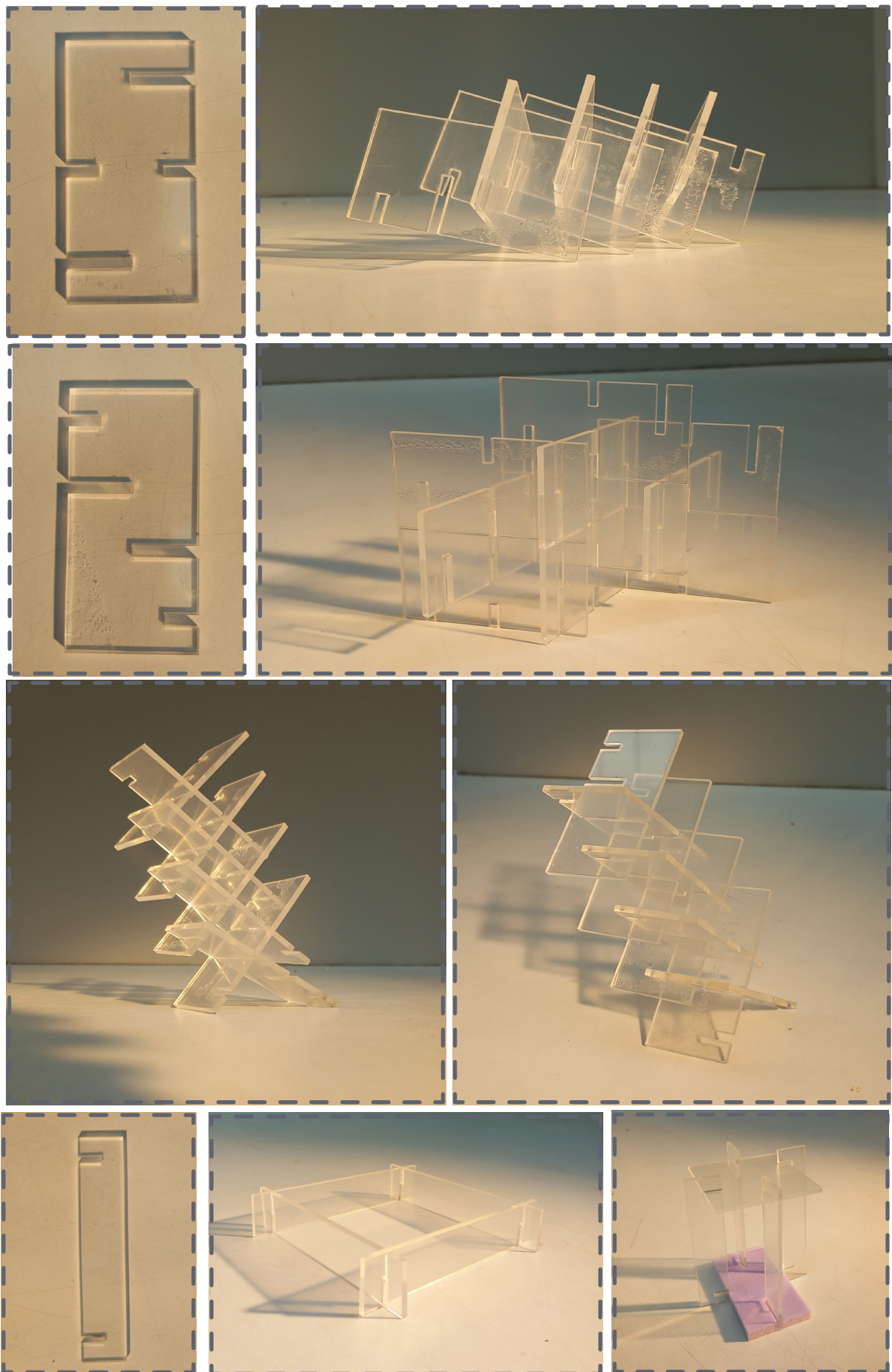


Figure 8.2.12 to 19, Modules Geometry variation prototypes and forms, Source: Author's own

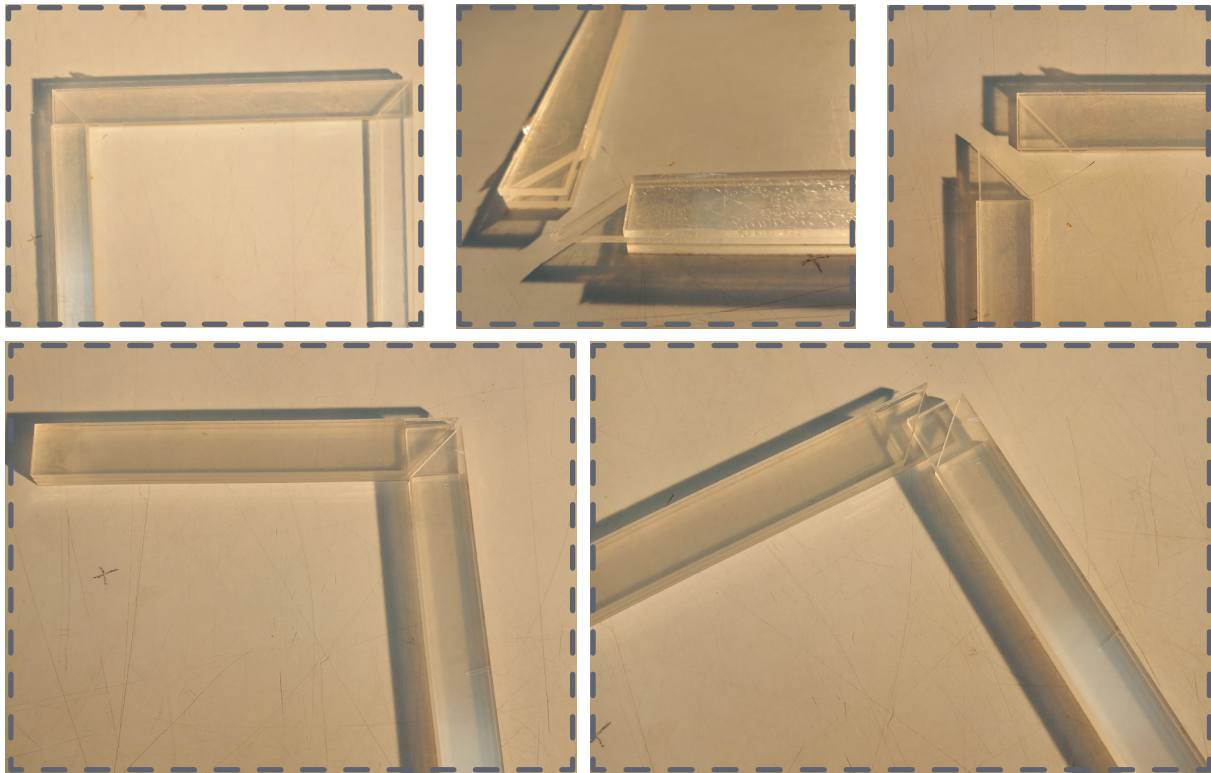


Figure 8.2.20 to 27, Modules Geometry variation prototypes and forms, Source: Author's own

Exploitative Connection Concept 1: Slot joints

This connection design was inspired by children's puzzles and traditional woodworking techniques, with the aim of adapting similar interlocking principles to glass elements. Various module geometries were defined, each incorporating slots positioned in different locations to test their potential performance. This exploration led to the development of several iterations, ultimately resulting in a more refined and detailed connection. Due to its promising structural and formability qualities, the slot joint became one of the possible candidates in the design process.

This requirement could be addressed in two main ways, as direct glass-to-glass contact was not intended. One option involved introducing a stiff material that would serve both as a protective layer and as part of the load-bearing assembly, ensuring that it participated in the overall load path while also preventing the formation of local stresses near grooves and slot corners.

Alternative 1: One proposed solution was to embed a steel or titanium plate within the laminated glass layers, creating a safe and secure connection between the modules.

Alternative 2: An alternative idea considered the use of acrylic sheets, shaped to cover the slot while simultaneously interlocking with the glass. For additional safety, the lower part of the acrylic component could be made thicker, with an embedded steel plate to help distribute loads evenly within the slot and minimize the risk of local stress concentrations.

Alternative 1:

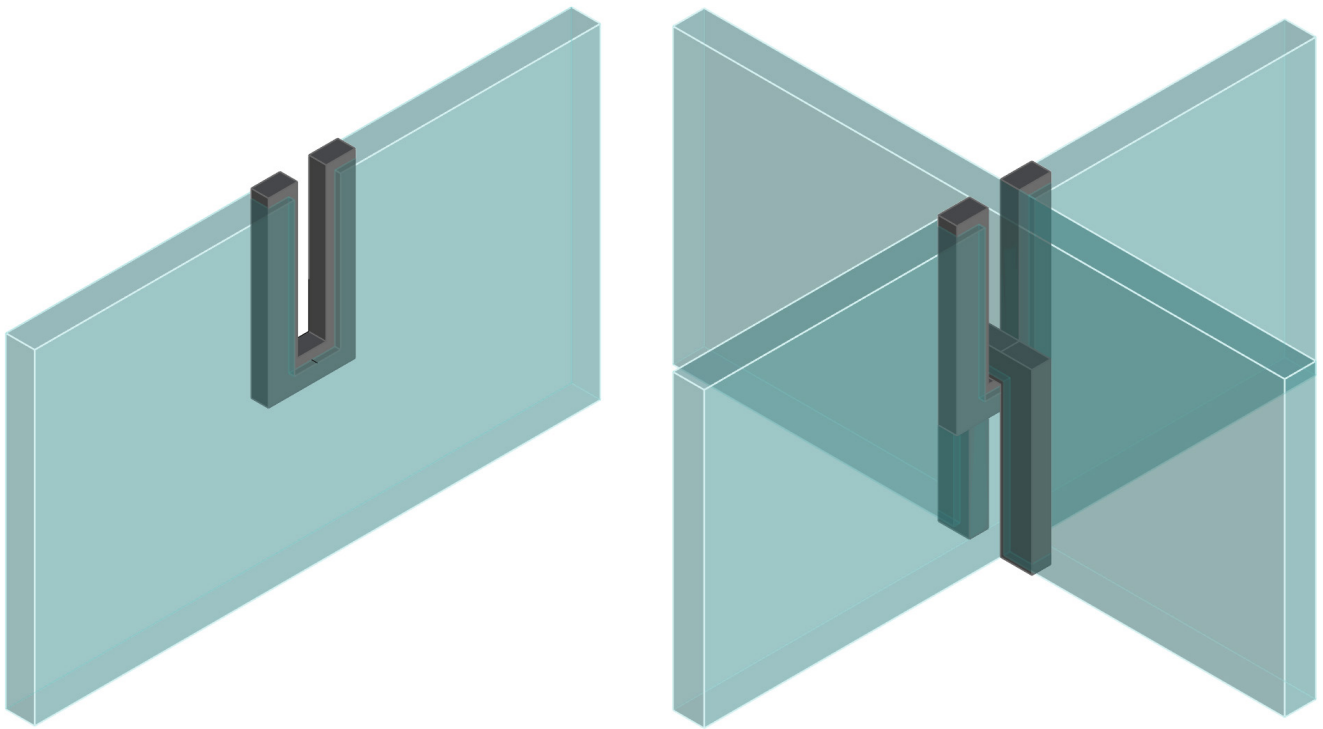


Figure 8.2.28 & 29, Slot joint connection design using embedded steel plate, Source: Author's own

Alternative 2:

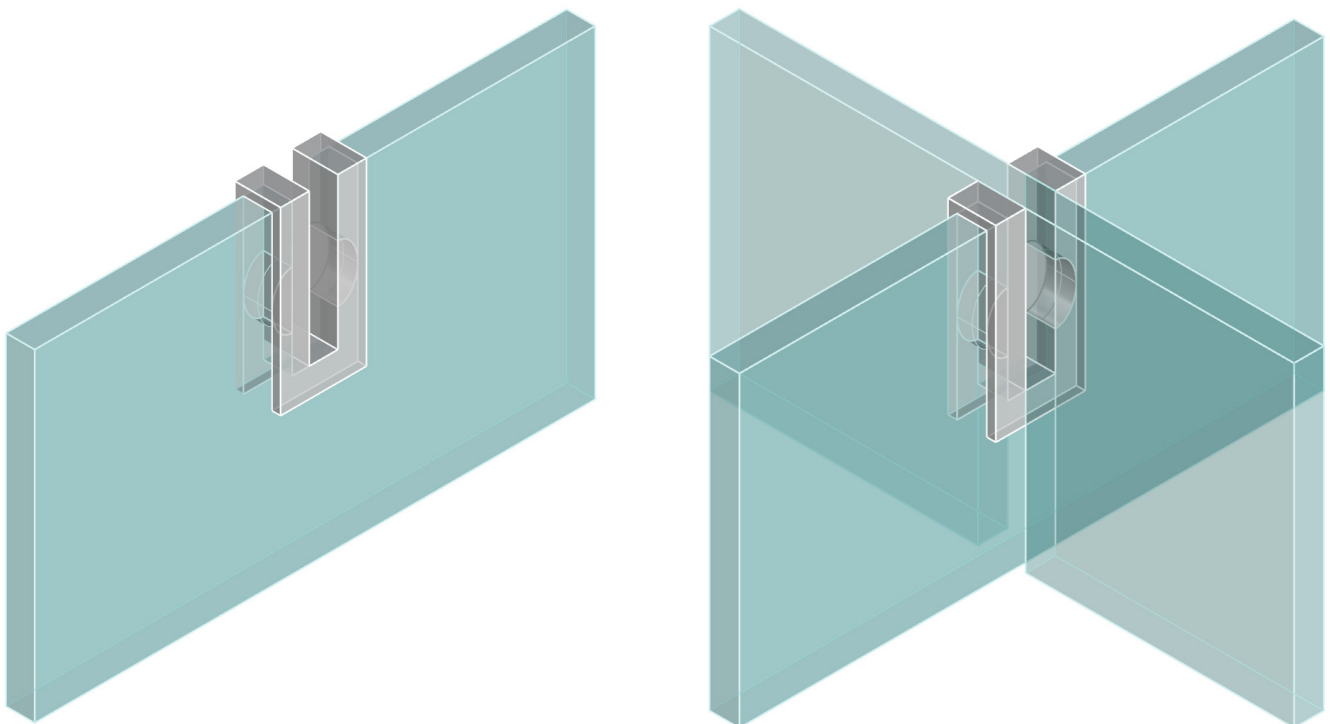


Figure 8.2.30 & 31, Slot joint connection design using Acrylic sheet with an embedded steel plate at bottom , Source: Author's own

Redefining Design Concept: Reciprocal Roof Structure, Basis for Modular Design

Further exploration focused on optimizing both the form and the connection to ensure that the system would not only be demountable but also reliable and adaptable for different configurations.

While initial module geometries, such as triangles and squares, provided some flexibility, they proved limited in generating diverse forms compared to simple rectangular modules. By adjusting the ratio of the glass beams, the rectangular modules offer greater versatility, enabling a wider range of applications—from pavilions and shelters to facades and even furniture. For the purposes of this graduation project, the concept of a Reciprocal Roof Structure was selected as a first step toward potential future adaptations into full shell structures or three-dimensional spaces.



Figure 8.2.1, Figure 8.2.34, Figure 8.2.35, *Forests of Venice Pavilion*, Venice Architecture Biennale 2016. Source: Kjellander Sjöberg, Arvet, Source: <https://www.dezeen.com/2016/05/29/forests-of-venice-pavilion-venice-architecture-biennale-2016-kjellander-sjoberg-folhem-wood>



Figure 8.2.36, *Wood and Shadow Pavilion*, 2016: (a) general view of the pavilion; (b) interior of the Wood and Shadow Pavilion, 2016, reproduced with permission from the Chamber of Polish Architects branch in Opole. Source: <https://www.mdpi.com>

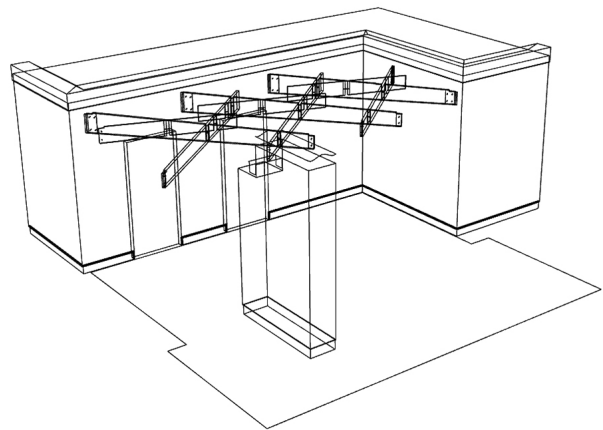
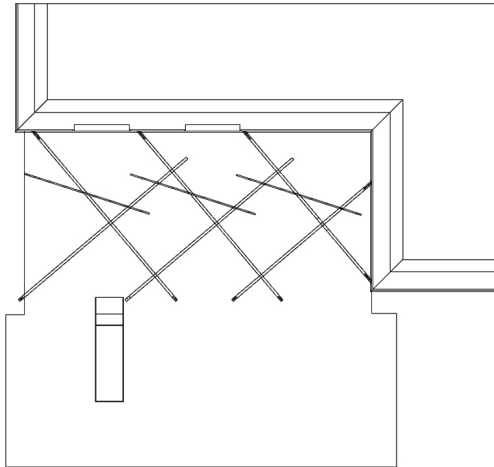


Figure 8.2.37 to 40 , Reciprocal Roof, 2014, Outdoor Covering | Reutlingen | Germany, Source: Aalto University Design of Structures. <https://www.ads-aalto.fi/reciprocal-roof>



Figure 8.2.41, Reciprocal Frame Canopy Structure by Gramazio Kohler / ETH Zurich. Source: <https://www.designboom.com>

Further developments could focus on adapting the connection design and system composition to replicate the projects shown on the next page, replacing permanent connections with demountable alternatives. This approach would allow for the creation of simple cubic or minimal forms, which are highly practical and widely used in temporary architectural applications like pavilions or exhibitions.



Figure 8.2.42 & 43, left, Glass house, Milan, Italy, By Carlo Santambrogio and Ennio Arosio. Right, Apple store, new york, by Eckersley O'Callaghan

1. Final Module Geometry:

To begin the process, a single module measuring 1800 mm in length and 300 mm in depth was defined as the initial basis, with the understanding that it would be further reviewed and refined in later stages.

Designing a system based on this module, initial sketches were developed using simple line compositions, inspired by the grid-like aesthetics of Mondrian's paintings, aiming to create architecturally authentic layouts. The focus was on exploring the junctions where the lines intersected—which would later define the key positions for the shear connections.

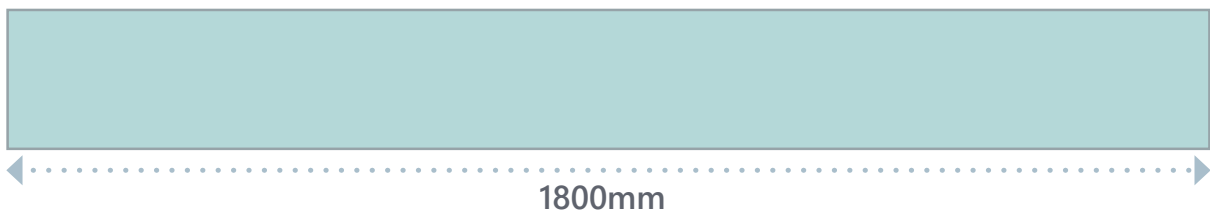


Figure 8.2.44, Modules Sizing diagram , Source: Author's own

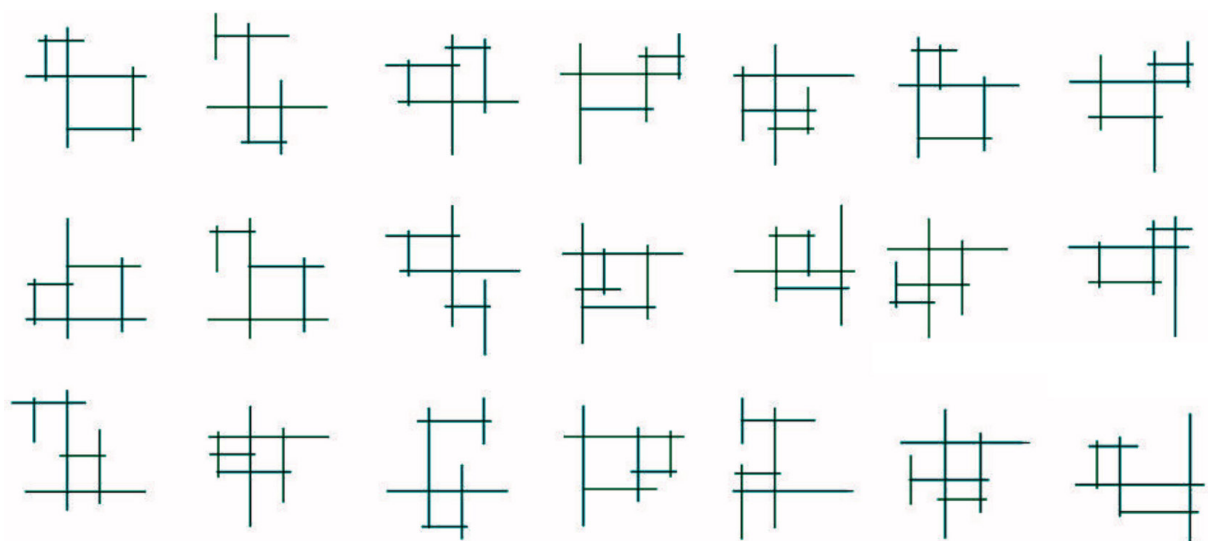


Figure 8.2.45, Composition sketches of roof structure , Source: Author's own

- **Redefine Module Geometry:**

Establishing clearer design principles and enable parametric development of the modular roof structure, the modules were defined in three sizes to allow for greater variation and adaptability to different spans and site conditions. These were designed in three length, with a ratio of $L = 600\text{ mm}$, $2L = 1200\text{ mm}$, and $3L = 1800\text{ mm}$ in length. This proportional system introduced a set of rules for connecting the modules: for example, connections could occur at $1/2$ the length of the second module and at $1/3$ or $2/3$ of the third module. These ratios not only added flexibility but also ensured coherence in the overall structural logic.

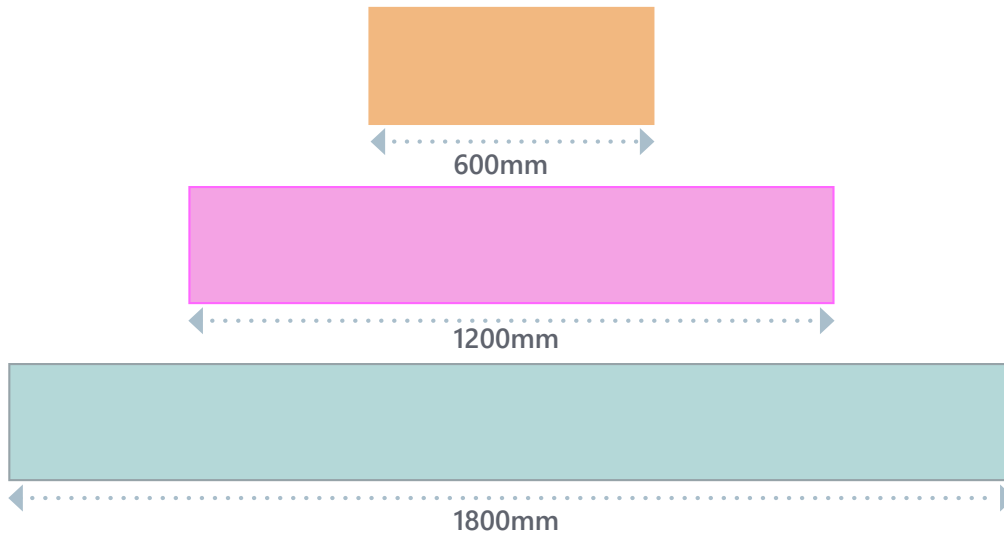


Figure 8.2.46, Modules Sizing variation diagram , Source: Author's own

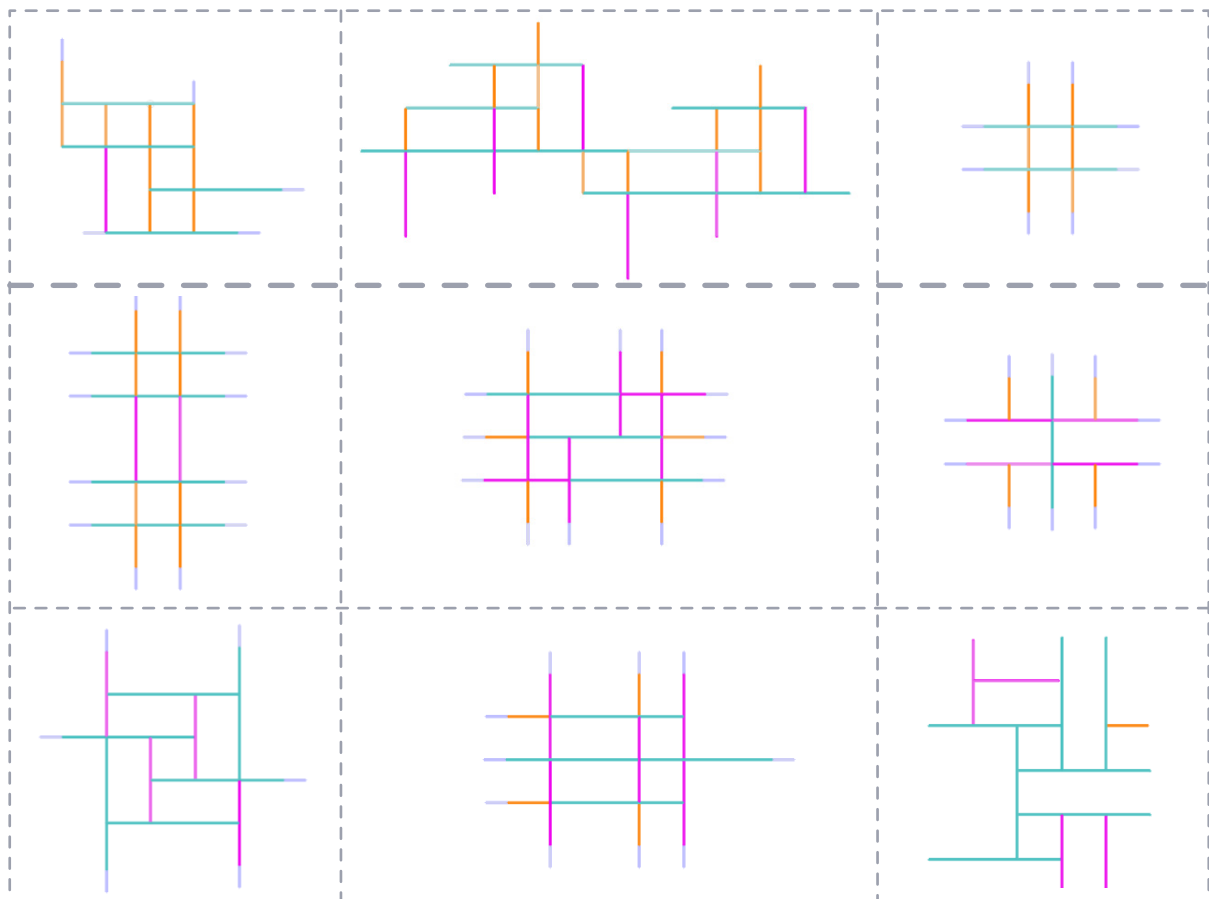


Figure 8.2.47, Reciprocal Roof Structure design sketches , Source: Author's own

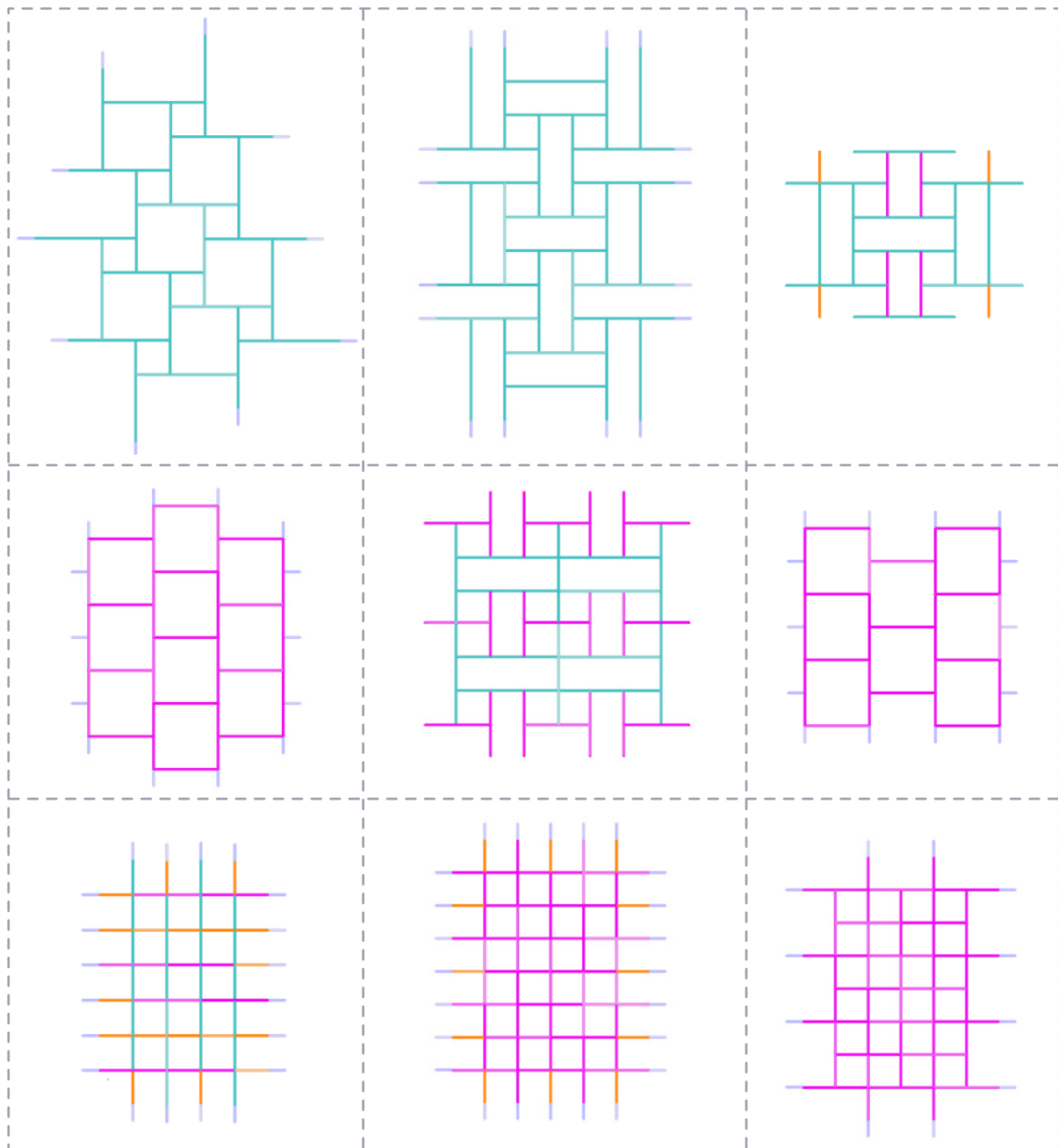


Figure 8.2.48, Reciprocal Roof Structure design sketches , Source: Author's own

The figures shown above represent various top-view composition patterns achievable using the designed module sets. Some configurations use just one type of module in combination with fins, while others incorporate combinations of two or all three module types. All these arrangements consistently follow the connection principles outlined previously.

Several patterns are inspired by Mondrian's famous geometric paintings, while others reference well-known Pattern, easily recognizable design patterns, and some are based on creativity of author.

However, the true value of this system lies in its limitless confrontational possibilities, allowing anyone—regardless of their expertise—to intuitively engage with the modules. Users can creatively experiment, producing countless variations that are both structurally clear and visually appealing.

2. Connection Design Alternatives

- **Connection Categories**

Reviewing the sketches for the modular glass reciprocal roof system, results in 3 types of intersections. Either the panels aligned, or 2 modules are perpendicular to one module, or one module is perpendicular to the other.

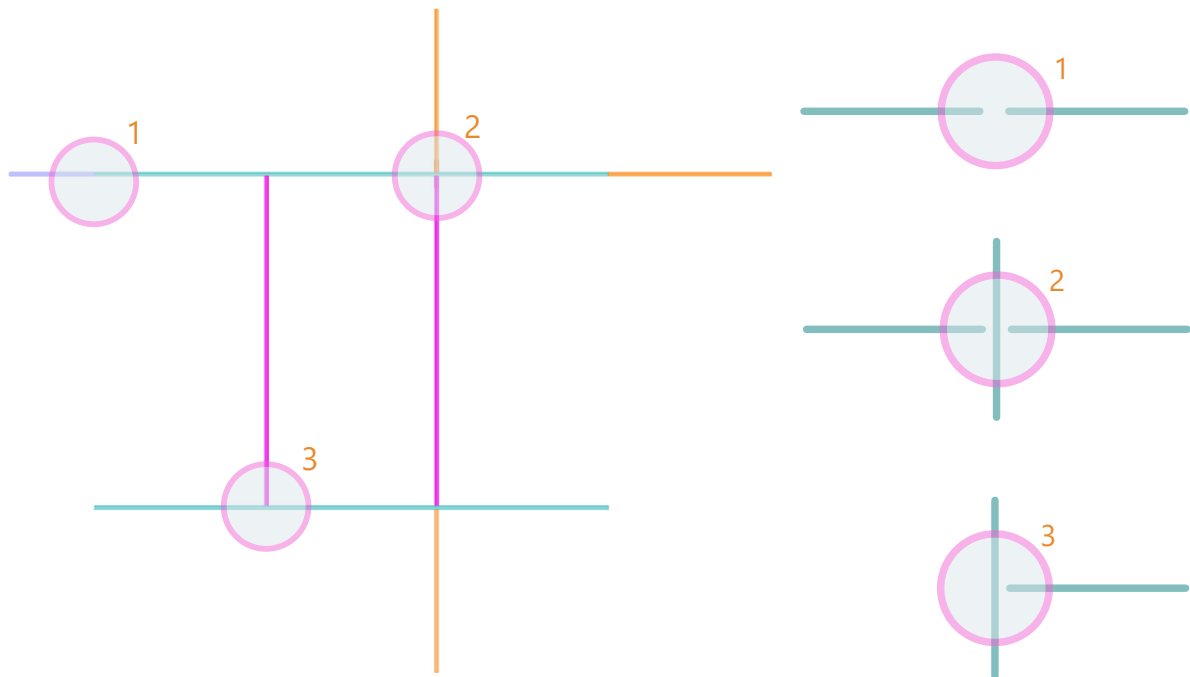


Figure 8.2.49, Joint Types Diagram , Source: Author's own

Shear connections:

The aim for the connection design of this reciprocal roof structure is to develop a shear connection. Shear connections are generally simpler, more cost-effective, and easier to fabricate and assemble compared to more complex moment connections. Given that the structure functions as a roof and primarily resists vertical loads, shear connections are well-suited to the structural requirements.

- **Connection Design Options**

During the connection design process, a wide range of woodworking techniques was explored, including traditional Japanese interlocking joinery, simple hanging systems, slot joints, tongue-and-groove methods, and various other types of joints.

While many variations were initially explored, ultimately, six key connection types were developed, all inspired by woodworking joinery principles, and they were identified as the most promising candidates—capable of supporting the three main connection conditions defined in the system. They formed the basis for the sketched connection concepts and modular system forms shown above.

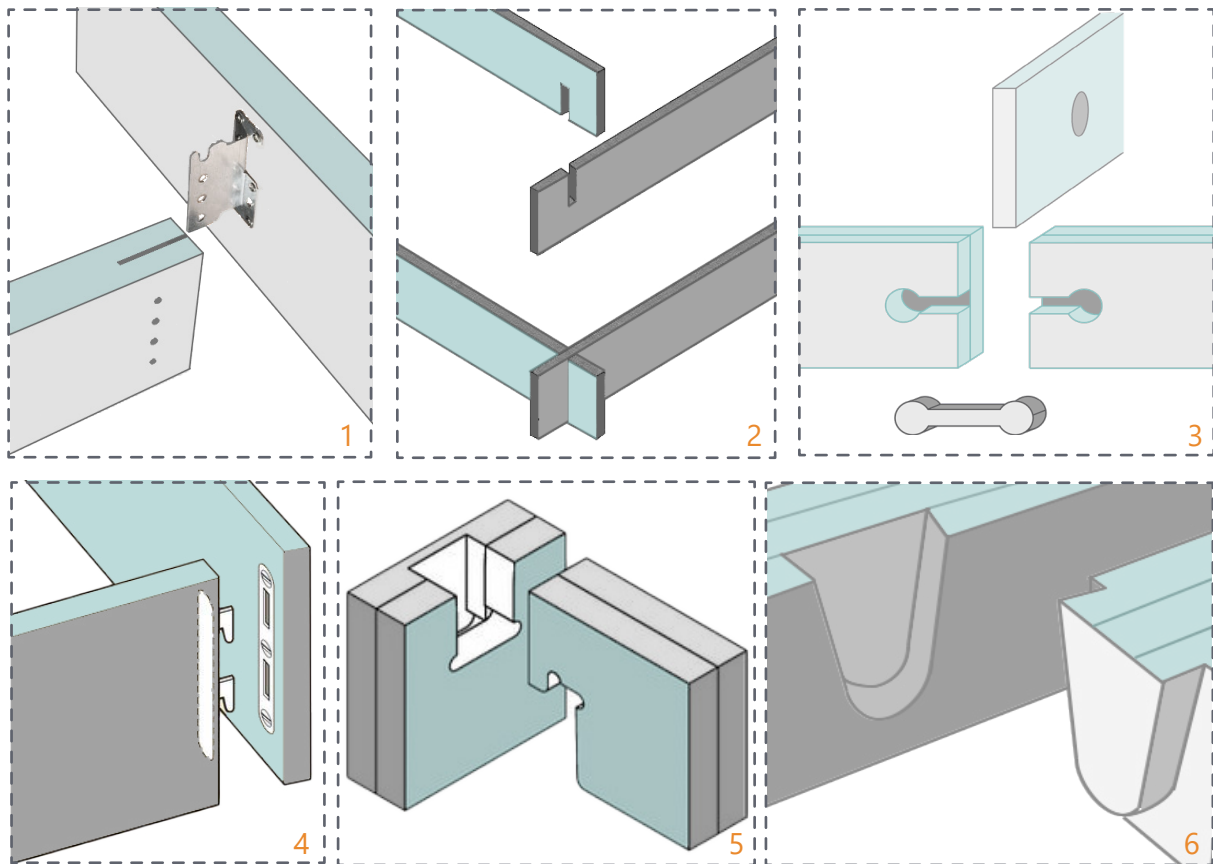


Figure 8.2.50 to 55, Possible connection design sketches for this system , Source: Author's own

While exploring different connection strategies, some concepts relied on the layered nature and thickness of laminated glass. However, these introduced unnecessary stress into the interlayer and bonding zones, as seen in options like Figures 5 and 6.

On the other hand, embedded steel plates, hooks, or metal inserts were dismissed because they did not align with the guiding principles of the project. These elements were neither novel nor fully reversible.

Among all the options explored, I ultimately chose to proceed with the “dog bone” shaped connection (Figure 3). This decision was based on several key factors. First, the geometry was relatively straightforward to fabricate, making it practical within the constraints of the project. Second, its application within a glass-based system felt innovative and offered a new design opportunity. The intermediate material not only functioned as a structural connector but also acted as a protective buffer between the glass elements. Since glass-to-glass interlocking was not feasible due to the limited thickness and brittleness of the panels, the dog bone connector provided a realistic, safe, and materially compatible solution.

• Development of Connection Design

Eventually, the decision was made to continue with the dog bone-shaped connection. This option stood out because it was relatively simple to fabricate and presented a novel application for glass, offering both structural and protective functions in a single element. Unlike embedded connections, which are a common and well-established solution in glass construction, the dog bone connection introduced a fresh approach by creating an interlocking

mechanism that did not rely on embedding components within the glass itself. The dog bone connection effectively addressed these challenges by using an external protective layer that could interlock and secure the modules while remaining practical and innovative.

The inspiration for this connector came from cabinet-making techniques, particularly a type of zip bolt used to fasten two wooden panels. This precedent offered a useful analogy—a simple, effective connection using intermediate elements, but applied here in a new material and architectural context. That translation from carpentry to structural glass became a central idea in the development of the final design.



Figure 8.2.56 to 58, Zip Bolts widely used in cabinet construction , Source: <https://www.zipbolt.com.au>

- **Material Choice for Connection**

Glass Type

Heat-strengthened laminated glass was chosen over fully toughened laminated glass for this structural system because of its failure behavior and load-sharing characteristics. Unlike fully toughened glass, which shatters into small fragments and loses its structural integrity immediately upon breakage, heat-strengthened glass breaks into larger shards that often remain in place. This allows the panel to continue carrying some load temporarily, maintaining the load path within the system. In a reciprocal roof structure, where each element supports and is supported by the others, this behavior is critical for preventing sudden collapse in case of localized failure. For this reason, heat-strengthened glass was considered a safer and more reliable option for the type of connection and overall structural logic used in the project.

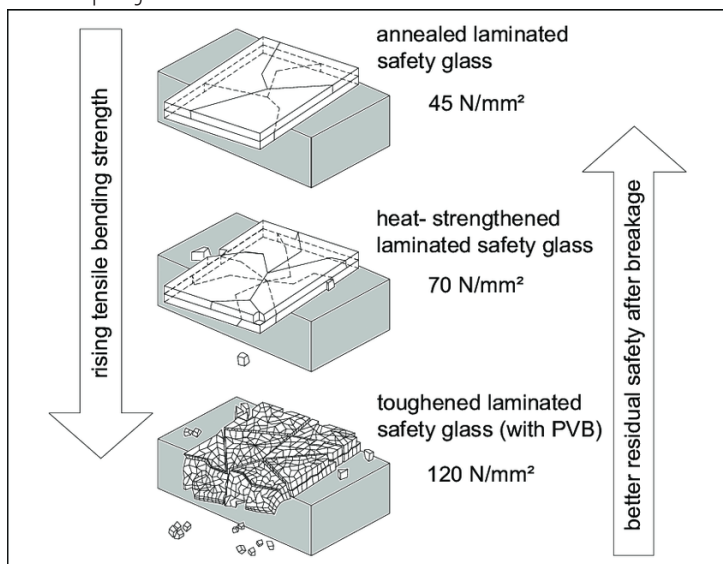
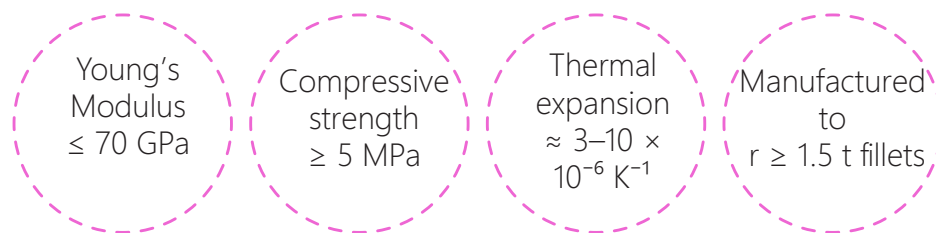


Figure 8.2.59, PFLS of fully toughened and heat strengthened glass diagrams, Source: <https://www.researchgate.net/>

Connection Material Type

In exploring material options for the connector, I adopted and adapted the two-tier selection method outlined by Dimas et al. (2022), a key source in my literature review. The process begins by establishing a set of primary criteria—essential mechanical and physical properties that the dog bone connector must satisfy to function safely alongside heat-strengthened glass. Only materials that meet all these criteria advance to the next stage. Then, a secondary set of criteria is used to rank the remaining candidates based on sustainability, cost, and visual performance. These factors, while important, are more flexible and context-dependent.

Primary criteria – must have



- Young's modulus ≤ 70 GPa (slightly less than glass)
- Tensile/compressive strength \geq design load \times safety factor
- Thermal expansion close to glass ($\approx 3-10 \times 10^{-6} \text{ K}^{-1}$)
- Can be machined or molded into smooth dog-bone geometry with $r \geq 1.5$ t fillets

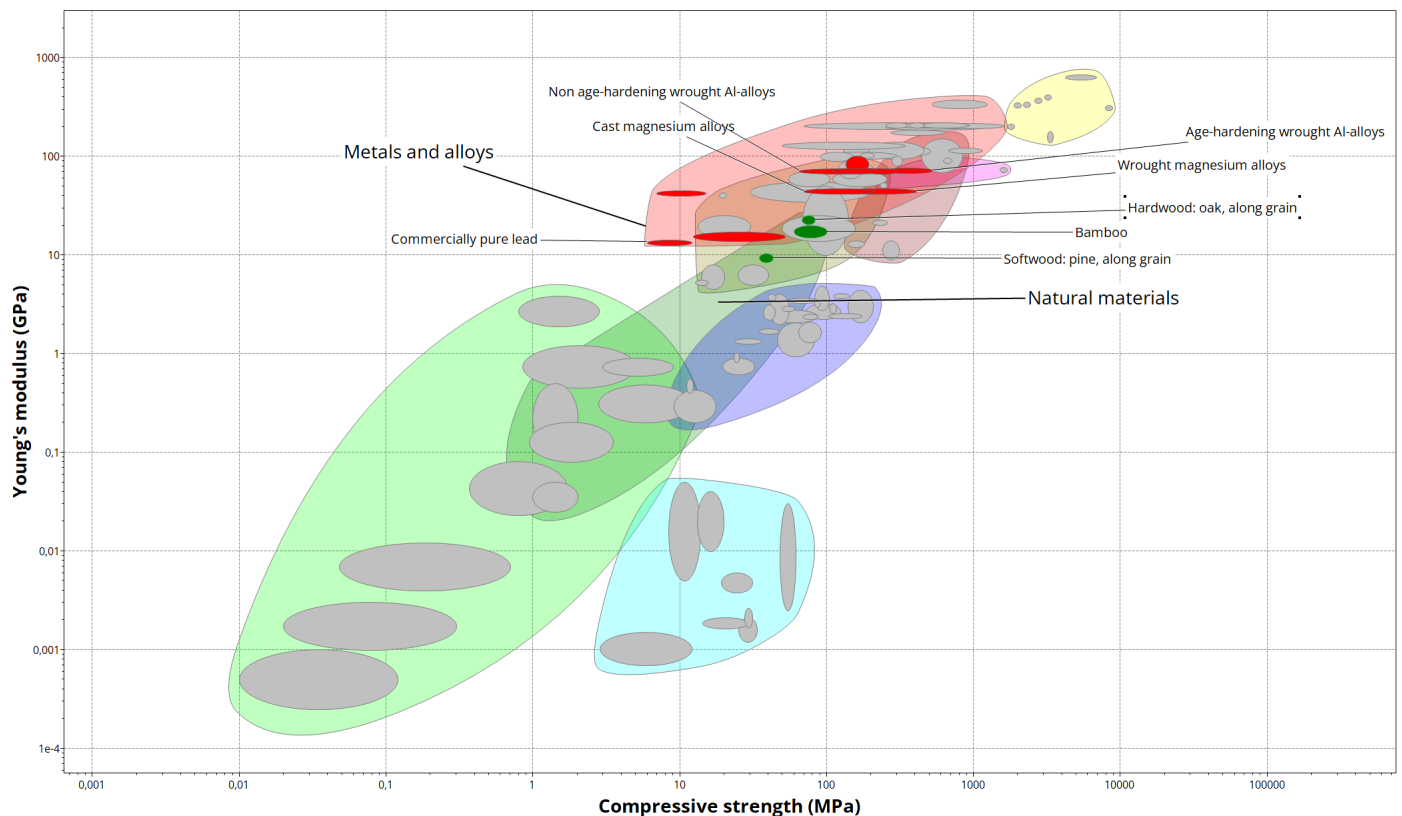
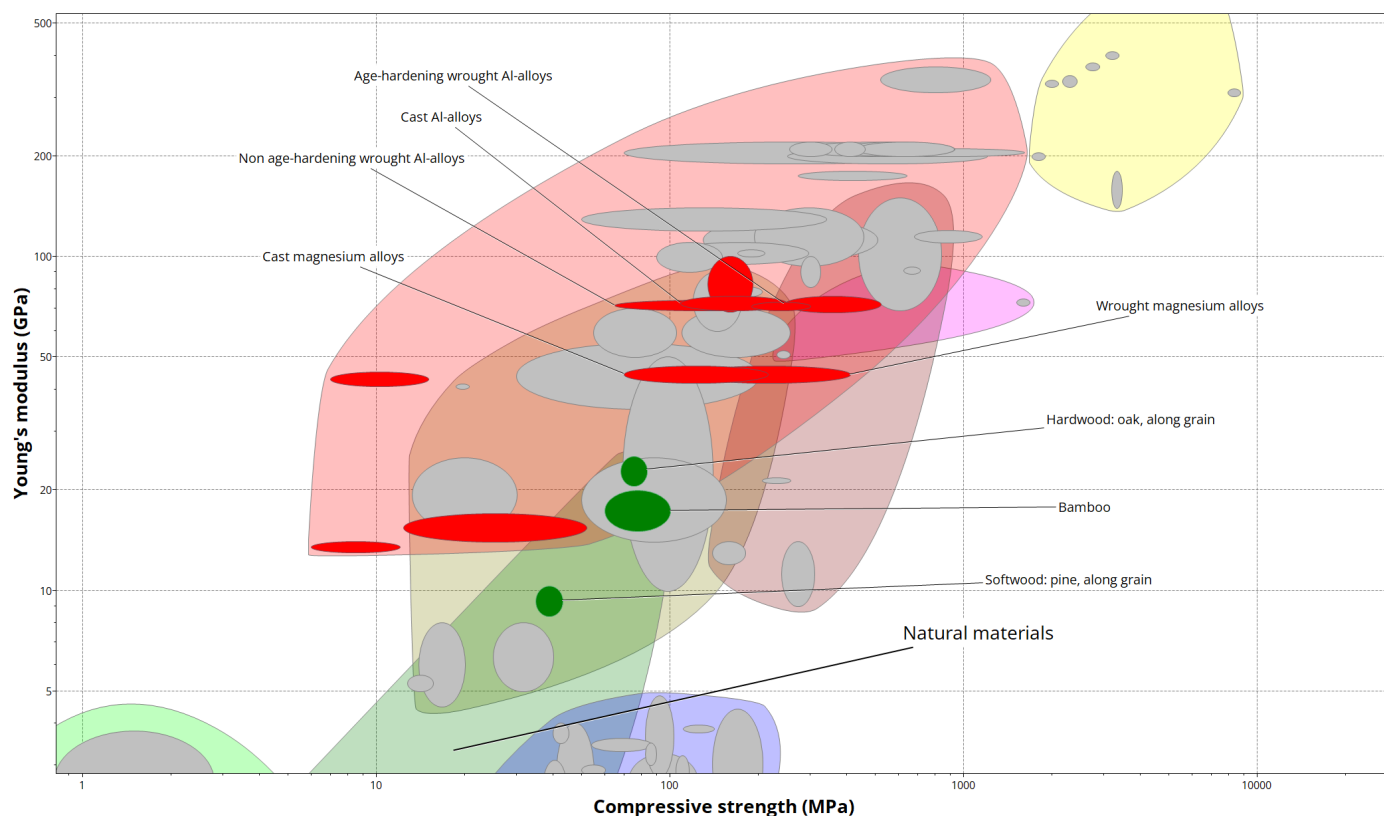


Figure 8.2.60, Granta Edu pack results show casing the materials which are with in the range of compression >5 Mpa and $10 < E$ value <70 Gpa, the one on the next page is zoomed in , Source: Author's own



Material	Typical E (GPa)	Strength (MPa)	Pros	Watch-outs
6061/6082 aluminium	69 – 70	150 – 290	Near-perfect modulus match; easy CNC; mature fatigue data	CTE $22 \times 10^{-6} \text{ K}^{-1}$ —add 0.5–1 mm PU/PTFE washer
Magnesium alloys	≈ 45	160 – 240	Very light; E safely below glass; CNC + anodise	Needs coating against corrosion; limited façade record
Short-carbon-fibre PEEK	18 – 25	160 – 200	High temp, chemical and creep resistance; matte black finish	Expensive; mould-only, anisotropic if fibres mis-aligned
Hardwood oak (quartered, kiln-dried)	20 – 25	70 – 100 (parallel grain)	Renewable, very low CO ₂ ; easy to machine; warm look	Anisotropic; moisture-sensitive —seal well; fire rating needs treatment

Figure 8.2.61, Comparison table for Primary Criteria , Source: Author's own

Secondary criteria – nice to have



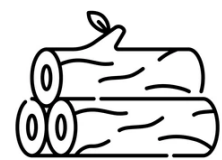
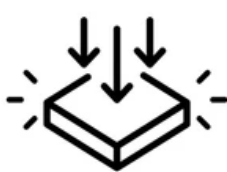
- Low embodied CO₂ per kg
- Competitive material and processing cost
- High recycled content / easy to recycle
- Durability against water, UV and fire

Material	Embodied CO ₂ (kg CO ₂ e kg ⁻¹)	Cost level*	Recycled content / recyclability	Durability – water / UV / fire
6061/6082 aluminium (75 % recycled)	≈ 7	medium	High scrap capture; remelts to billet	Excellent corrosion; loses strength above 500 °C
Magnesium alloy	≤ 5	high	Technically recyclable, thin scrap stream	Needs coating; melts at 650 °C
Short-carbon-fibre PEEK	> 20 (virgin)	very high	Closed-loop mechanical recycling emerging	Outstanding chemical & UV stability; V-0 self-extinguishing
Hardwood oak	≈ 0.07 (fossil CO ₂)	low-medium	Fully renewable; offcuts chip/compost; repairable	Needs moisture control; greys in UV; requires fire-retardant coating

Figure 8.2.62, Comparison table for secondary Criteria , Source: Author's own

In exploring material options for this connection, ultimately a middle-ground material was sought: something with a lower Young's modulus than glass, sustainable, and regionally accessible. Based on these criteria, hardwood was selected. Hardwood serves effectively as a protective buffer for glass, helping prevent scratches and flaw propagation. It also offers a balance between being soft enough to cushion the glass (unlike steel) and stiff enough to carry structural loads (unlike silicone or softwoods).

In terms of sustainability, hardwood also performed well against the secondary criteria. It is cost-efficient, widely available—particularly across Europe—and supports low-carbon, reversible construction methods. This combination of mechanical reliability and environmental performance made it the most suitable material for the connector.



Young's modulus + Sustainable + Locally Sourced► Hard wood

Through research into this type of connection, it became clear that a key-shaped interlocking geometry was essential for securely joining glass panels. However, considering the range of connection categories required by the system—such as cases where two panels must connect perpendicularly along the same axis—the design had to evolve further. This insight led to a revision of the connection, aiming to develop a uniform solution capable of accommodating multiple joint configurations. The diagram below illustrates the revision process and the key steps in optimizing this connection system.

Because of the shape of this connection, the module design had to be updated to include holes and slots that follow the form of the connection itself. One key part of this process was dealing with how the connections meet perpendicularly to one module. Different options were tested, but after optimization, the current solution was chosen. On the left side, there is a single connection aligned with the neutral axis of the beam, while on the right side, a double-connection setup is shown. The double version is meant to handle higher loads, making it useful for longer spans or situations with more demanding loading.

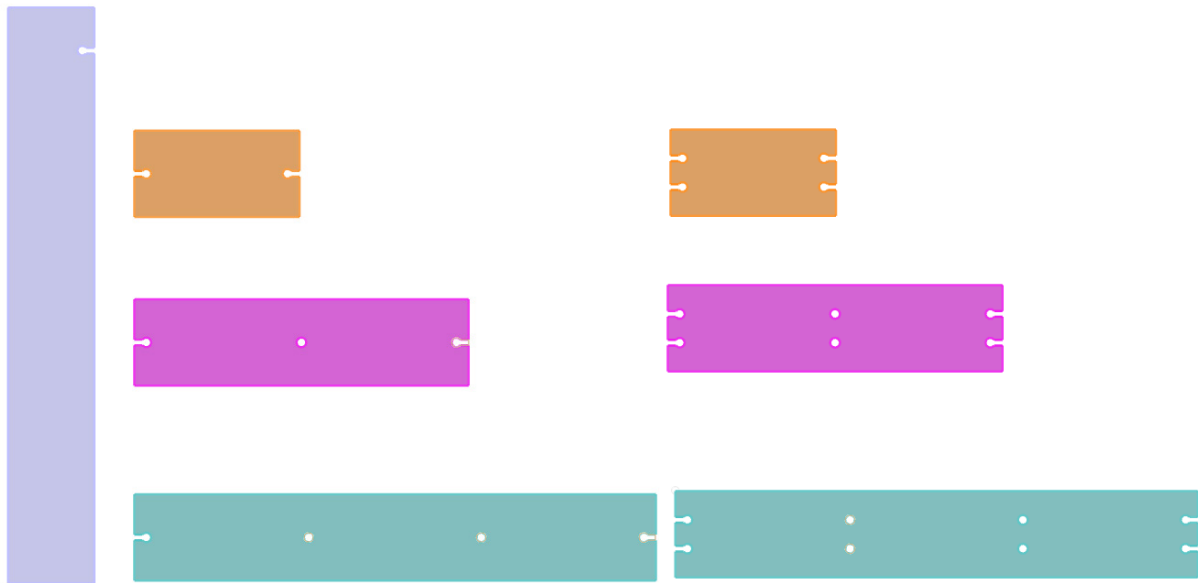


Figure 8.2.63, Module Revision, Source: Author's own

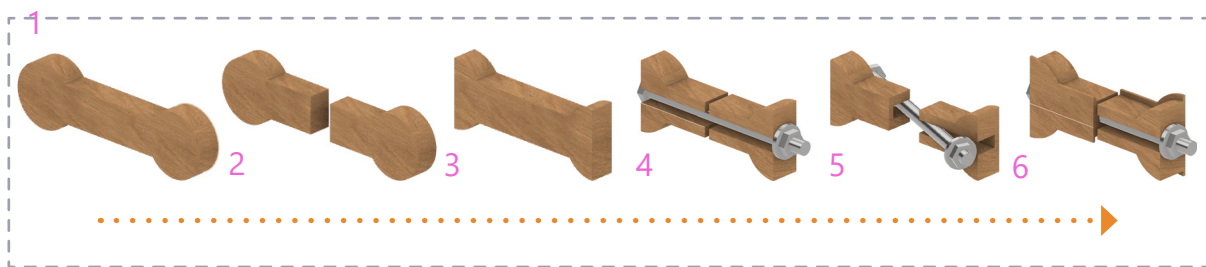


Figure 8.2.64, design process of connection diagram, Source: Author's own

The diagram above illustrates the step-by-step development of the connection design. Because structural glass alone cannot carry all the required loads, and given the need to accommodate multiple joint configurations, the initial concept had to be revised. The design began with a simple "+"-shaped connector intended to align two modules through a perpendicular middle panel.

In Step 2, the key-shaped connector was split into two separate wooden components. However, this created the challenge of how to reconnect the pieces effectively. Step 3 introduced a trimmed bolt access area—half of the bolt head's circle was cut away to allow a tool to reach and fasten it. Then in Step 4, a central groove was added to house a bolt running through both wooden parts, providing the necessary structural link.

To ensure better balance and simplify assembly, one of the two wooden halves was flipped in Step 5. This adjustment allowed the bolt to rotate 45 degrees during tightening, aligning it into position and enabling the application of preload to secure the joint. Finally, in Step 6, an additional backing layer was added to the rear of the wooden connector. This helped prevent slippage and reinforced the stability of the joint under load.

On the following page, the final design of the connection is presented through a 3D view and technical drawings. These represent the resolved geometry and dimensions developed through iterative feedback and multiple design revisions.

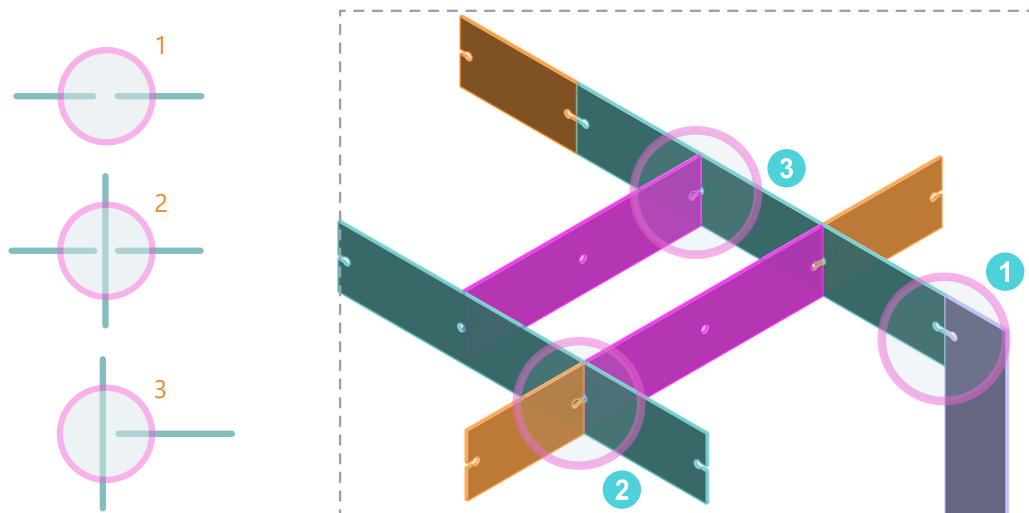
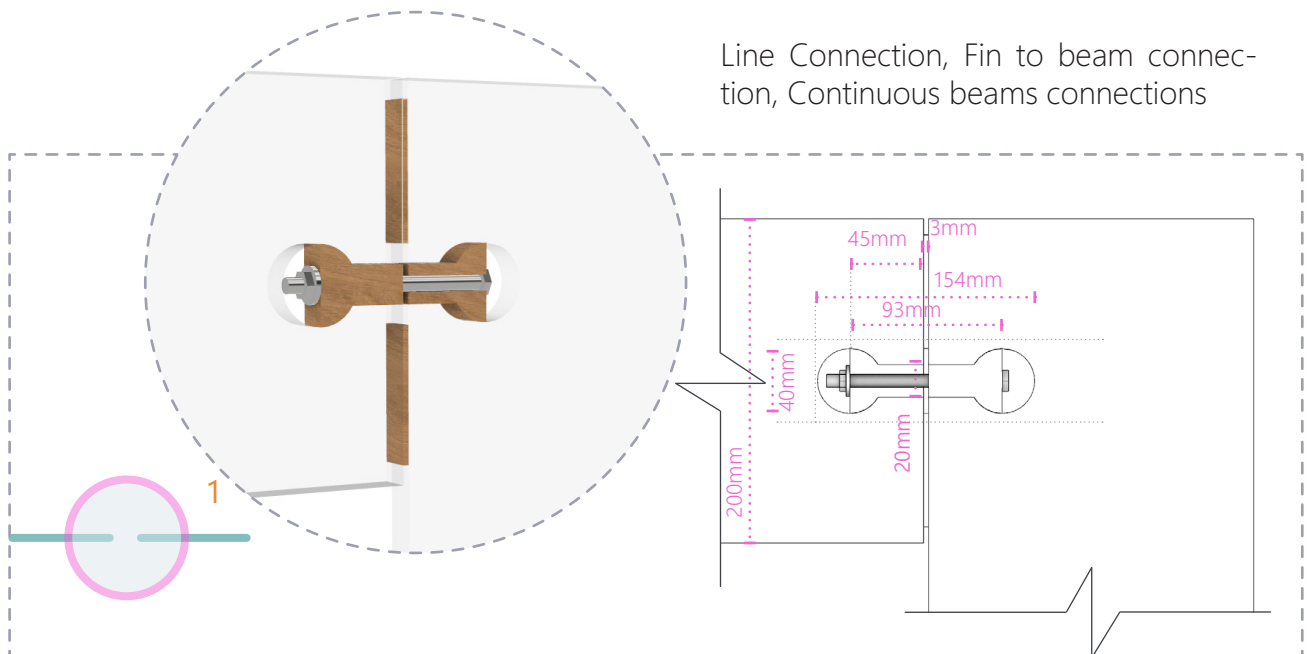
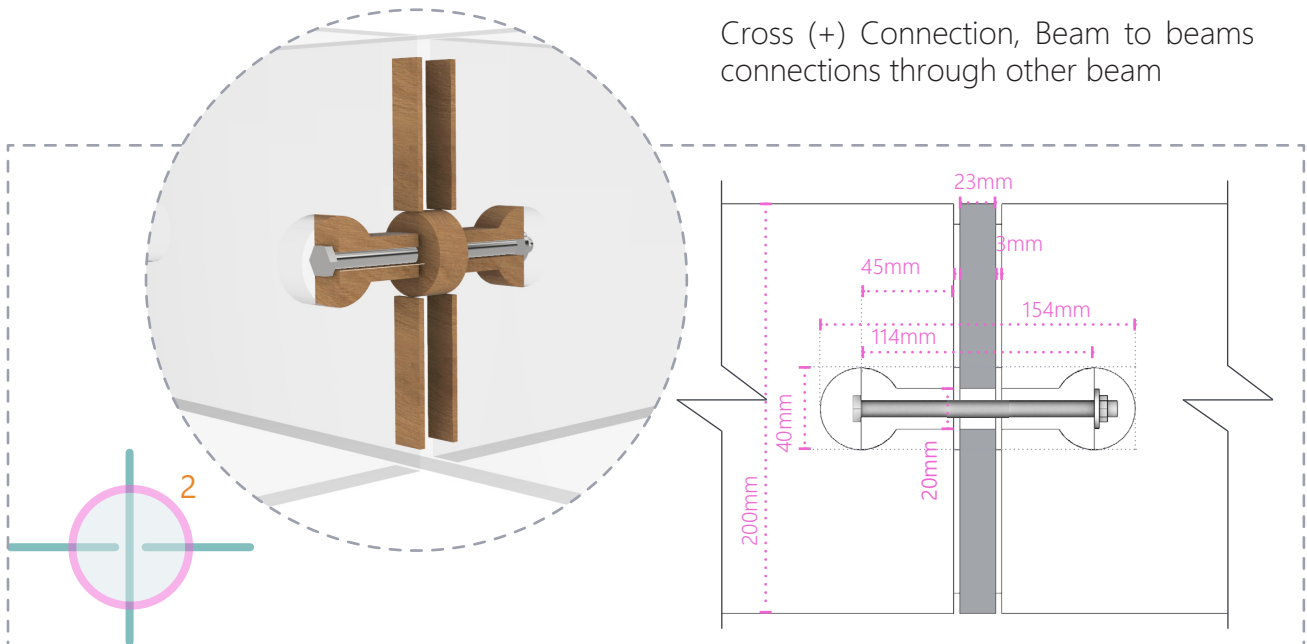


Figure 8.2.65, Categories of connection 3D diagram, Source: Author's own

Line Connection, Fin to beam connection, Continuous beams connections



Cross (+) Connection, Beam to beams connections through other beam



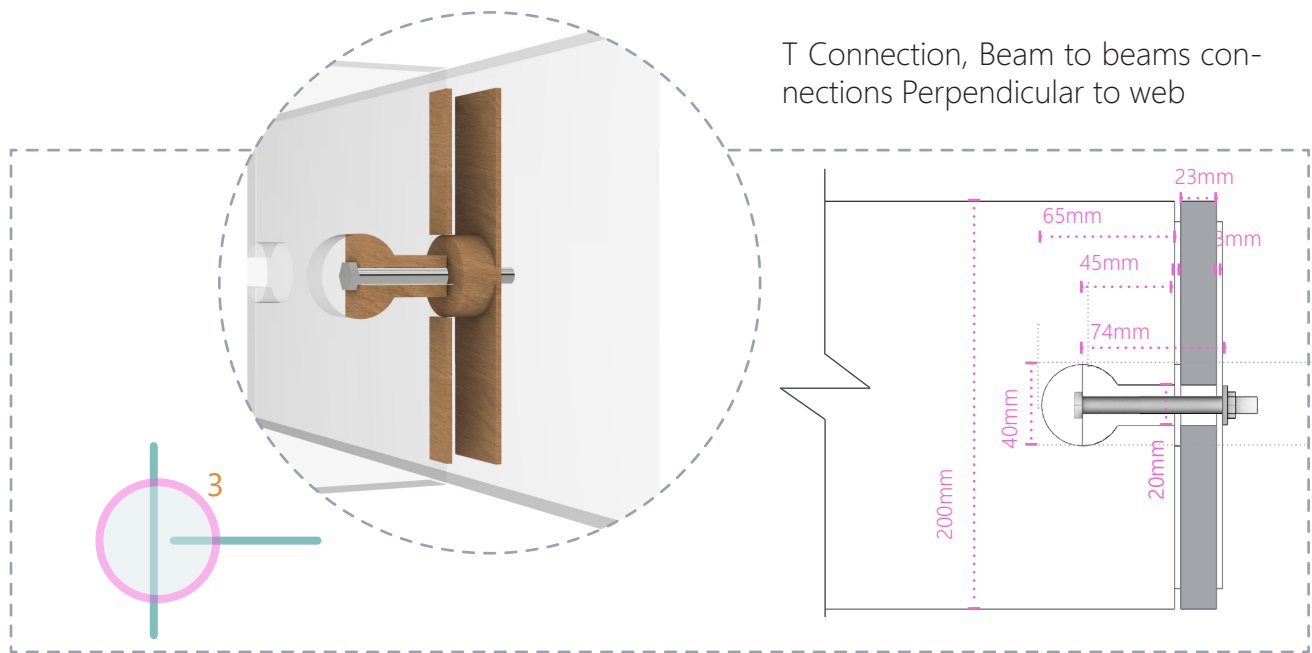


Figure 8.2.66 to 68, Connection detail drawings and diagrams, Source: Author's own

For the wooden components, a detailed material study was conducted to select a hardwood species with the highest possible strength in shear and compression, while also considering its thermal expansion properties. Since the wood is used in direct contact with heat-strengthened glass, choosing a species with a thermal expansion coefficient close to that of glass was essential to avoid generating additional stresses due to differential movement. In addition to thermal expansion, swelling behavior due to moisture changes was also a critical factor. For this reason, the grain direction of the wood was carefully considered—not only in terms of structural loading, but also to minimize dimensional changes that could affect the fit and stress distribution in the connection. These factors together informed the choice of a dimensionally stable hardwood, capable of maintaining performance and alignment under both mechanical and environmental conditions.

The next two pages present a comparison between different hardwood species, focusing on key mechanical and thermal properties. Parameters such as compressive strength, shear capacity, thermal expansion coefficient, and Young's modulus were evaluated to support the material selection process. Based on the comparison results, I decided to select oak (*Quercus robur*, abbreviated as OAK), which is widely available across Europe and ranked as the strongest among the hardwood species I evaluated for this project.

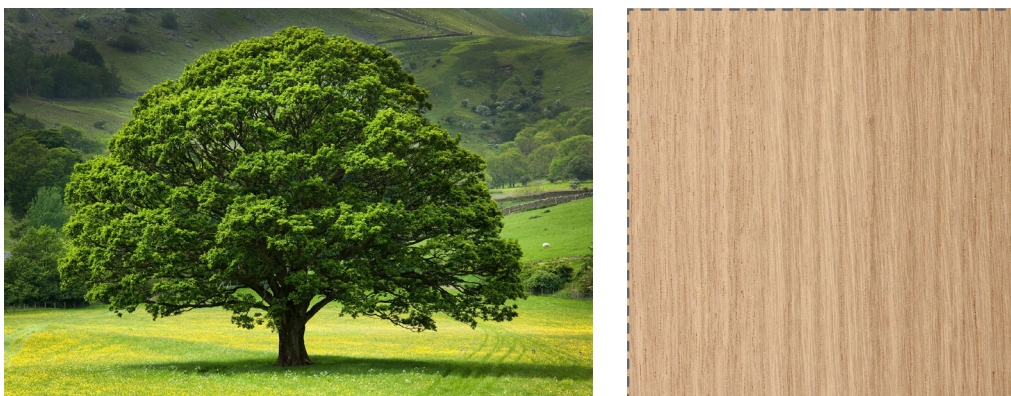


Figure 8.2.69, Oak tree and grain pattern, Source: <https://www.ober-surfaces.com>

Figure 8.2.70 to 75, Granta Edu pack results in comparing hard wood species, Parallel to grain , Source:Authors Own

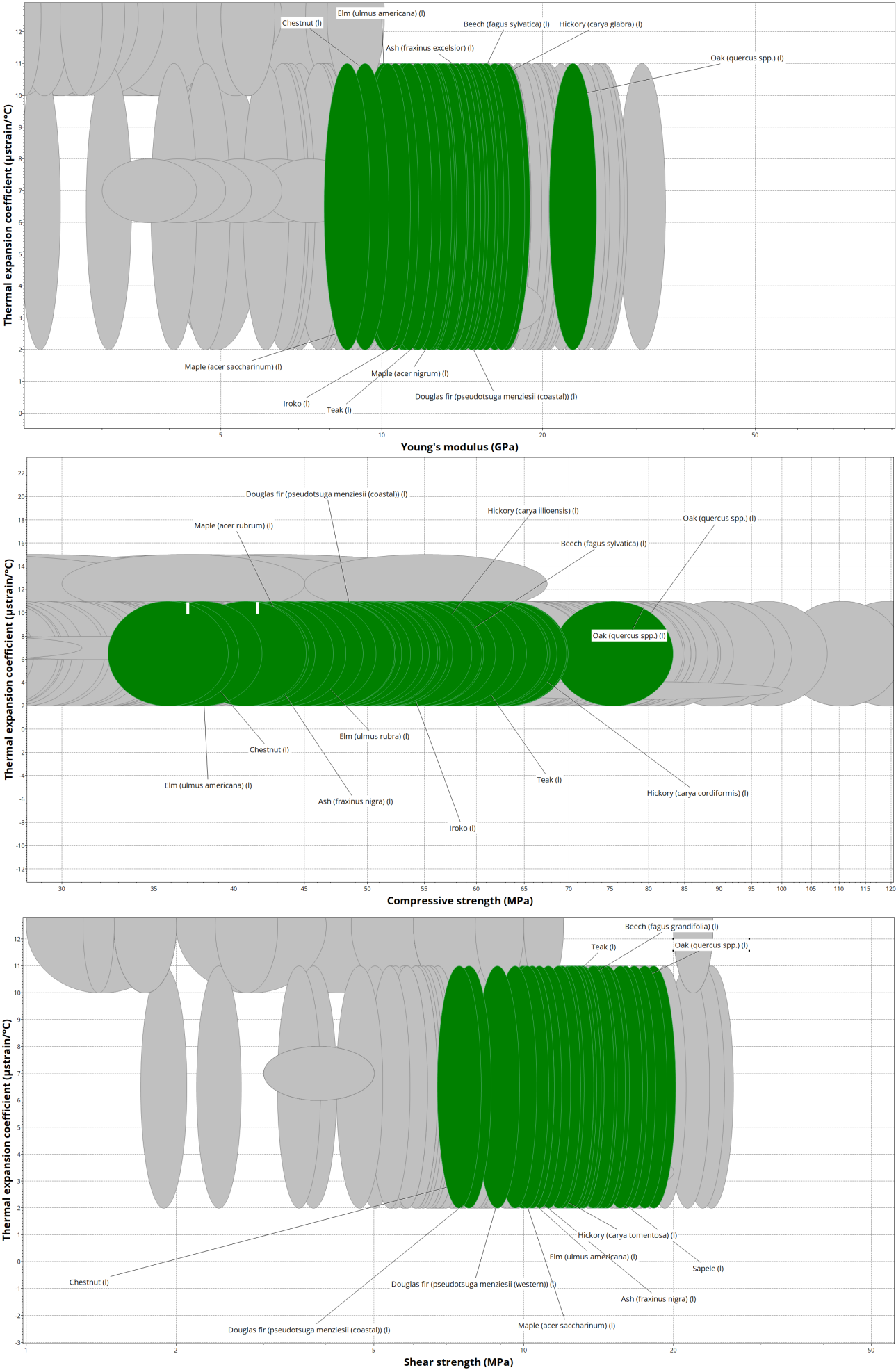
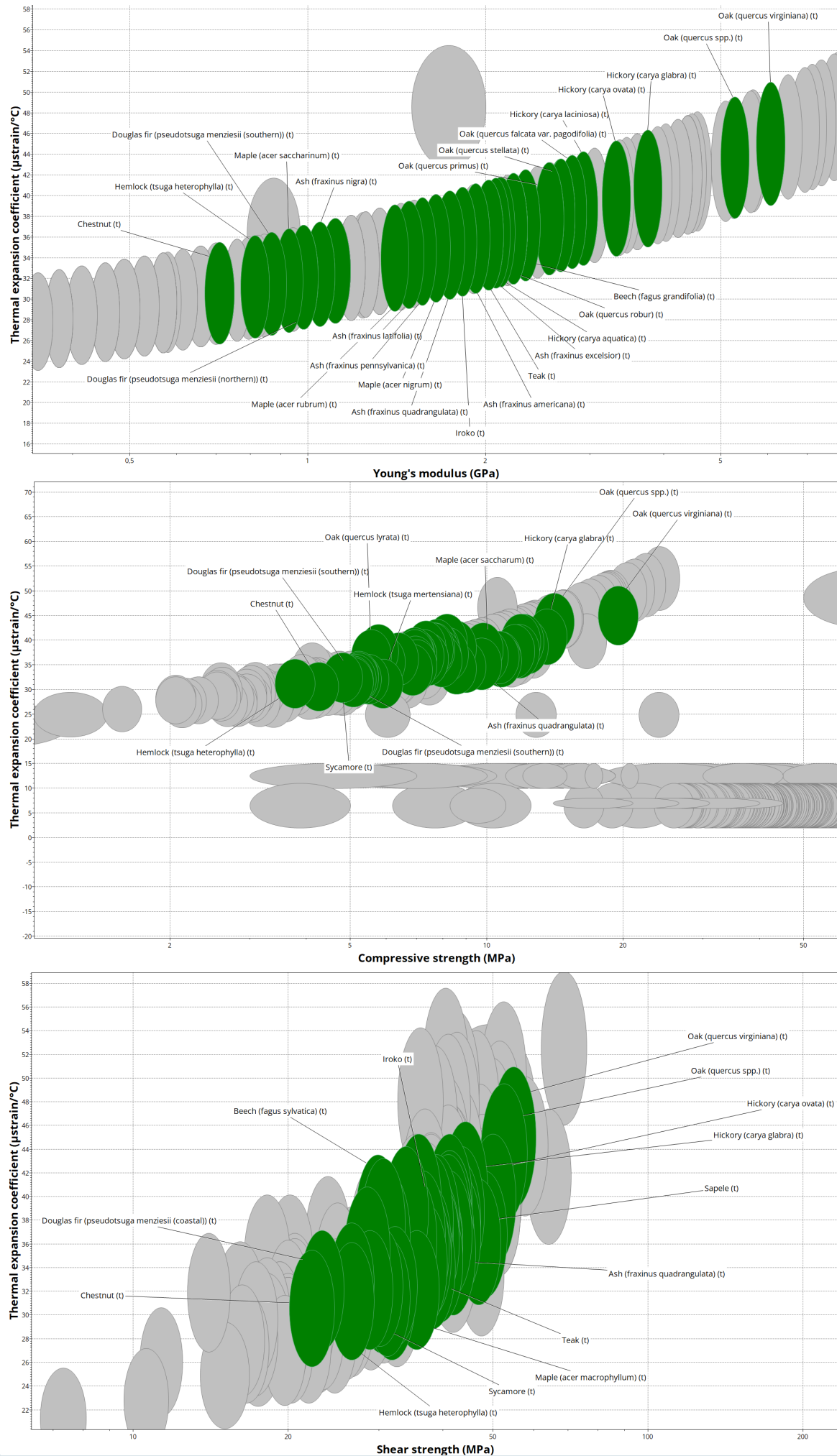


Figure 8.2.70 to 75, Granta Edu pack results in comparing hard wood species, perpendicular to grain , Source:Authors Own



Oak was selected after comparing several hardwood options due to its strong overall mechanical performance, compatibility with glass, and reliable behaviour in both directions of the grain. It offered the best balance of strength, stiffness, and thermal stability, making it a dependable and sustainable choice for this connector system.

Property	Parallel to Grain	Transverse to Grain
Compressive Strength (MPa)	~90	~15–20
Tensile Strength (MPa)	~130	~10–15
Shear Strength (MPa)	~18–19	~11–12
Young's Modulus (GPa)	20–25	5–6
Thermal Expansion ($\mu\text{strain}/^{\circ}\text{C}$)	~3.5–4.5	~35–40

Figure 8.2.76, A concise comparison table showing oak's mechanical and thermal properties in both parallel and transverse directions (based on your EduPack graphs) , Source:Authors Own

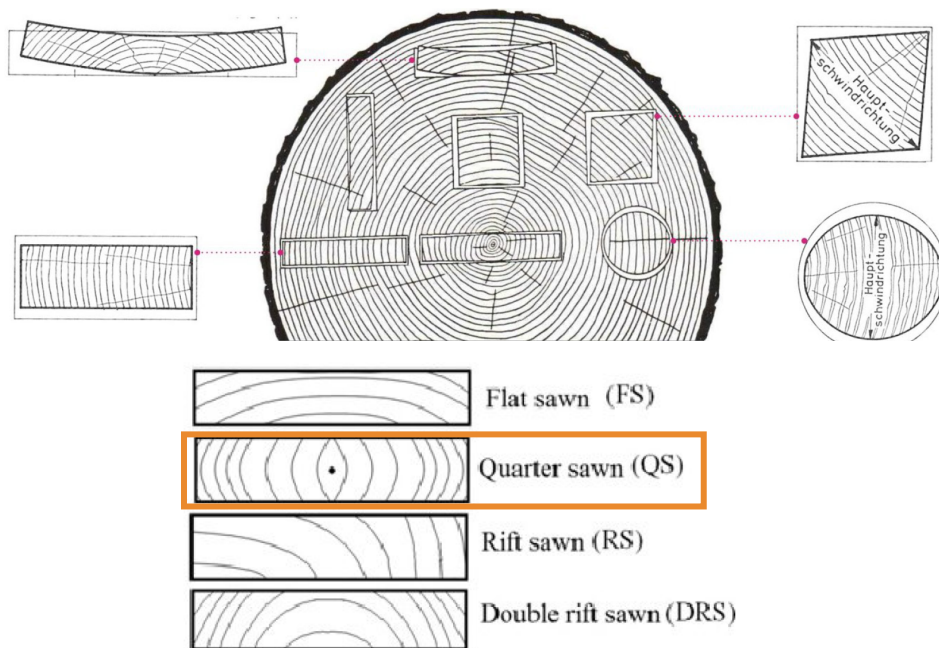


Figure 8.2.76 and 77, Timber Sawn directions, Source: <https://www.researchgate.net>

To improve dimensional stability and reduce the risk of swelling-related deformation, I selected quarter-sawn timber, and managed to use pieces cut near the heart of the log. Quarter-sawing produces boards where the growth rings are more perpendicular to the face, which results in less warping, cupping, and expansion—especially in the tangential direction. The heartwood is also typically more stable and stronger than sapwood, making it a suitable choice for this connection system, where both mechanical performance and tight tolerances are essential.

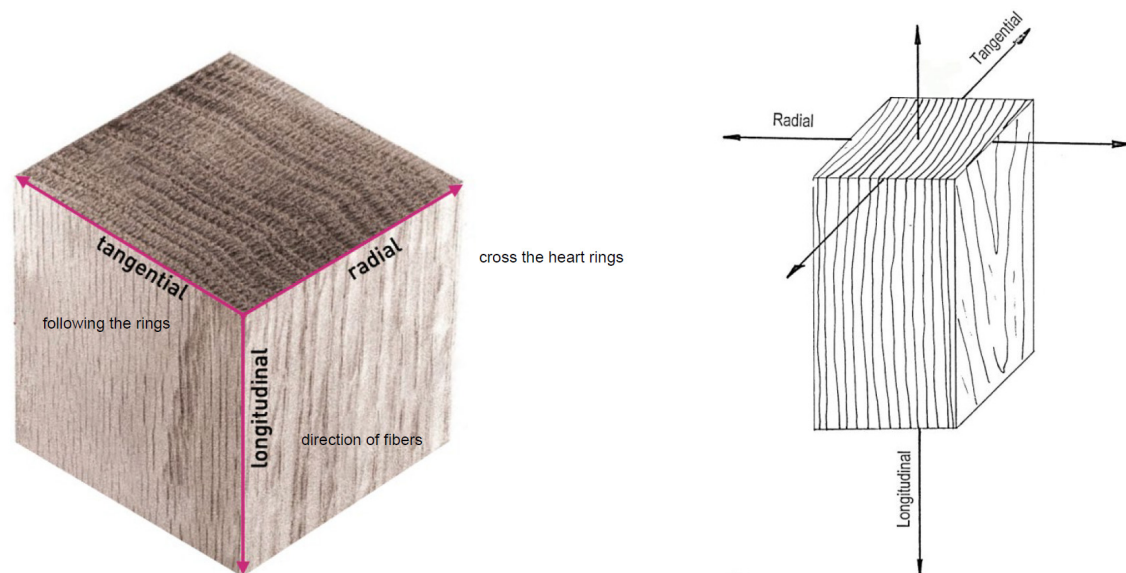


Figure 8.2.78, Wood grain direction, Source: <https://www.researchgate.net/>

After selecting the wood species, it became important to consider which cut of the timber would be used and how the grain direction would align with the applied loads. Wood has the highest strength in the longitudinal direction (along the grain), especially when resisting compression or tension. This is followed by the radial direction, while the tangential direction is the weakest in both strength and dimensional stability. In terms of swelling, wood also behaves best along the grain, followed by radial, with tangential showing the most expansion.

Due to the specific geometry of my connection design, one direction experiences compressive forces from the glass, while another is compressed by the bolt preload. For the vertical loads from the glass, I aligned the grain in the longitudinal direction to take advantage of its higher strength and lower swelling in that orientation—helping to avoid local stresses in the glass. However, I also had to ensure that the shear strength in that direction was not exceeded. The preload from the bolts acts mainly along the radial direction, which is acceptable as swelling in that direction is moderate and more predictable. The tangential direction—which is most prone to dimensional changes—was oriented where no direct load is applied, allowing it to expand more freely without affecting the structural integrity or putting stress on the glass.

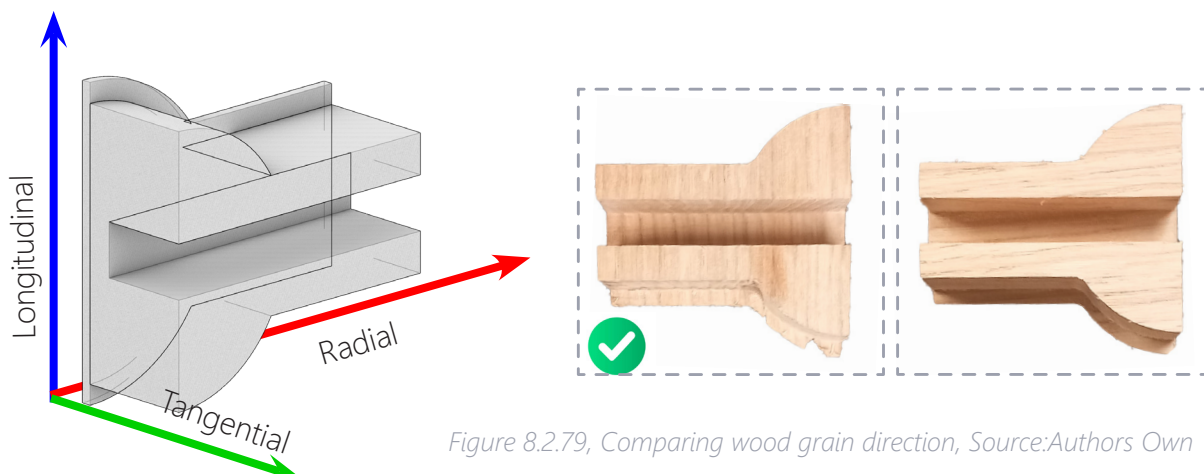


Figure 8.2.79, Comparing wood grain direction, Source: Authors Own

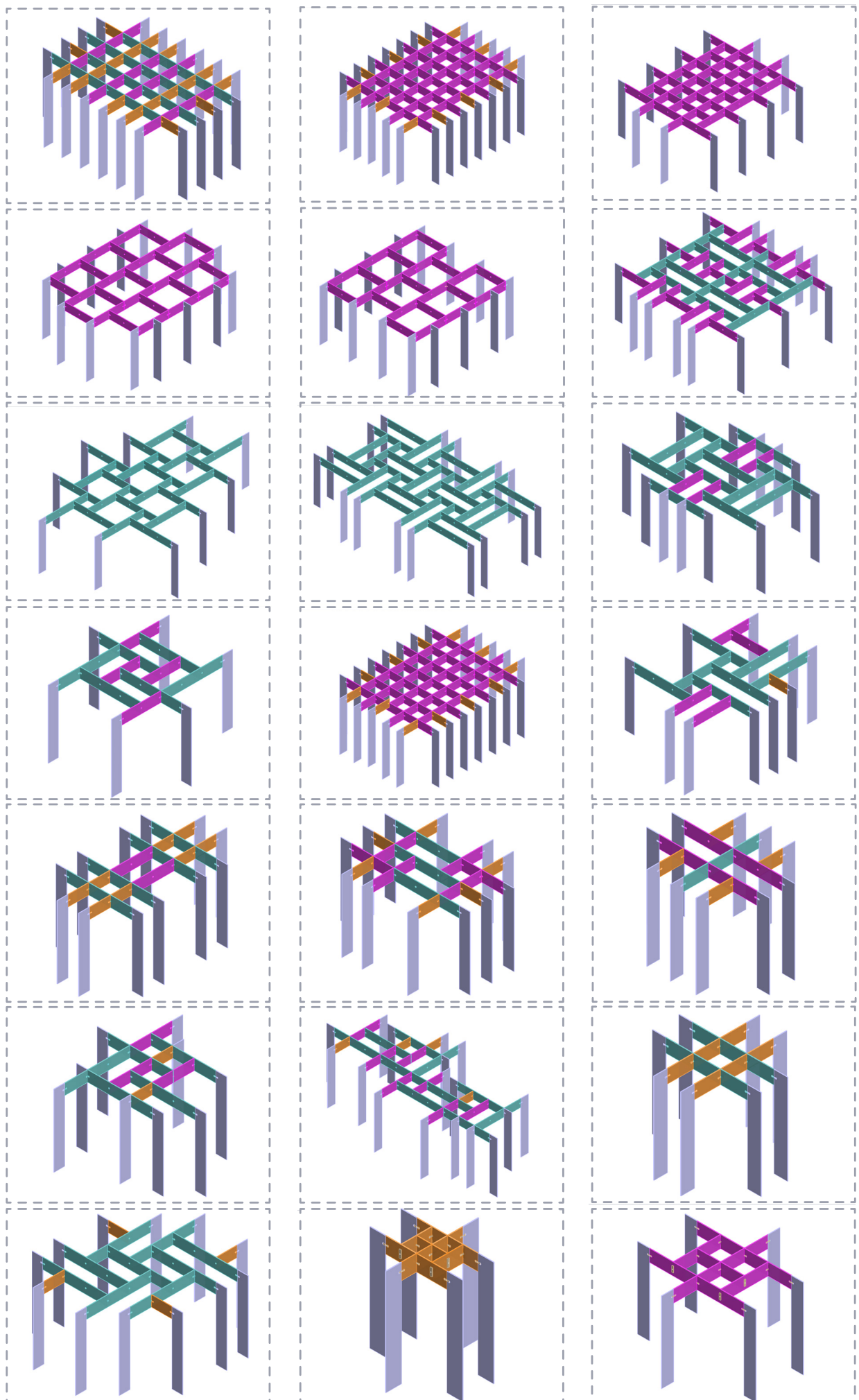


Figure 8.2.80 to 100, Variations of modular systems using defined modules and connection types, Source: Author's own

8.2. Structural Analysis

8.2.1 Primarily sizing and calculations (Glass Module)

Hand Calculations for Preliminary Sizing

To support the early design phase, a set of hand calculations was performed to estimate the appropriate cross-section dimensions of the glass modules. These calculations focused on three main aspects: bending stress, and stress concentration around bolt holes, and overall deflection. To maintain a consistent design approach, three module geometries were selected and analyzed using the same design principles. Each module was calculated individually to compare performance across different sizes and to evaluate how varying lengths and depths influence structural behavior. These estimations provided a first validation for the proposed geometry before moving on to detailed simulations.

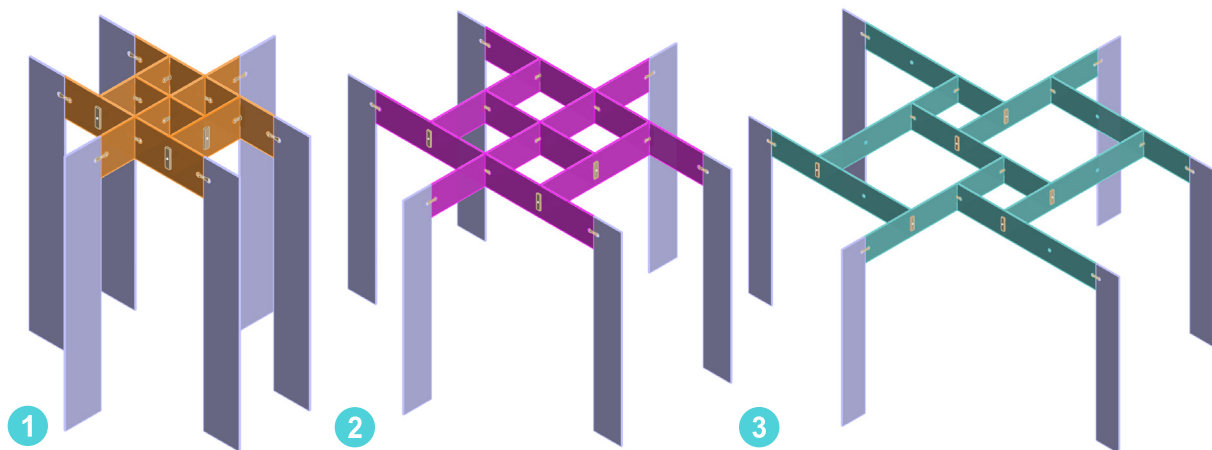
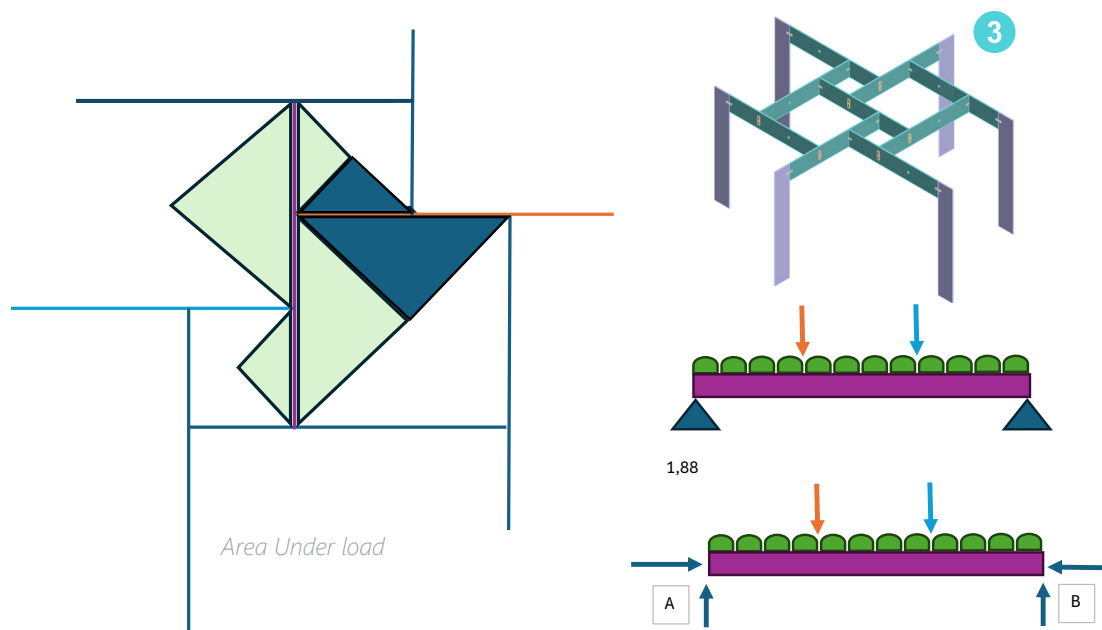
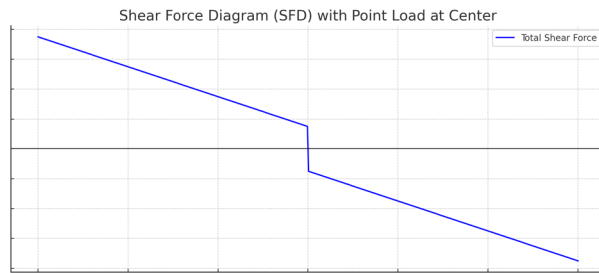


Figure 8.2.1, 3 system designs with same principle but using modules size S,M and L. . Source: Author's own

Starting with the third configuration, the loaded area and the corresponding free body diagram of the supporting beams have been illustrated below.



length	m	1,8
Depth	m	0,2
Layers of glass	-	2
Thickness of each layer	m	0,008
Total Thickness	m	0,016
Volume	m3	0,00576
Cross section area	m2	0,0032
Second Moment of Inertia	m4	1,06667E-05
Y= H/2	m	0,1
Loading area	m2	0,9



LOADS

Maintenance Load	KN/m2	0,5	KN/m	0,25
Snow Load	Kpa(KN/m2)	0,6	KN/m	0,3
Panel loads	KN/m2	0,2	KN/m	0,1
Self weighth	KN	0,144	KN/m	0,08
Point Load	KN	0,657	KN/m	0,19

UDL on panel	1,3	KN/m2
	1,17	KN

ULS

factored loads		
Snow Load	0,45	KN/m
Maintenance load	0,375	KN/m
Panel loads	0,135	KN/m
Self weighth	0,108	KN/m
Point Load	0,88695	KN

SLS

factored loads		
Snow Load	0,3	KN/m
Maintenance Load	0,25	KN/m
Panel loads	0,1	KN/m
Self weighth	0,108	KN/m
Point Load	0,657	KN

Max Bending Moment

M max UDL	0,43254	KNm
M max point	0,57672	KNm
M total	1,00926	KNm

$$\sigma_{\max} = M_{\max} \cdot y/I$$

σ Applied stress	9461,813	KN/m2	9461,8125
	9,461813	Mpa	

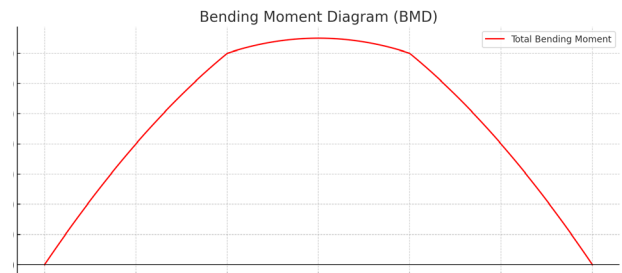
$$\sigma_{\max} = f_{gd}$$

$$W = M_{\max} / \sigma_{\max} = 6bh^2$$

$$\text{assuming } b$$

$$h$$

$$W = I/Y ; y = \text{depth}/2$$



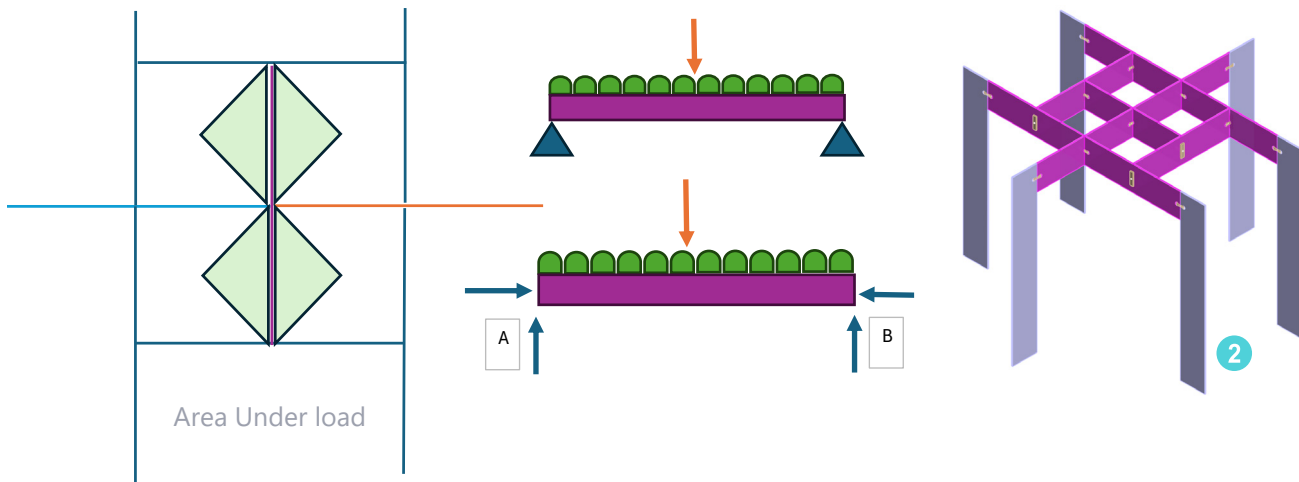
$$f_{gd} = \frac{k_e \cdot k_{sp} \cdot k_A \cdot k_{mod} \cdot f_{gk}}{\gamma_m} + \frac{k_p \cdot k_{ep} \cdot f_{pk}}{\gamma_p}$$

fgd	22,25	Mpa	N/mm2
	22250	KN/m2	
	640,8	KN	

Utilization Ratio 42,525

Max Deflection

δ max UDL	8,326E-05	m	0,083257333	mm
δ max Point	6,304E-05	m	0,063042589	mm
δ max total	0,0001463	m	0,146299922	mm
δ max Allowed	L/250	0,0072	m	7,2 mm



length	m	1,2
Depth	m	0,2
Layers of glass	-	2
Thickness of each layer	m	0,008
Total Thickness	m	0,016
Volume	m3	0,00384
Cross section area	m2	0,0032
Second Moment of Inertia	m4	1,07E-05
Y= H/2	m	0,1
Loading area	m2	0,36

LOADS

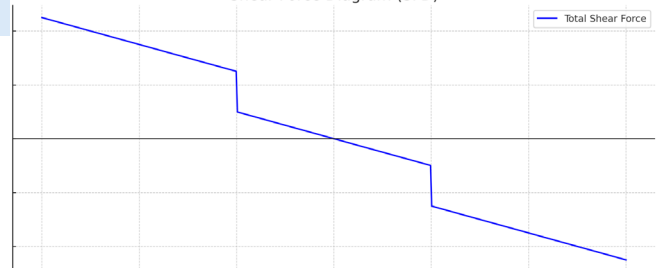
Maintenance Load	KN/m2	0,5	KN/m	0,15	UDL on panel	1,3	KN/m2
Snow Load	Kpa(KN/m2)	0,6	KN/m	0,18		0,468	KN
Panel loads	KN/m2	0,2	KN/m	0,06	two side point load	0,564	KN
Self weigth	KN	0,096	KN/m	0,08			
Point Load	KN	0,282	KN/m	0,13			

ULS

factored loads

Snow Load	0,27	KN/m
Maintenance load	0,225	KN/m
Panel loads	0,081	KN/m
Self weigth	0,108	KN/m
Point Load	0,3807	KN

Shear Force Diagram (SFD)



SLS

factored loads

Snow Load	0,18	KN/m
Maintenance Load	0,15	KN/m
Panel loads	0,06	KN/m
Self weigth	0,108	KN/m
Point Load	0,282	KN

Max Bending Moment

M max UDL	0,12312	KNm
M max point	0,16416	KNm
M total	0,28728	KNm

$$\sigma_{\max} = M_{\max} \cdot y / I$$

σ Applied s	2693,25	KN/m2	2693,25
	2,69325	Mpa	

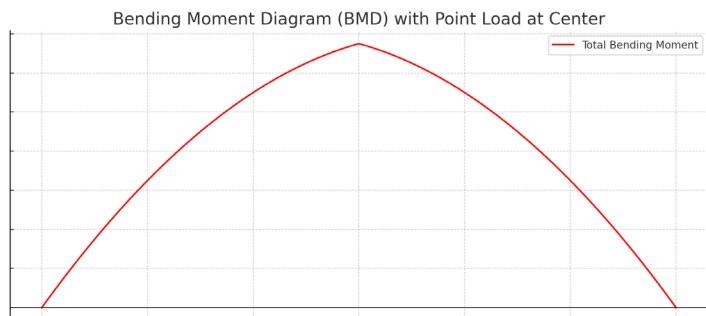
$$\sigma_{\max} = f_{gc} \quad 427,2$$

$$W = M_{\max} / \sigma_{\max} = 6bh: \quad 0,000672 \quad m^3$$

$$\text{assuming } l \quad m \quad 0,016$$

$$h \quad m \quad 0,083695$$

$$W = I / Y; y = c \quad m^3 \quad 0,000107 \quad 0,000107$$



Max Deflection

δ max UDL	1,08E-05	m	0,010805	mm
δ max Point	1,23E-05	m	0,012272	mm
δ max total	2,31E-05	m	0,023077	mm

δ max Allow	L/250	0,0048	m	4,8	mm
--------------------	-------	--------	---	-----	----

$$f_{gd} = \frac{k_e \cdot k_{sp} \cdot k_A \cdot k_{mod} \cdot f_{gk}}{\gamma_m} + \frac{k_p \cdot k_{ep} \cdot f_{pk}}{\gamma_p}$$

fgd	22,25	Mpa	N/mm2
	22250	KN/m2	
	427,2	KN	

$$K_t = 1.5 + 1.25 \left(\frac{H}{d} - 1 \right) - 0.0675 \left(\frac{H}{d} \right)$$

Where the stress concentration factor

$$K_t = \frac{\sigma_{\max} (H - d) t}{P}$$

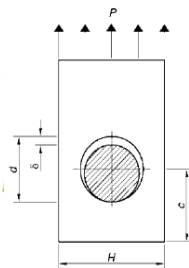


Fig 6.12 Pin and lug notation

Min clear edge distance = 1,5*t	0,024	m
Min clear corner distance = 4*t	0,064	m
Min clear bolt spacing = 4*t	0,064	m
Min Hole Diameter >= t	0,016	m

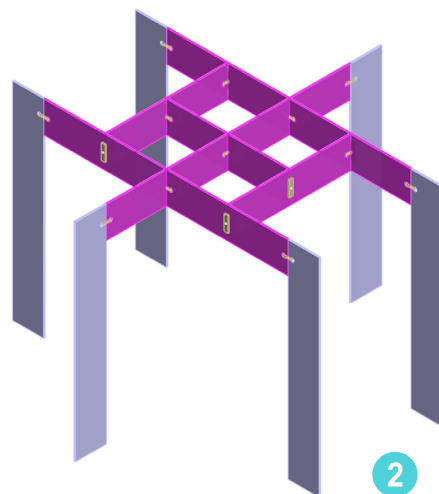
H	0,2 m
d	0,017 m

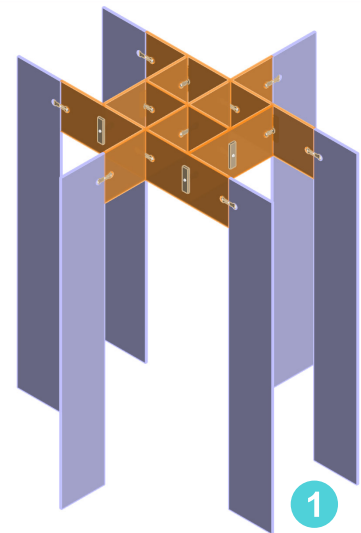
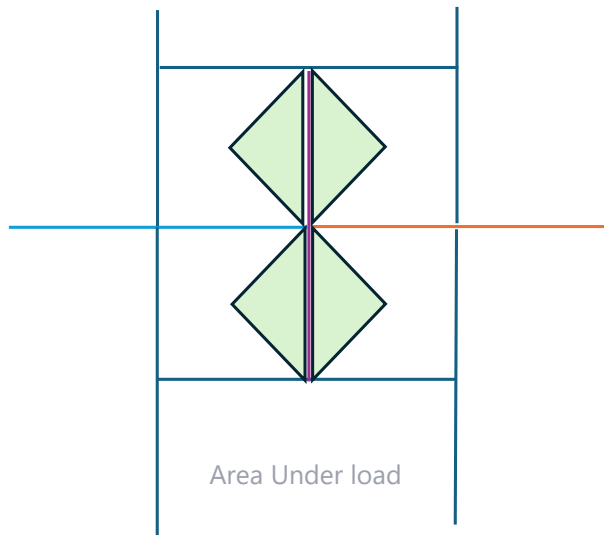
$$K_t \quad 7,134057$$

σ_{\max}	927,5736	KN/m2
	0,927574	N/mm2

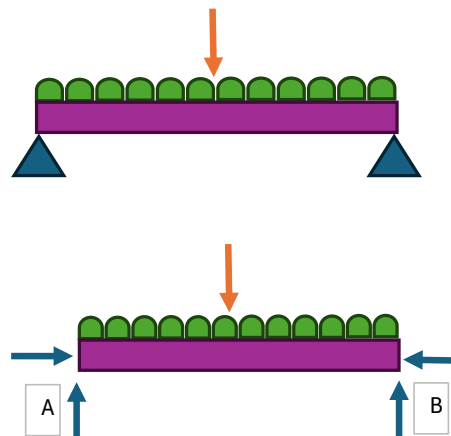
area	441,23	mm2
under		
stress(Pre	0,862815	N/mm2
ssure) on	862815,3	Pa

Utilization 12,10449





length	m	0,6
Depth	m	0,2
Layers of glass	-	2
Thickness of each layer	m	0,008
Total Thickness	m	0,016
Volume	m3	0,00192
Cross section area	m2	0,0032
Second Moment of Inertia	m4	1,07E-05
Y= H/2	m	0,1
Loading area	m2	0,09



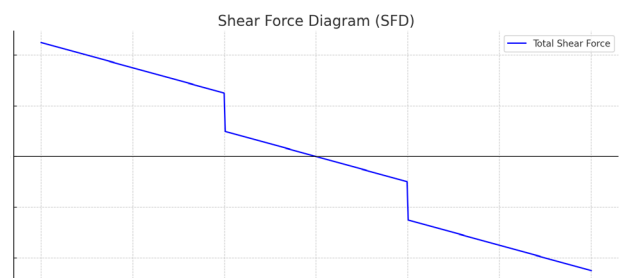
LOADS

Maintenance Load	KN/m2	0,5	KN/m	0,075	UDL on panel	1,3	KN/m2
Snow Load	Kpa(KN/m2)	0,6	KN/m	0,09		0,117	KN
Panel loads	KN/m2	0,2	KN/m	0,03	two side point load	0,165	KN
Self weigth	KN	0,048	KN/m	0,08			
Point Load	KN	0,0825	KN/m	0,085			

ULS

factored loads

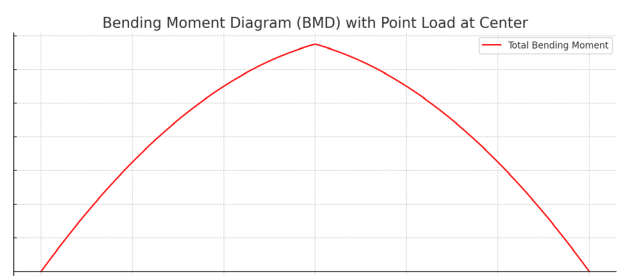
Snow Load	0,135	KN/m
Maintenance load	0,1125	KN/m
Panel loads	0,0405	KN/m
Self weigth	0,108	KN/m
Point Load	0,111375	KN



SLS

factored loads

Snow Load	0,09	KN/m
Maintenance Load	0,075	KN/m
Panel loads	0,03	KN/m
Self weigth	0,108	KN/m
Point Load	0,0825	KN



Max Bending Moment

M max UDL	0,01782	KNm
M max point	0,02376	KNm
M total	0,04158	KNm

$$\sigma_{\max} = M_{\max} \cdot y / I$$

σ Applied s	389,8125	KN/m2	389,8125
	0,389813	Mpa	

$\sigma_{\max} = f_{gc}$	213,6		
$W = M_{\max} / \sigma_{\max} = 6bh^3$	0,000195	m3	
assuming t	m	0,016	
h	m	0,04503	
$W = I / Y ; y = c$	m3	0,000107	0,000107

$$f_{gd} = \frac{k_e \cdot k_{sp} \cdot k_A \cdot k_{mod} \cdot f_{gk}}{\gamma_m} + \frac{k_p \cdot k_{ep} \cdot f_{pk}}{\gamma_p}$$

Ke	1			
Ksp	1			
KA	1	1,353772		
Kmod	0,29			
fgk	45	Mpa		
Ym	1,8			
Kp	1			
Kep	0,6			
		Fully	heat	
		Thoughe	strengthen	
		d	ed	
fpk	40	40	90	Mpa
Yp	1,6	1,6	1,8	

fgd	22,25	Mpa	N/mm2
	22250	KN/m2	
	213,6	KN	

Utilization 1,751966

Max Deflection

δ max UDL	4,11E-07	m	0,000411	mm
δ max Point	9,33E-07	m	0,000933	mm
δ max total	1,34E-06	m	0,001344	mm

δ max Allo	L/250	0,0024	m	2,4	mm
-------------------	-------	--------	---	-----	----

$$K_t = 1.5 + 1.25 \left(\frac{H}{d} - 1 \right) - 0.0675 \left(\frac{H}{d} \right)$$

Where the stress concentration factor

$$K_t = \frac{\sigma_{\max} (H-d)t}{P}$$

Fig 6.12 Pin and lug notation

Min clear edge distance = 1,5*t	0,024	m
Min clear corner distance = 4*t	0,064	m
Min clear bolt spacing = 4*t	0,064	m
Min Hole Diameter >= t	0,016	m

H	0,2 m
d	0,017 m

Kt	7,134057
----	----------

σ_{\max}	271,3646	KN/m2
	0,271365	N/mm2

area	441,23	mm2
under		
stress(Pre	0,252419	N/mm2
ssure) on		252419,4 Pa

8.2.2 Detailed analysis and calculations (Connection)

Load Path: From General to Detail

In this structural system, the load path begins at the glass roof panels, where vertical loads such as self-weight and live loads are applied. These forces are transferred into the glass beams or modules, which carry the loads longitudinally. From there, the loads are passed through the timber-glass friction fit connections, which act as critical transfer points. The preloaded bolts within the wooden connectors ensure contact and friction, helping to distribute shear and compressive forces effectively. These connections then pass the loads into the adjacent modules, continuing the flow across the reciprocal roof structure, and ultimately transferring the loads into the supporting fins or columns. On a detailed level, the stress is concentrated around the bolt holes and contact surfaces, especially in the wooden connectors

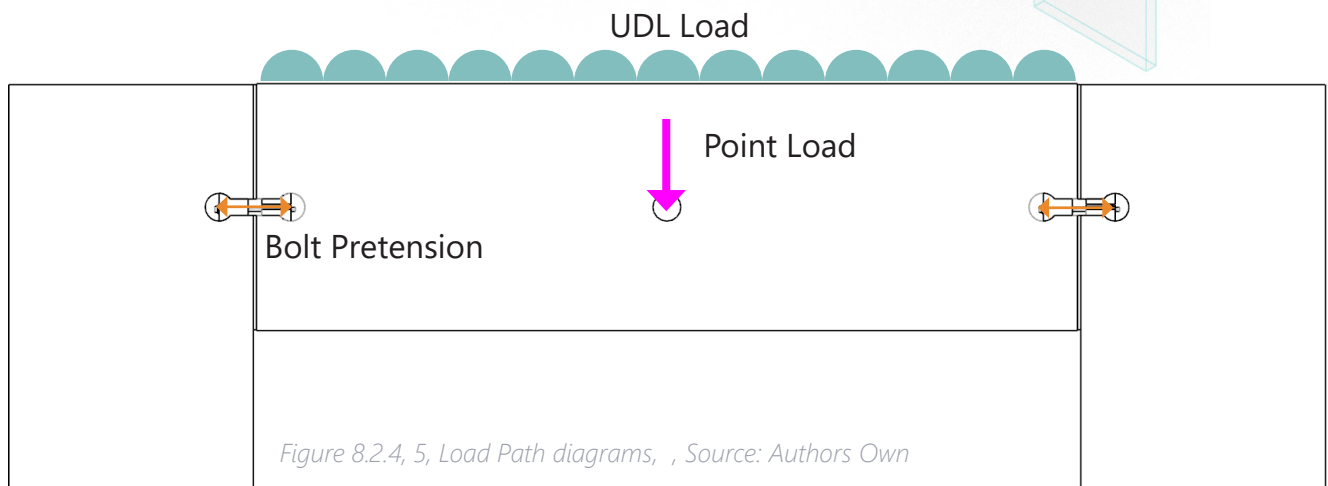
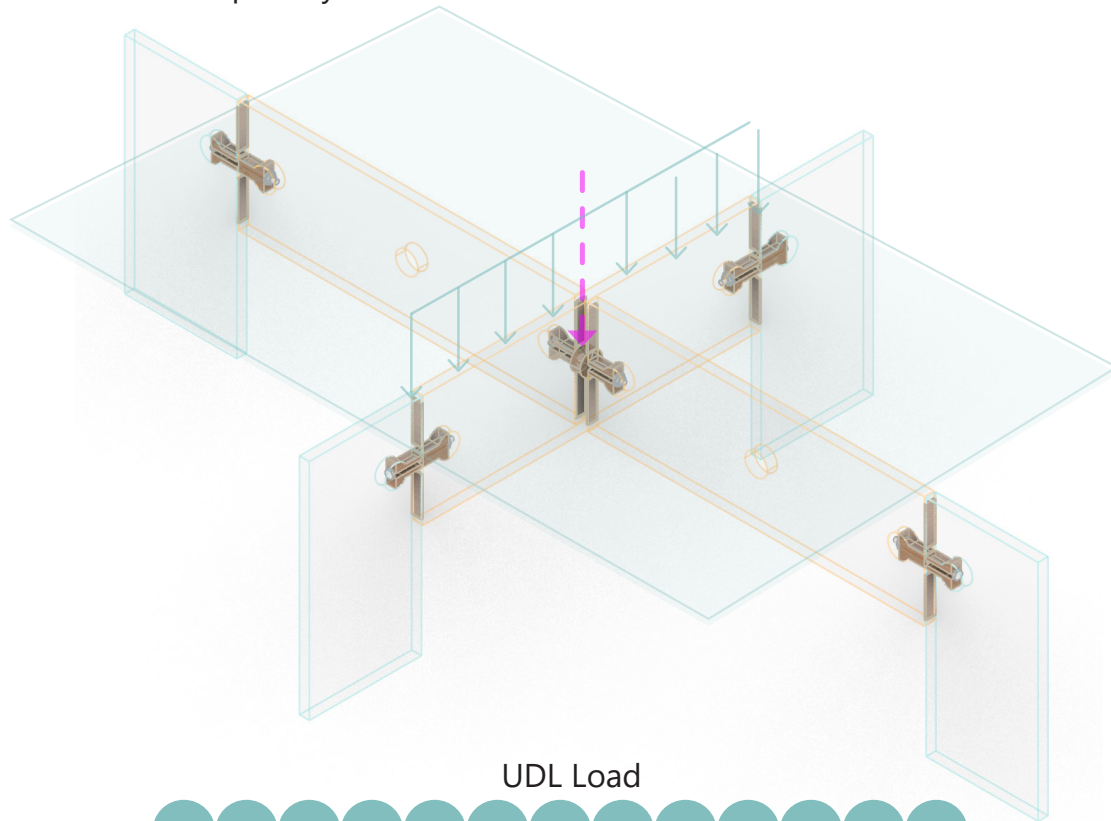
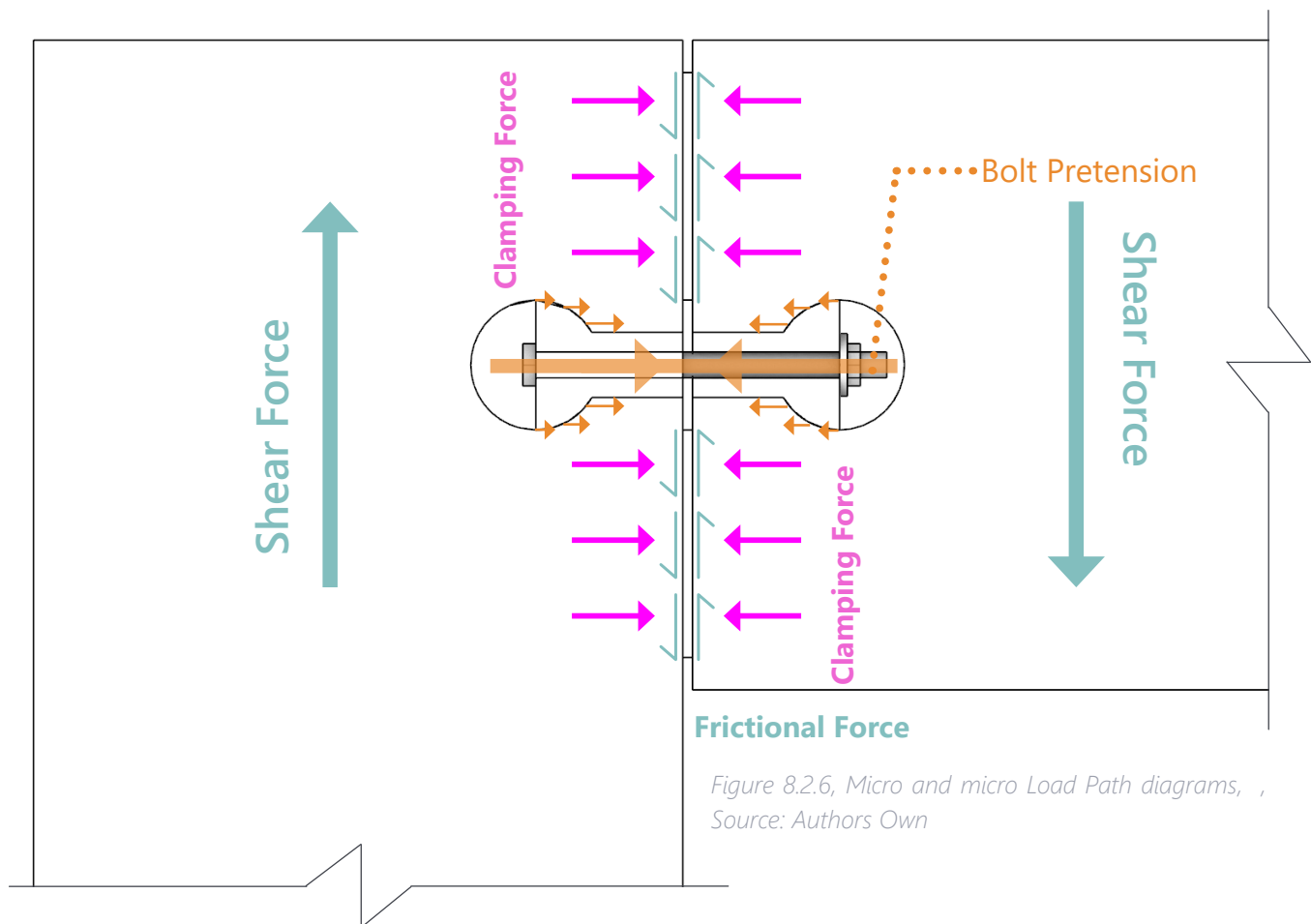


Figure 8.2.4, 5, Load Path diagrams, , Source: Authors Own



At the module level, the load is resisted primarily through the clamping force generated by the preload in the bolts, which presses the wooden connectors tightly against the glass panels. This results in a frictional force at the interface between the wooden strips and the glass surfaces. Together, the bolt pretension and frictional contact allow the system to resist shear forces effectively, without relying on direct tension in the glass or chemical bonding. This dry, mechanical friction fit approach not only supports the structural behavior but also aligns with the project's goal of creating a fully demountable and reusable connection system.

1. Calculations (Clamp force, Preload , Friction force)

$F = \mu \cdot N$

Frictional Force ← Normal Force

Friction coefficient

UDL Loads converted to point load=0.117kN

Point loads= 0.170 KN

Total loads= 0.285KN

Therefore, to ensure that the connection can resist the applied shear forces through friction alone, the clamping force (produced by the bolt preload) must be equal to or greater than the shear force divided by the friction coefficient between the wood and glass. This relationship can be expressed as:

$$\begin{aligned} F_{\text{Clamp}} &= F_{\text{Preload}} \\ F_{\text{Friction}} &= F_{\text{Shear}} \end{aligned}$$

$$F_{\text{clamp}} \geq \frac{F_{\text{shear}}}{\mu}$$

Coefficient of friction (typically around 0.4 for wood–glass interface)

$$0.285 / 0.4 = 0.7125 \text{ kN}$$

This equation was used to determine the minimum preload needed in the bolts to prevent slippage and ensure safe load transfer through friction.

2. Preload calculation in bolt:

- **Proof strength = 0.85 * yield strength**

$$0.85 * 275 = 233.75 \text{ MPa}$$

Choosing a random bolt, M8

- **Proof strength = F / At**

$$285 \text{ N} / 50.3 \text{ mm}^2 = 5.66 \text{ MPa}$$

$$\text{Proof strength} = 233.75 \text{ MPa} > 5.66 \text{ MPa},$$

Then the bolt is enough and safe for this loads.

- **Proof Load = Proof strength * At**

$$233.75 * 50.3 = 1157.625 \text{ N}$$

- **Preload = 0.75 * Proof Load**

Then the **maximum preload allowed to apply to** this specific bolt M8 is,

$$1157.625 * 0.75 = 881.821 \text{ N}$$

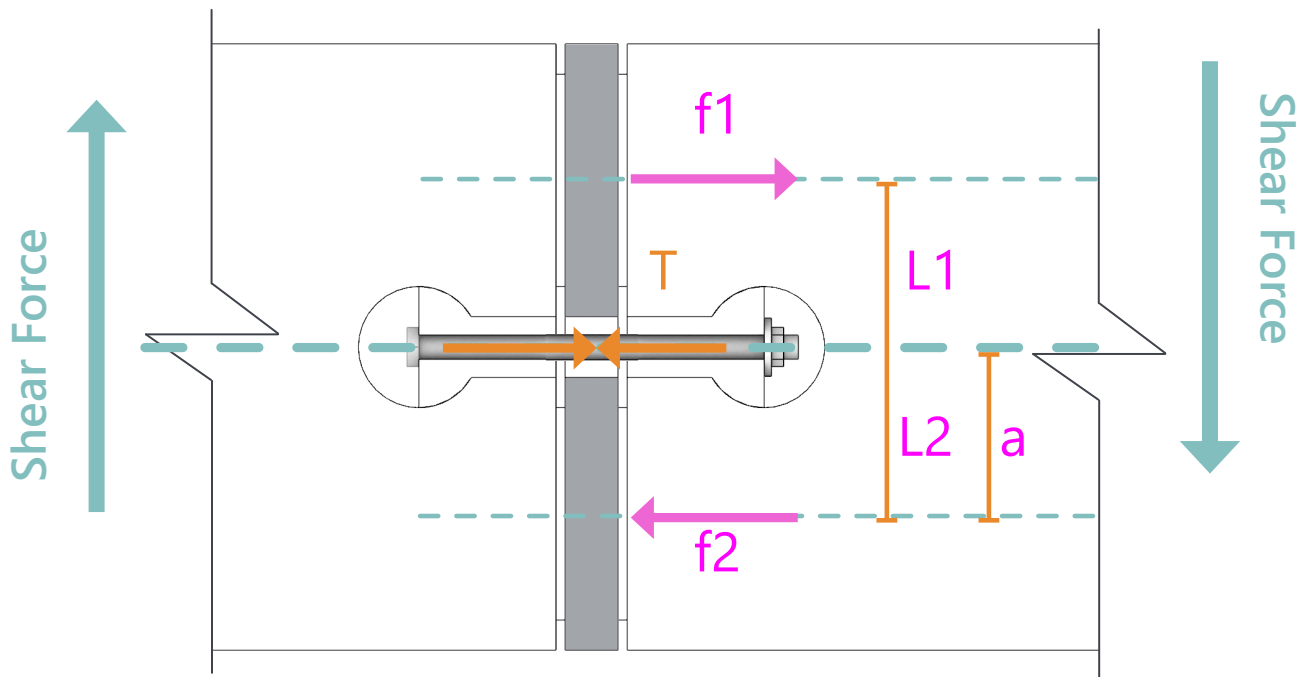


Figure 8.2.7, Internal tension and compression and lever arm diagram , Source: Authors Own

- $M_s = F \cdot \text{Length of beam} / 4$

$$0.285 \text{ KN} \cdot 0.6 \text{ m} / 4 = 0.042 \text{ KNm}$$

- $f_1 = f_2 = M_s / L_1 \text{ or } L_2$

$$0.042 \text{ KNm} / 0.1 \text{ m} = 0.42 \text{ KN}$$

- $\text{Preload} = f_1 / 0.4$

$$0.42 \text{ KN} / 0.4 = \mathbf{1.068 \text{ KN}}$$

The **final amount of preload needed** to apply to the **smallest module's each side** bolt to resist its responding loads.

3. Torque calculation:

$$T = K \cdot F \cdot d$$

- F = normal force
- T = torque
- K = torque coefficient
- d = bolt diameter

$$T = 0.2 \cdot 1068 \cdot 8 = 1.708 \text{ Nmm}$$

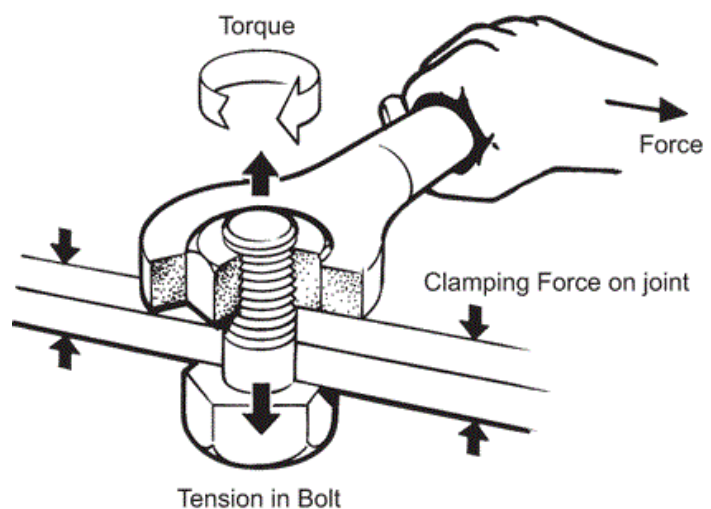
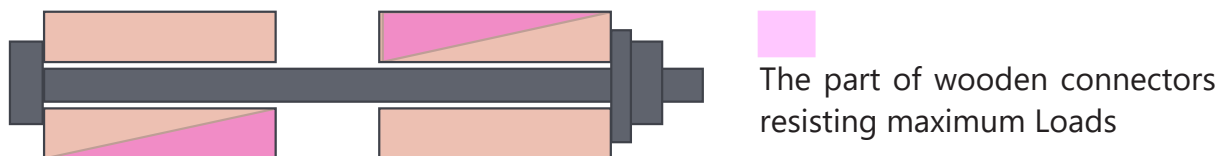


Figure 8.2.8, Torque diagram , Source: <https://smartbolts.com/>

Based on the micro-level load path within the joints, the most critical stress concentrations are expected to occur in two primary regions: the bottom face of the supporting module's connector and the top face of the connector belonging to the supported module, as illustrated in the figure below. These areas are subject to the highest compressive stresses during load transfer. Therefore, they must be specifically evaluated in the ANSYS simulation to ensure that the compressive stresses do not exceed the allowable strength of the wood in the corresponding fibre direction. This verification is essential to ensure structural safety and material integrity under service conditions.



Due to the preloading applied to the bolts and the nature of the shear forces acting on the module, the connection initially resists external loads through friction alone. As long as the applied loads remain below the frictional resistance created by the bolt preload, the system maintains stability without direct stress on the bolt body. However, once the external load surpasses the friction capacity, the system transitions to a second stage of resistance in which the load is transferred directly to the bolt. In this case, shear forces act on the bolt cross-section, causing it to deform as illustrated in the diagram below.

Although this scenario is not ideal from a long-term performance perspective, it provides an additional safety mechanism. If the system experiences loading beyond its design limit, the bolts still offer a secondary means of load transfer, helping to protect the structure from sudden failure.

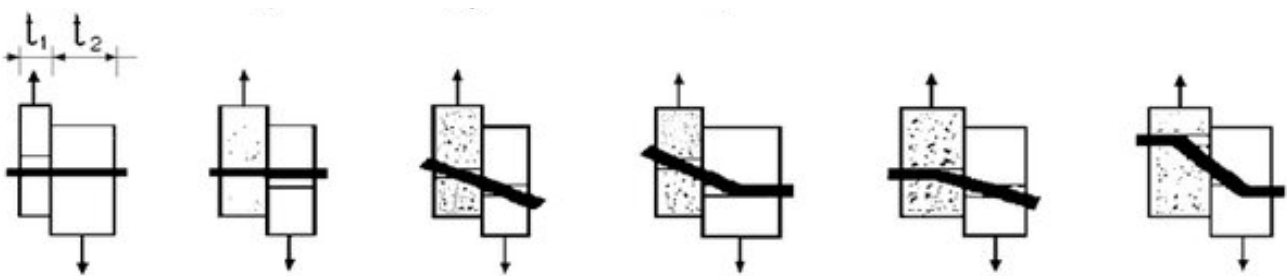


Figure 8.2.9, Single shear connection diagram, max stress in wood, and bolt deformation , Source: Authors Own

8.2.3 System analysis (Karamba 3D)

Based on the project objectives, the design focuses on creating a pavilion intended for an interior exhibition space, using the defined modules and connection system. A key requirement is that the structure can be disassembled and reassembled in different configurations for outdoor use as well. To demonstrate this adaptability, two different forms have been designed using the same modules and connection types. These variations will be structurally analyzed in Karamba to evaluate whether they meet the required performance criteria in terms of stress and displacement for the chosen spans.

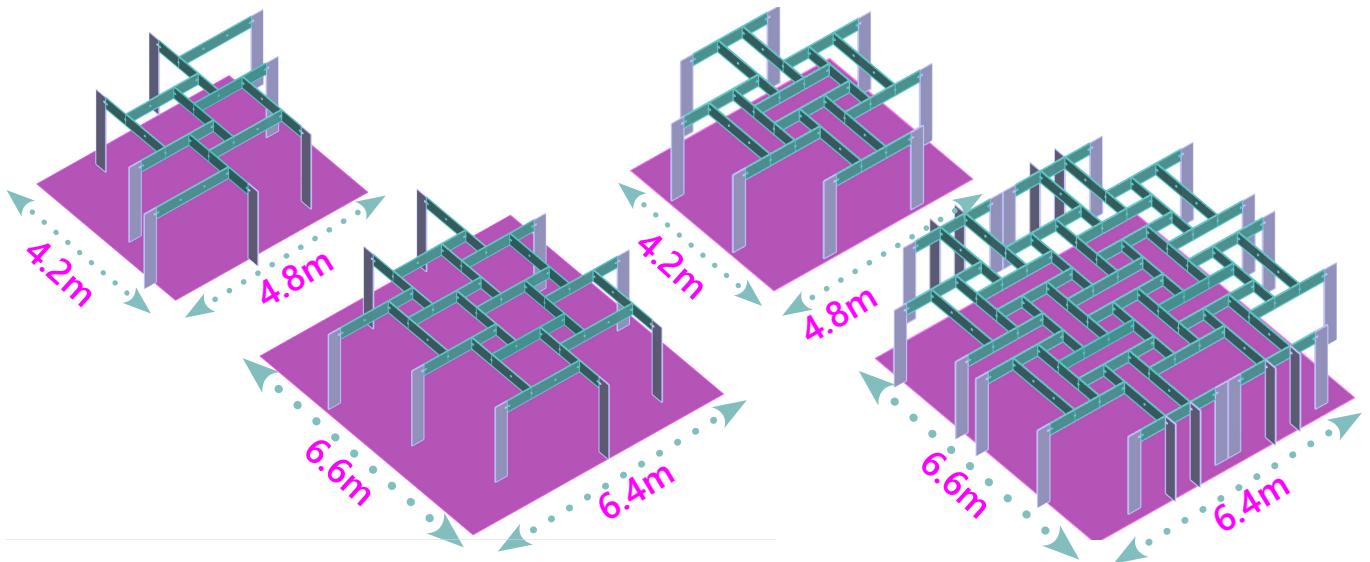


Figure 8.2.10, 2 variation with same modules for two spanning scenarios, Source: Author's own

Set ups in Karamba

1. Material Properties

Note on Glass Thickness Assumption:

Although the actual design incorporates a safety factor by doubling the nominal glass thickness to 16 mm—to account for accidental breakage and unforeseen loads—all structural calculations and simulations in this thesis were conservatively carried out using an 8 mm glass thickness. This approach ensures that the system remains structurally safe even under worst-case scenarios.

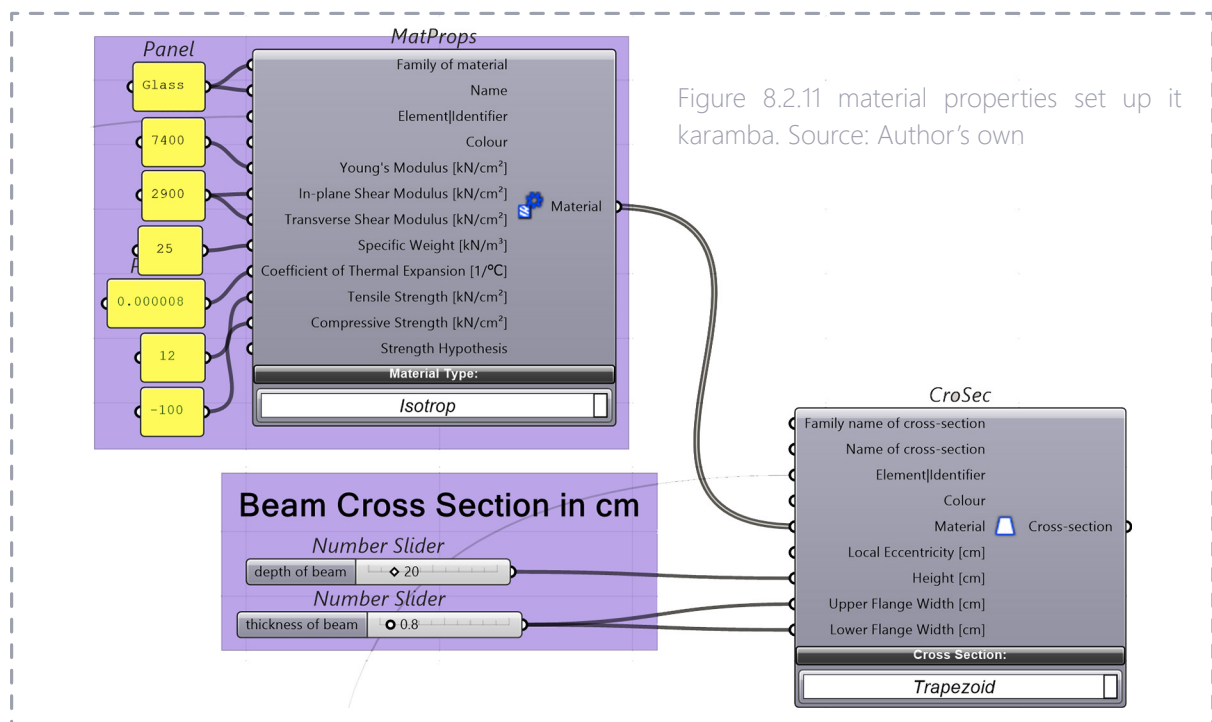
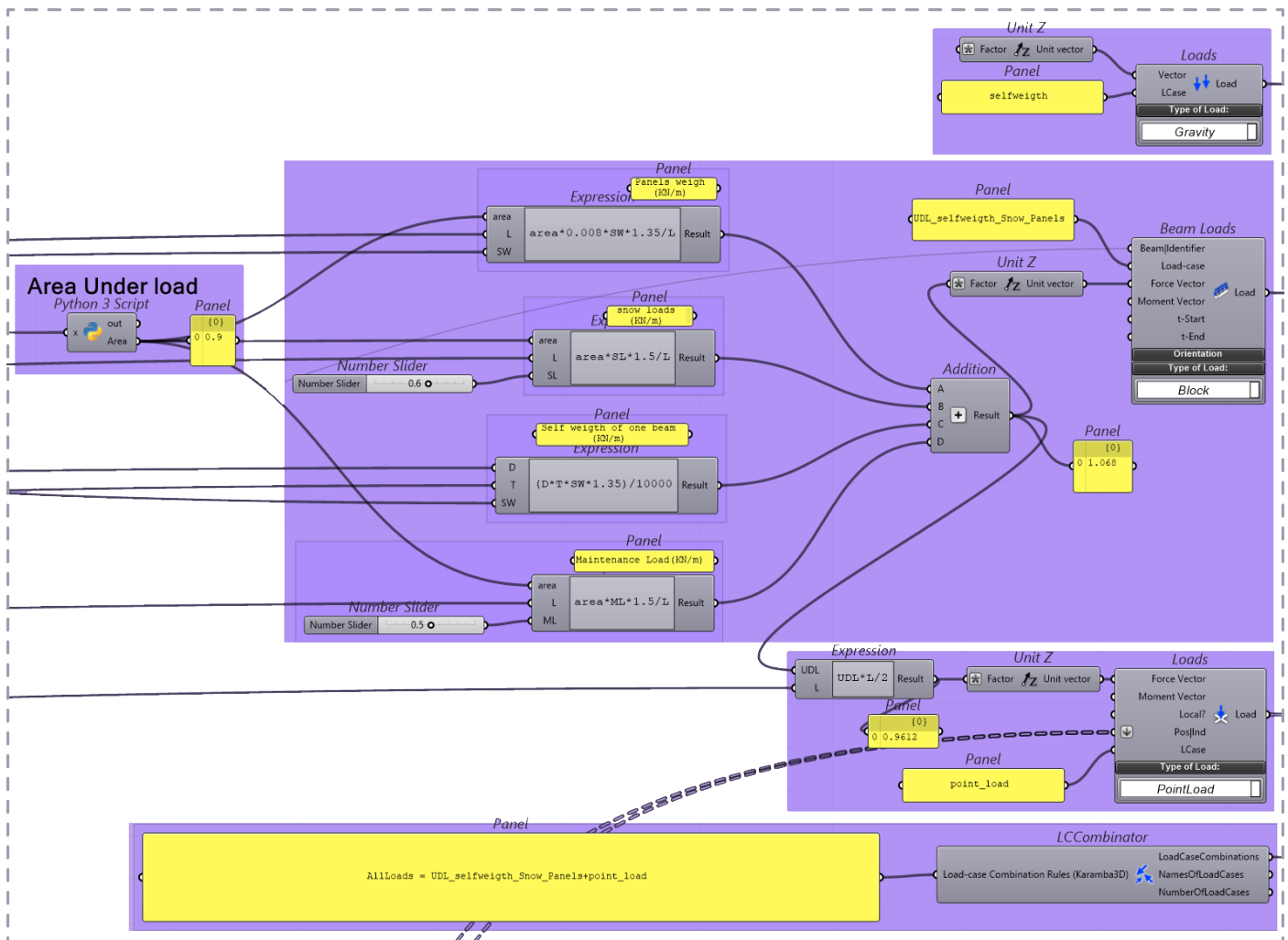


Figure 8.2.11 material properties set up in karamba. Source: Author's own

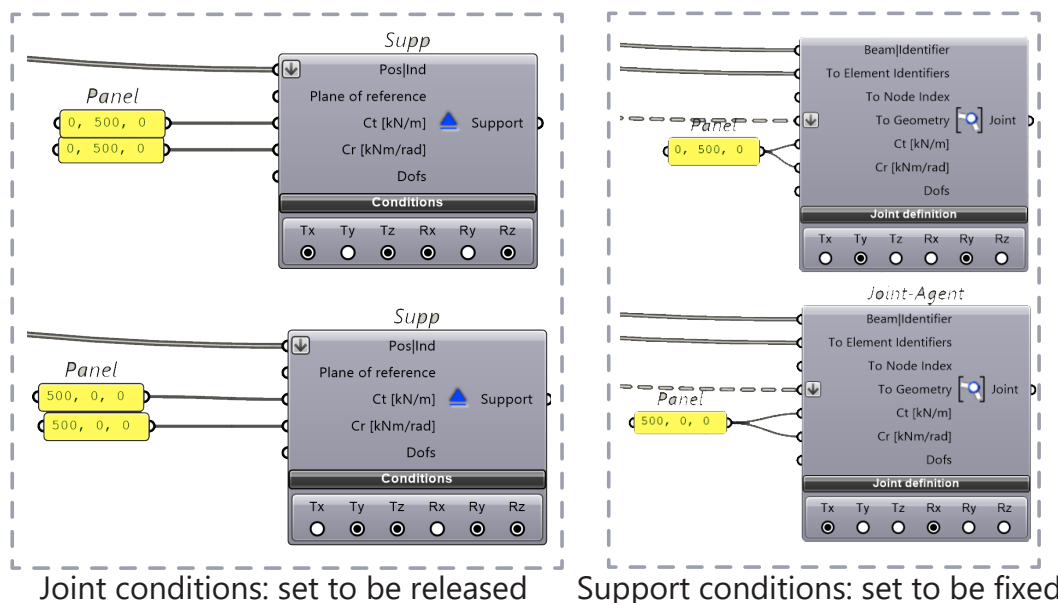


- Initial joint-stiffness input for Karamba

In Karamba 3D each Support or Joint-Agent can be given a spring in any individual degree of freedom. For the oak-glass "dog-bone" connector this is essential, because the joint is neither a perfect hinge nor a rigid weld: up to a very small slip it behaves as a stiff friction-fit, after which it slides.

To represent that "semi-rigid" behaviour I need two initial-tangent springs:

a translational stiffness C_t and a rotational stiffness C_r Both are taken directly from calculations based on the results of Force against movement in the laboratory test.



- Initial joint-stiffness input for Karamba

The joint behaves as a friction-fit that is practically rigid up to the first perceptible movement and then softens as slip develops. To capture that behaviour in Karamba the initial elastic (tangent-) stiffness is taken from the earliest portion of the laboratory shear-slip curve and expressed as two linear springs:

a translational spring C_t acting in the slip direction

a rotational spring C_r acting about the same plane

The three central load steps (still within the stick phase) are used to obtain representative secant values; averaging removes scatter and gives a single, conservative spring for the FE model.

Step	Shear FF(kN)	Slip Δ (mm)	$C_t = F / \Delta C_t$ (kN m ⁻¹)	Rotation $\theta = \Delta / 115$ (rad)	$C_r = M / \theta C_r$ (kN m rad ⁻¹)
2	1.5	4	375	0.0348	460
3	2.3	5	460	0.0435	370
4	3	6	500	0.0522	308

Governing formulae

$$C_t = \frac{F}{\Delta}, \quad C_r = \frac{2\mu Nr}{\theta}, \quad \theta = \frac{\Delta}{2r}$$

where

$\mu = 0.40$ (static friction glass–oak)

$N = 3.5$ kN (bolt preload from 5.5 N·m tightening torque)

$r = 57.5$ mm (half the 115 mm pad spacing)

* Gauge length = $2r = 115$ mm

** $M = 2\mu Nr = 0.161$ kN·m ($\mu = 0.4$, $N = 3.5$ kN, $r = 57.5$ mm)

Averaged stiffness

$$C_t = \frac{375 + 460 + 500}{3} \approx 445 \text{ kN m}^{-1}, \quad C_r = \frac{460 + 370 + 308}{3} \approx 379 \text{ kN m rad}^{-1}$$

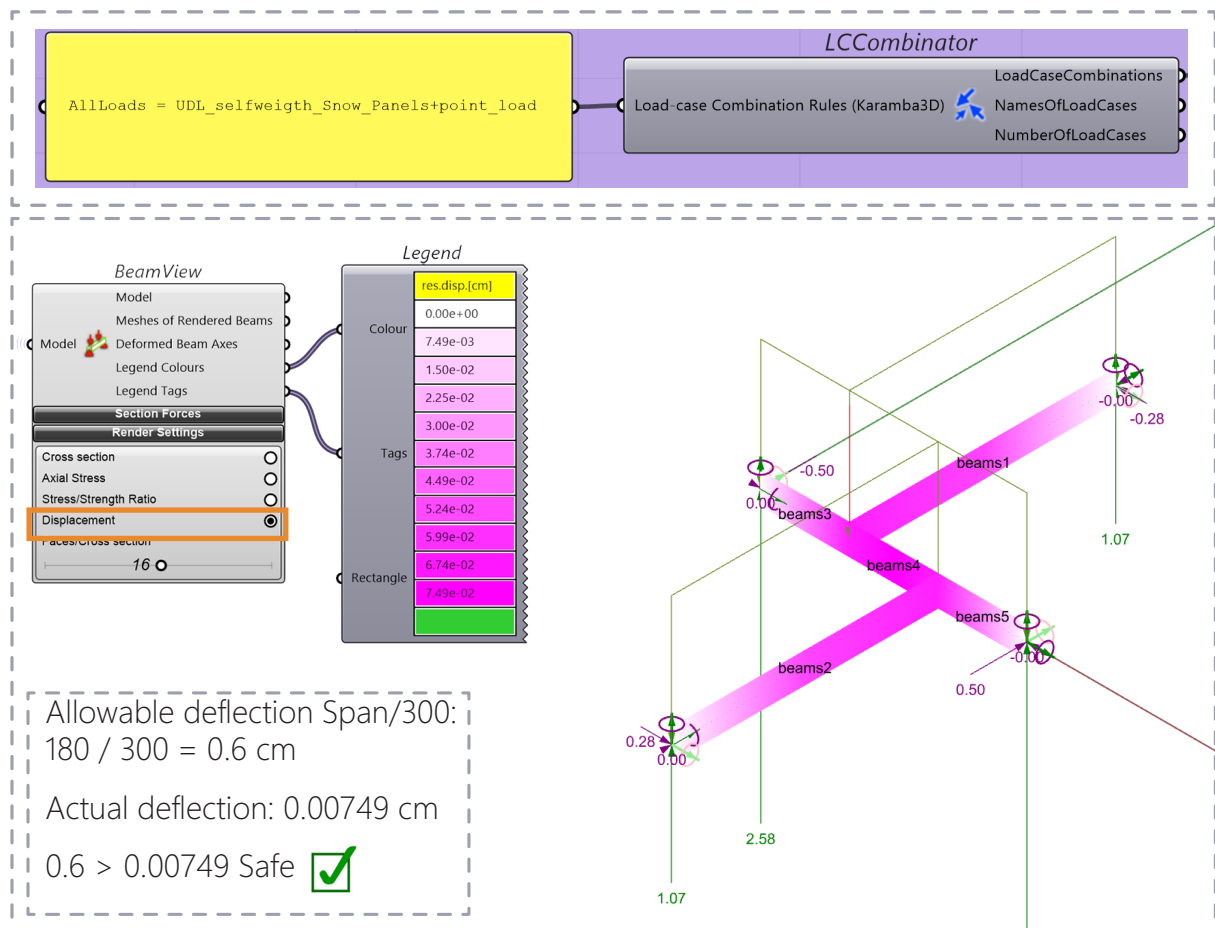
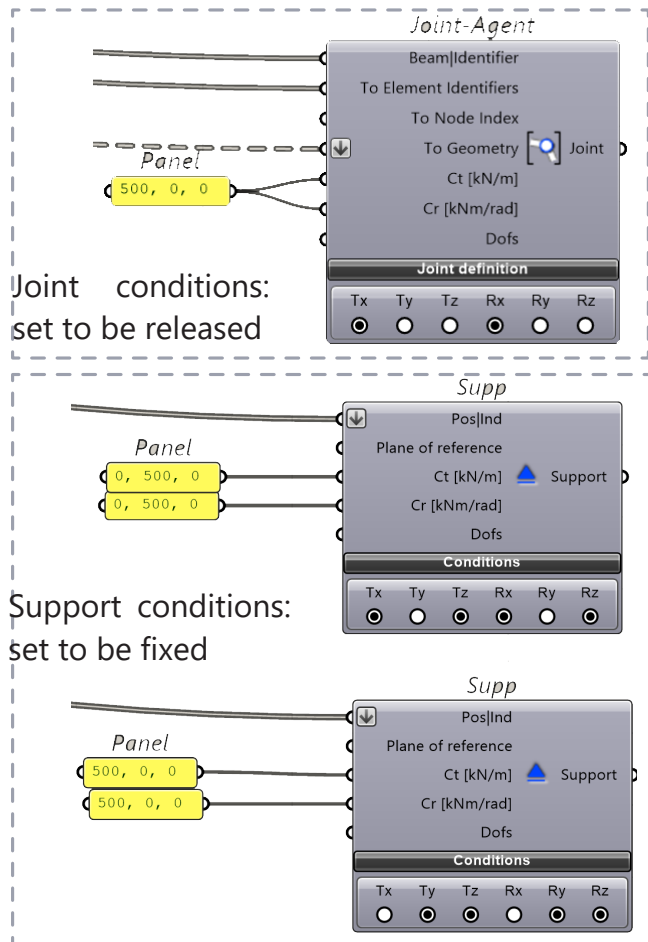
Rounded to the nearest hundred for simplicity.

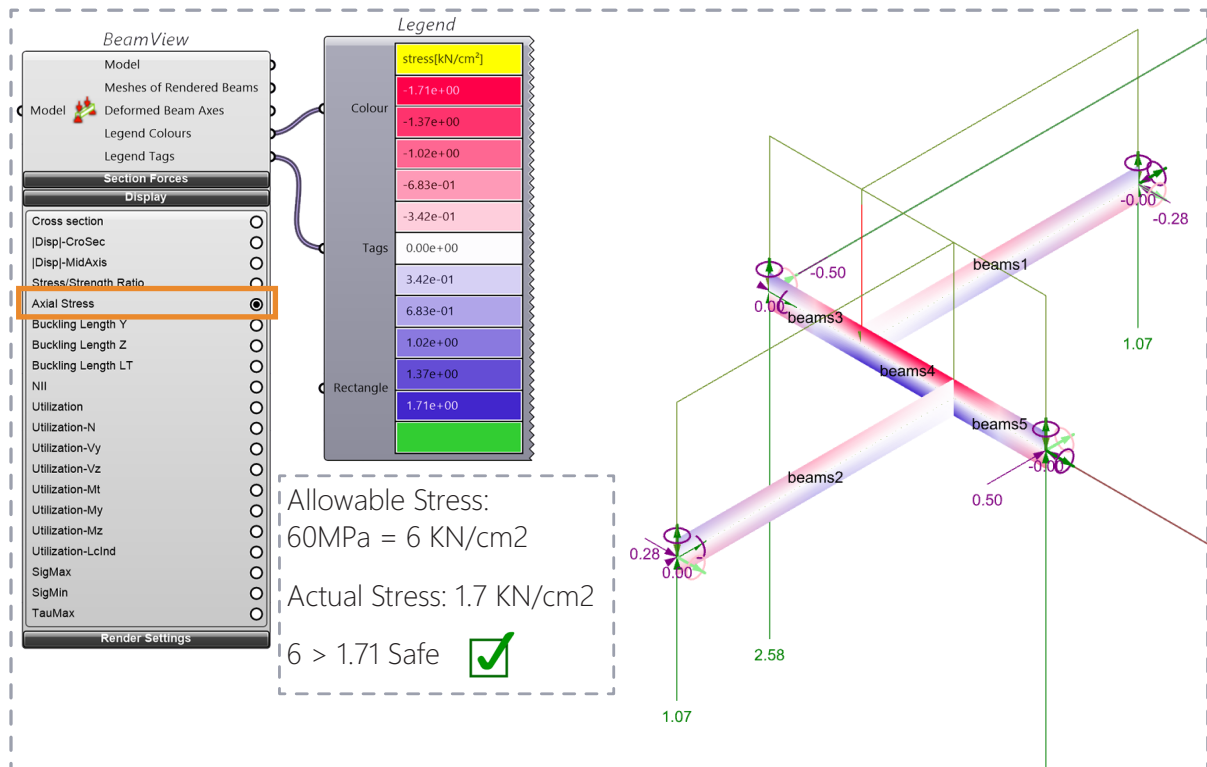
Alternative one:

Simplified beam model



The support conditions, joint configuration, and applied load combination for this simplified model are illustrated below. This setup represents the smallest possible composition of three interconnected beams using the proposed connection system, serving as a representative case for structural assessment.





Below the Max Bending Moment (My) Diagram and Shear Force diagram (Vz) are shown.

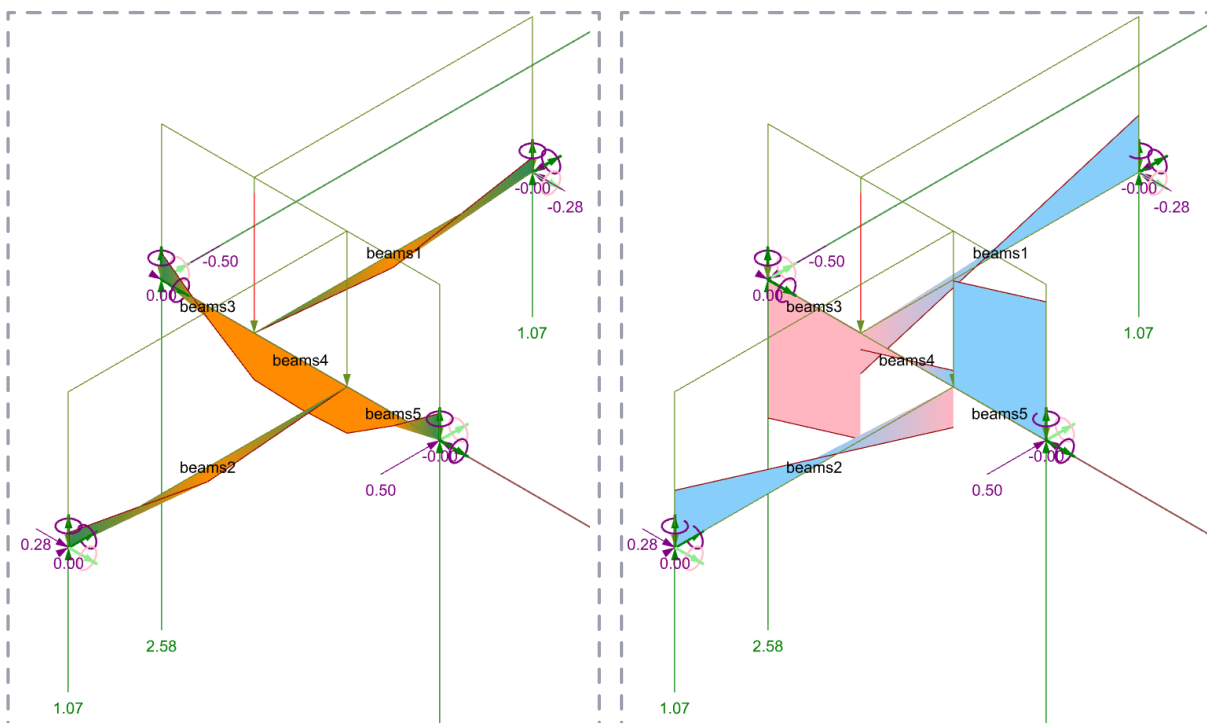


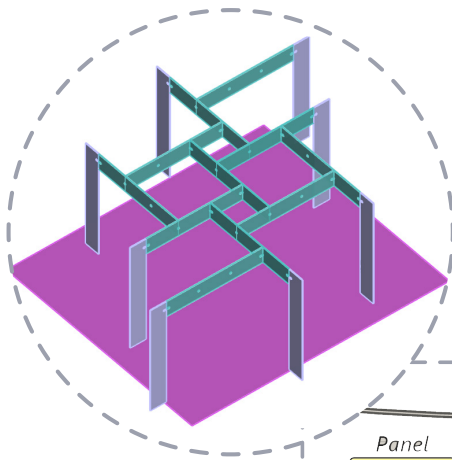
Figure 8.2.12 to 19, Simplified version of systems reciprocal connections as a starting point, Displacement in the module, Axial stresses, and support conditions and load cases, Source: Author's own

Alternative Two:

Pergola Design Span 4.2 * 4.8m

Note on Glass Thickness Assumption:

Although the actual design incorporates a safety factor by doubling the nominal glass thickness to 16 mm—to account for accidental breakage and unforeseen loads—all structural calculations and simulations in this thesis were conservatively carried out using an 8 mm glass thickness. This approach ensures that the system remains structurally safe even under worst-case scenarios.



Joint conditions:
set to be released

Support conditions:
set to be fixed

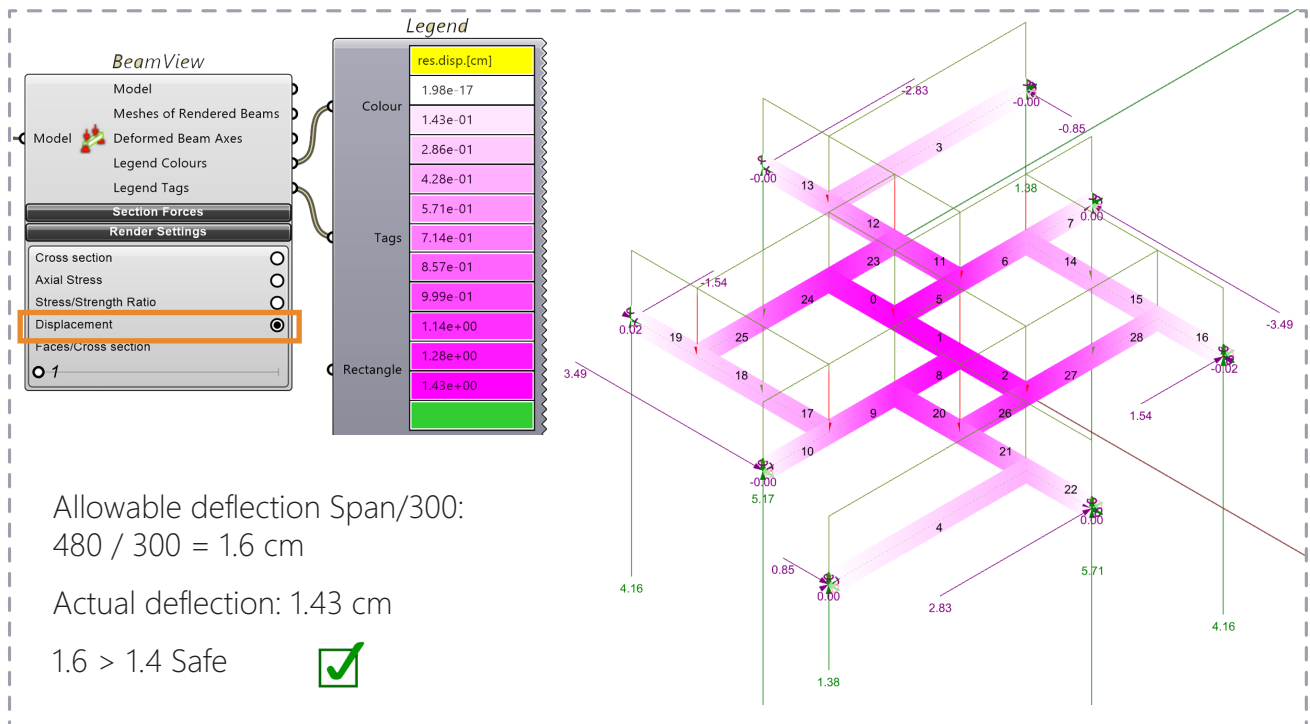
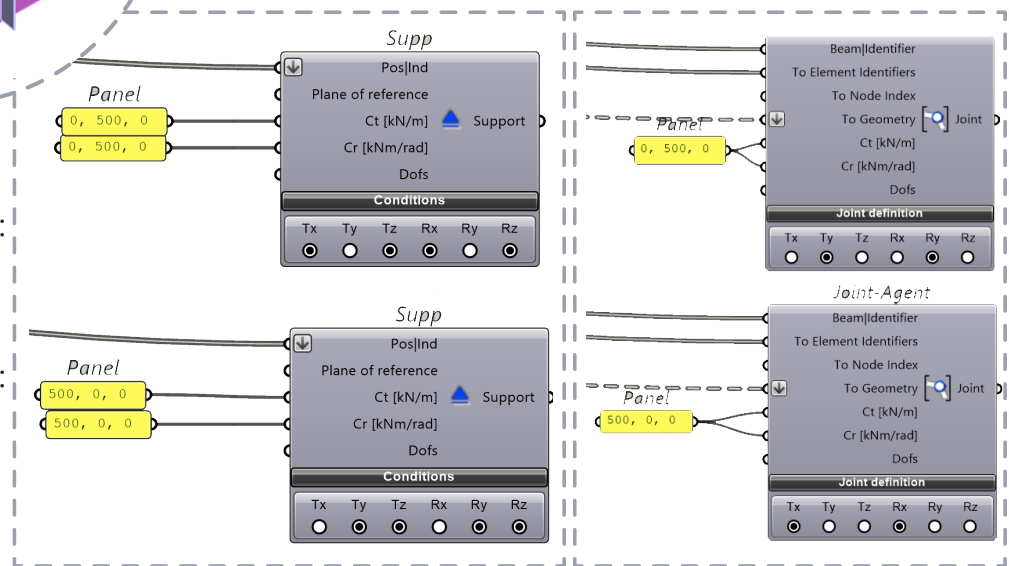


Figure 8.2.20, Displacement, Source: Author's own

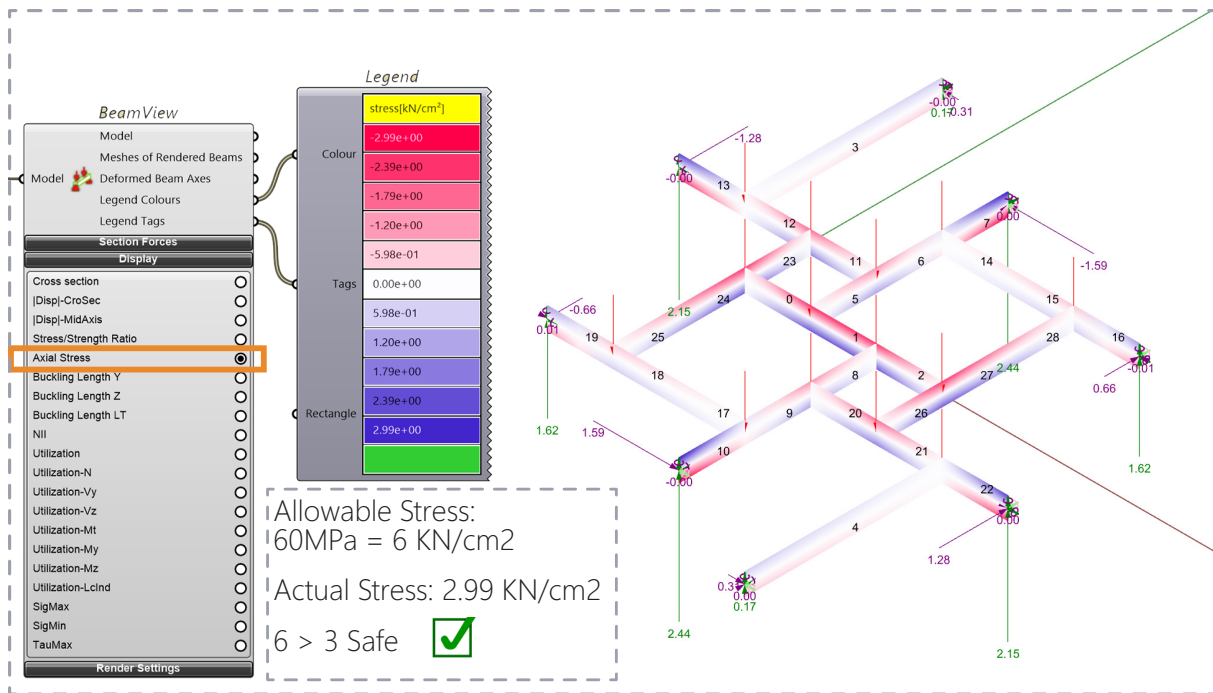


Figure 8.2.22, Axial stress and stress/strain ratio , Source: Author's own

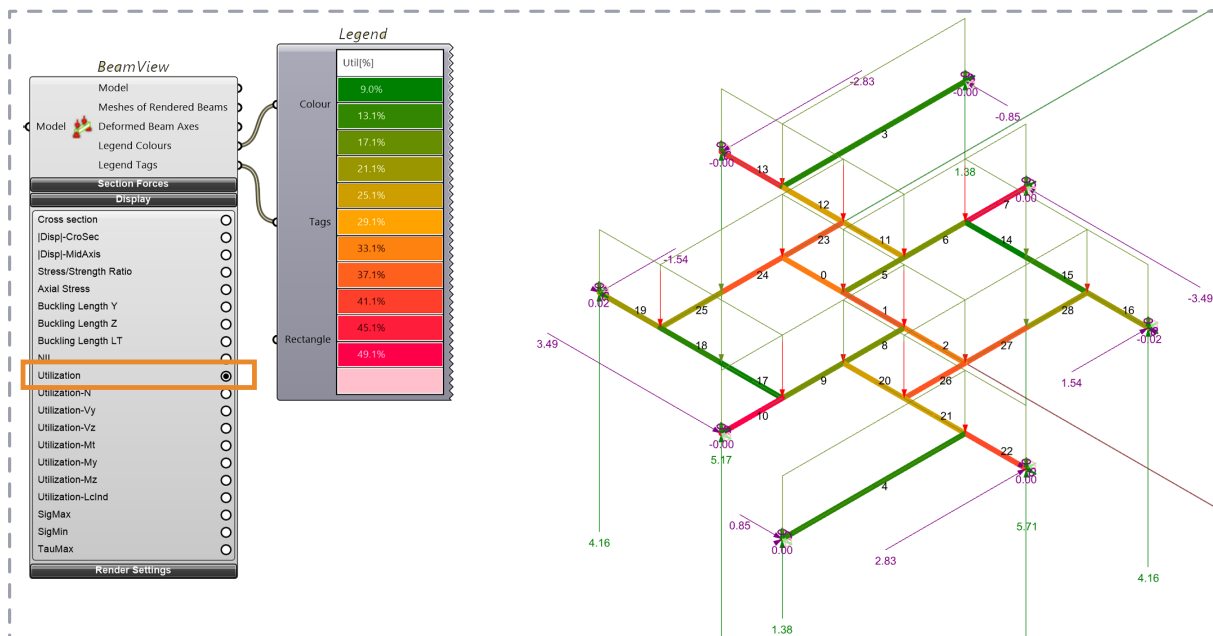


Figure 8.2.23, Utilization , Source: Author's own

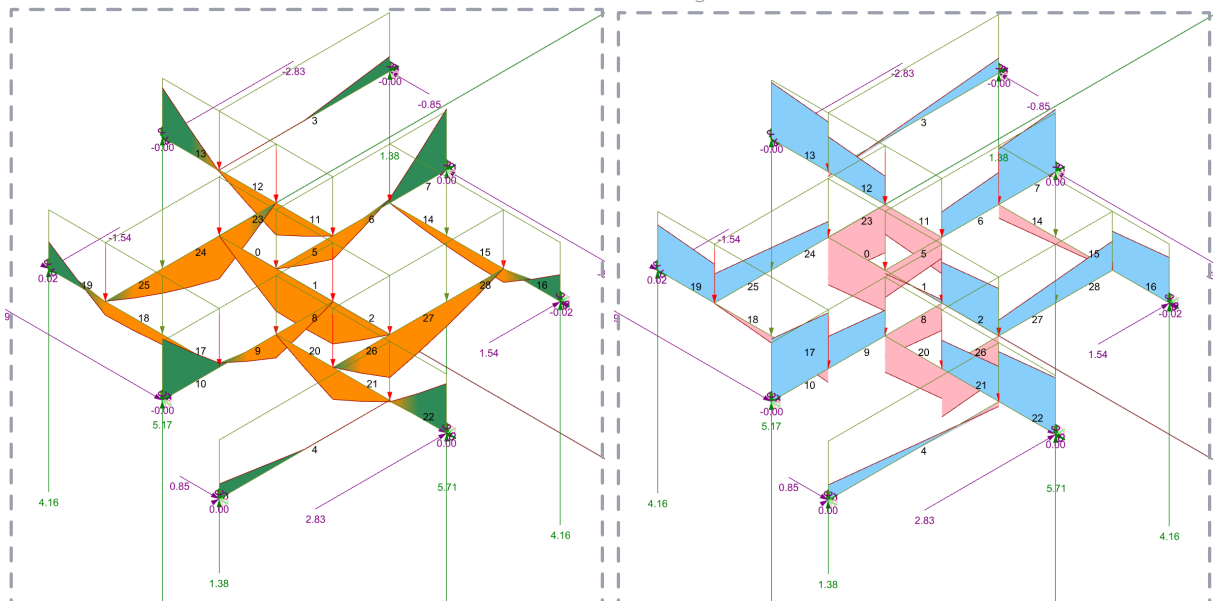
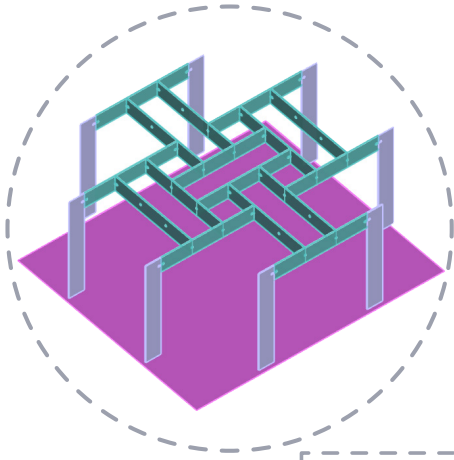


Figure 8.2.24 & 85, My and Vz , Source: Author's own

Alternative Three:

Pergola Design Span 4.2 * 4.8m



Note on Glass Thickness Assumption:

Although the actual design incorporates a safety factor by doubling the nominal glass thickness to 16 mm—to account for accidental breakage and unforeseen loads—all structural calculations and simulations in this thesis were conservatively carried out using an 8 mm glass thickness. This approach ensures that the system remains structurally safe even under worst-case scenarios.

Joint conditions:
set to be released

Support conditions:
set to be fixed

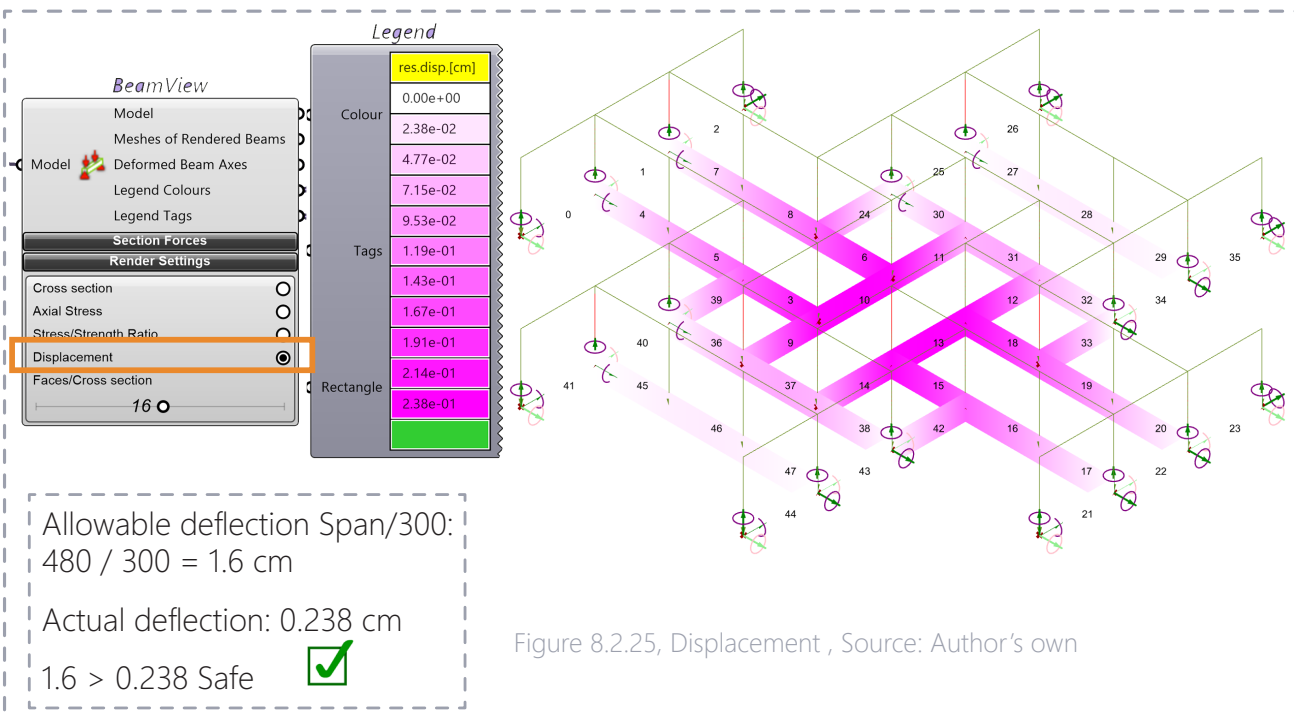
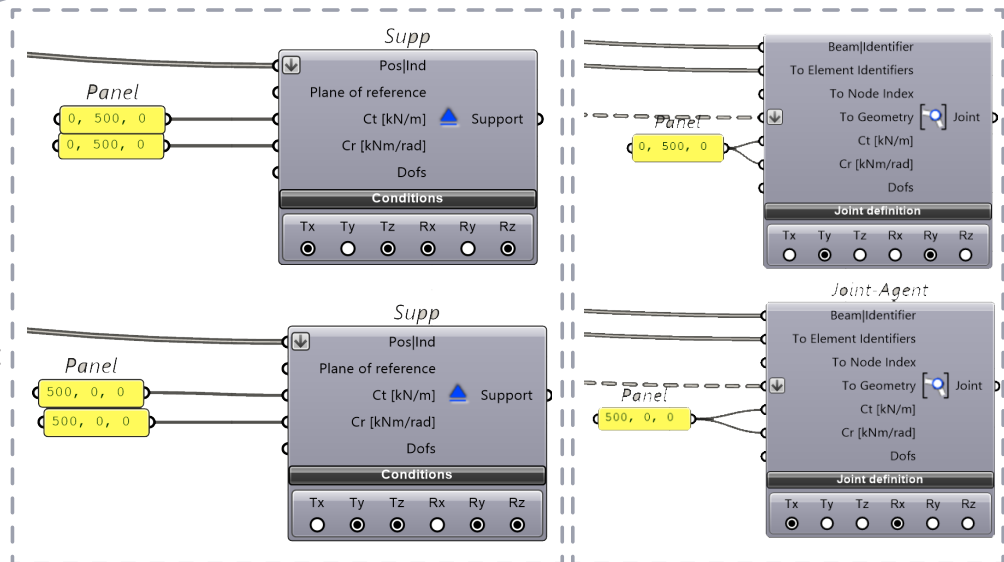


Figure 8.2.25, Displacement , Source: Author's own

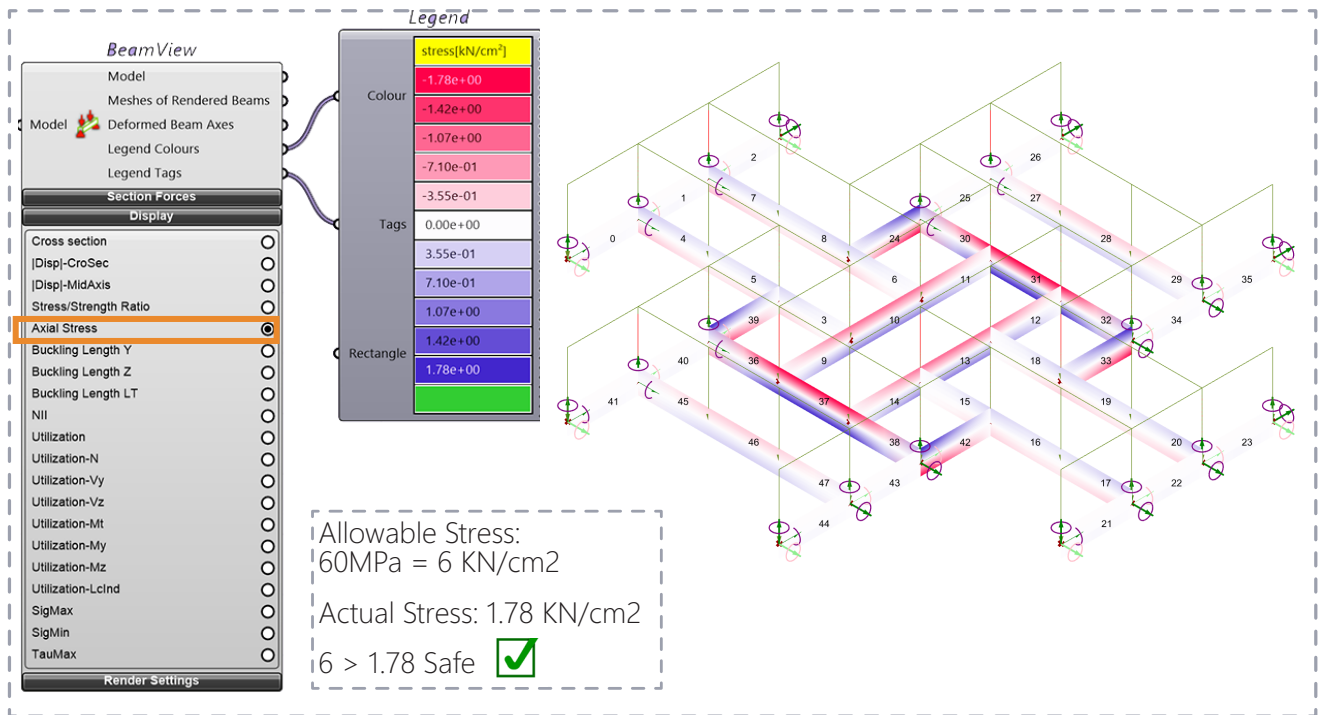


Figure 8.2.26, Axial stress and stress/strain ratio , Source: Author's own

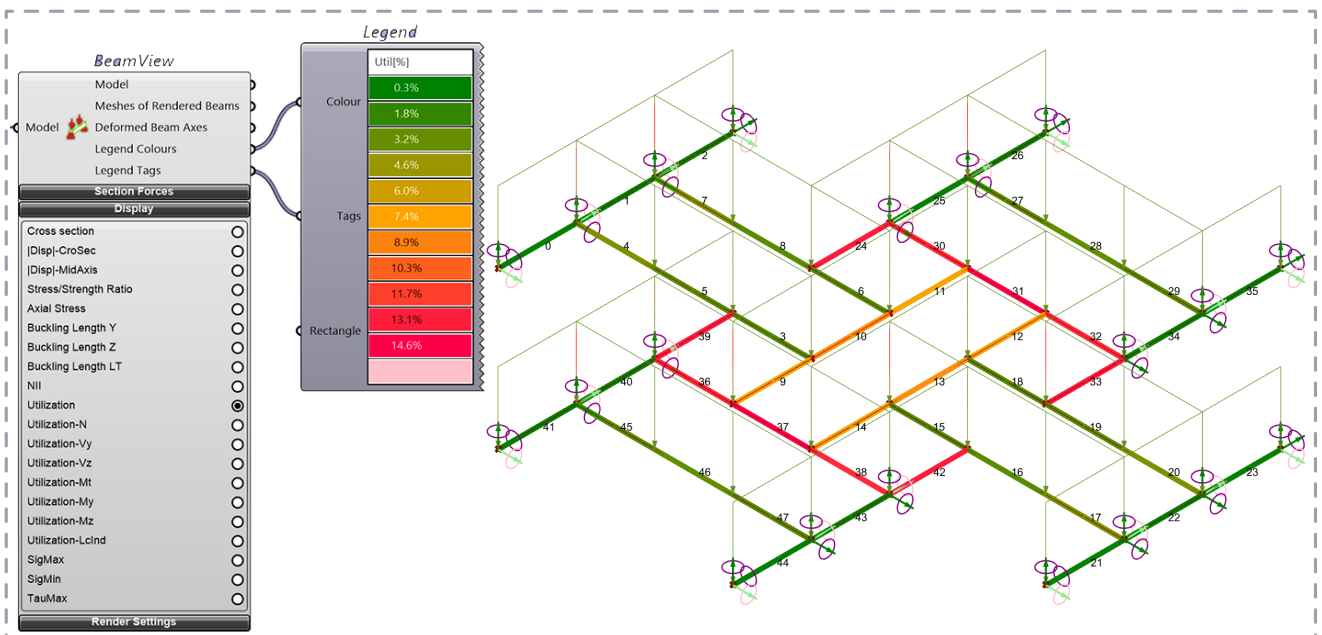


Figure 8.2.27, Utilization , Source: Author's own

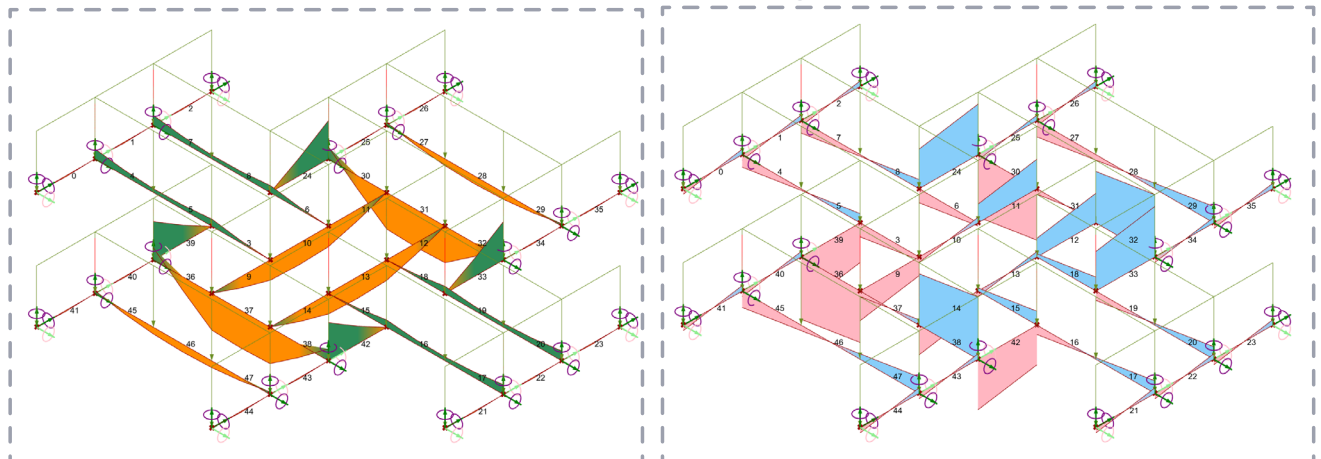
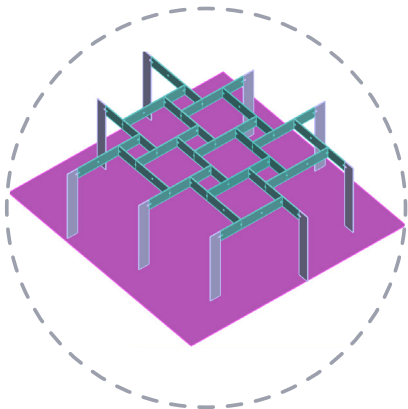


Figure 8.2.28 & 85, My and Vz , Source: Author's own

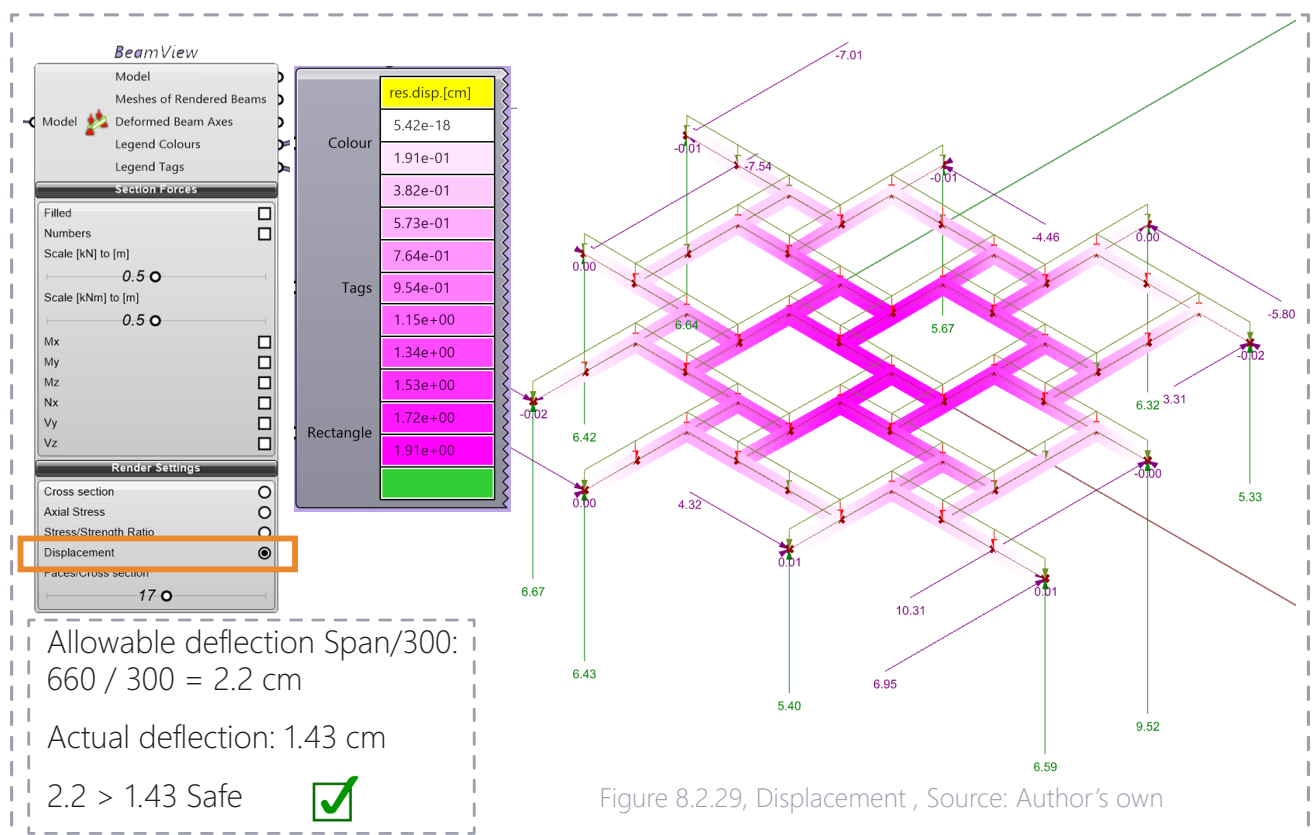
Alternative Four:

Pergola Design Span 6.6 * 6.4m



Note on Glass Thickness Assumption:

Although the actual design incorporates a safety factor by doubling the nominal glass thickness to 16 mm—to account for accidental breakage and unforeseen loads—all structural calculations and simulations in this thesis were conservatively carried out using an 8 mm glass thickness. This approach ensures that the system remains structurally safe even under worst-case scenarios.



Allowable deflection Span/300:
 $660 / 300 = 2.2 \text{ cm}$

Actual deflection: 1.43 cm

$2.2 > 1.43$ Safe



Note: The deformation shown in the simulation is exaggerated by a factor of 10 for visual clarity and does not represent the actual displacement

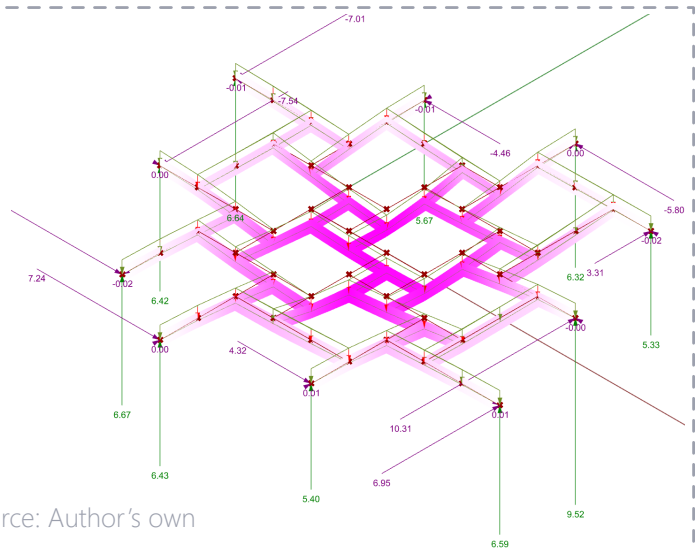


Figure 8.2.30, 10x Exaggerated Displacement , Source: Author's own

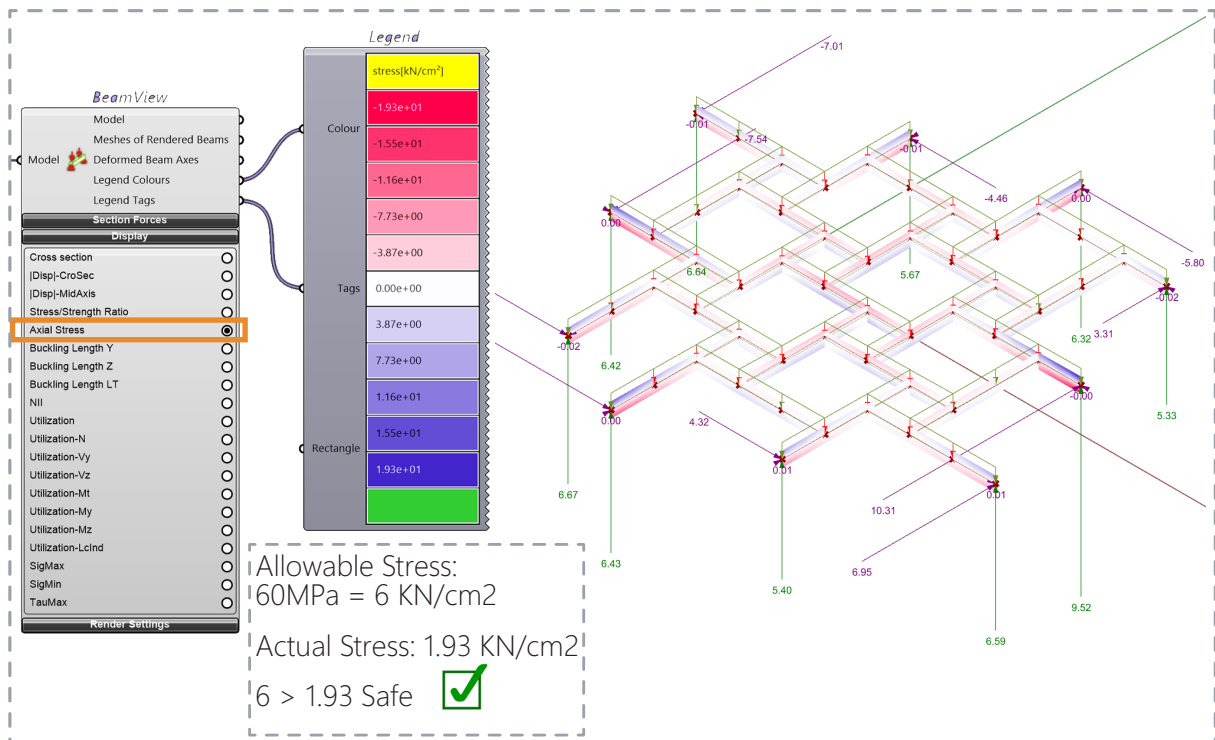


Figure 8.2.31, Axial stress and stress/strain ratio , Source: Author's own

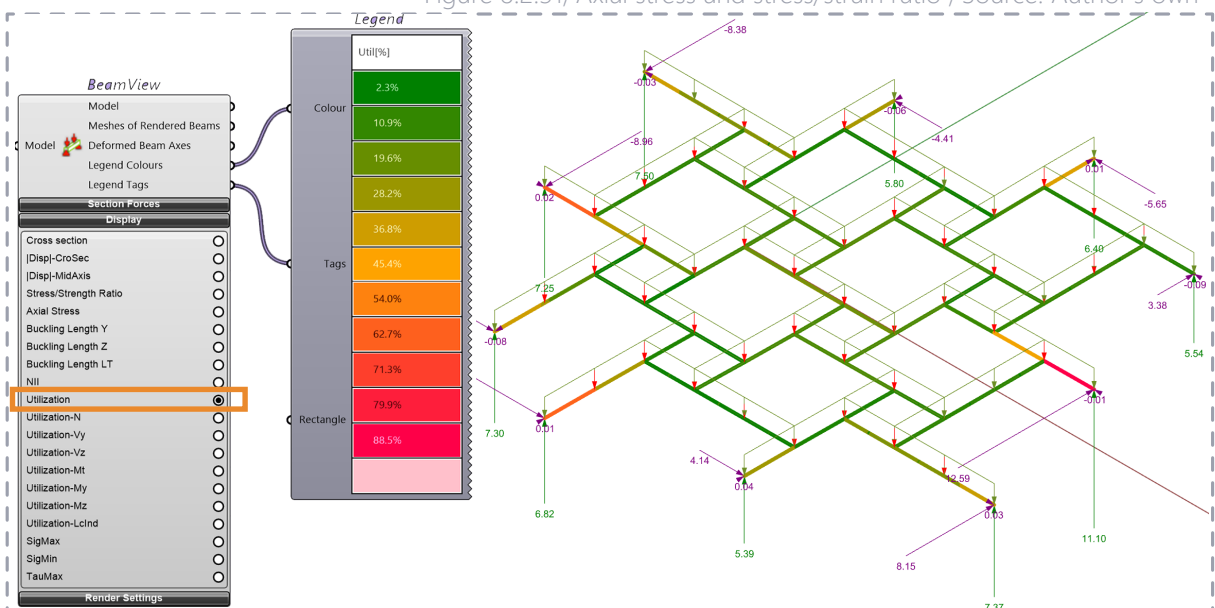


Figure 8.2.32, Utilization , Source: Author's own

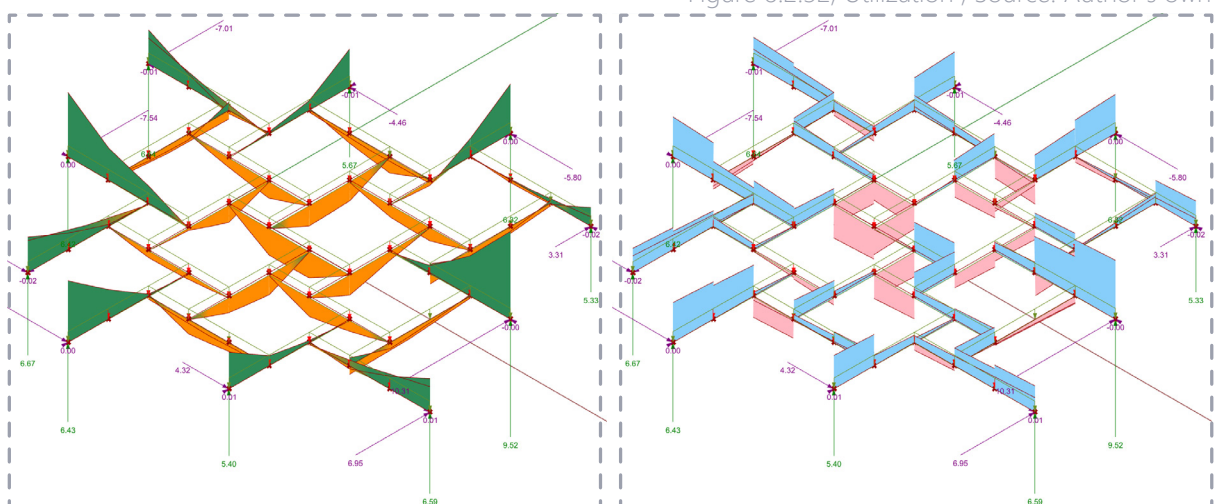
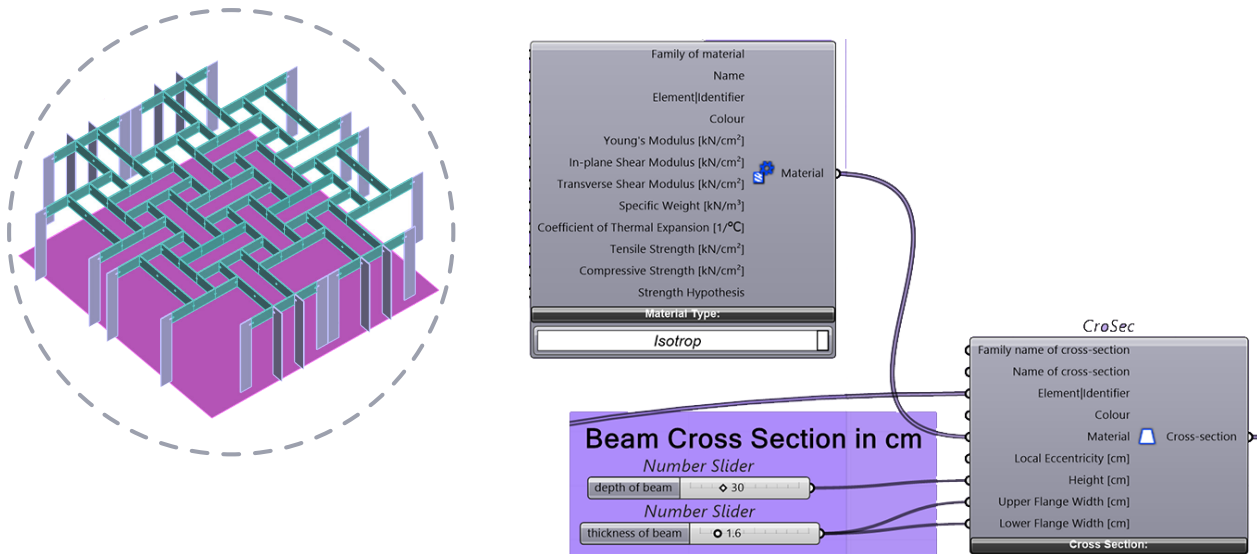


Figure 8.2.33 & 34, My and Vz , Source: Author's own

Alternative Four:

Pergola Design Span 6.6 * 6.4m



Note on **Change** in Glass Thickness Assumption:

Initially, the glass thickness was assumed to be 8 mm as a conservative baseline for analysis. However, simulations of longer spans revealed that this thickness, combined with the limited module depth, was inadequate to satisfy serviceability requirements—particularly with respect to deflection. While axial stresses remained within acceptable limits, the deflection values exceeded the allowable threshold. Consequently, the glass thickness was increased to 16 mm and the module depth stayed same as 200 mm. Despite these adjustments, the revised configuration still did not meet Deflection limits for the intended application. The updated simulation results based on these parameters are presented below. Further developments and the next design decisions taken from this point onward are described in detail on page 126.

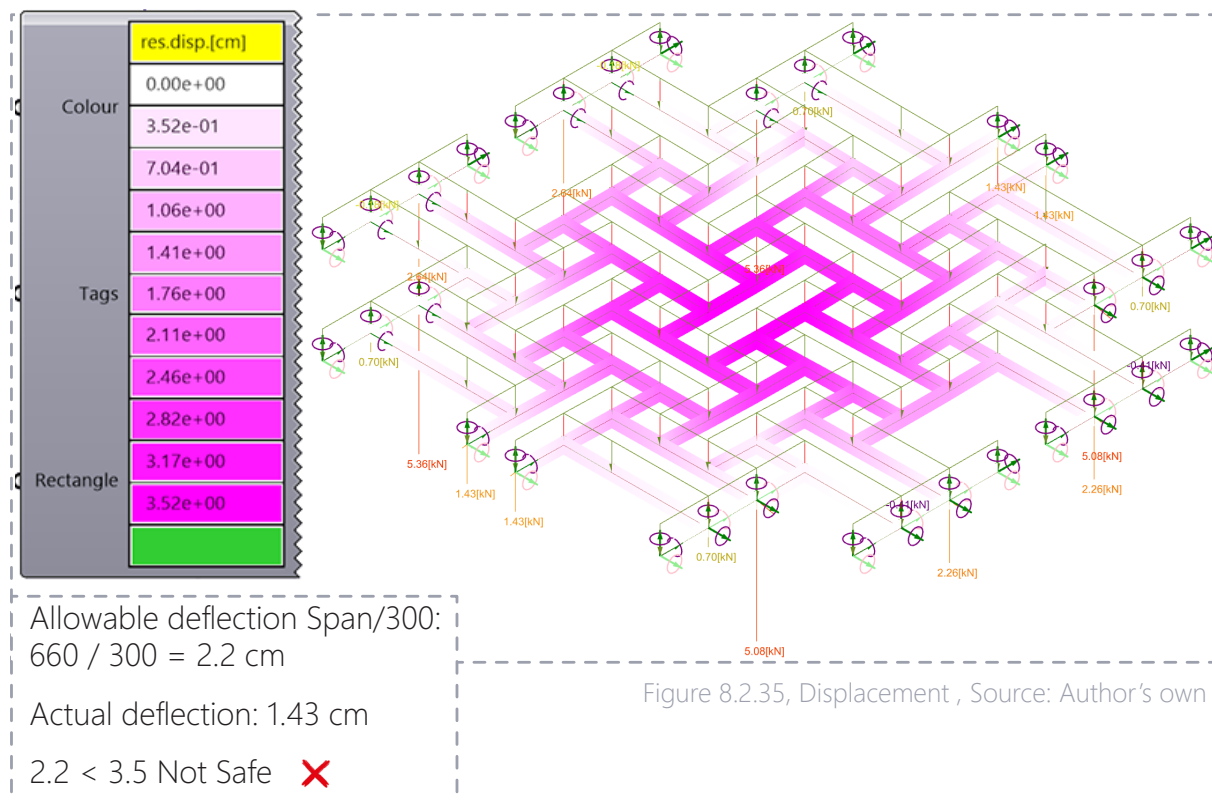
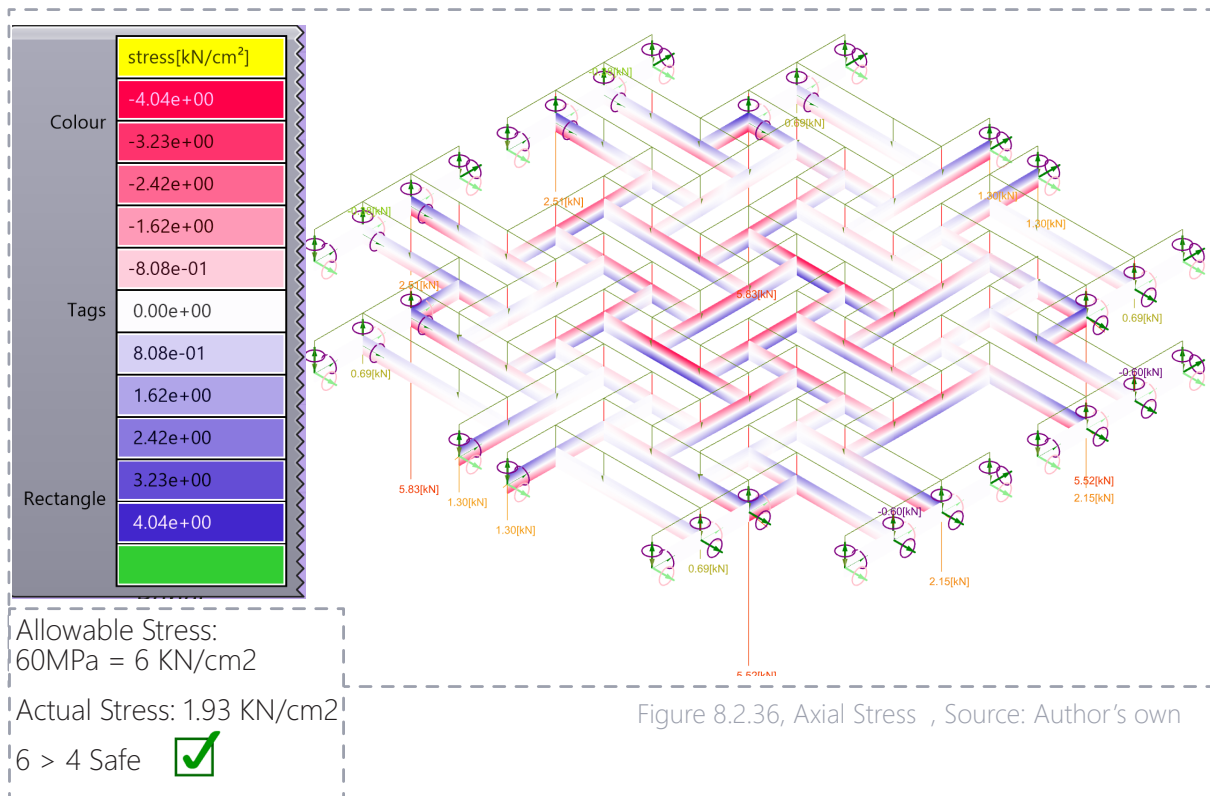


Figure 8.2.35, Displacement, Source: Author's own



Further iterations showed that acceptable deflection could only be achieved either by increasing the thickness to 24 mm with a 50 cm depth, or 32 mm with a 30 cm depth—both of which were inefficient and impractical from a material and aesthetic point of view.

To overcome this, a more strategic and material-conscious approach was introduced: combining modules of varying depth. This hybrid configuration allows deeper beams to be concentrated in areas of high bending (typically at mid-span), while shallower modules are used where bending moments are lower (near supports or edges). As shown in the diagram, modules with a 50 cm depth and 24 mm glass thickness are positioned at the centre of the structure, while 20 cm deep modules with 16 mm glass are placed along the perimeter. This strategy balances structural efficiency, aesthetic clarity, and material economy.

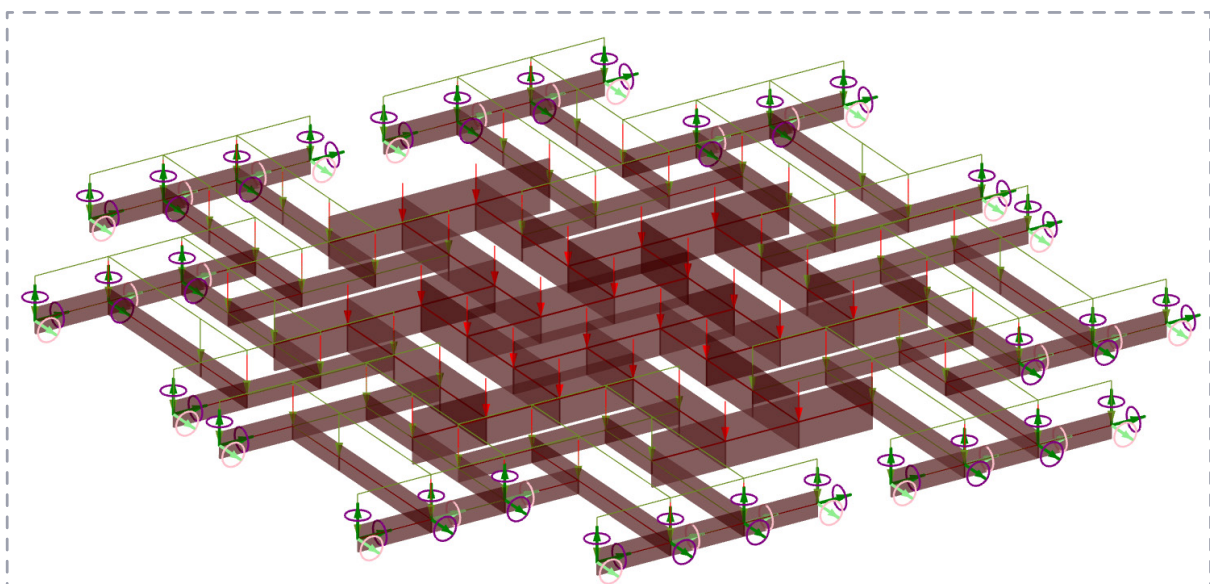


Figure 8.2.37, Cross section variation in depth and thickness to resist the load in allowable deflection , Source: Author's own

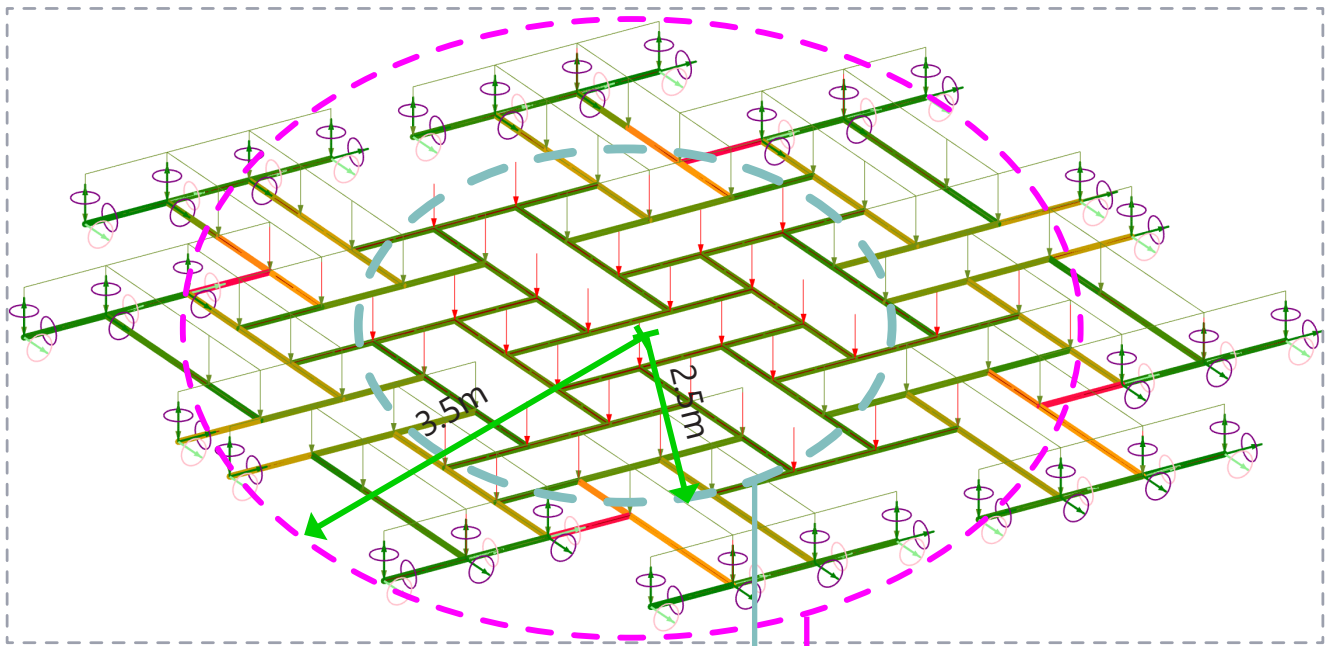
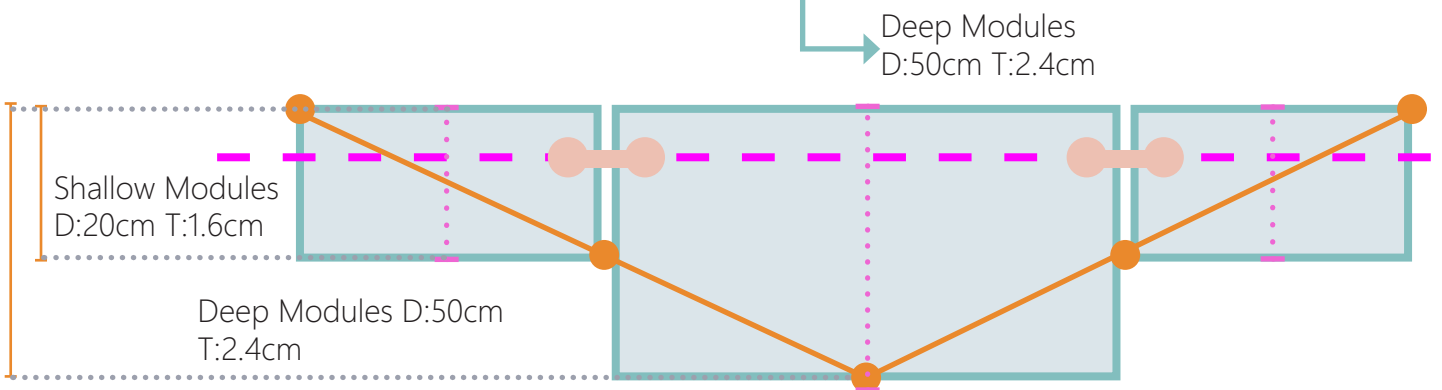


Figure 8.2.38, Cross section variation in depth and thickness in span radius , Source: Author's own



Beam Configuration:

Total span (L): Composed of three segments, each of length

Segment arrangement: Shallow – Deep – Shallow

Glass thickness (b): Constant across all beams

Depth (h): Shallow segments with smaller h_1 , deep segment with larger h_2

Material: Heat-strengthened glass with modulus of elasticity E

Moment of Inertia and Flexural Rigidity: The moment of inertia

I for each beam segment is calculated based on its cross-sectional geometry using:

Flexural rigidity EI is then derived for each section:

- $EI_1 = E \cdot \frac{b \cdot h_1^3}{12}$ for shallow segments
- $EI_2 = E \cdot \frac{b \cdot h_2^3}{12}$ for the deep central segment

- Dividing the span into three sections (**two shallow and one deep**).
- Determining **bending moments** in each section:
- Using standard beam theory for combined **loading conditions (UDL + point loads)**
- **Each section** can be approximated as a **simply supported beam segment**
- Computing **maximum deflection** using the principle of superposition: For each load type (UDL, point loads), calculating deflection contribution in each segment
- Using appropriate flexural rigidity E1 or E2 for the segment
- Comparing the total deflection at mid-span with allowable deflection: $\delta_{\max} < \text{Span} / 300$

$$\delta_{\text{total}} = \delta_{UDL}^{\text{deep}} + \delta_{UDL}^{\text{shallow-left}} + \delta_{UDL}^{\text{shallow-right}} + \delta_{P1} + \delta_{P2}$$

One important design question that arose was what happens to the connections when the modules have different depths. To address this, the modules were kept aligned at the top surface, allowing variation only on the bottom side. This approach maintains a consistent top level for panel placement while enabling structural optimization through varying depths. Based on simple calculations (shown below), this configuration is also structurally advantageous: since the deeper elements are positioned where compression is higher, and the shallower ones where it's lower, the compression on the bottom side decreases, reducing the required preload in the bolts. This not only improves the efficiency of the connection but also simplifies assembly and reduces stress concentrations around the holes.

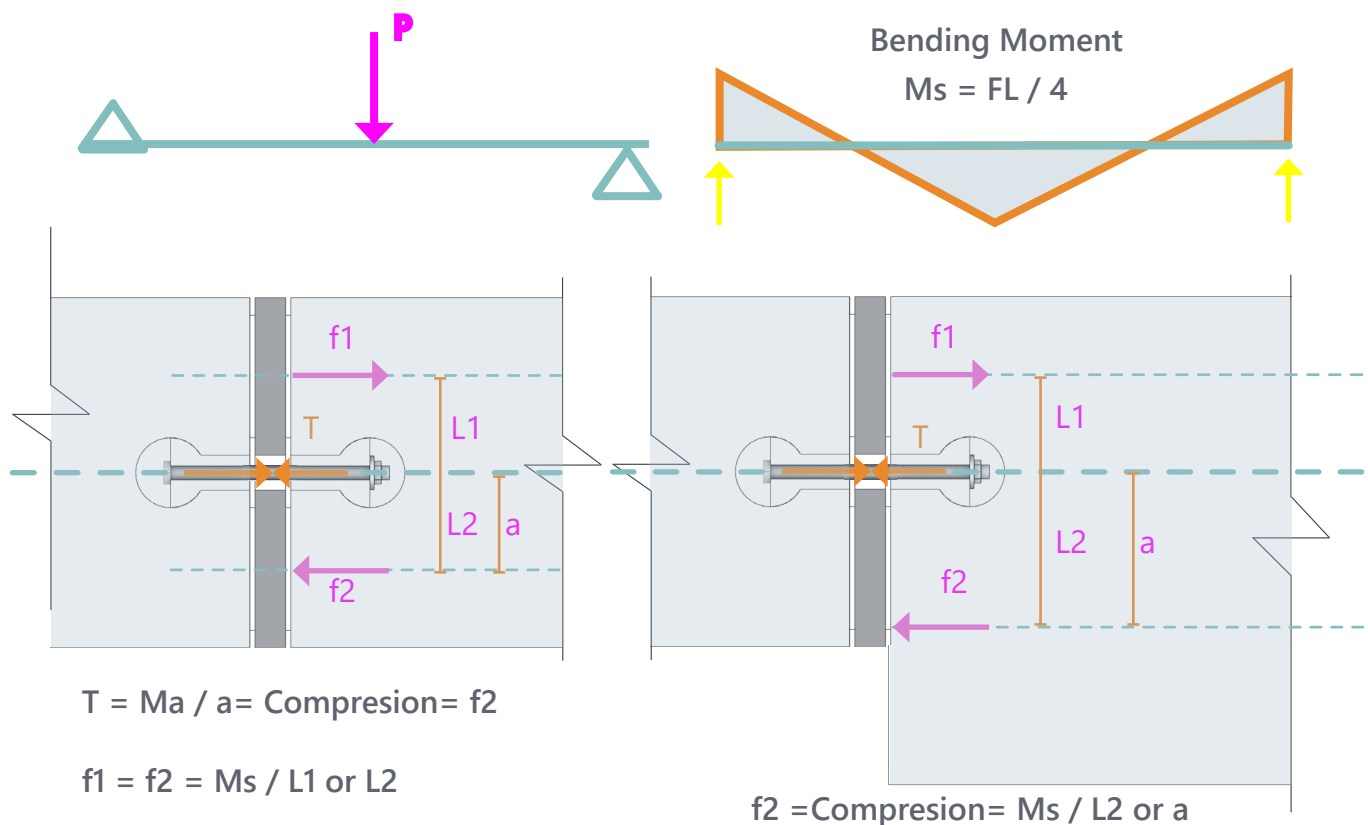
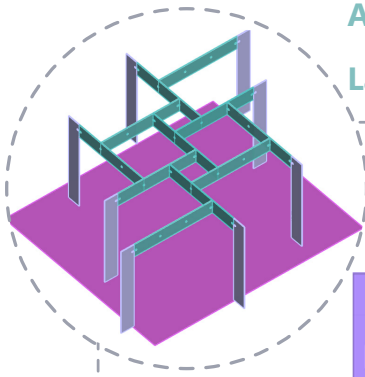


Figure 8.2.39 to 41, 1) Tension-Comparison between equal-depth and variable-depth modules. Source: Author's own

Tension-Comparison between equal-depth and variable-depth modules. By maintaining top alignment and allowing the depth to vary at the bottom, compressive forces near the lower internal forces (f_2) are reduced. This results in a lower required preload to resist internal moment (M_s), improving material efficiency and connection safety.

Analysis Five:

Lateral Loads Pergola Design Span 6.6 * 6.4m



Beam Cross Section in cm

Number Slider
depth of beam

Number Slider
thickness of beam

Family name of cross-section
Name of cross-section
Element Identifier
Colour
Material
Local Eccentricity [cm]
Height [cm]
Upper Flange Width [cm]
Lower Flange Width [cm]
Cross Section:

Area Under load

Expression
D
L
D * L
area
Panel

Panel
wind load (kN/m)
Number Slider

Expression
area
L
WL
area*WL*1.5/L
Result

Unit Y
Factor Unit vector
Unit X
Factor Unit vector

Beam Loads
Beam Identifier
Load-case
Force Vector
Moment Vector
t-Start
t-End
Orientation
Local to element
Global
Global proj.
Type of Load:

Panel
AllVerticalLoads = UDL_selfweighth_Snow_Panels+point_load

LCCombinator
LoadCaseCombinations
NamesOfLoadCases
NumberOfLoadCases

Panel
AllLoads = AllVerticalLoads + Lateral_Load

LCCombinator
LoadCaseCombinations
NamesOfLoadCases
NumberOfLoadCases

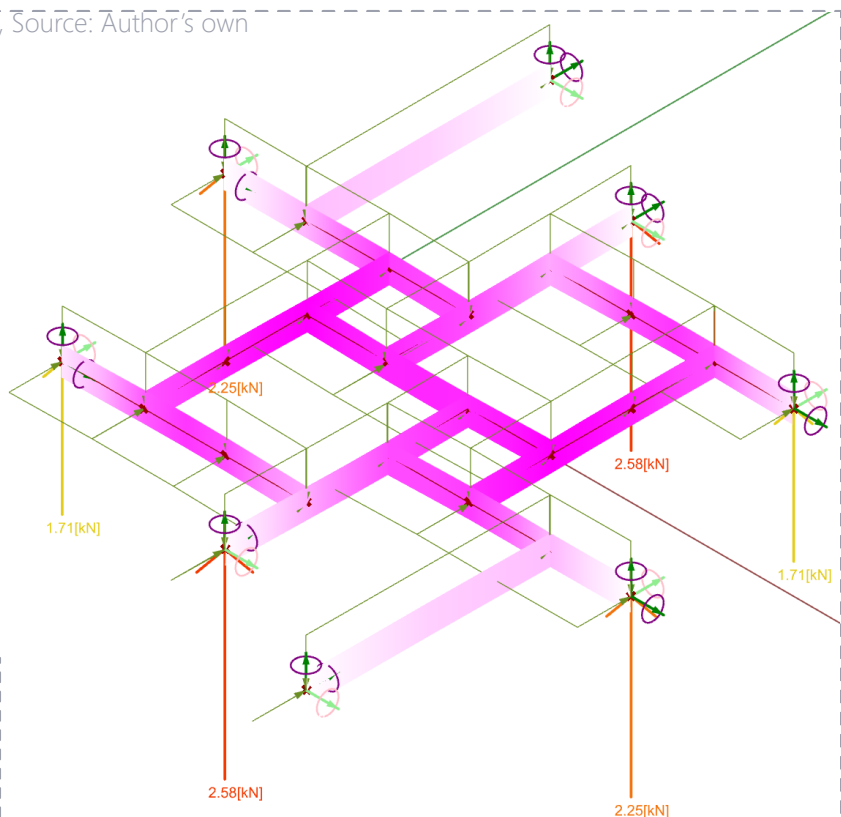
Figure 8.2.42, Displacement, Source: Author's own

	res.disp.[cm]
Colour	8.56e-03
	1.57e-01
	3.05e-01
	4.53e-01
	6.01e-01
Tags	7.49e-01
	8.98e-01
	1.05e+00
	1.19e+00
	1.34e+00
Rectangle	1.49e+00

Allowable deflection
Span/300: 660 / 300 = 2.2 cm

Actual deflection: 1.43 cm

2.2 > 1.49 Safe ☒



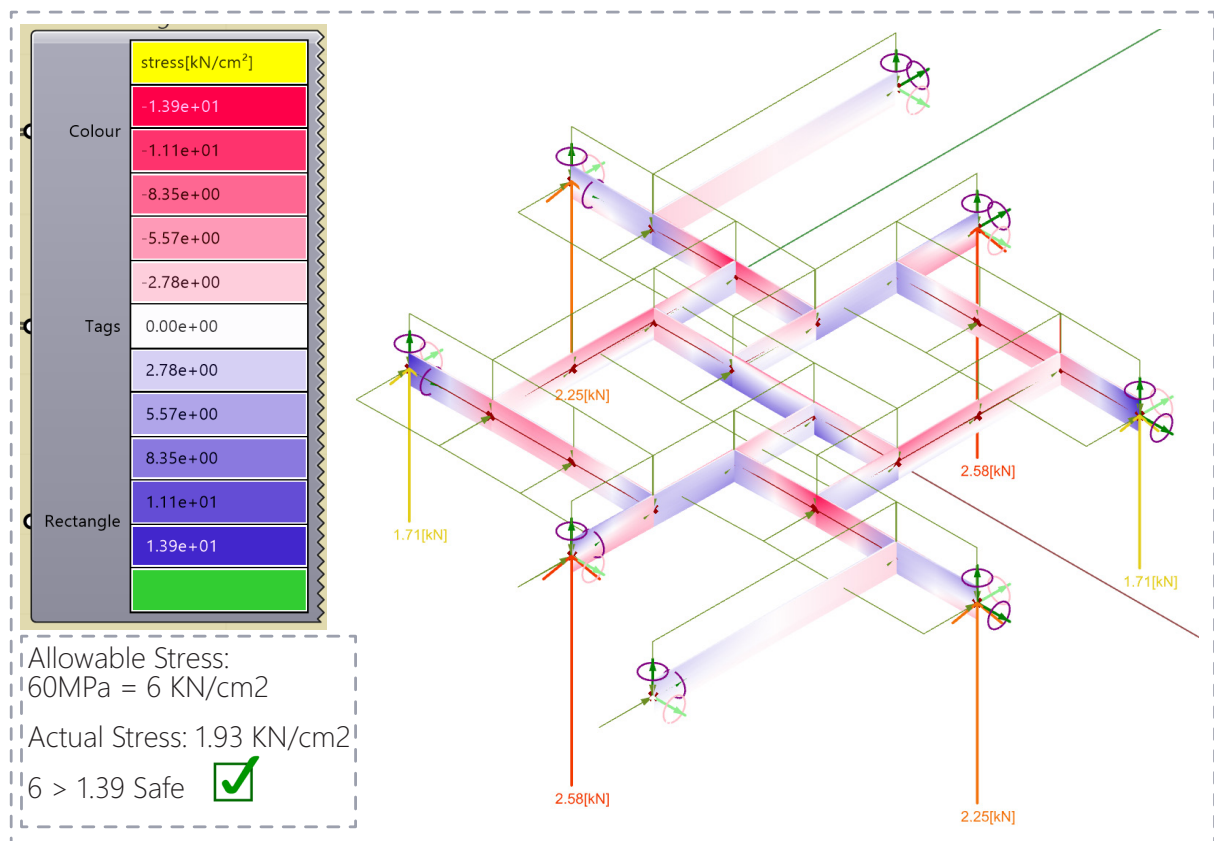


Figure 8.2.43, Axial stress and stress/strain ratio , Source: Author's own

Overall, the results demonstrate that the friction-fit connection designed for this system is capable of safely resisting a wind load of 0.5 kN/m². This value corresponds to the average wind pressure in cities such as London and Düsseldorf, the proposed locations for potential pavilion deployment. Provided that the application does not require strict air- or water-tightness, and assuming no exposure to extreme climatic conditions, the current design performs adequately. However, for use in harsher environments or where additional performance criteria are required—such as improved airtightness, waterproofing, or increased load resistance—further adaptations to the system would be necessary.

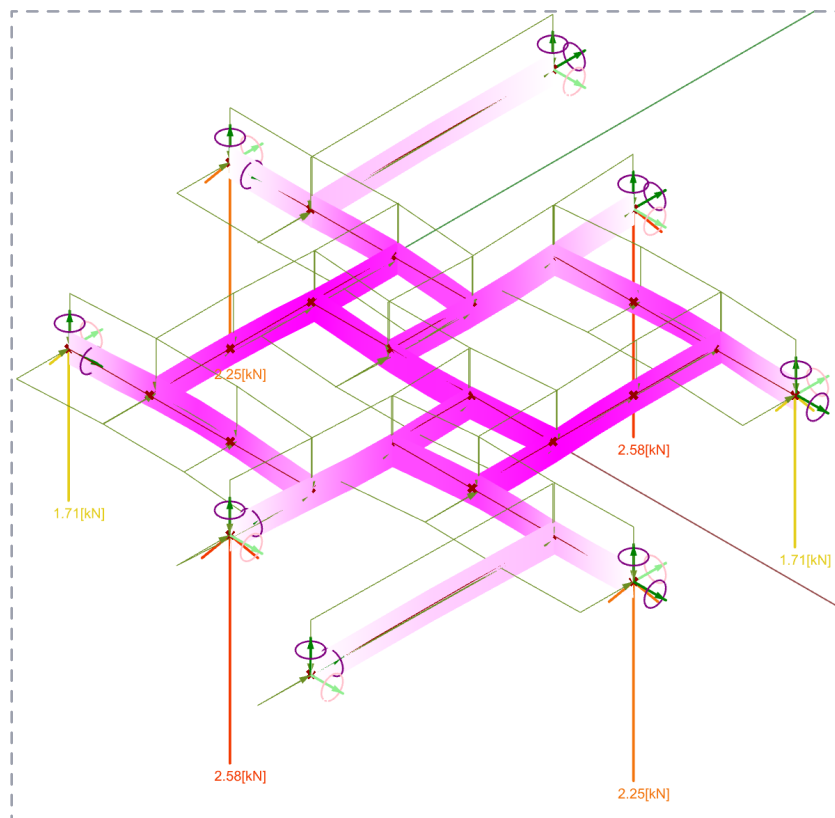
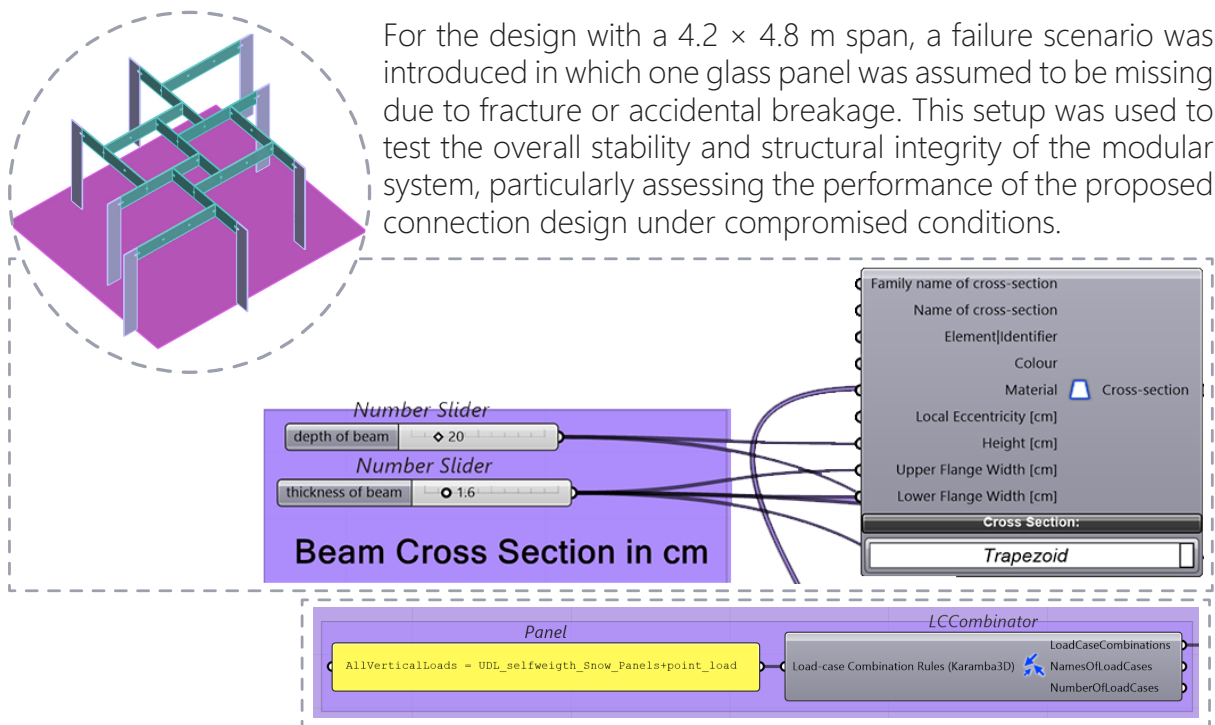


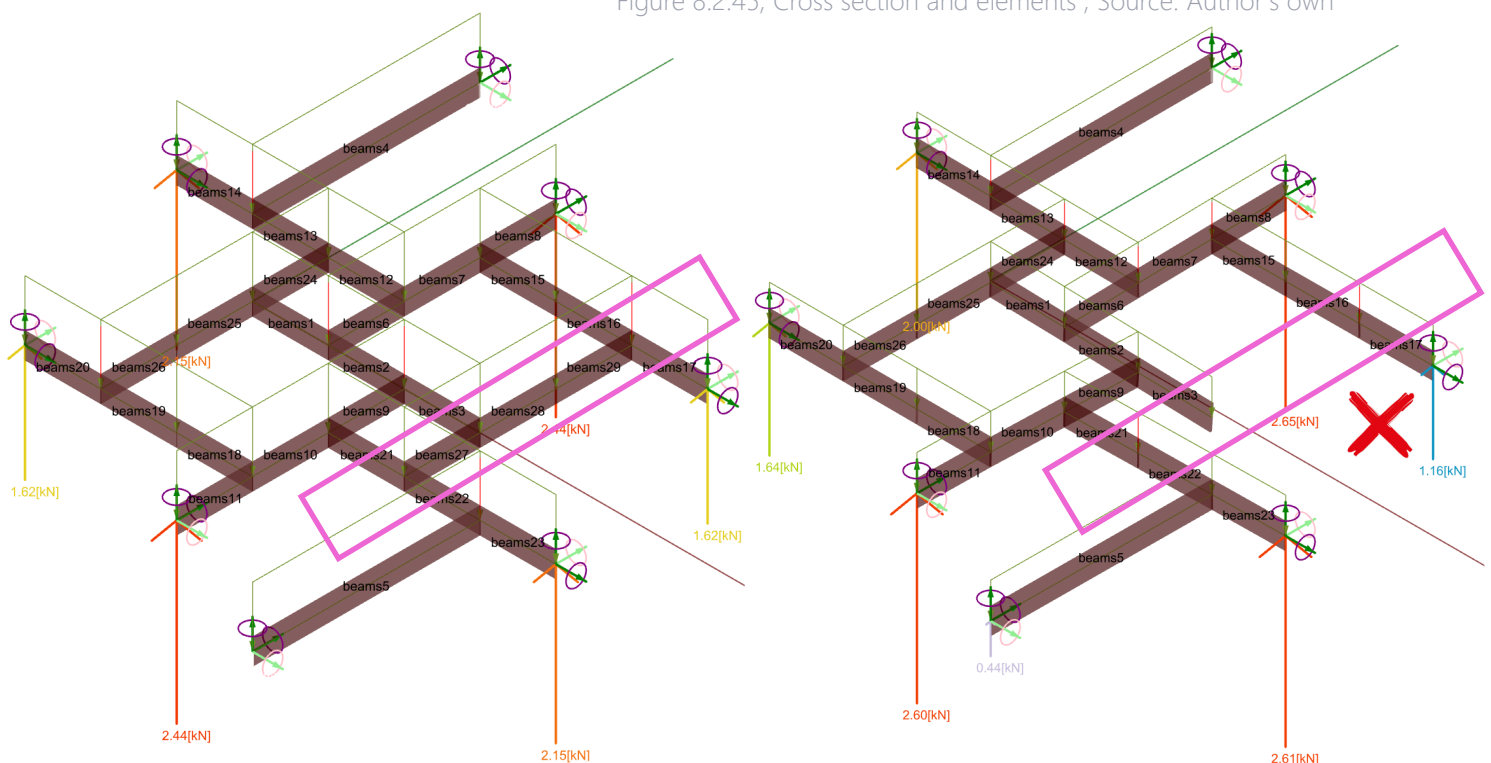
Figure 8.2.44, 5 x times exaggerated Displacement , Source: Author's own

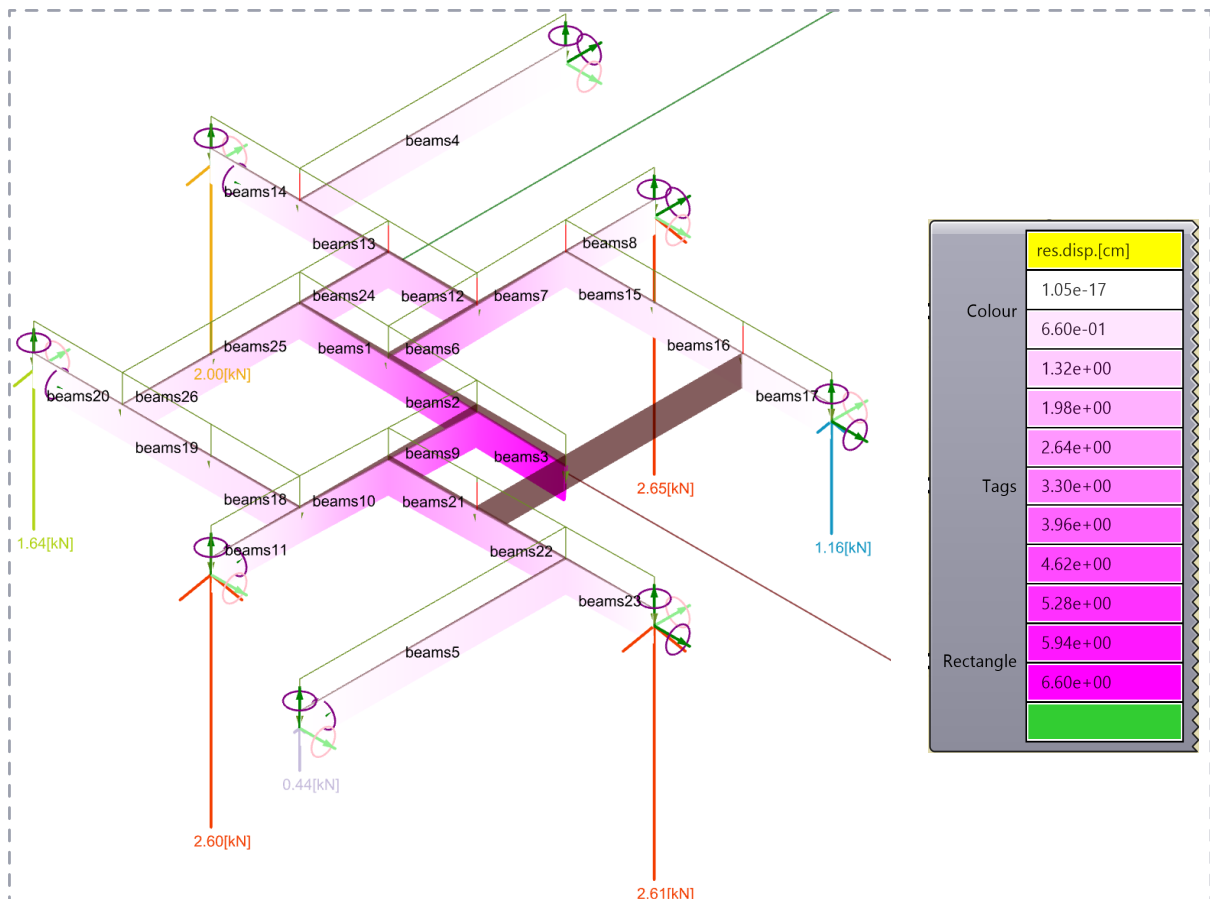
Failure Scenario Analysis



This section illustrates the load paths and deflection behaviour in the event of failure or breakage of one of the glass modules. As previously mentioned, all structural analyses were conducted using a glass thickness of 8 mm. This was intentionally done to maintain a conservative design approach, assuming that the second 8 mm layer in the actual 16 mm laminated assembly would act as a redundant safety measure under unforeseen or extreme loading conditions. To simulate a breakage scenario, one of the glass panels was virtually removed and the system was re-analysed to assess its behaviour. The results showed a maximum deflection of approximately 6 mm on the open-ended side and stress levels reaching 59 MPa—well below the typical failure threshold for heat-strengthened glass. This confirms that the system retains a notable degree of residual capacity and structural integrity even in the case of partial glass failure.

Figure 8.2.45, Cross section and elements , Source: Author's own





As shown above, the brown geometry illustrates the complete structural system, including the location of the missing or broken glass panel. In contrast, the overlaid pink layer represents the deflection results from the simulation. The maximum displacement occurred at the free edge adjacent to the missing panel and was measured at 6.6 cm. This significantly exceeds the allowable deflection limit for the given span, which is approximately 2.2 cm. However, despite the excessive deformation, the maximum principal stress observed in this failure scenario was 59 MPa—still within the permissible range for heat-strengthened glass. This outcome demonstrates that although serviceability criteria (specifically deflection) are compromised, the structure retains a certain level of load-bearing capacity, and catastrophic failure is avoided due to the redundancy built into the design.

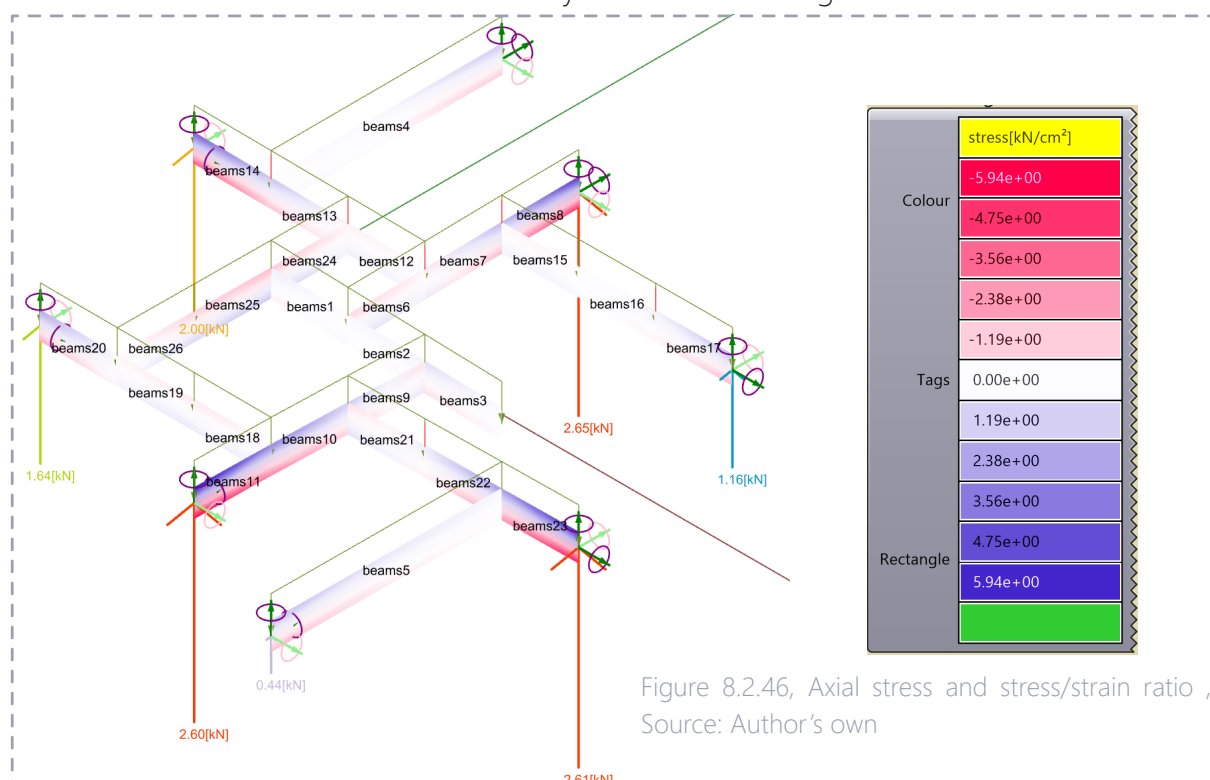


Figure 8.246, Axial stress and stress/strain ratio
Source: Author's own

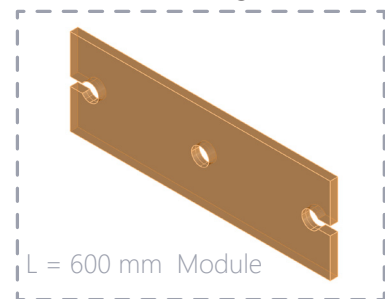
8.2.4 Ansys Simulations(FEM)

Simulation Strategy

Given the large number of possible combinations—arising from three module lengths and three connection types—a total of 54 configurations could theoretically be analysed. However, simulating every case would be inefficient and unnecessary. Instead, a strategic simplification was adopted to capture key structural behaviours while keeping the process manageable:

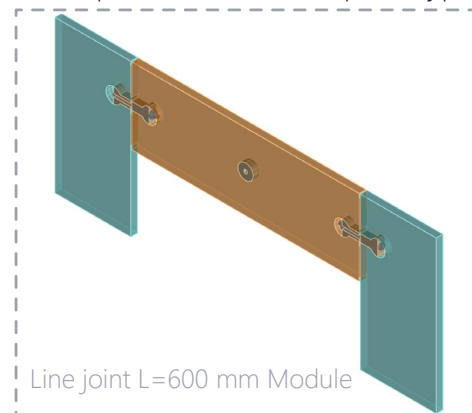
1. Single Module Evaluation

Used to verify whether the selected glass thickness could safely resist applied design loads. Also, observing stress concentration around wholes and edges.



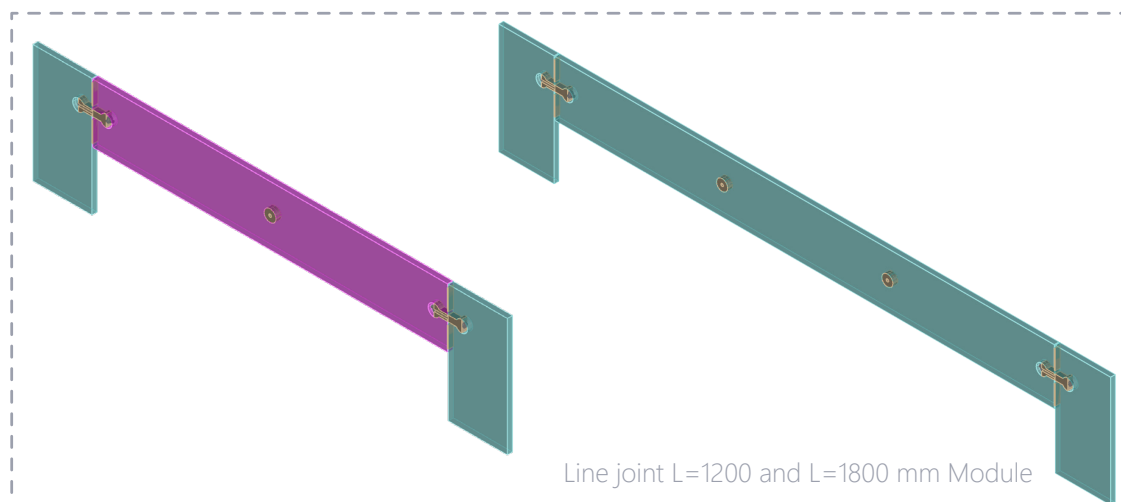
2. Linear Joint Simulation

A line-type connection was modeled (simplified) to replicate the tested prototype and validate the digital model.



3. Module Length Variations

All three lengths were analysed to confirm that different spans remained within safe performance limits.



4. Joint Type Simulations

T-shaped and **cross-shaped** connections were simulated to assess local stress behaviour and compensate for lack of testing opportunity to validate the 2 other connection types..

This targeted method allowed for meaningful insight while maintaining consistency with experimental observations.

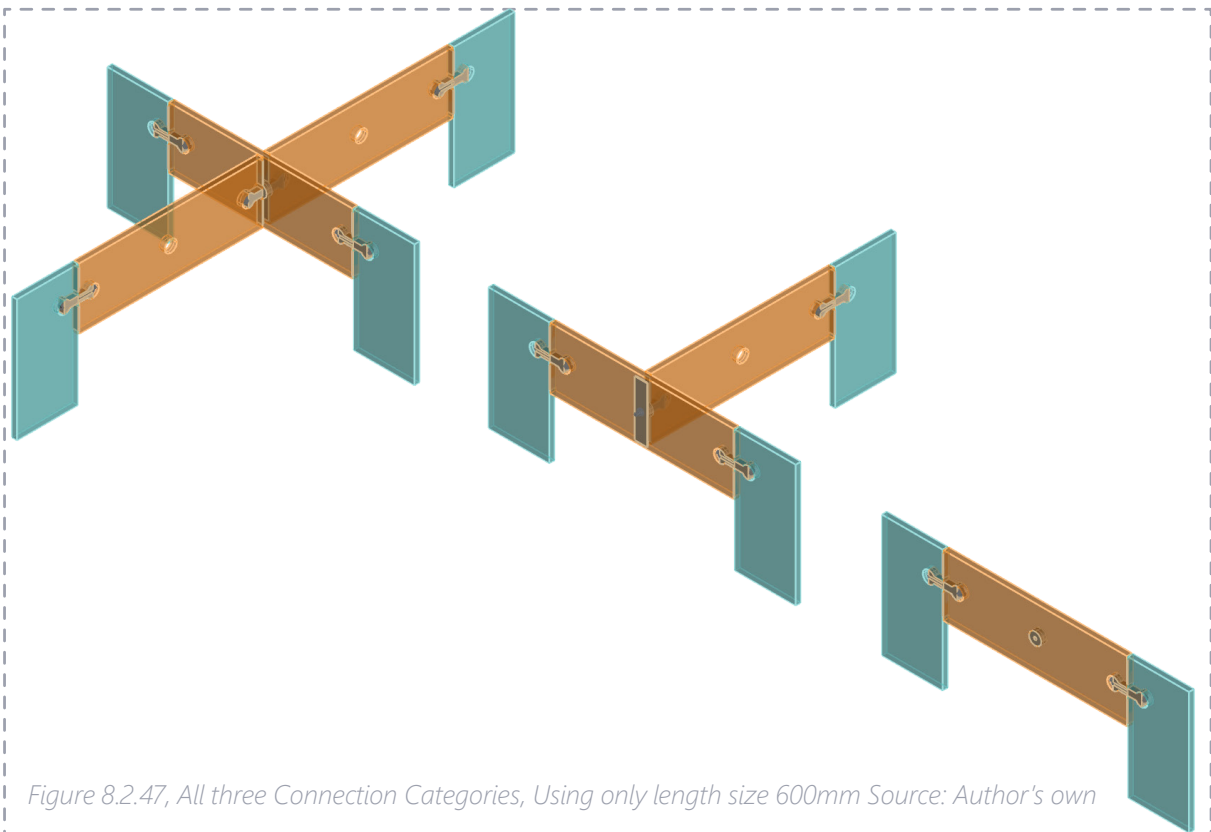


Figure 8.2.47, All three Connection Categories, Using only length size 600mm Source: Author's own

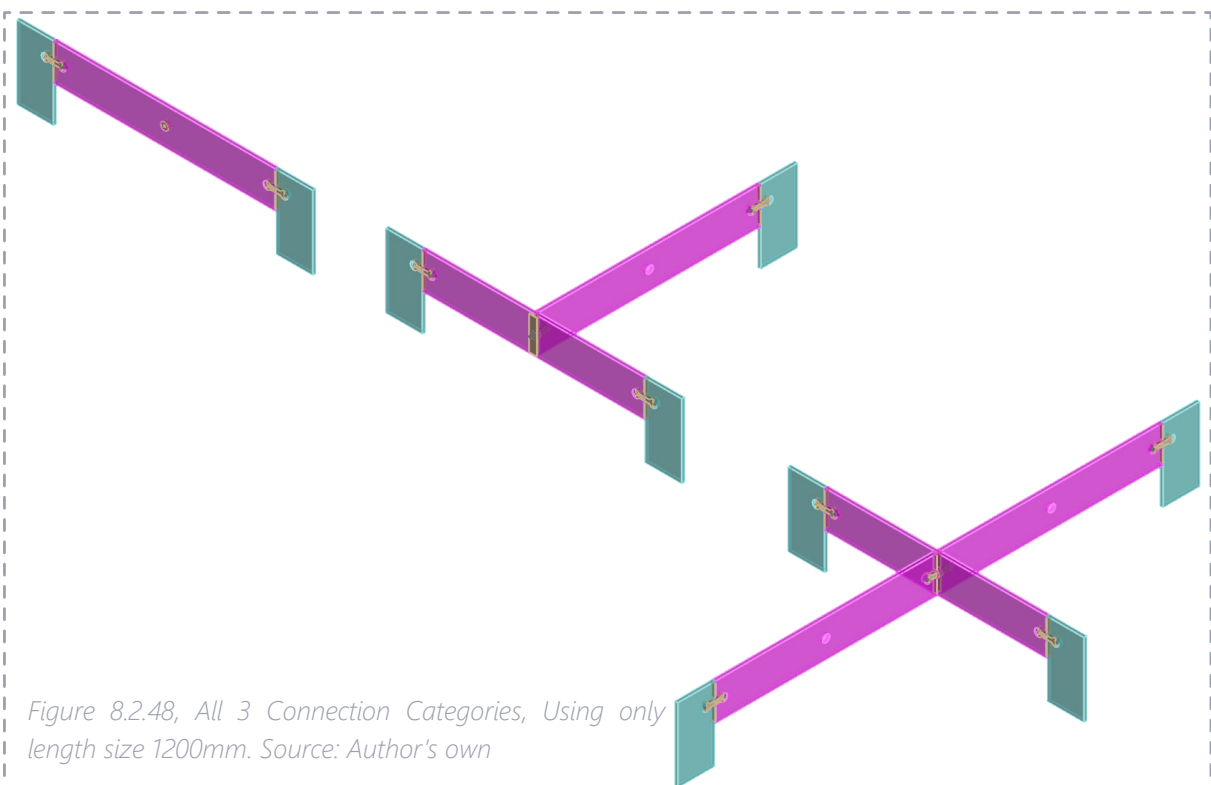


Figure 8.2.48, All 3 Connection Categories, Using only length size 1200mm. Source: Author's own

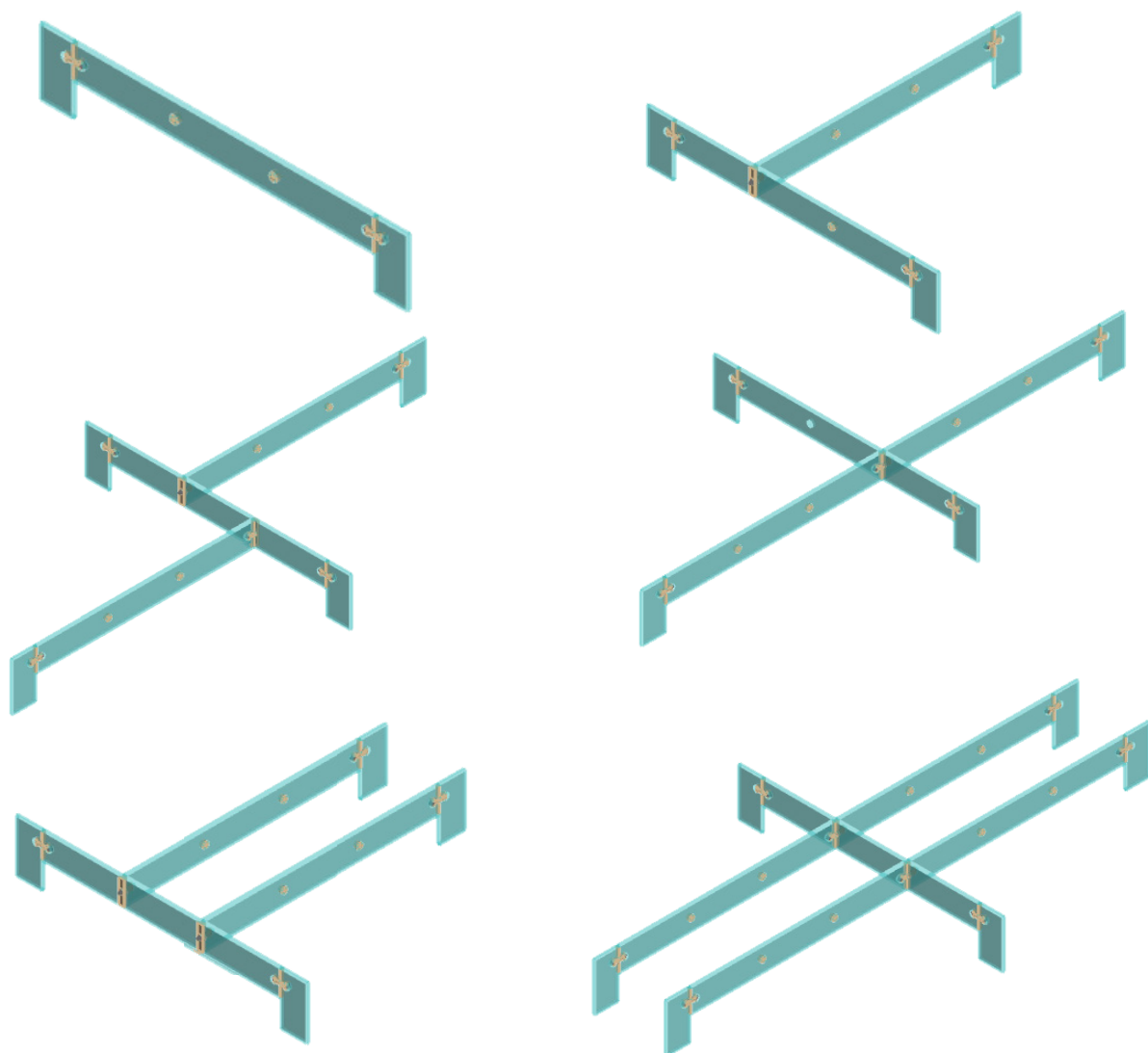


Figure 8.2.49, All 3 Connection Categories, Using only length size 1800mm. Source: Author's own

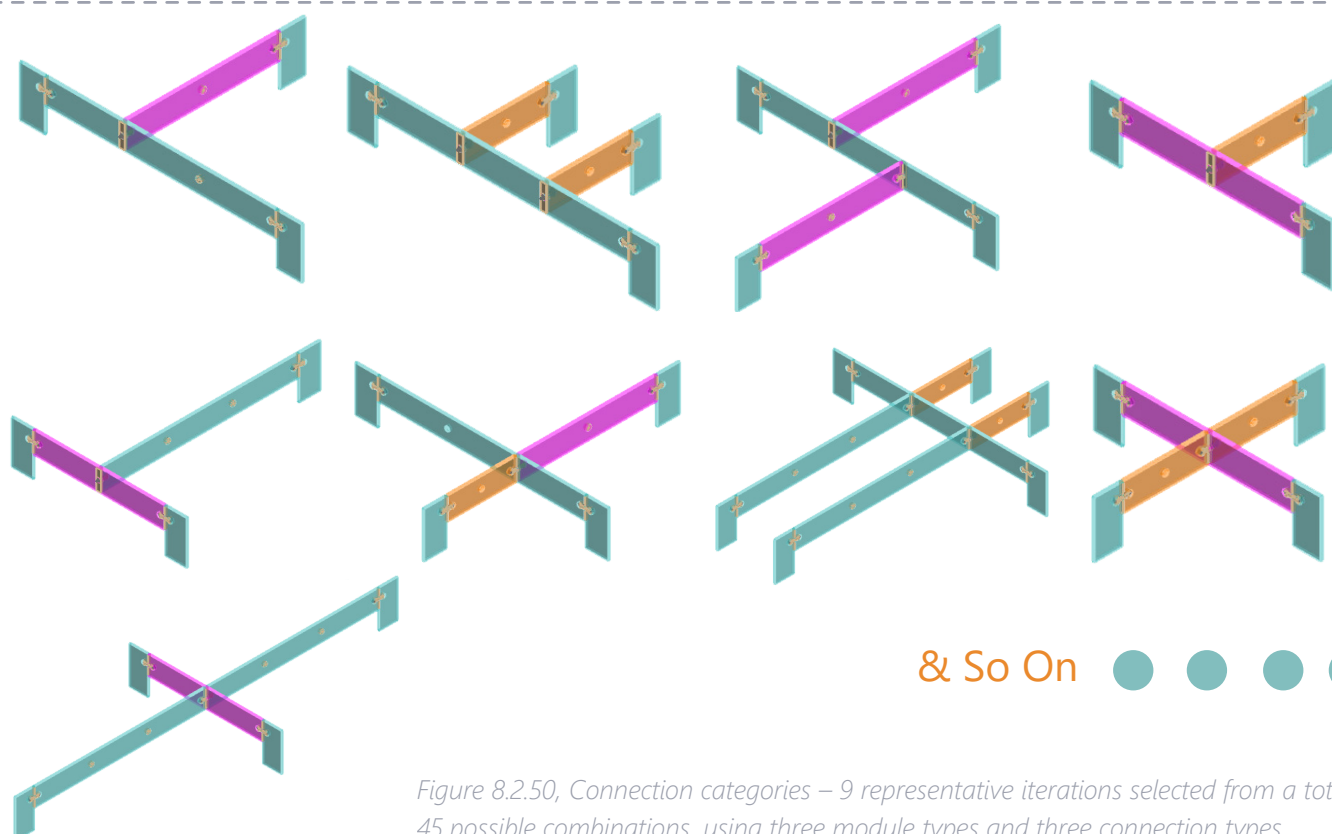


Figure 8.2.50, Connection categories – 9 representative iterations selected from a total of 45 possible combinations, using three module types and three connection types.

1. Single Module Evaluation

- L600mm module

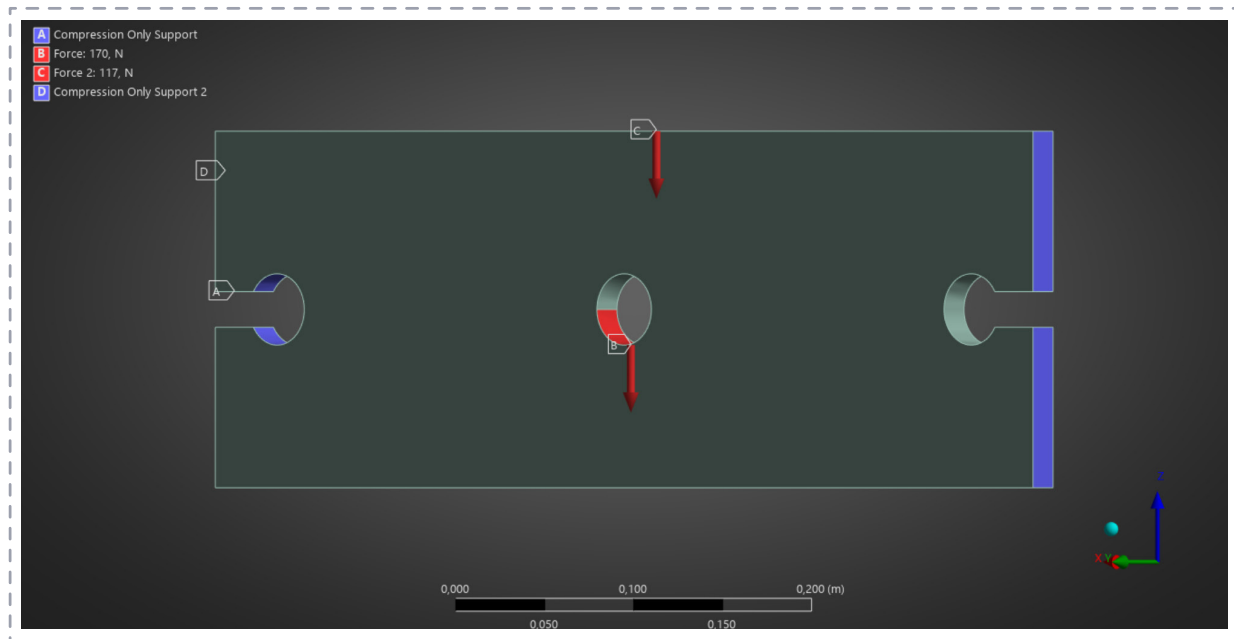


Figure 8.2.51, Simulation set up. Source: Author's own

Simulation setup showing two times point loads applied through the middle hole and a uniformly distributed load on the top surface. Compressive supports were defined around the holes and at the contact interface with the wooden strips.

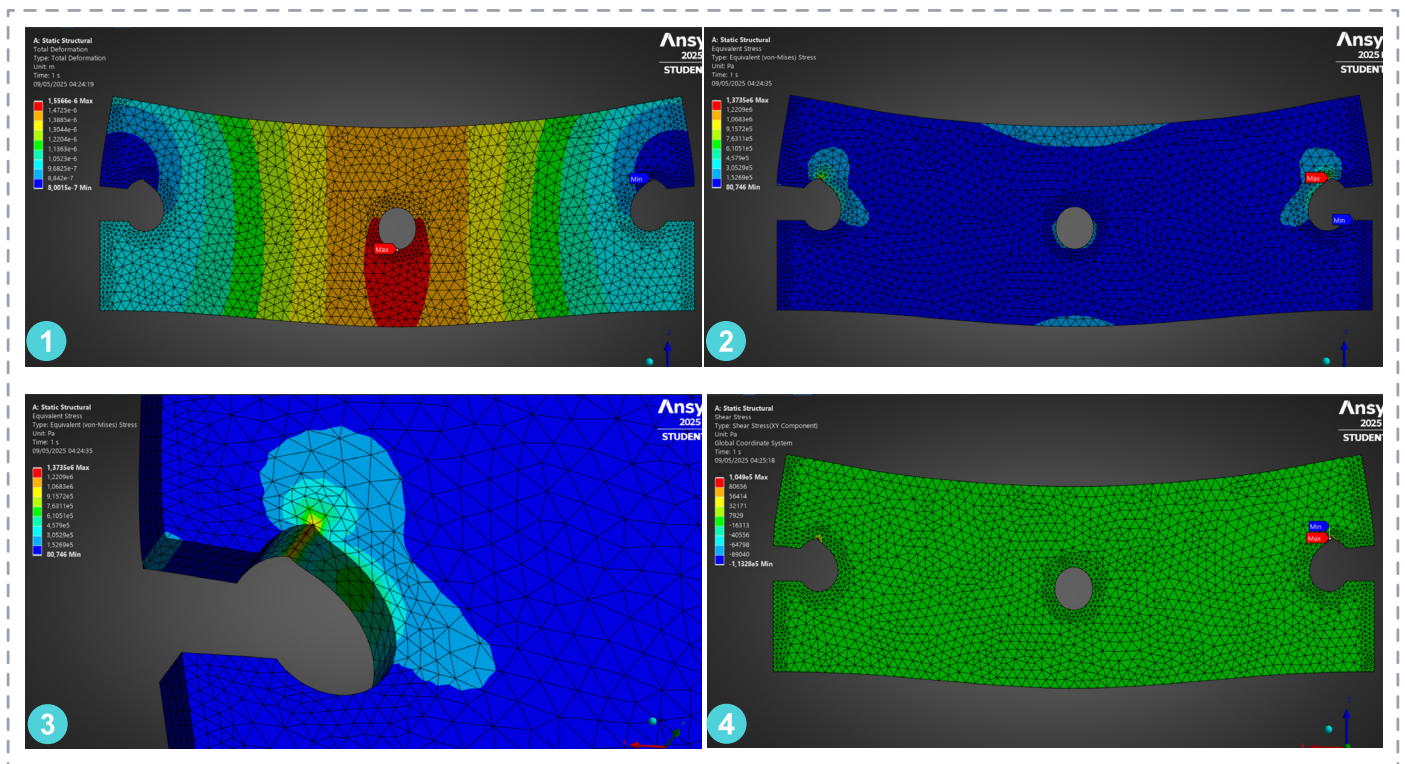


Figure 8.2.52, Simulation Results. 1) Deformation 2) Equivalent stresses 3) Closer view to max stress position 4) shear stress Source: Author's own

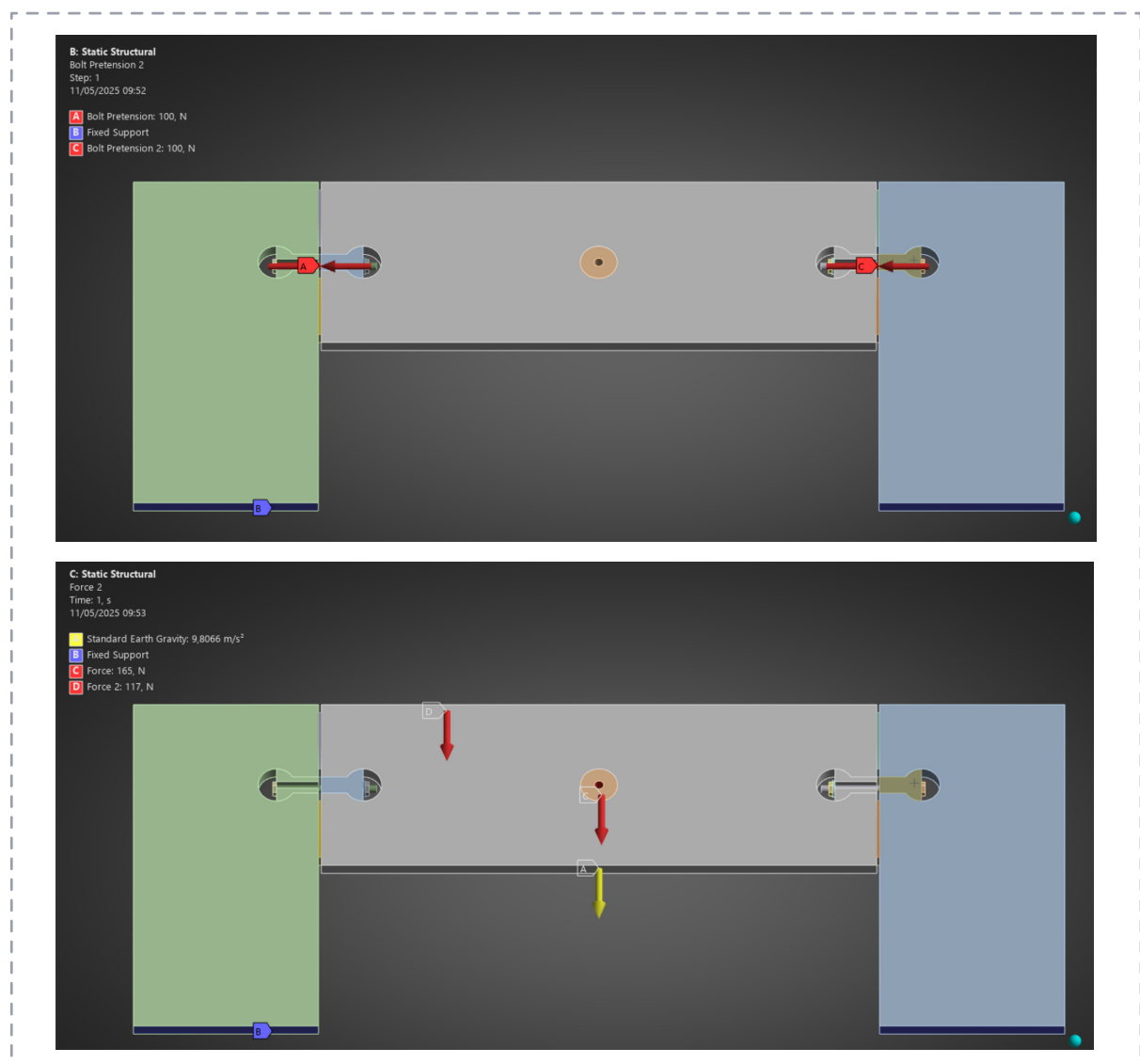
2. Linear Joint Simulation

- L600mm module
 - Set Ups

In the this simulation, a full assembly of all three connected modules was analyzed to better simulate the connections and obtain more accurate results for the glass panels by **defining contact surfaces**.

The simulation followed a **two-step loading process**. In the **first step**, only the **preload** was applied to the bolts, and **fixed supports** were assigned at the **ends of the fins** (clamping points). In the **second step**, **Loads** namely, uniformly distributed loads (UDL), point loads, and gravity **were applied** while keeping the fixed supports active. **The results showed stress values well below 60 MPa, which is within the safe tensile strength range for heat-strengthened glass.**

Three types of contact definitions were used in the model: **frictional**, **rough**, **frictionless**. The **interface between the glass and wooden connectors and wooden spacers** was defined as **frictional**, with a **coefficient of friction of 0.4**. The **contact between the nut and washer with the bolt** was defined as **rough**, while the **bolts' contact with the wooden parts** was modeled as **frictionless**.



- Set Ups

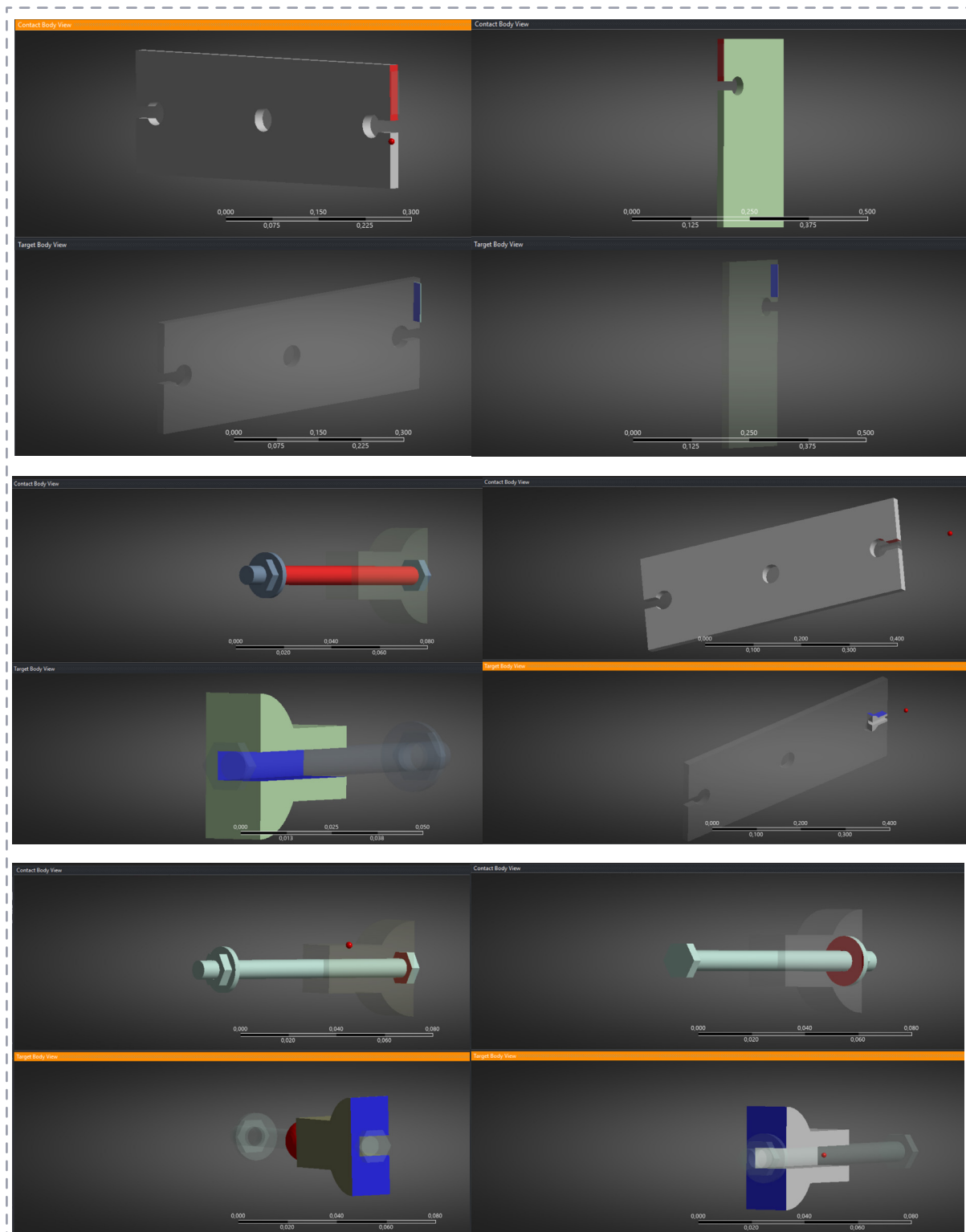


Figure 8.2.53, Simulation Contact set up. Source: Author's own

- Results

Equivalent Stress

The maximum observed stress is 5.9 MPa, which is significantly lower than the allowable tensile strength of heat-strengthened glass (60 MPa), confirming that the design remains well within the safe range under these loading conditions.

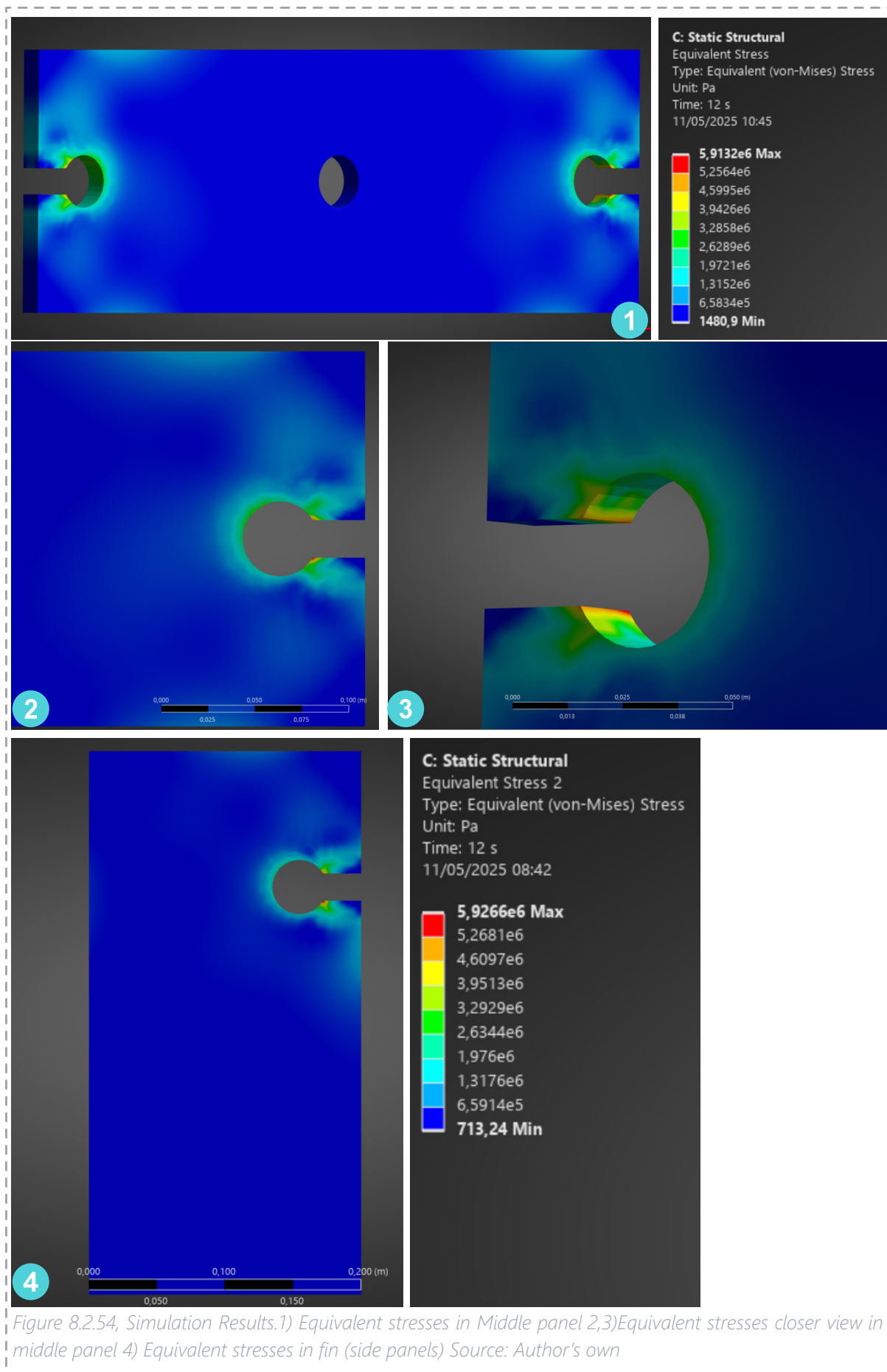


Figure 8.2.54, Simulation Results.1) Equivalent stresses in Middle panel 2,3)Equivalent stresses closer view in middle panel 4) Equivalent stresses in fin (side panels) Source: Author's own

The images below show the equivalent (von Mises) stresses and Equivalent elastic strain (von Mises strain) in the Wooden connectors and strips separately. The maximum equivalent elastic strain in the wooden connector was 0.00045, which is well below the typical elastic strain limit for hardwood (approximately 0.001–0.002). This confirms that the wood remains in the elastic range and is not at risk of local failure or permanent deformation under the applied loading conditions.

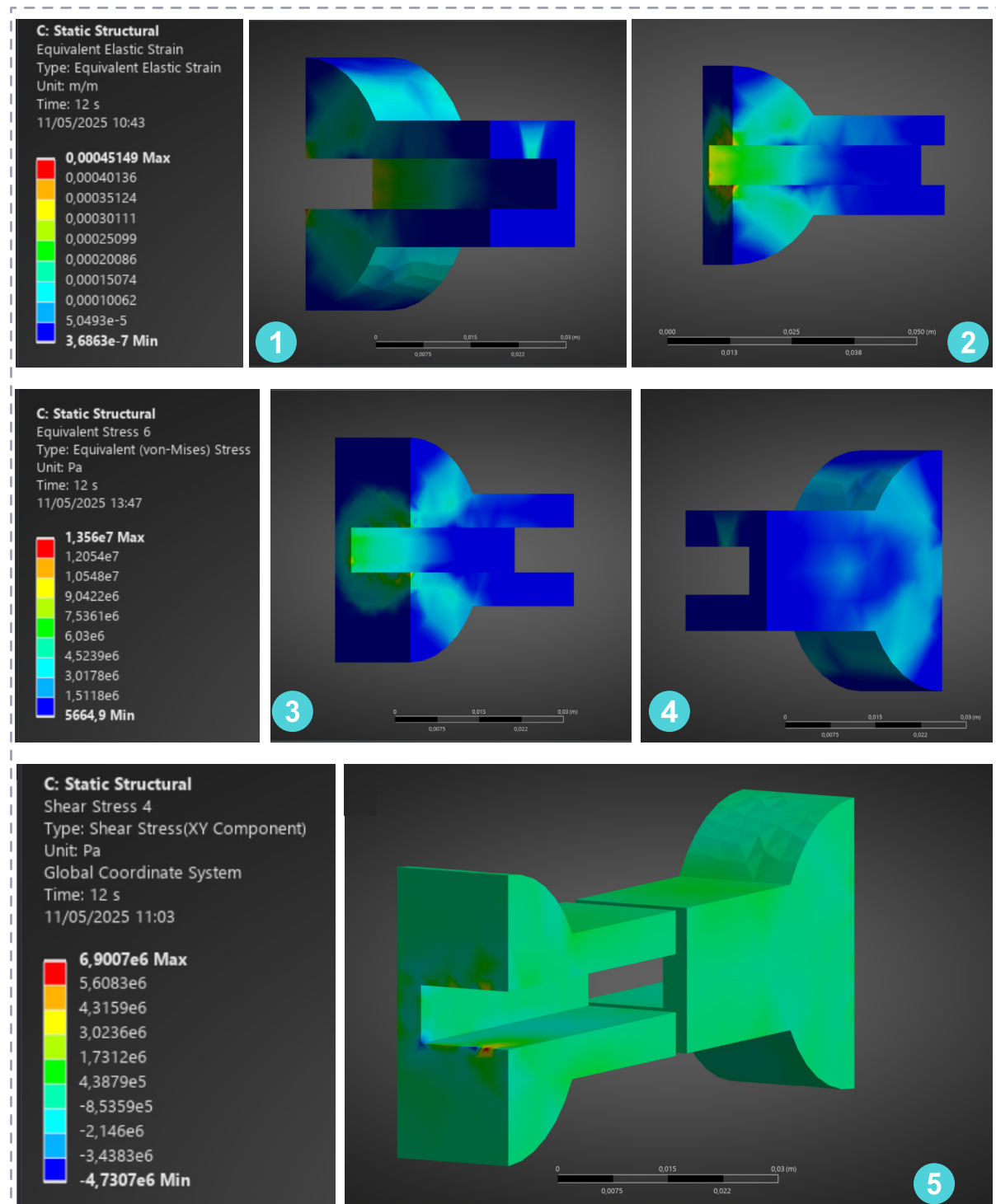
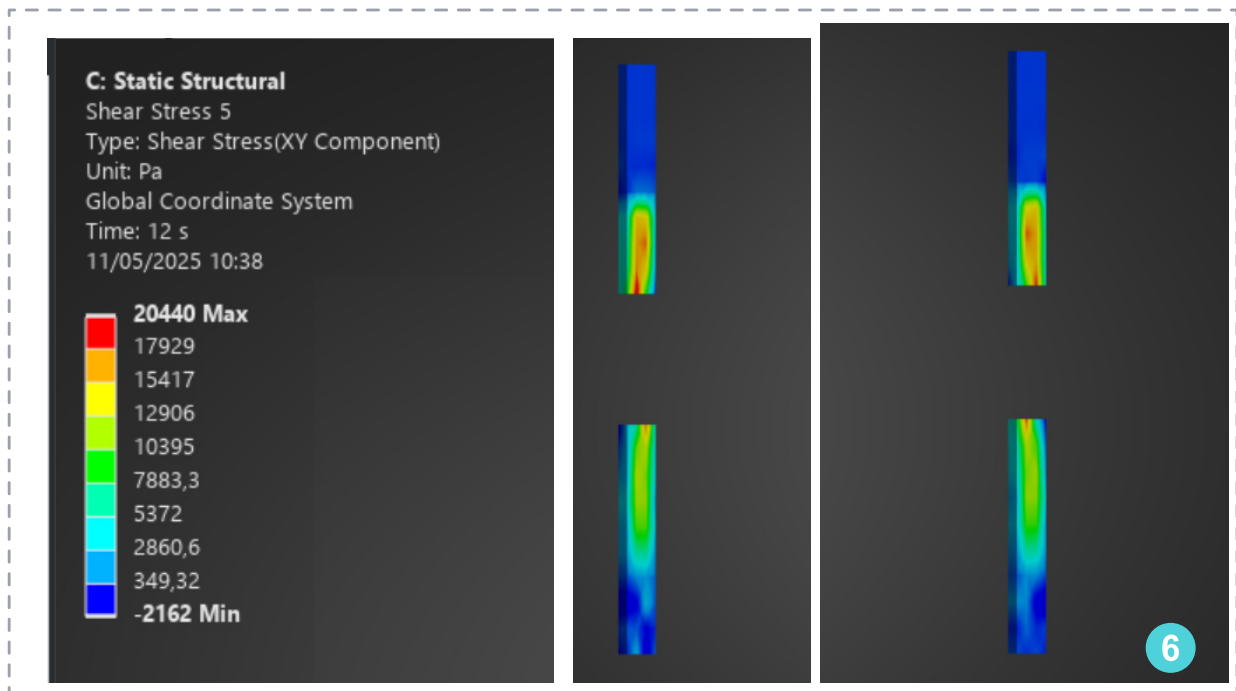
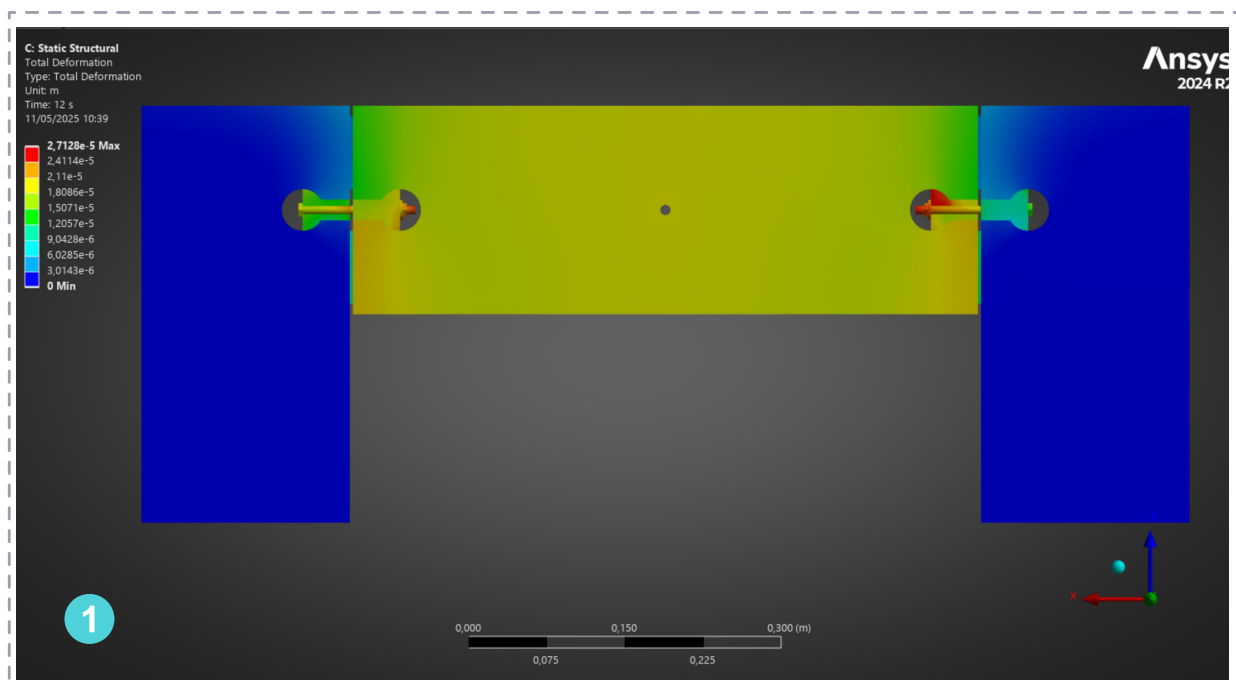


Figure 8.2.55, Simulation Results.1,2) Equivalent elastic strain in wooden connectors 3,4)Equivalent stresses in wooden connectors panel 5) equivalent stresses in wooden strips 6) Shear stresses in wooden connectors
Source: Author's own



The simulation shows that the equivalent (von Mises) stress in the wooden connector is approximately 13 MPa. Since the loading is applied in transverse (perpendicular) compression to the grain, the relevant material strength is around 20 MPa for hardwood. This means the simulated stress remains within the allowable range, confirming that the wooden component is safely loaded and no local crushing or failure is expected under the given conditions. Based on data from EduPack, the maximum shear strength of oak along the grain is approximately 18 MPa. As shown in the image above, the simulated shear stress in the wooden connector reaches around 7 MPa, which remains well below the material limit, indicating that the connection is safe under the given loading conditions. To resist these loads, the amount of preload required was calculated to be only 717 N. In the simulation, a preload of 1 kN was applied to provide an additional safety margin. Also stress in wooden strips with 0.02 Mpa is lower than the compressive strength of wood perpendicular to the grain which is 20Mpa



Based on EN 16612, which provides guidelines for structural glass, the deflection limit for glass beams is typically set at $L/300$. For a span of 600 mm, this results in a maximum allowable deflection of 2 mm (0.002 m). In the simulation, the observed deflection was 2.7128×10^{-5} m (0.027 mm), which is significantly lower than the allowable limit. This confirms that the beam satisfies the serviceability criteria for deflection under the applied loading conditions.

0.000027128 m < 0.002 m → Well within the allowable limit

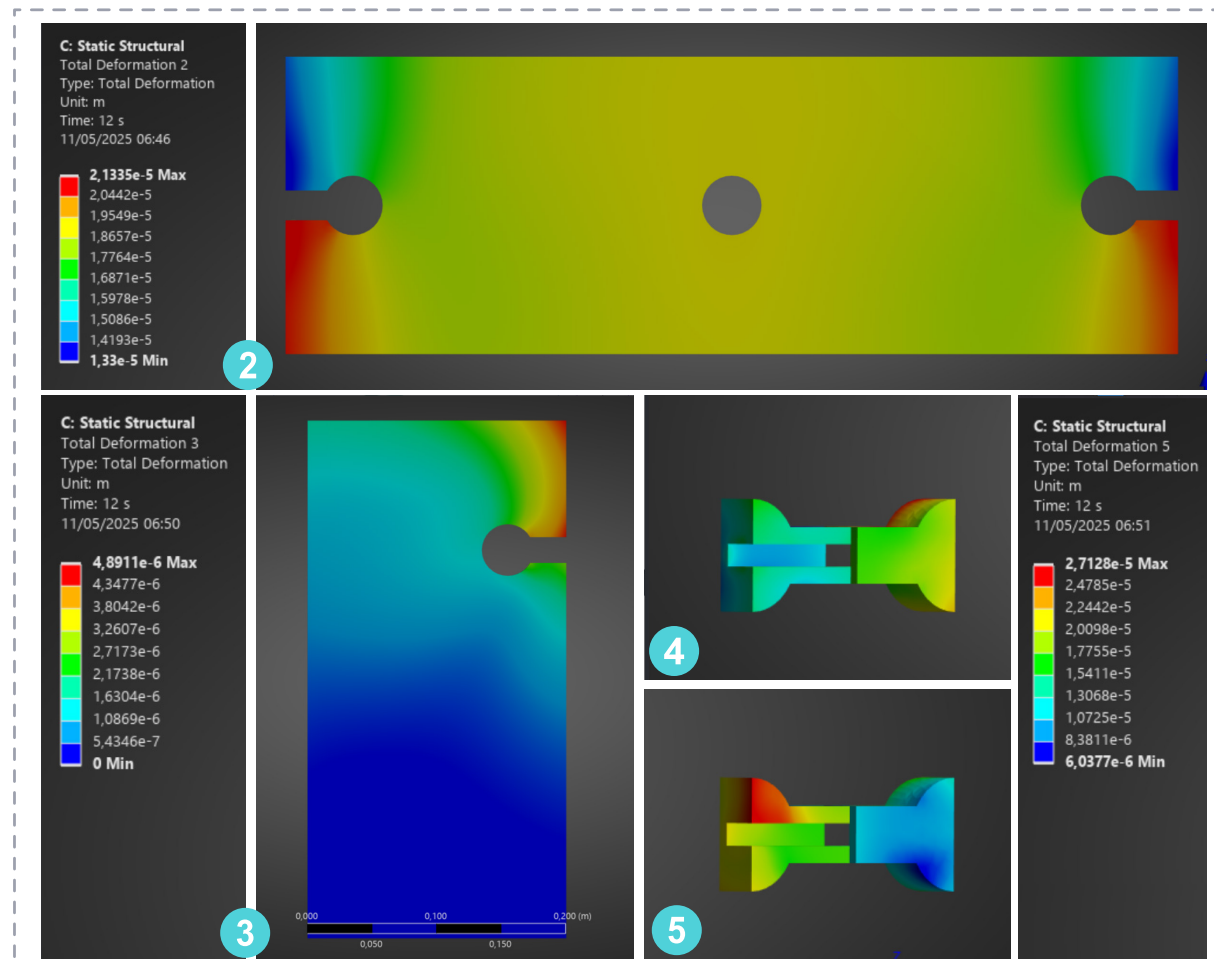
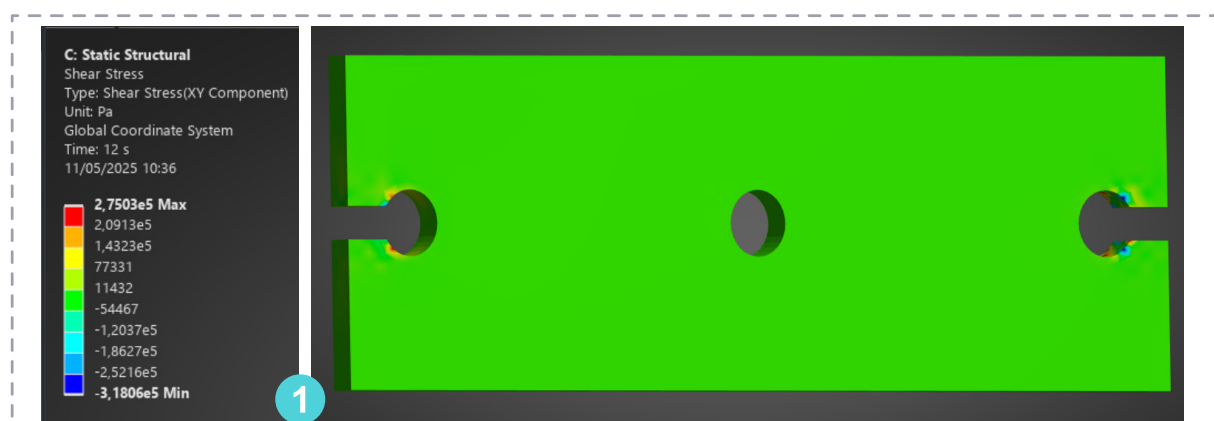


Figure 8.2.56, Simulation Results. 1) Total deformation . 2) Deformation in middle panel . 3) deformation in side panel (fins). 4) deformation in wooden connectors Source: Author's own

Based on the simulation, the shear stress around the holes is approximately 0.33 MPa, which is significantly lower than the shear strength and tensile strength of heat-strengthened glass. With a typical tensile strength of around 60 MPa and a shear strength in the range of 20–25 MPa, the observed stress levels indicate that the glass remains well within a safe range under the applied loading.



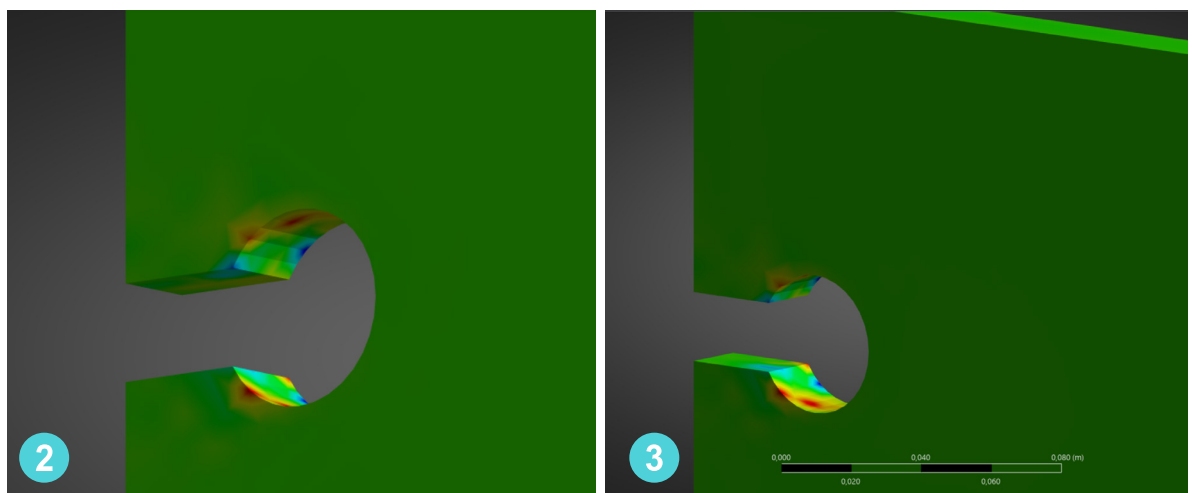


Figure 8.2.57, Simulation Results.

1) Overall shear stress in middle module. 2,3) Shear stress around the holes of middle module close view

Source: Author's own

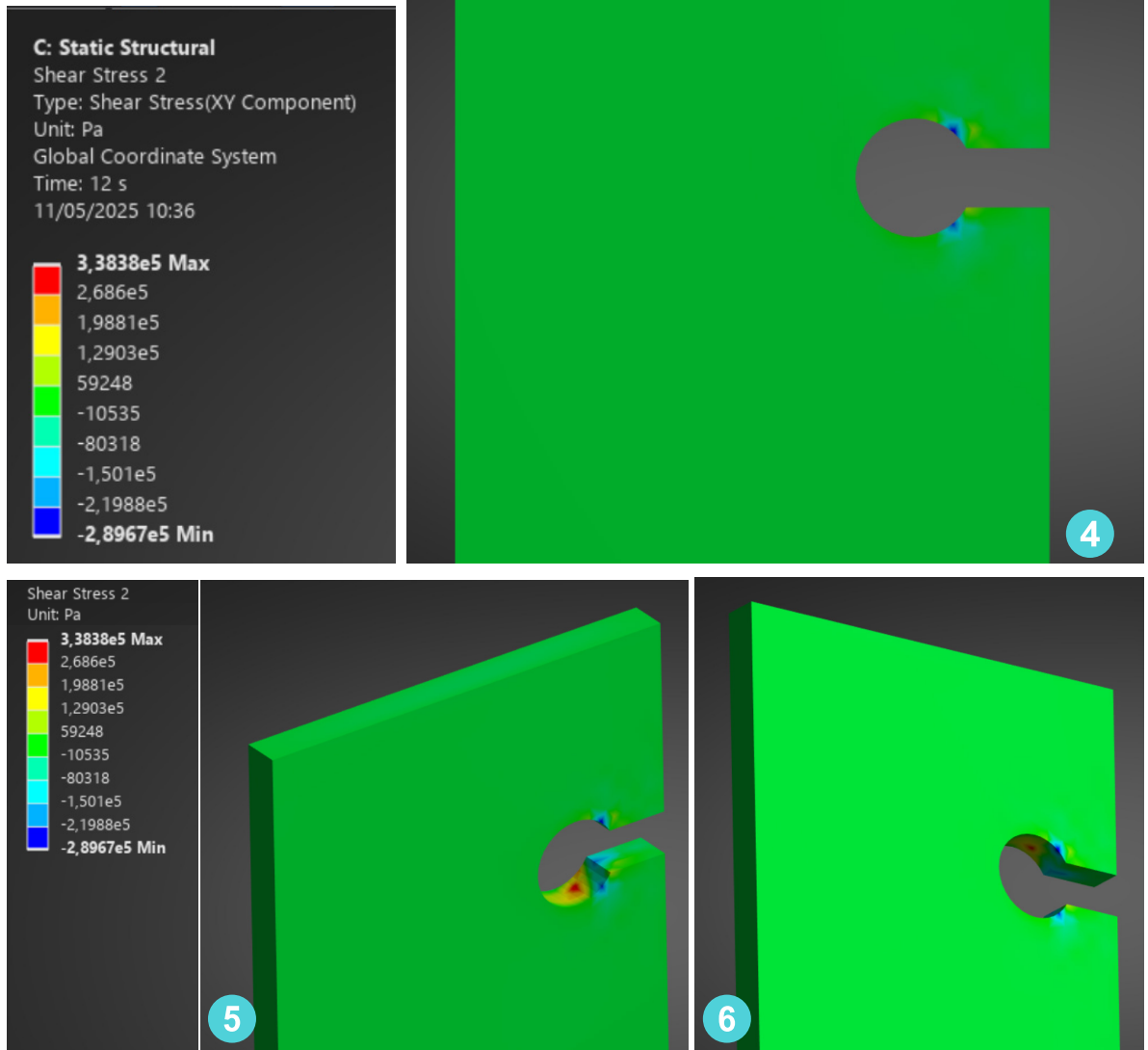


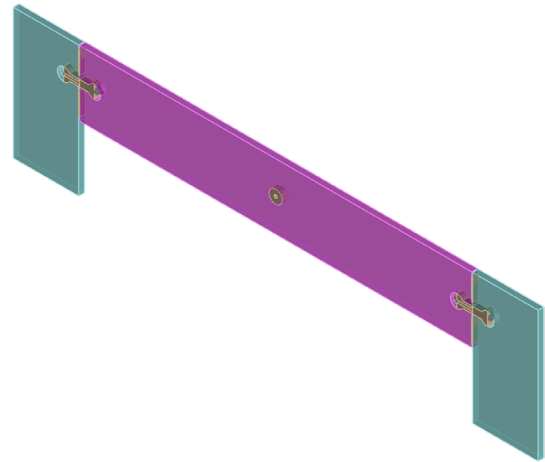
Figure 8.2.58, Simulation Results.

4) Overall shear stress in side panel (fins)

5,6) Shear stress around the holes of side module close view. Source: Author's own

2. Linear Joint Simulation

- L1200mm module
- Results



Equivalent Stress

The maximum observed stress is 10.86 MPa, which is significantly lower than the allowable tensile strength of heat-strengthened glass (60 MPa), confirming that the design remains well within the safe range under these loading conditions.

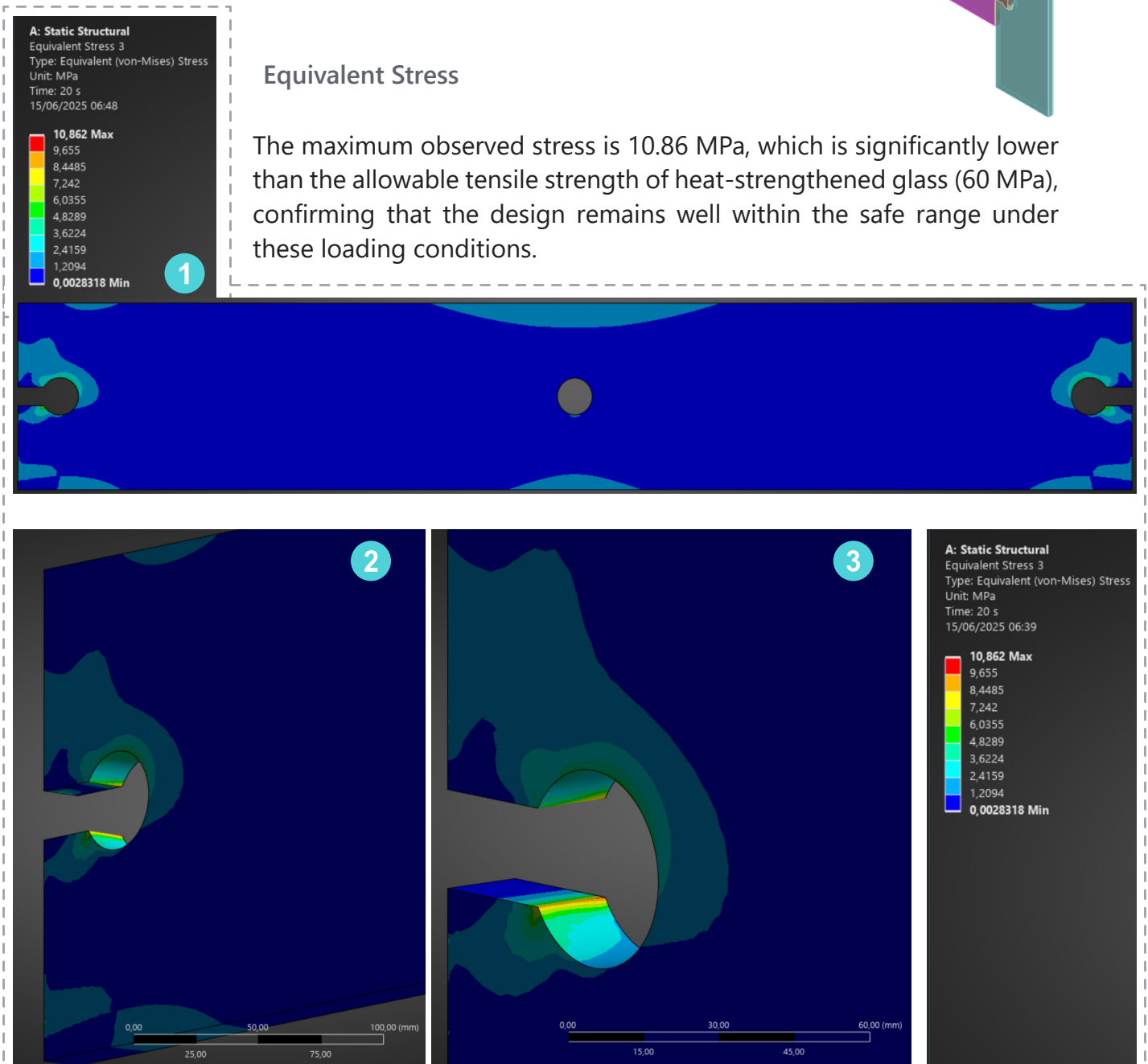


Figure 8.2.59, Simulation Results.1) equivalent stress on middle panel, 2,3) stresses around holes and edges from closer view
Source: Author's own

As shown in the close-up view, the maximum stress occurs around the bolt hole and along the edge of the glass panels; however, the magnitude of these stresses remains relatively low and within safe limits

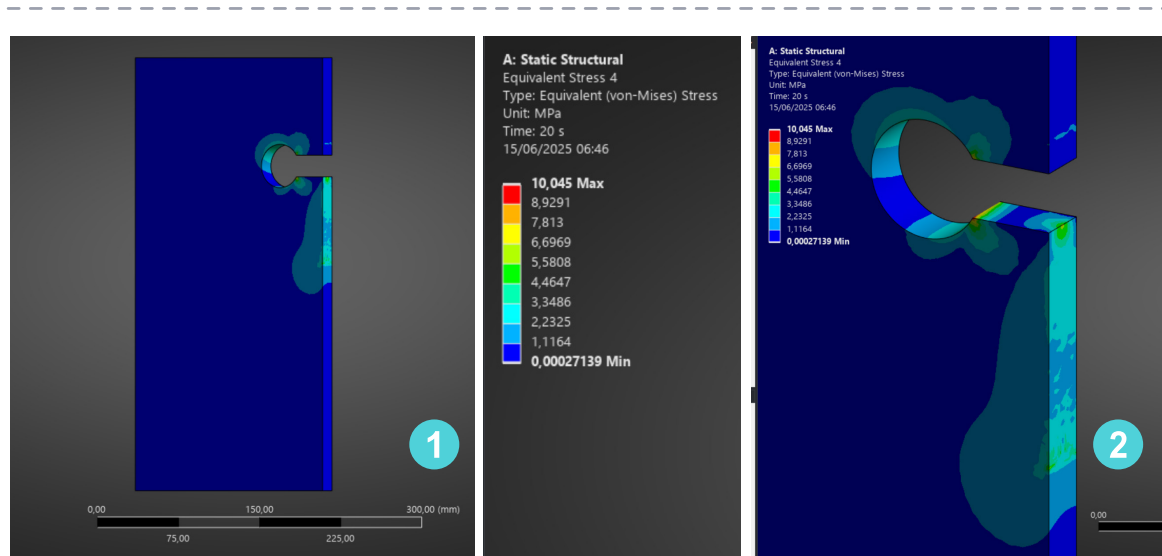


Figure 8.2.60, Simulation Results. 1) Equivalent stress on side panel, 2) stresses around holes and edges from closer view Source: Author's own

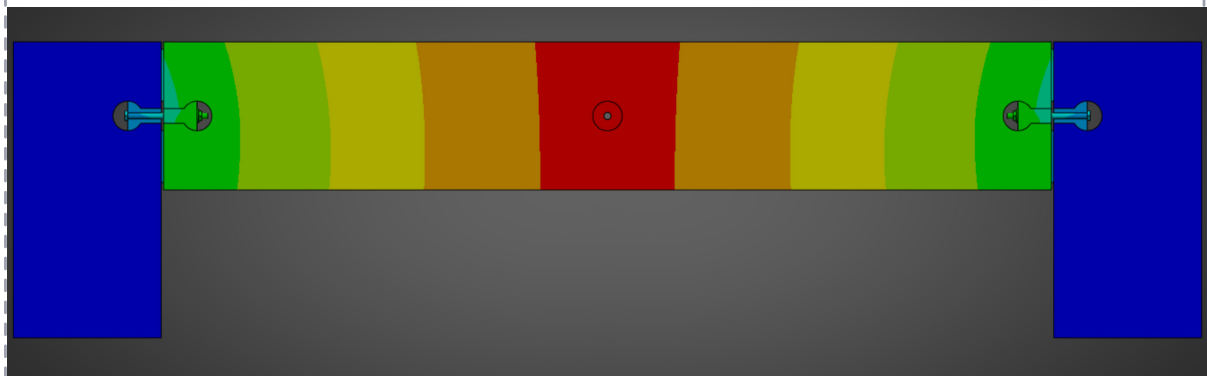
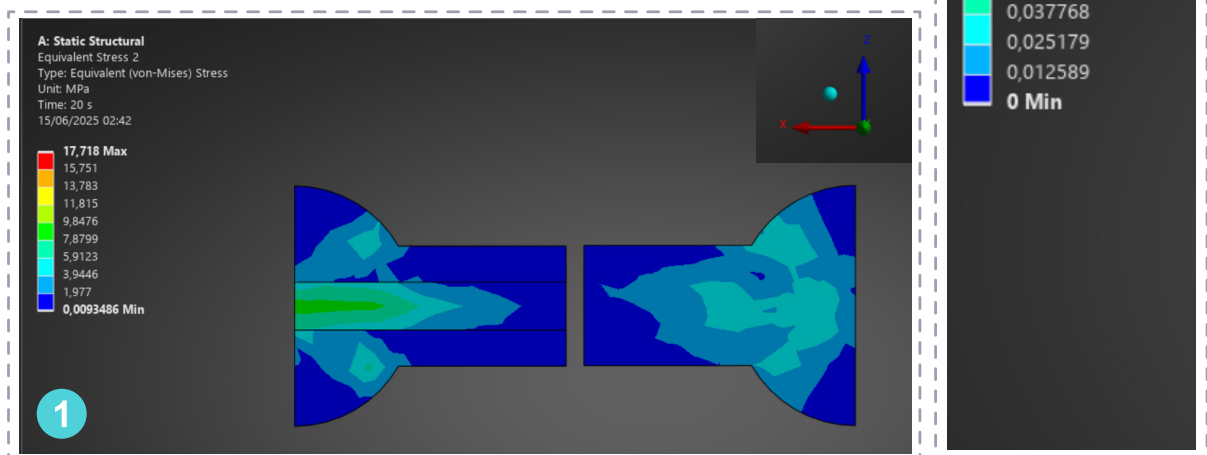
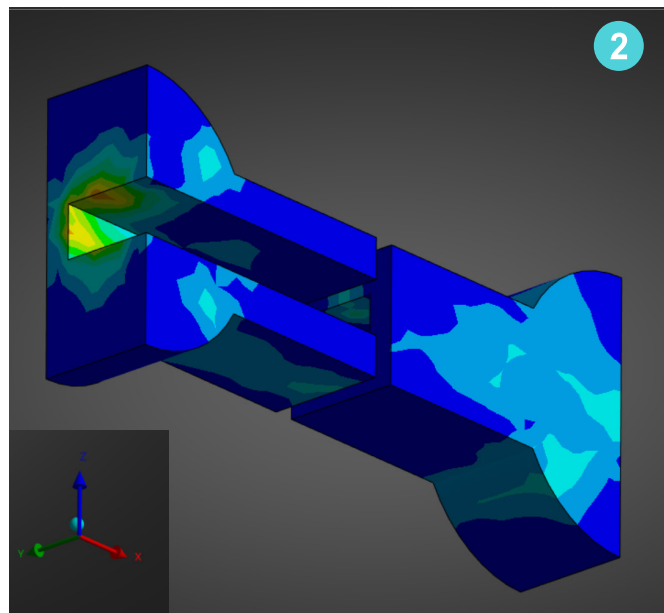
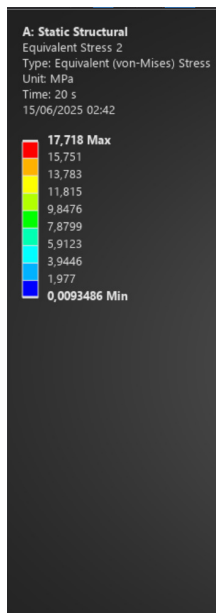


Figure 8.2.61, Simulation Results. Total deformation. Source: Author's own

Based on EN 16612, which provides guidelines for structural glass, the deflection limit for glass beams is typically set at $L/300$. For a span of 1200 mm, this results in a maximum allowable deflection of 4 mm (0.004 m). In the simulation, the observed deflection was 0.1133 mm, which is significantly (40 times) lower than the allowable limit. This confirms that the beam satisfies the serviceability criteria for deflection under the applied loading conditions.

0.1133 mm < 4 mm → Well within the allowable limit





Based on EduPack data, the **compressive strength** of hardwood parallel to the grain ranges between **75 to 80 MPa** and perpendicular to grain is **20 and 25 MPa**. In the simulation, the maximum compressive stress observed in this direction was approximately **17 MPa**, which confirms that the stress levels remain well within the **safe range** for the selected material.

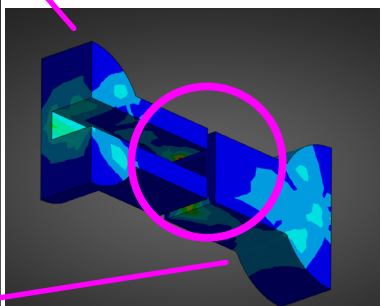
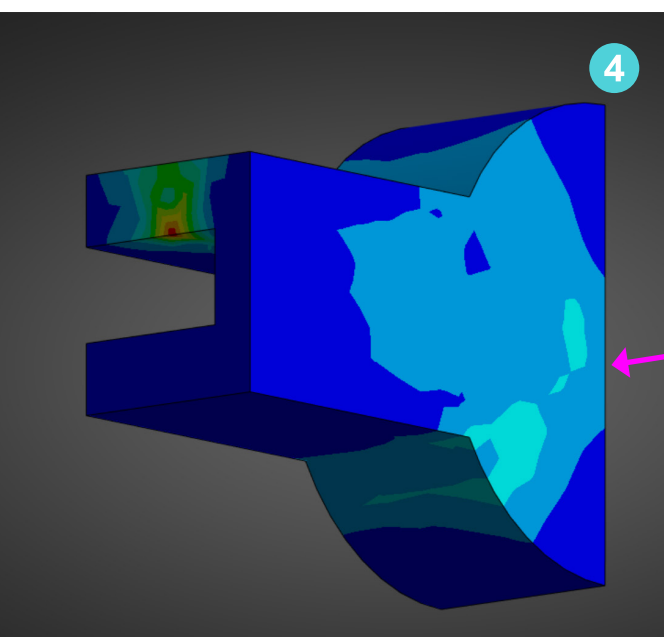
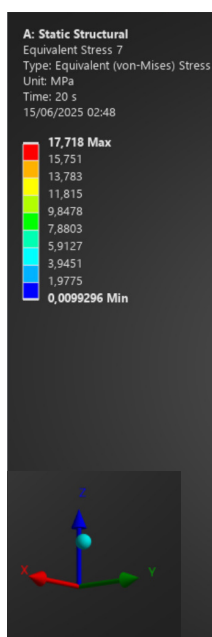
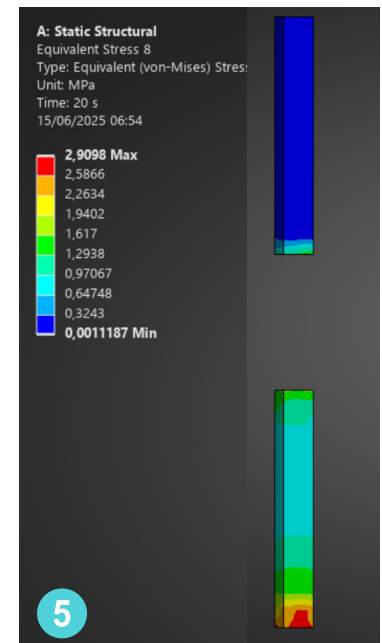
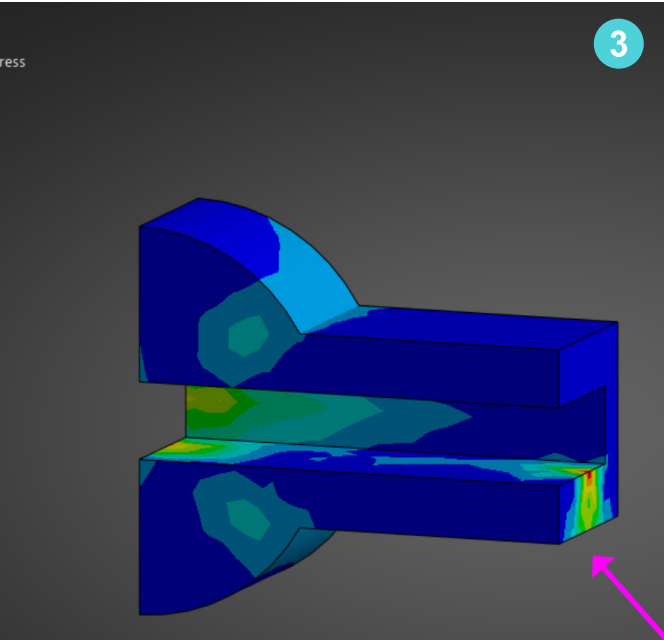
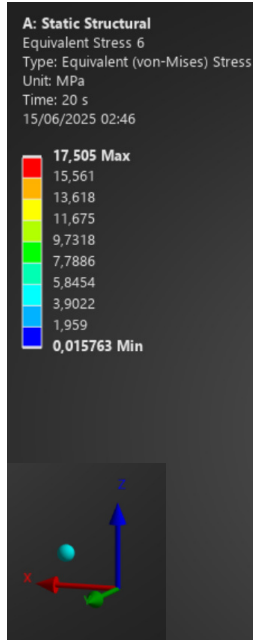


Figure 8.2.62, Simulation Results. Equivalent stress in all wooden connectors and wooden spacers from all angles, side wooden connector and middle connector . Source: Author's own

The shear stress distribution in the wooden connectors is illustrated below, addressing concerns regarding shear strength limitations. According to EduPack data, the shear strength of hardwood is approximately 18 MPa parallel to the grain and 50–55 MPa perpendicular to the grain. In both directions, the simulated shear stresses remain below these thresholds, confirming the safety of the connection under the given loading conditions.

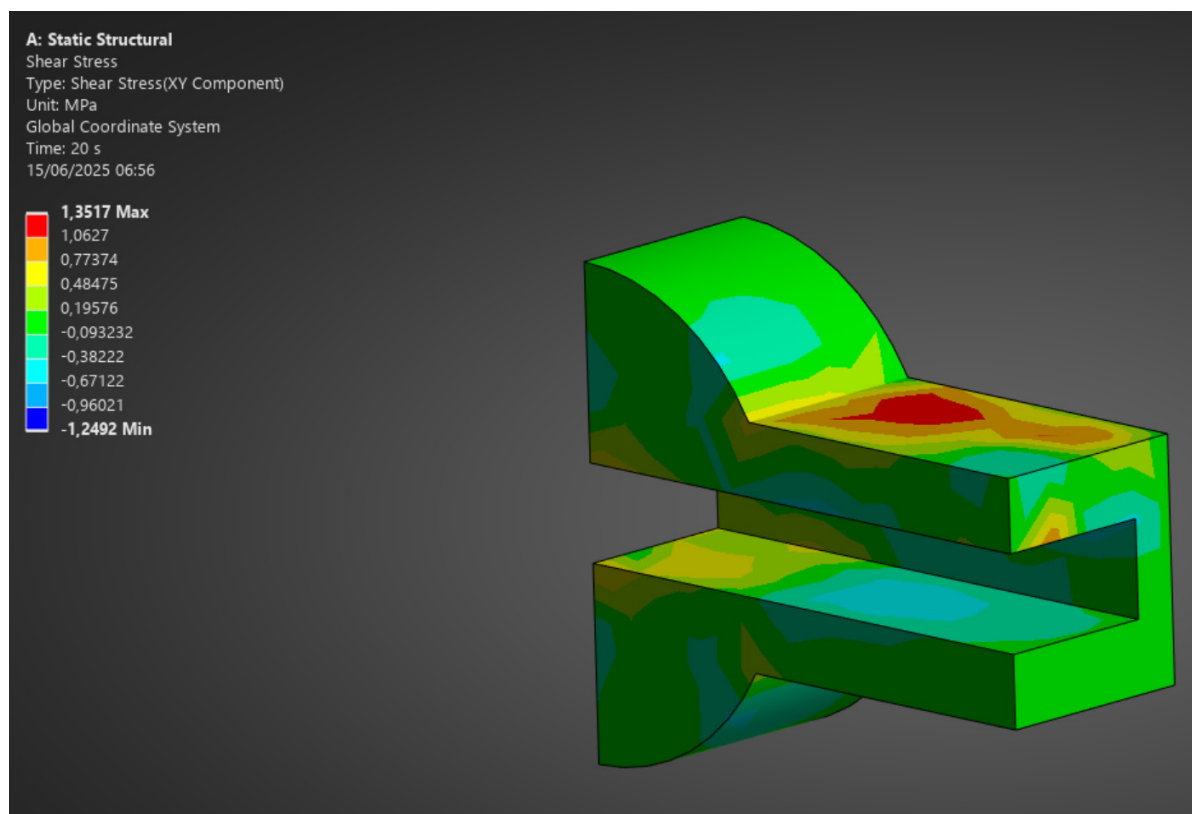
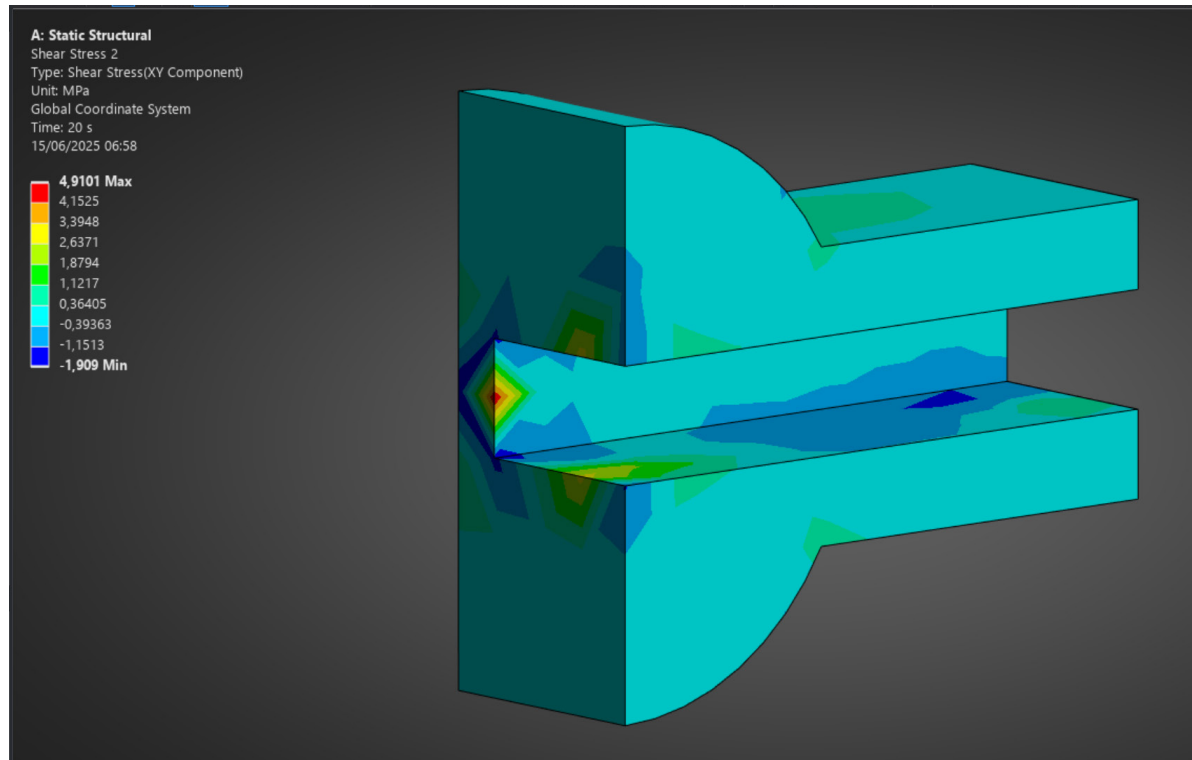
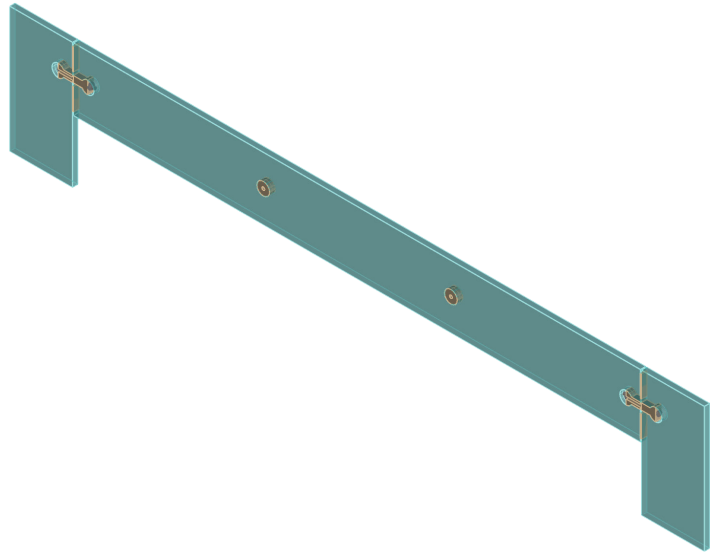


Figure 8.2.63, Simulation Results. Shear stress in wooden connectors, Top : side wooden connector and Bottom : middle connector . Source: Author's own

2. Linear Joint Simulation

- L1800mm module
 - Results



During the simulation of the 1800 mm module with a linear connection, the ANSYS model repeatedly **encountered errors** that could not be resolved. However, when the **glass panel was modeled independently**, the resulting stress levels **remained within the allowable strength range** of heat-strengthened glass. Given that the **setup and boundary conditions were consistent** with previously validated models, the errors were likely caused by **failure in the wooden connectors**. This module **required higher preload forces** and spanned a greater length, making the **wood a probable weak point**.

Based on this, the 1800 mm module was excluded from the catalogue of viable lengths when using wooden connectors. For longer spans, alternative strategies should be considered—either by **replacing wood with stiffer materials such as aluminum**, or by **increasing the number of connectors to distribute the load and reduce stress per joint**.

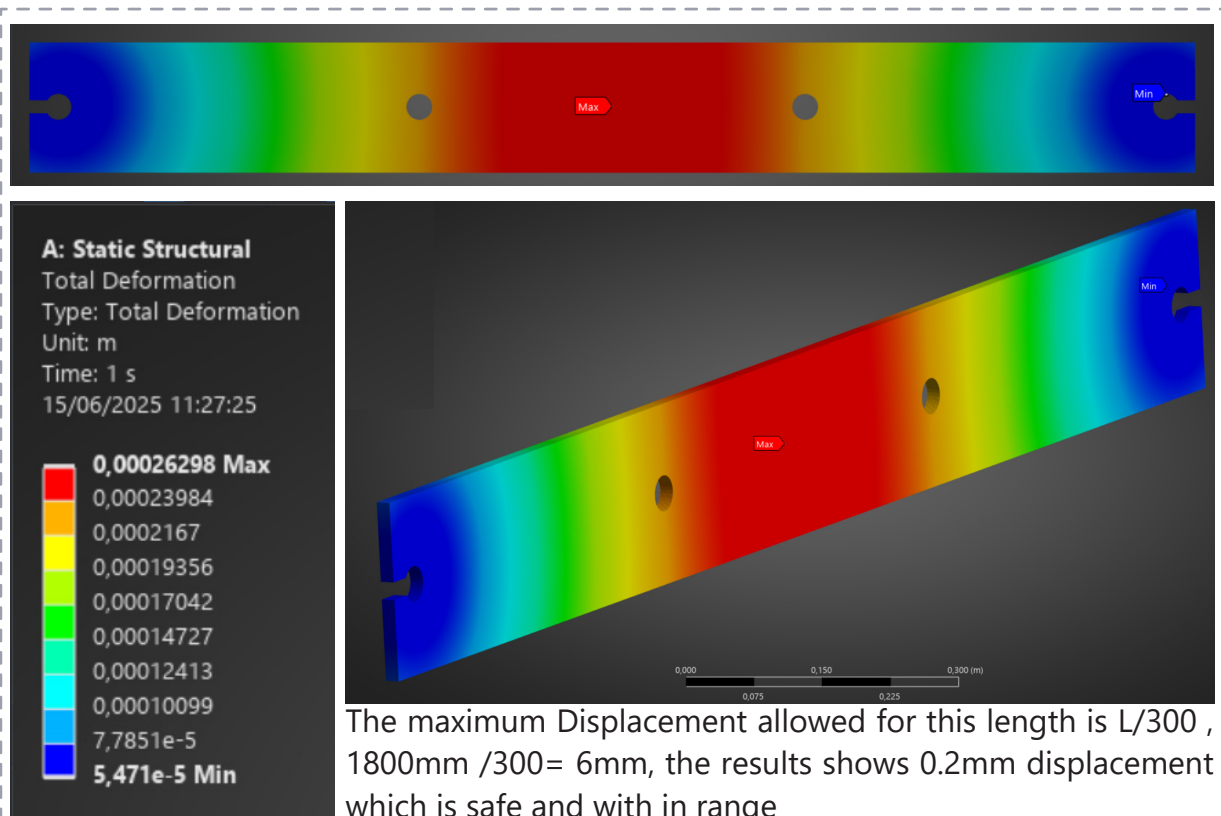


Figure 8.2.64, Simulation Results. Total Deformation in glass panel l1800mm . Source: Author's own

The maximum equivalent stress in the glass module is 9.5 Mpa, which is well below the typical stress limit for heat strengthened glass (approximately 60Mpa). This confirms that the module L 1800mm remains in the safe range and is not at risk of local failure under the applied loading conditions.

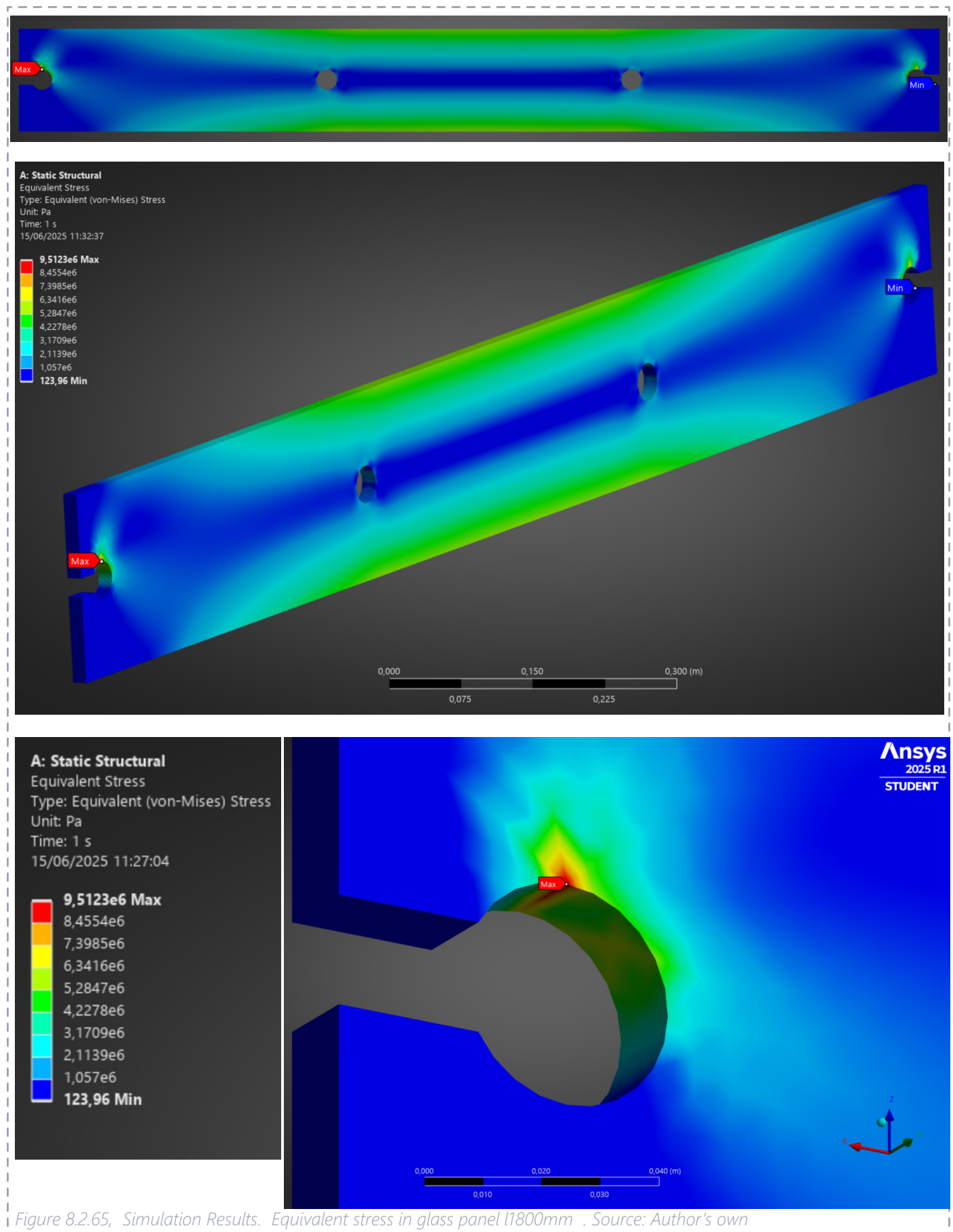


Figure 8.2.65, Simulation Results. Equivalent stress in glass panel l1800mm . Source: Author's own

2. T shape Joint Simulation

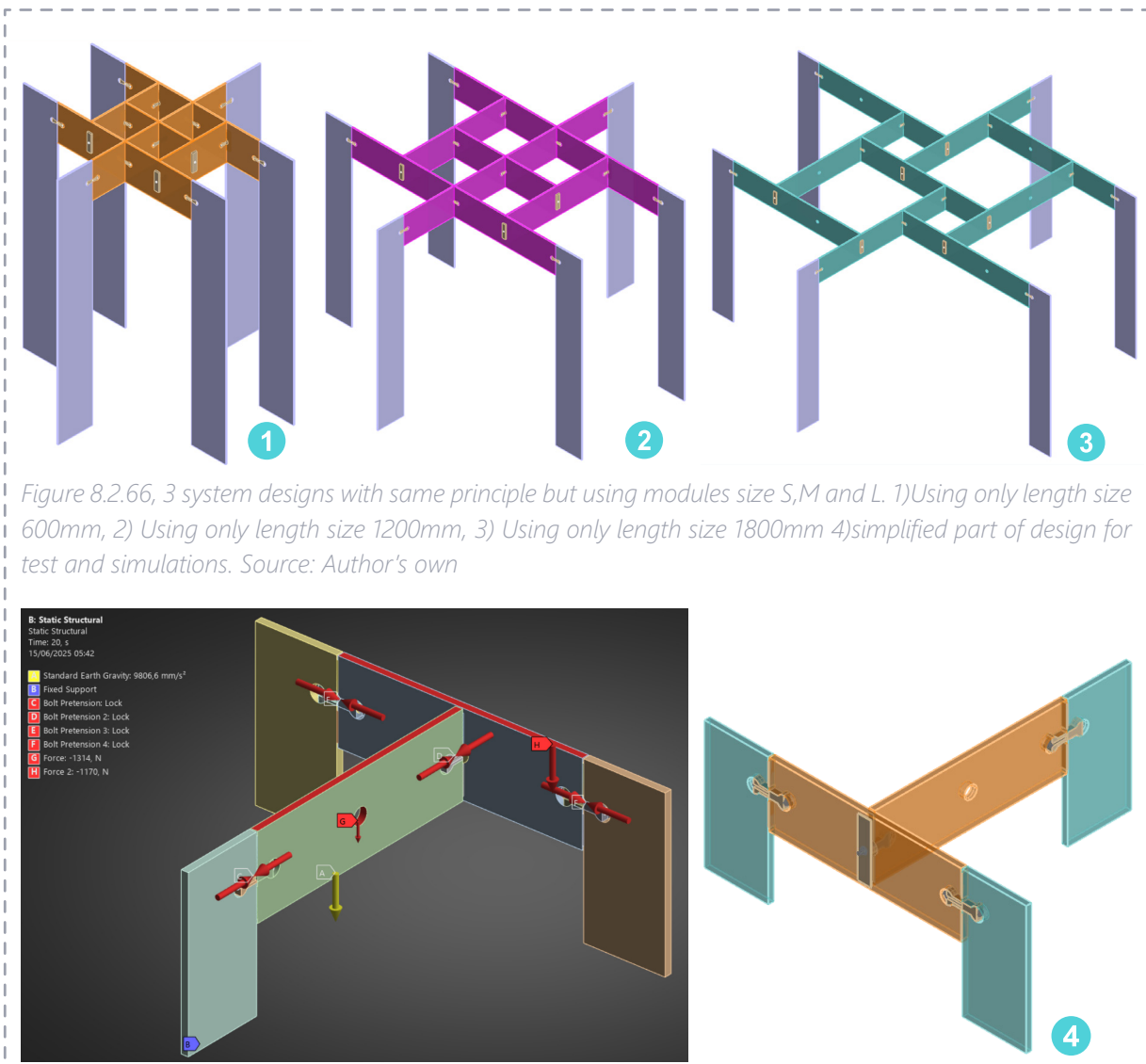
- L600mm module

- Results

To simulate the connection and module behaviour, a single representative configuration had to be selected from the many possible system variations. Due to constraints in the experimental setup—particularly the testing machine’s capacity, which was only suitable for the shortest module length—a system using this smaller module was chosen as the baseline for simulation.

To evaluate the connection’s performance under more demanding conditions, the same design logic (using one connection type and composition principles) applied using longer modules. The expected loads from these larger modules were then proportionally applied to the shorter module. This allowed the simulation to capture the stresses and deformation at the connection point under equivalent load conditions, without altering the physical test specimen.

The simulation process followed a **three-step loading sequence**, reflecting the real-world scenarios tested in the design phase. However, to maintain clarity and focus in the report, only the most critical scenario—maximum load applied to the smallest module—is presented and discussed here.



The simulation shows a maximum equivalent elastic strain of 0.0005, it is 50% of the allowable strain, for heat-strengthened glass, the typical strain limit is approximately 0.001 (or 0.1%) before failure. Meaning the design remains well within the safe limit for elastic deformation. The maximum deflection observed is 0.5 mm, which is well below the allowable limit of 2 mm for a 600 mm span ($L/300$).

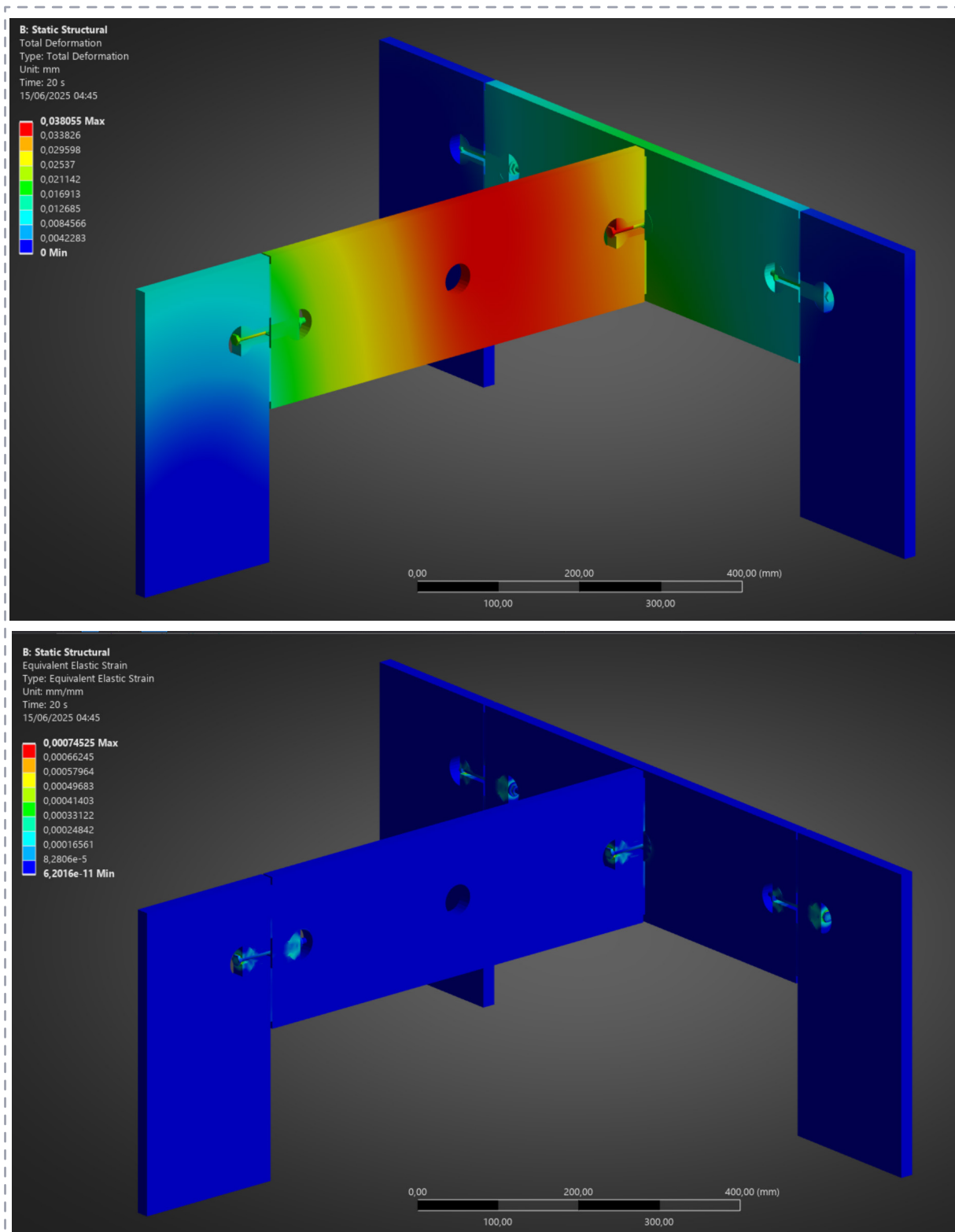


Figure 8.2.67, 3 Top, Total deformation, bottom Equivalent Elastic strain. Source: Author's own

The maximum stress observed in the simulation was approximately 7.2 MPa, which is significantly below the typical allowable stress limit for heat-strengthened glass, commonly taken as 60 MPa.

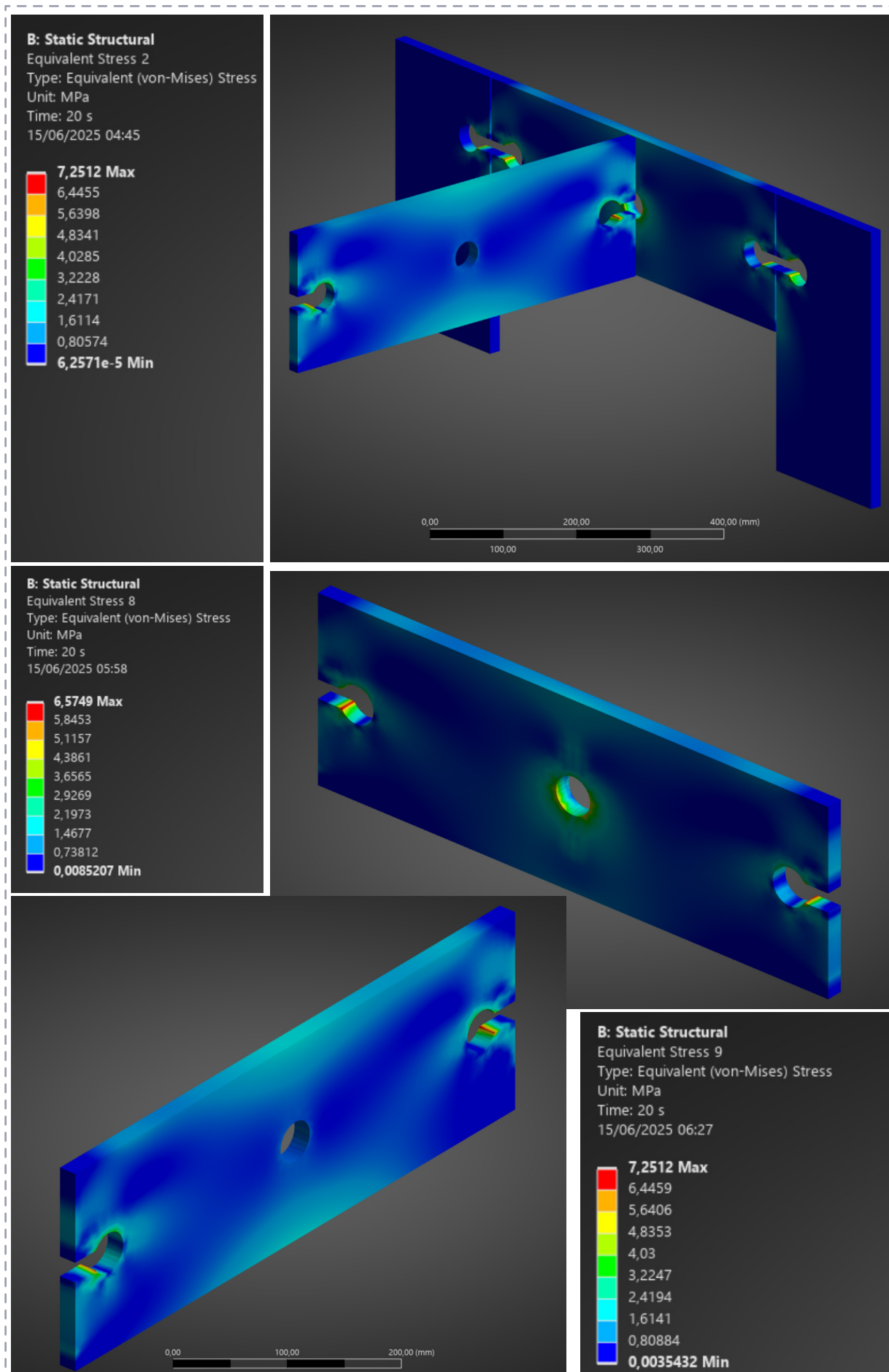


Figure 8.2.68, 3 Top, Total deformation, bottom Equivalent Elastic strain. Source: Author's own

The maximum stress observed in the fin or side panels simulation was approximately 6.8MPa, which is significantly below the typical allowable stress limit for heat-strengthened glass, commonly taken as 60 MPa.

Based on EduPack data, the **compressive strength** of hardwood parallel to the grain ranges

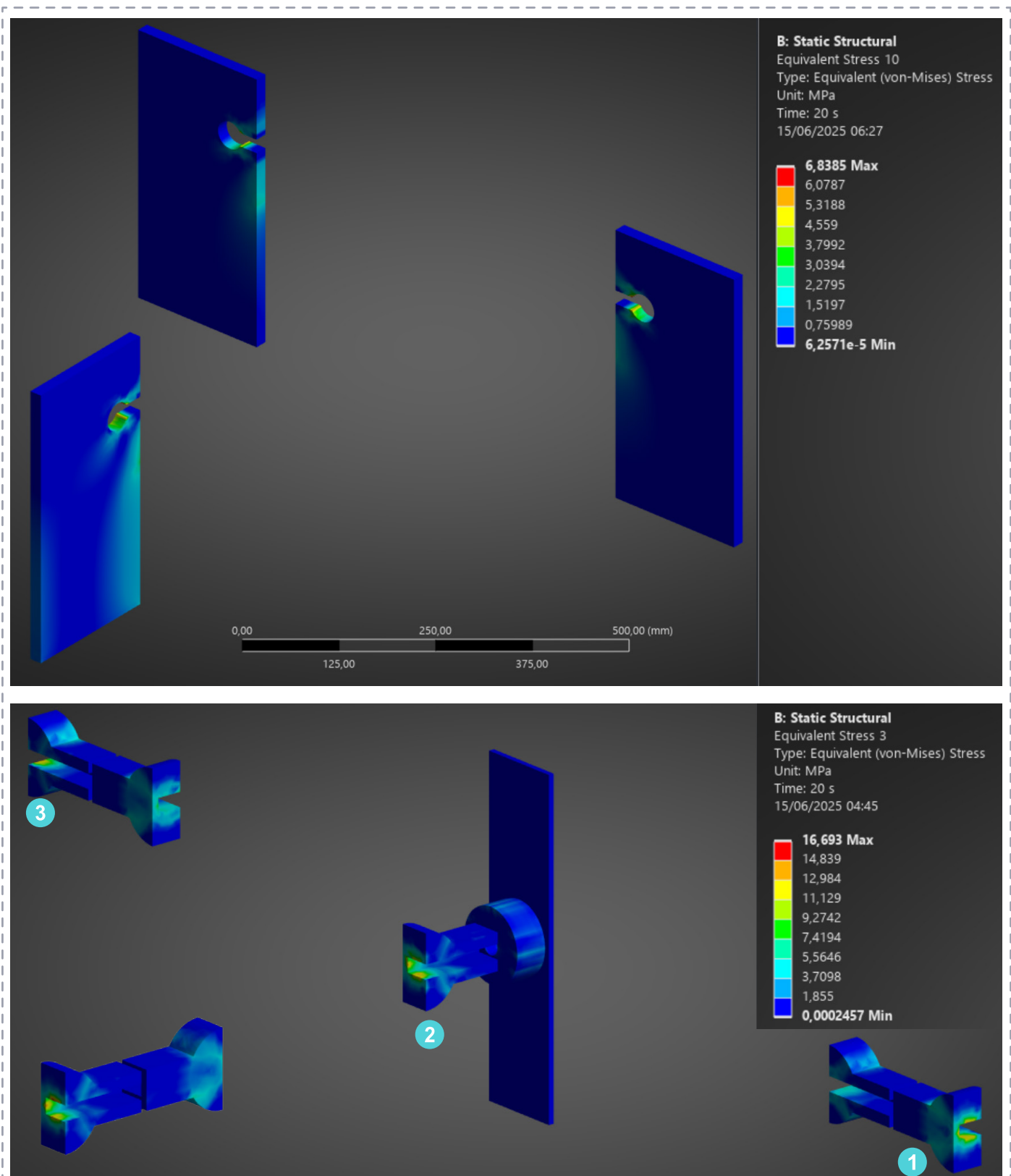


Figure 8.2.69, 3 Top, Equivalent stress in side panels (fin), bottom Equivalent stress in wooden components. Source: Author's own

between 75 to 80 MPa and perpendicular to grain is 20 and 25 MPa. In the simulation, the maximum compressive stress observed in this direction was approximately 15 MPa, which confirms that the stress levels remain well within the **safe range** for the selected material.

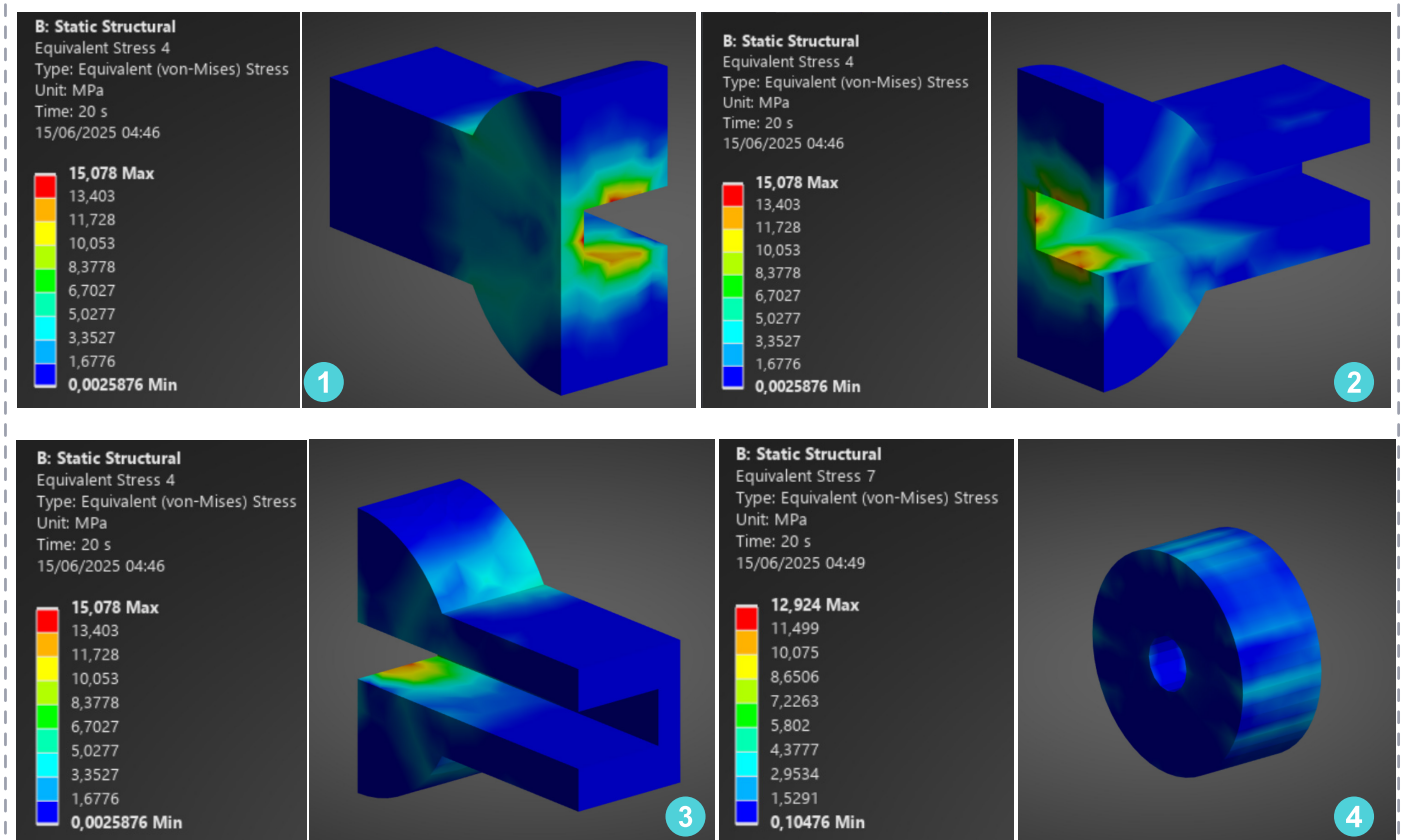


Figure 8.2.70, Simulation Results. 1)Middle panel connector, 2) T shape joint 3) side panel connector 4) cylinder connector . Source: Author's own

The simulated shear stress in the wooden connectors averages around 4.5 MPa, well below the hardwood's shear strength limits of 18 MPa (parallel) and 50–55 MPa (perpendicular), confirming the joint's safety.

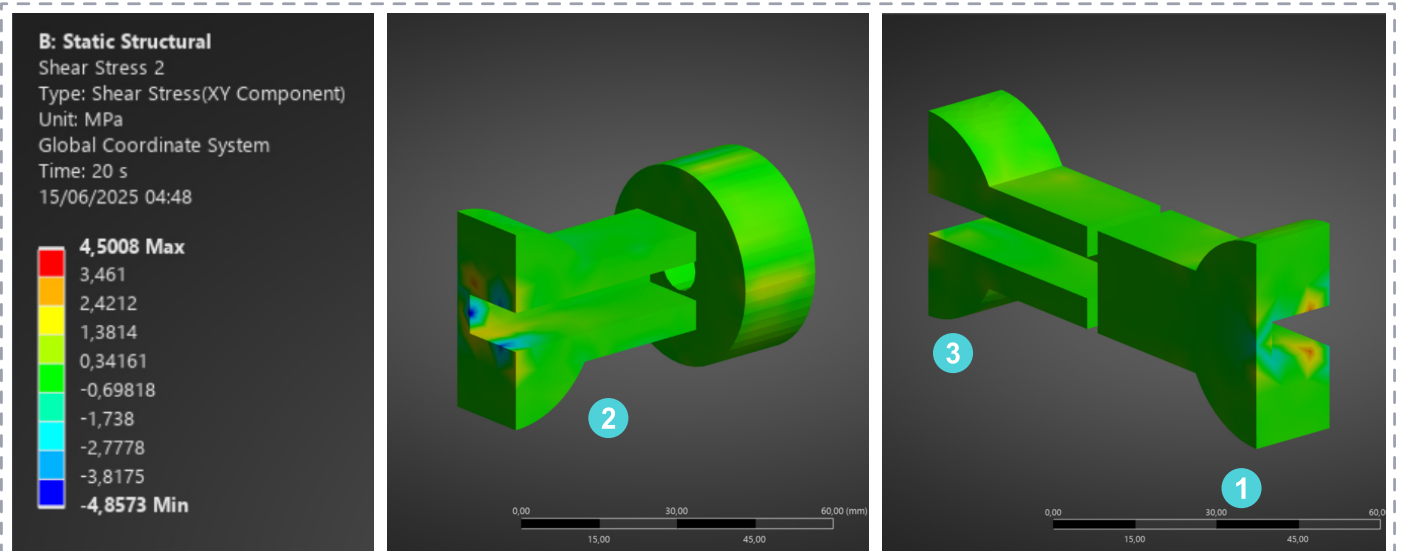


Figure 8.2.71, Simulation Results. Shear stress in wooden connectors, right : side wooden connectors like line joint and left : middle connector the T joint components . Source: Author's own

2. T shape Joint Simulation

- L600mm module
- Results

As mentioned before to simulate the connection behaviour, one representative system was selected due to limitations in the testing setup, which could accommodate only the smallest module. To assess how the connection would perform under higher loads, the same design logic was applied to

simulate larger modules by scaling their loads onto the smaller one. A three-step loading sequence was used to reflect realistic conditions, but for clarity, only the worst-case scenario—maximum loading on the smallest module—is discussed here.

The maximum stress in the glass was 8.4 MPa, which is well below the standard allowable limit for heat-strengthened glass (60 MPa). This confirms the glass performs safely under the applied load.

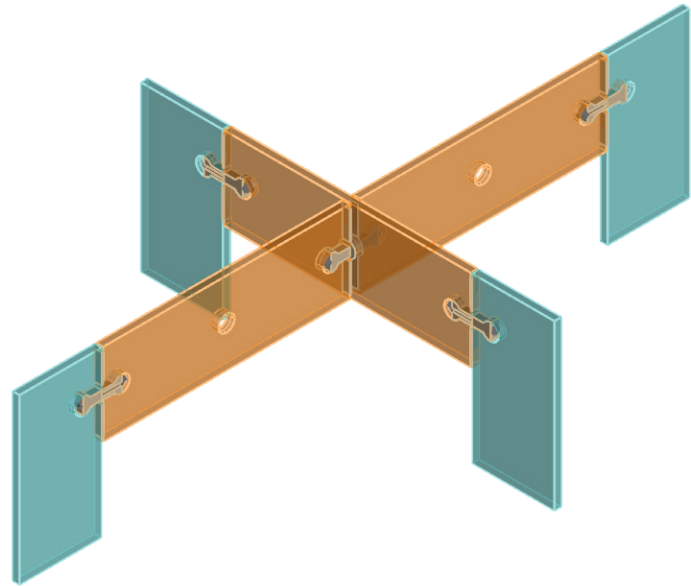
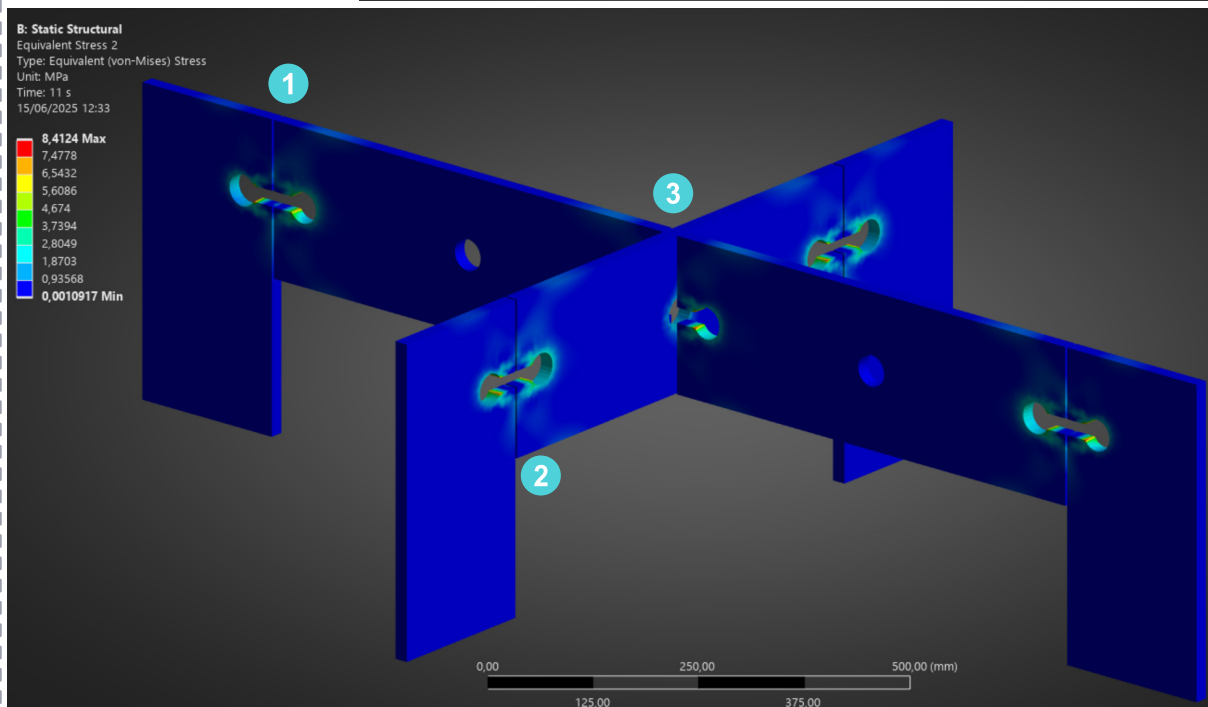
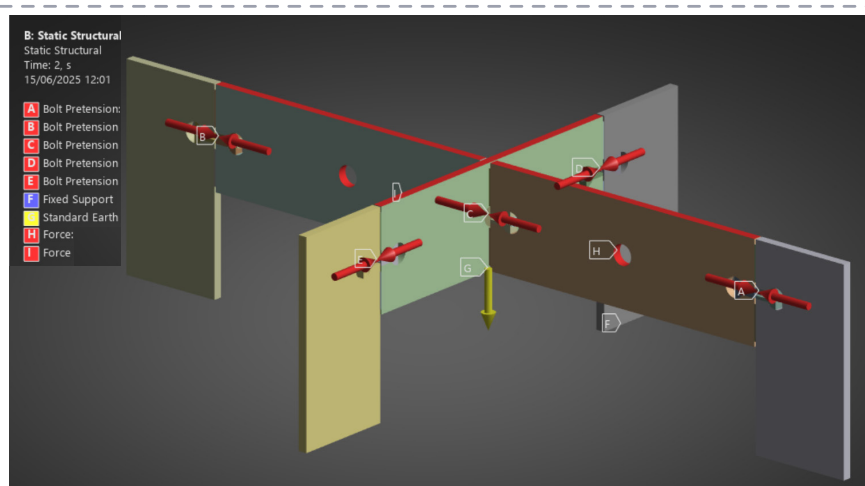


Figure 8.2.72, Simulation Results. Top: set ups, bottom: Equivalent stresses of glass modules. Source: Author's own



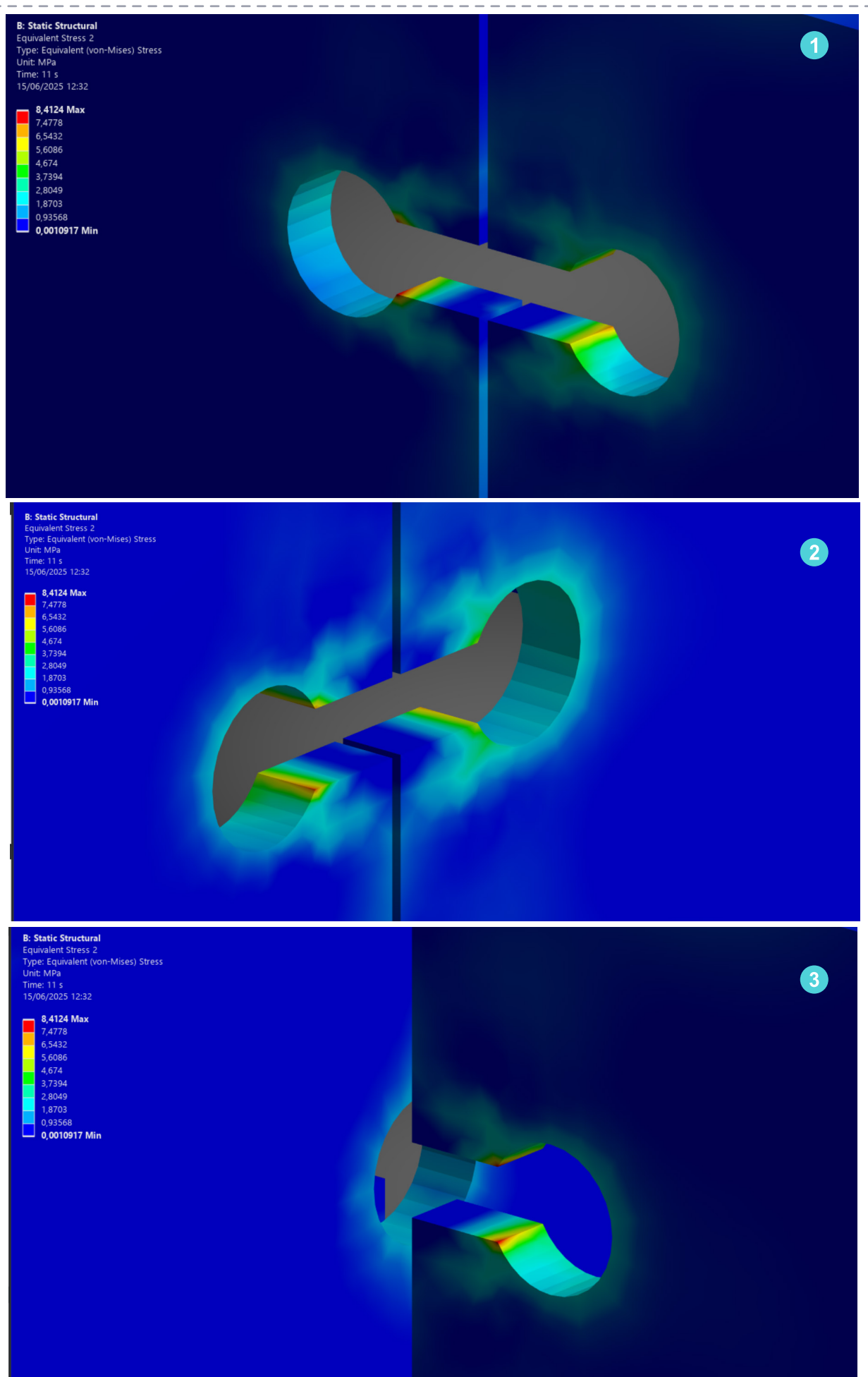
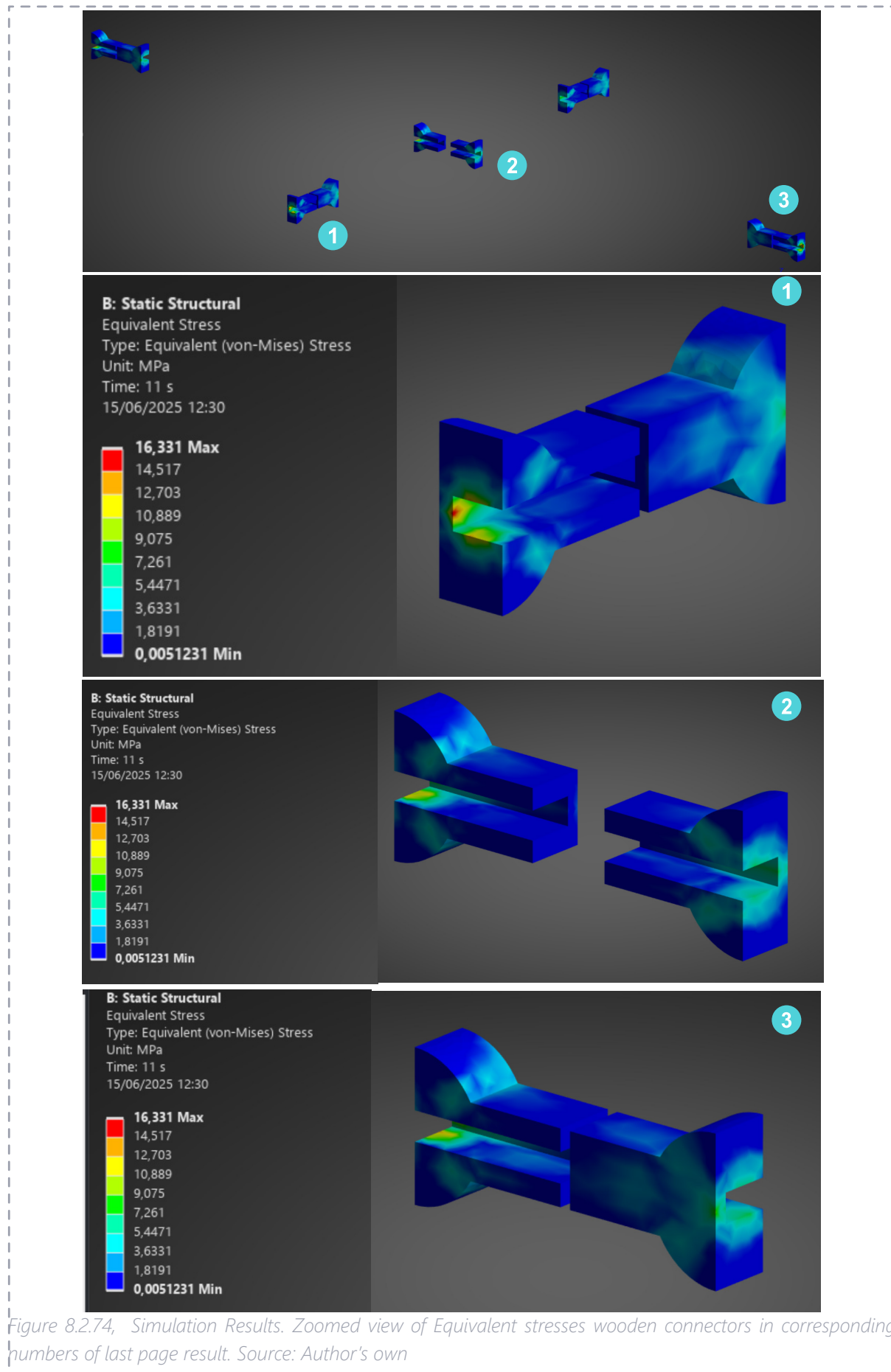


Figure 8.2.73, Simulation Results. Zoomed view of Equivalent stresses of glass modules in corresponding numbers of last page result. Source: Author's own

The stress in the wooden connector reached 16 MPa, which remains within the safe range for oak under parallel-to-grain loading. So, the wood also passed the safety check.



Stress in wooden connector is 16 MPa, within the limit for oak—safe. The stress in the steel bolt was 6 MPa, far below the yield strength of steel, which makes it structurally safe as well.

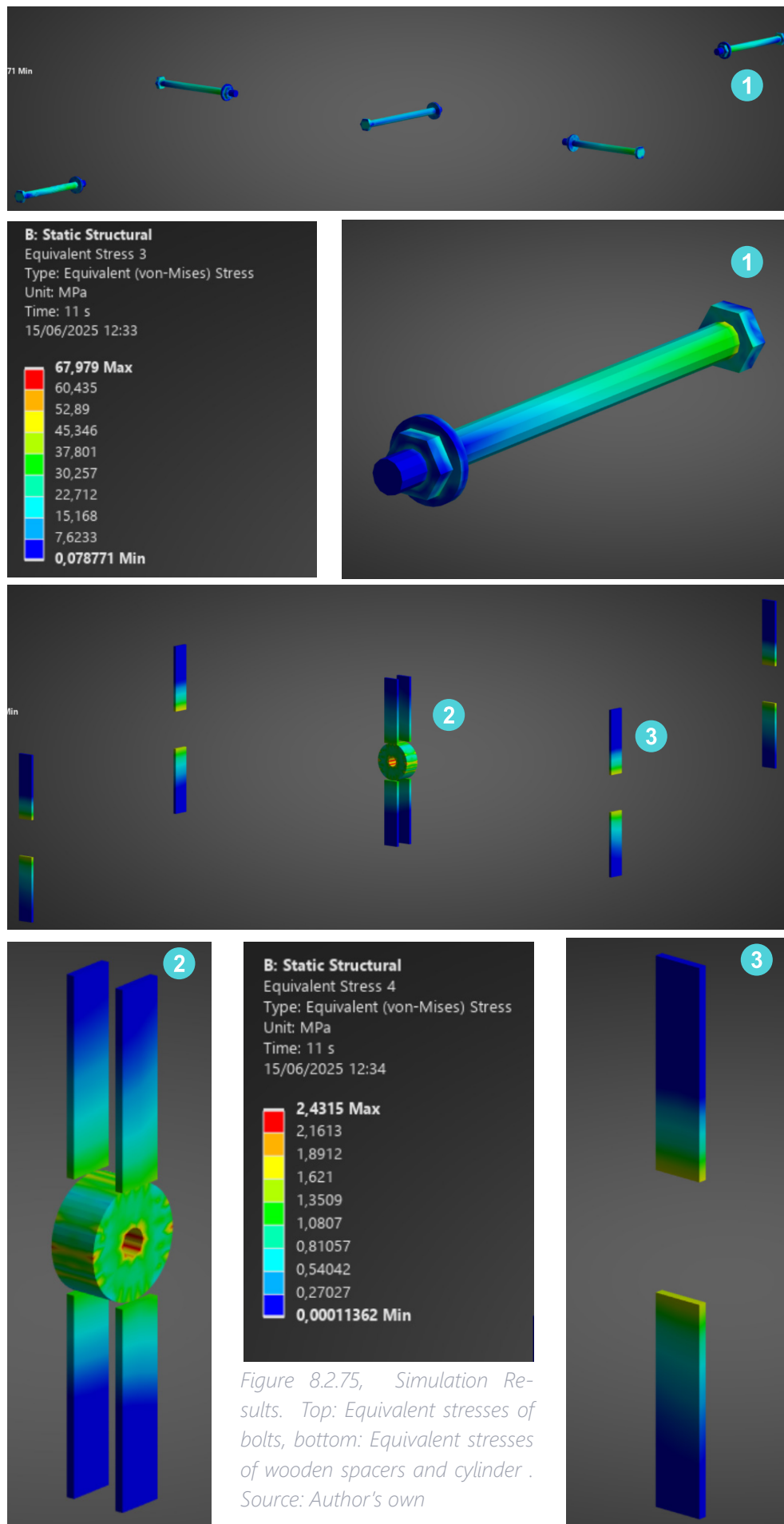


Figure 8.2.75, Simulation Results. Top: Equivalent stresses of bolts, bottom: Equivalent stresses of wooden spacers and cylinder. Source: Author's own

Stress in wooden connector is 16 MPa, within the limit for oak—safe. The stress in the steel The total deformation measured was 0.04 mm for a 600 mm span. According to the span/300 rule, the maximum allowable deflection would be 2 mm, so this result is well within limits and serviceability is guaranteed.

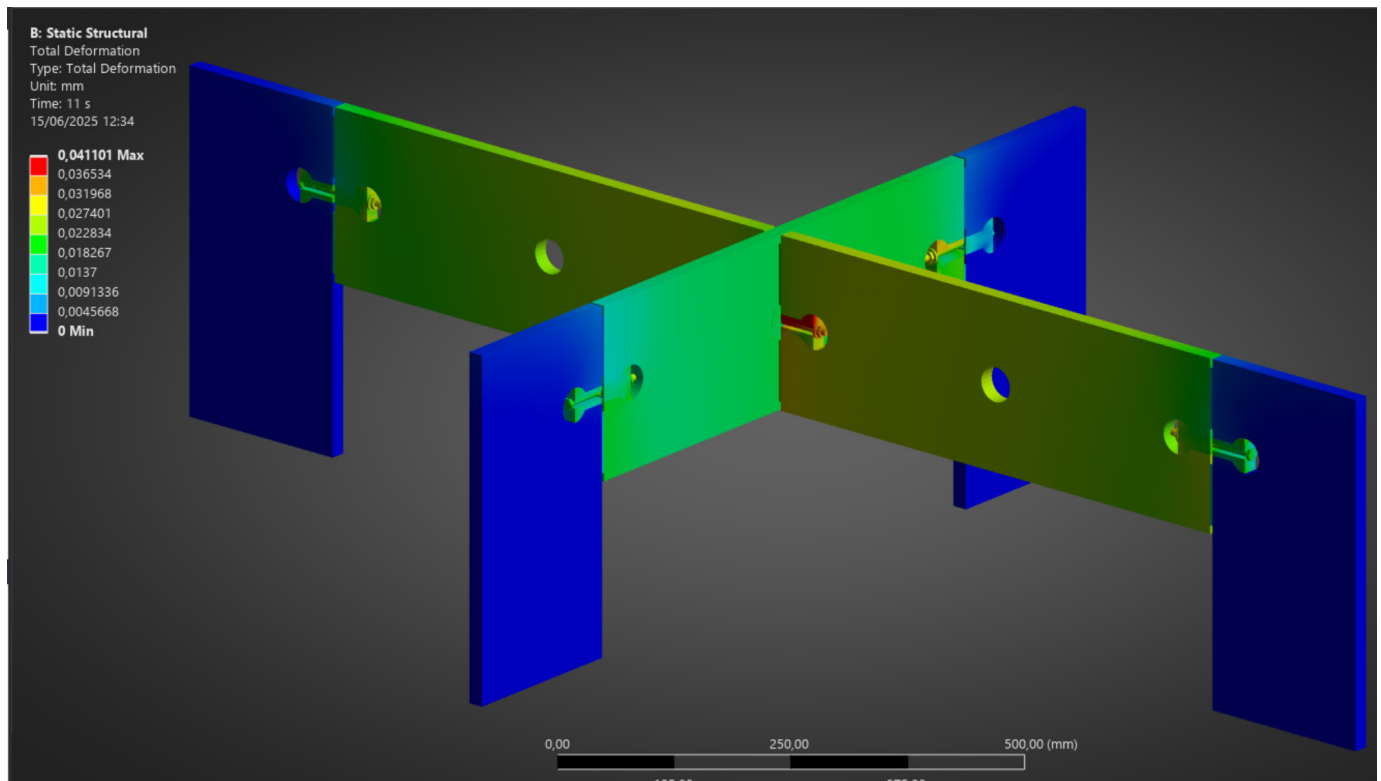
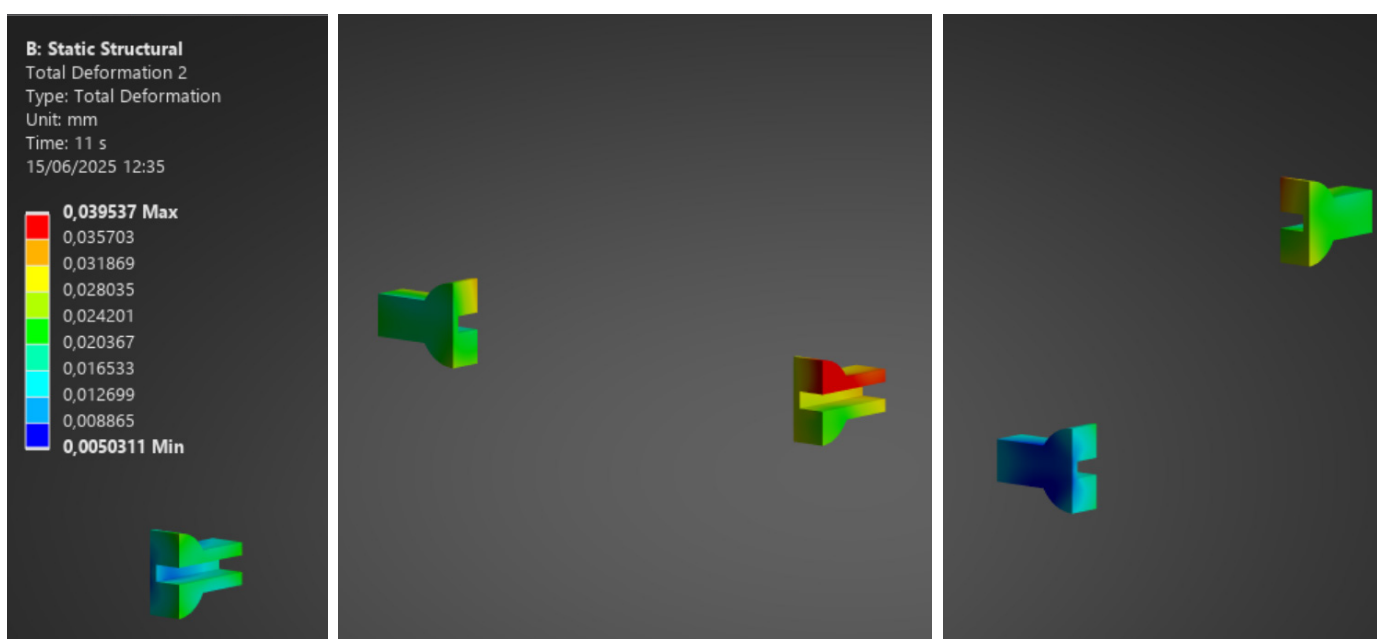


Figure 8.2.76, Simulation Results. Top: Total deformation, bottom: zoomed deformation of wooden connectors.
 Source: Author's own



8.3. Prototyping & Experiment

Experiment Question

How do mechanical interlocking timber-glass connections perform under vertical loading in terms of load-bearing capacity, displacement, and Short-term stability?

This experiment investigates the performance of timber-glass connections that rely on mechanical interlocking and bolted assemblies. The goal is to understand their structural behaviour under vertical forces, focusing on the following aspects:

- Quantifying the maximum load capacity before failure occurs.
- Monitoring displacement, slippage, and any relative movement between timber and glass elements.
- Observing the interaction between hardwood and glass when subjected to compressive or shear forces.
- Identifying potential failure mechanisms and recommending adjustments to geometry, material choice, or assembly method.

Monotonic Vertical Load Test (Ultimate Load Test)

1. Objective

- To verify that the connection system can safely support the expected design loads.
- To determine the ultimate load capacity, defined as the maximum vertical force the system can sustain before failure (such as glass cracking, wood crushing, bolt yielding, or full separation of components).

2. Test Setup

- A vertical load will be applied gradually to the middle (beam) panel while both ends are connected to fixed side fins through the designed interlocking joints. The load will be applied in three steps:
- Apply the design load and hold briefly.
- Increase to twice the design load as a safety check and hold again.
- Continue increasing until structural failure is observed.

3. Measured Parameters

- Load at which failure occurs.
- Type and location of failure (e.g. glass fracture, bolt deformation, wood damage).
- Load–displacement relationship (linear and non-linear response zones).

Pretension Sensitivity & Friction Capacity Check

1. Objective

To determine whether the bolt pretension (tightening force) is sufficient to prevent slip-page between the glass and wood under vertical load. This test also assesses whether friction alone provides adequate resistance to movement at the interface.

- To evaluate the practicality of the connection design and assess tolerances during manual assembly.
- To determine whether the geometry of the wooden interlocks and bolt holes allowed for a proper fit without excessive force or misalignment or proper space for fastening bolts.
- To identify early indications of failure mechanisms, such as wood crushing, bolt deformation, or slippage between components.
- To simulate basic loading conditions, including both uniform and point loads, in order to observe system response, load path, and deformation patterns.

8.3.1. Preliminary Prototype Testing (Plexiglas/Perspex and Meranti Wood)

Before performing tests with the final materials (heat-strengthened glass and oak hardwood), a preliminary prototype was constructed using plexiglass panels, meranti hardwood connectors, and low-carbon steel bolts. The aim of this pre-test was to validate the feasibility of the **proposed connection concept**, identify **potential assembly challenges**, and gain **insight into the behaviour of the system** under vertical loading conditions.

The substitute materials were chosen for practical reasons:

Plexiglass provided a safe, transparent, and accessible stand-in for glass, while meranti, a softer hardwood species, served as a temporary replacement for oak to evaluate the timber-bolt interface under load. **This test allowed for direct observation of the connection behaviour in a physical mock-up, without the risk of shattering or damaging high-cost glass elements.**



Figure 8.3.1 to 3, Pre-test prototype, Meranti wood Connector and spacers. Source: Author's own.

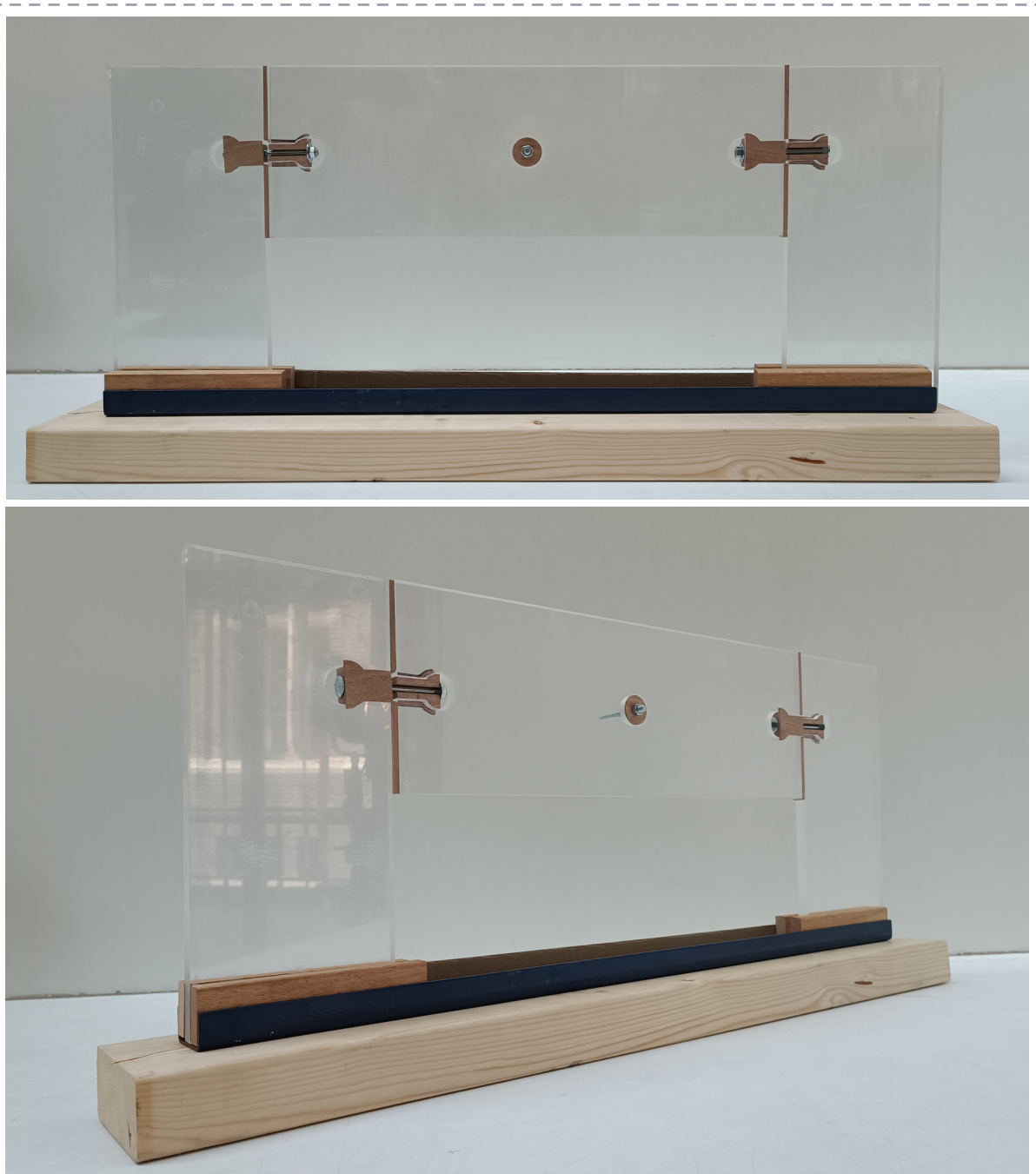


Figure 8.3.4 , 5, Pre-test prototype constructed from plexiglass and meranti wood, assembled by the author in the TU Delft model hall. Source: Author's own.

Fabrication of the Prototype

The plexiglass panels used in the prototype were constructed from two layers of precisely cut plexiglass sheets. The holes for bolt connections were drilled prior to lamination, and the layers were then bonded using double-sided transparent adhesive film. After lamination, all edges were manually sanded and finished to achieve smoothness, consistent dimensions, and accurate right-angle alignment at the corners. The timber connectors were produced manually in the modeling hall of the Faculty of Architecture at TU Delft using a range of woodworking tools, including drill presses, table saws, jigsaws, and sanding machines.

The wooden parts were carefully sanded after shaping to ensure a precise fit within the interlocking connection system and to allow proper alignment with the plexiglass panels. For the assembly, galvanized Carriage steel M8 bolts were selected and purchased from Hörnbach. These bolts featured squared neck along the shank, which allowed them to grip into the wooden part and prevent rotation during tightening. This facilitated easier installation and improved fastening reliability. Importantly, the bolts were designed with a threaded section only at the tip, leaving the shear zone between panels in contact with the shank of bolt with uniform and more cross sectional area rather than the threads.

Fabrication of the Prototype

The system was assembled manually by aligning the plexiglass panels with the meranti connectors and inserting bolts through the predefined holes. No torque control was applied; bolts were tightened manually until the components felt stable and secure. A uniformly distributed vertical load was first applied across the central beam panel, the released and loaded again by a point load applied at the centre hole of the same panel.

1. UDL Loading scenario

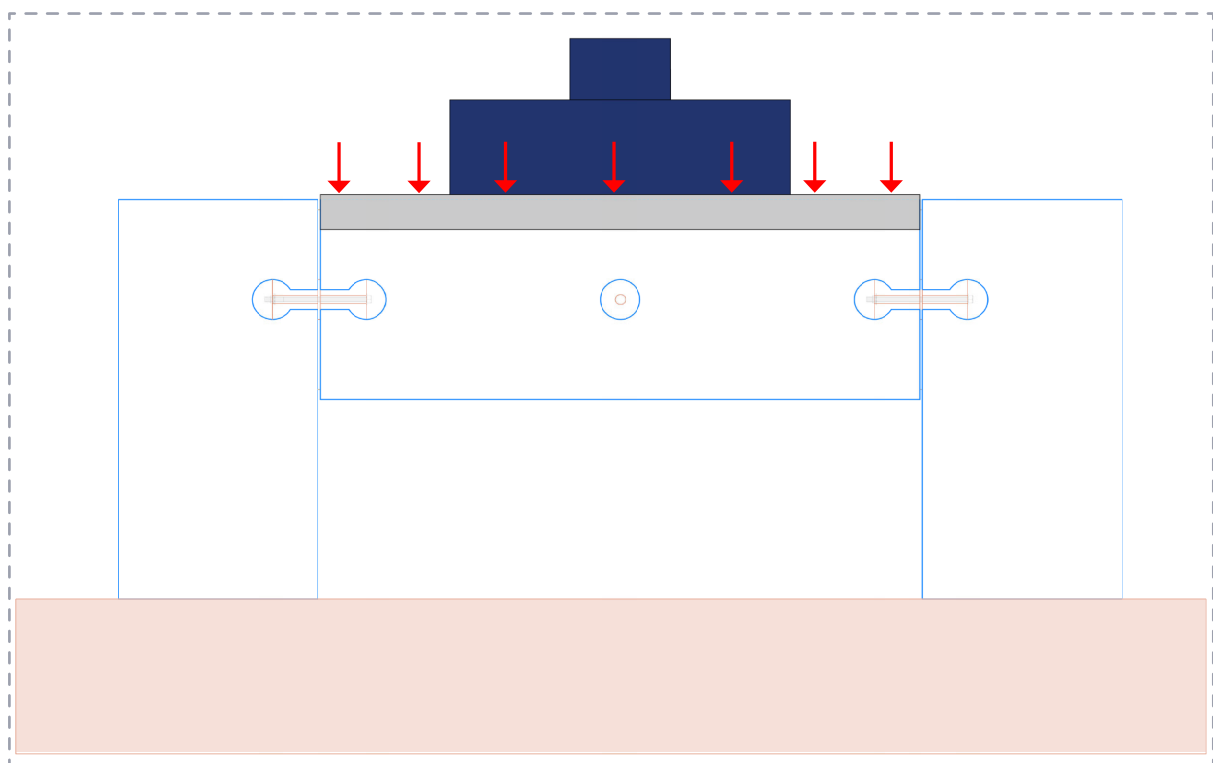


Figure 8.3.6, Pre-test prototype, UDL loading diagram. Source: Author's own.

To simulate the uniformly distributed load (UDL), a combination of snow load, maintenance load, and the dead weight of the panels above was considered. The load was applied to the top edge of the middle panel, representing a typical vertical loading scenario in the assembled system.

To ensure even load transfer from the testing machine to the plexiglass panel, a steel U-profile was used. This element served to distribute the load uniformly along the

panel's upper edge. To prevent direct contact between the steel and the plexiglass—which in the case of future glass testing could lead to stress concentrations or surface damage—a layer of protective wood was added. This wooden interface also allowed the panel to be clamped securely within the U-profile, while maintaining alignment and surface safety during the loading process.

At the bottom of the setup, a second steel U-profile was used to provide a stable clamping surface. Wooden support elements were placed inside this profile to secure the panel from below without direct contact between the plexiglass and steel.

This assembly was mounted on a wooden stand, which served as the reaction surface for the test. Together, these components ensured proper alignment, fixation, and load transfer during the loading sequence.

The U-profile was cut to a length of 600 mm, matching the exact length of the middle panel only, in order to solely apply load to the beam element and not to the fins on either side. This setup is critical, as it isolates the structural performance of the central panel and its connections, which are intended to carry vertical loads. In contrast, the side fins act more as supports or stabilizers, and loading them would introduce additional stress paths and altered boundary conditions, which is not the concern of this experiment.

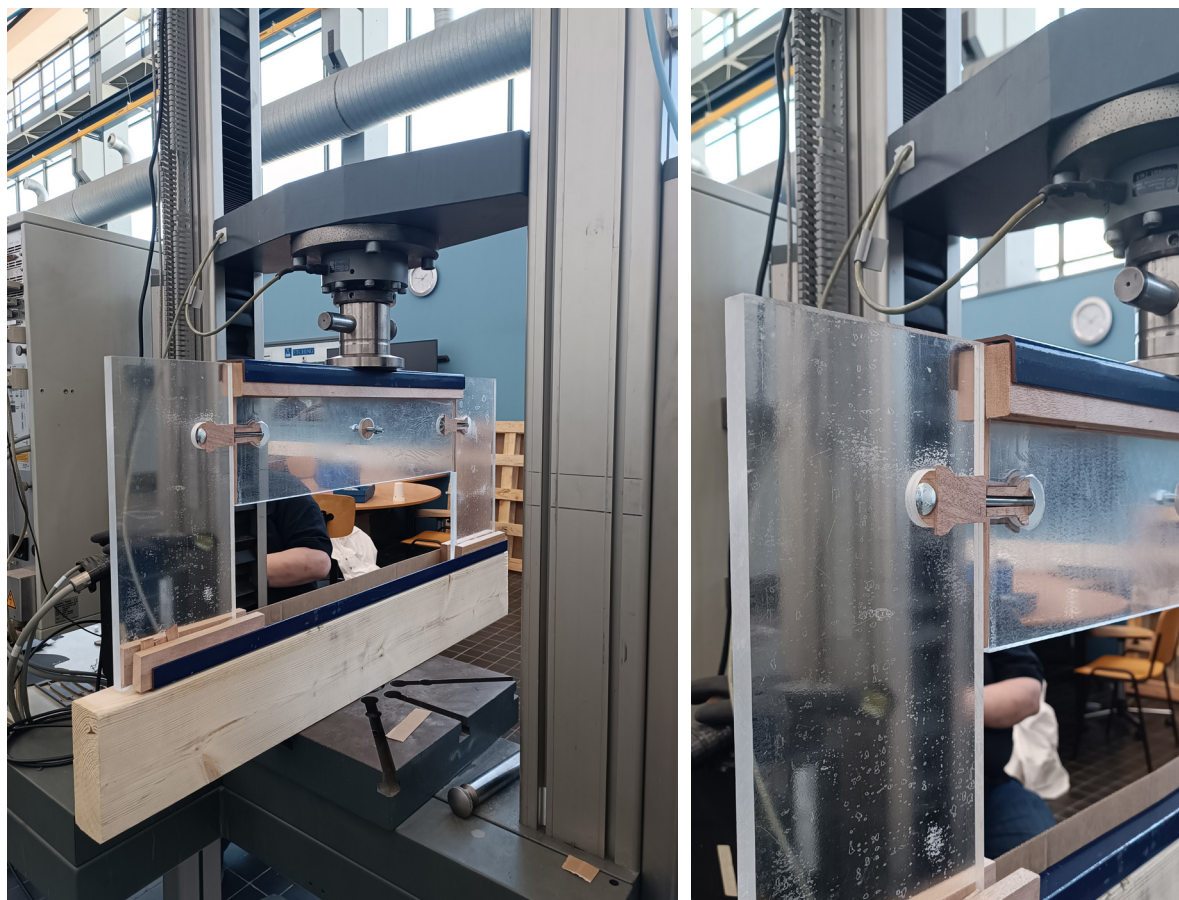
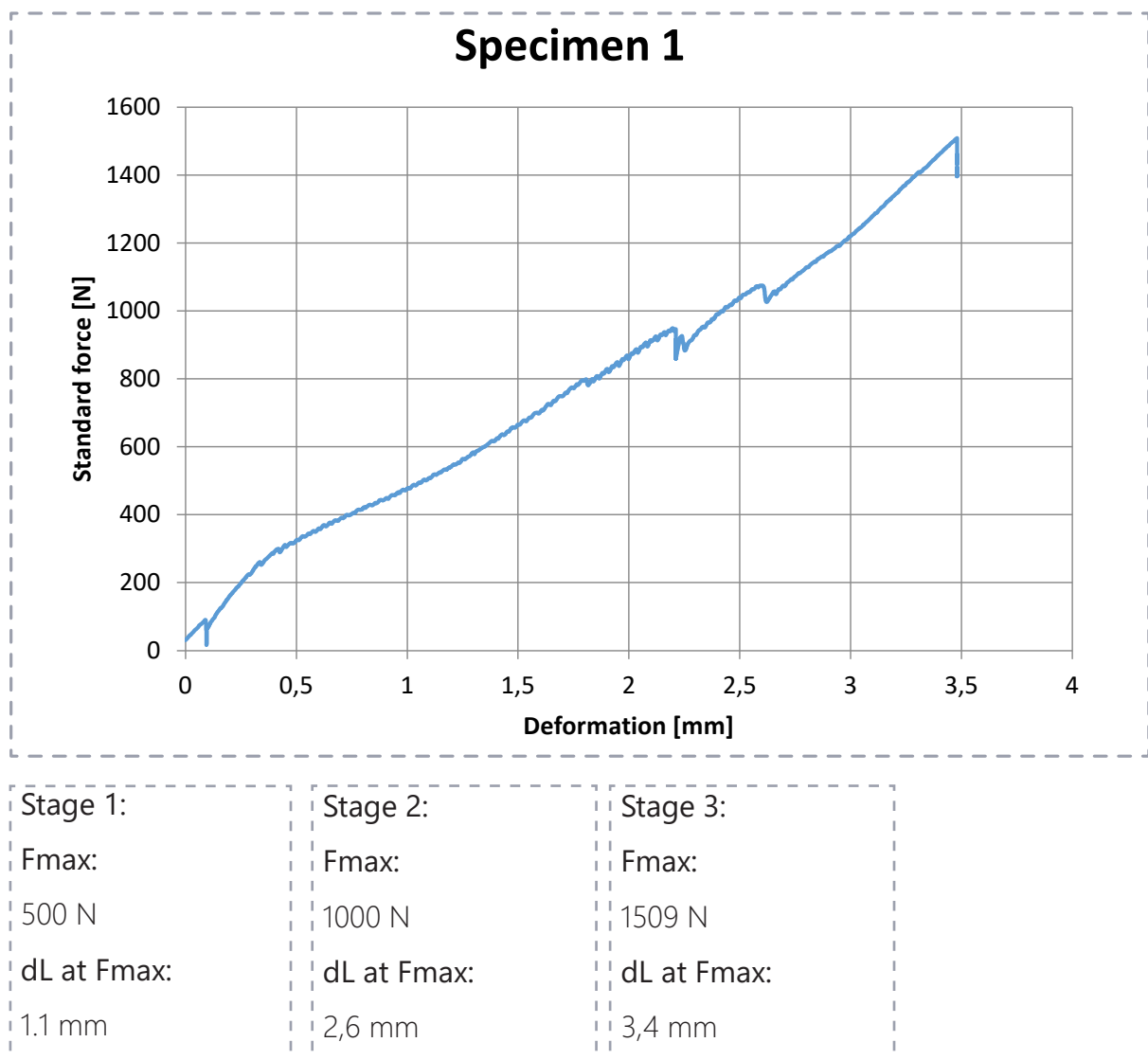


Figure 8.3.7 & 8, Pre-test prototype in lab set ups and under UDL loads. Source: Author's own.

- **Loading condition**

1. The module was loaded up to the design load and held for 10 minutes to simulate short-term conditions.
2. It was then overloaded to twice the design load to assess failure risk.
3. Additional 500 N increments were applied to test safety margins before releasing the module.

At this stage, the system performed successfully under both the design load and a doubled safety load, without any signs of failure or excessive deformation. The maximum load was maintained for approximately 10 minutes, after which the vertical displacement was recorded. The system was then fully unloaded, and the testing setup was reconfigured to apply a point load directly at the centre of the middle panel. **The results below are driven from excel file exported from machine in the lab:**



This second phase aimed to assess the behaviour of the connection under concentrated loading, focusing particularly on the bending response of the beam element and the interaction between the materials at the central connection.



Figure 8.3.9 to 11, Pre-test prototype, UDL loading results after 10 minutes. Source: Author's own.

2. Point Load scenario

To simulate the point load condition, two wooden panels of 18 mm thickness were used, made from perpendicularly oriented plywood to ensure strength and dimensional stability. These panels represented the connecting elements of the system and were positioned to apply a concentrated load at the centre of the middle module, in accordance with the design concept.

In the experimental setup, this condition was recreated by applying force symmetrically to the two wooden panels from opposite sides. These panels were connected using a steel pin that passed through the central hole of the cylindrical timber connector, transferring the load to the middle panel.

This method allowed to accurately mimic the intended load path in the real design, in which load is transmitted from two sides simultaneously through a central connection point.

This setup ensured symmetry in the application of the point load and provided a reliable means of evaluating how the middle panel and its connector behave under localized, concentrated loading.

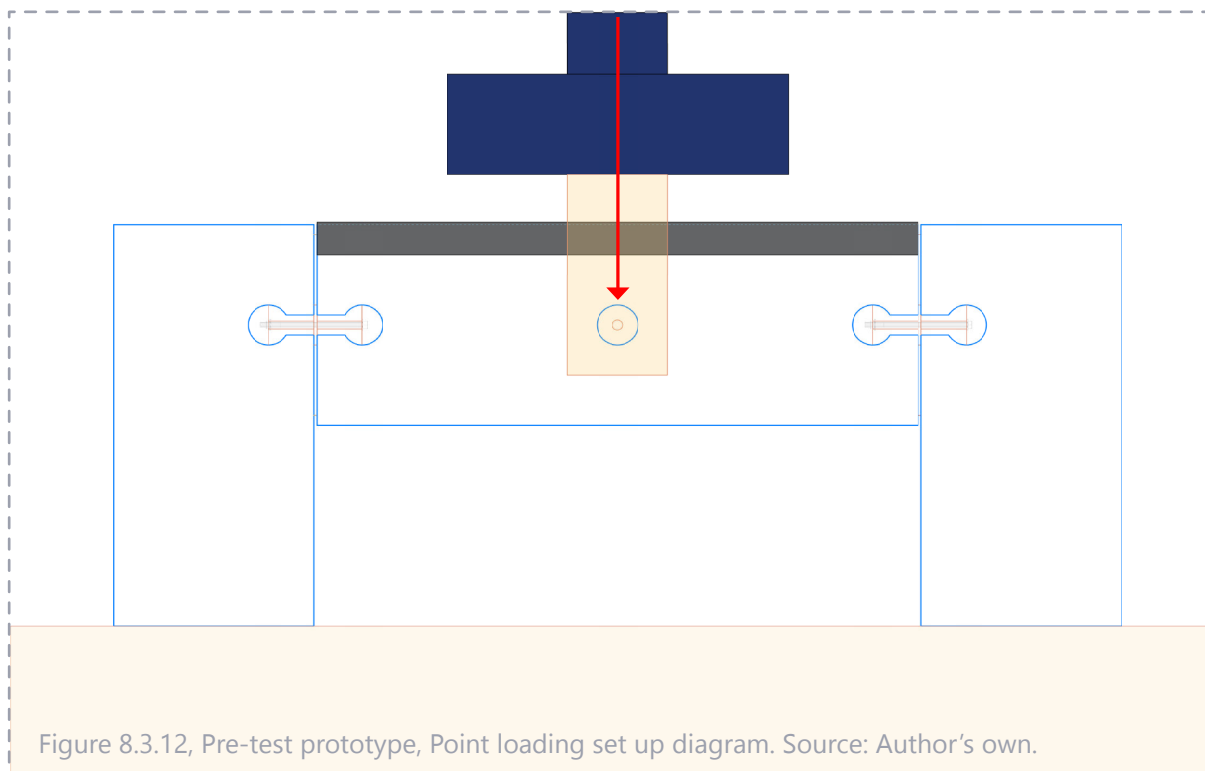


Figure 8.3.12, Pre-test prototype, Point loading set up diagram. Source: Author's own.

The diagram below (or the following section) illustrates the design detail, showing the location of the side panels and the central loading point within the overall connection system.

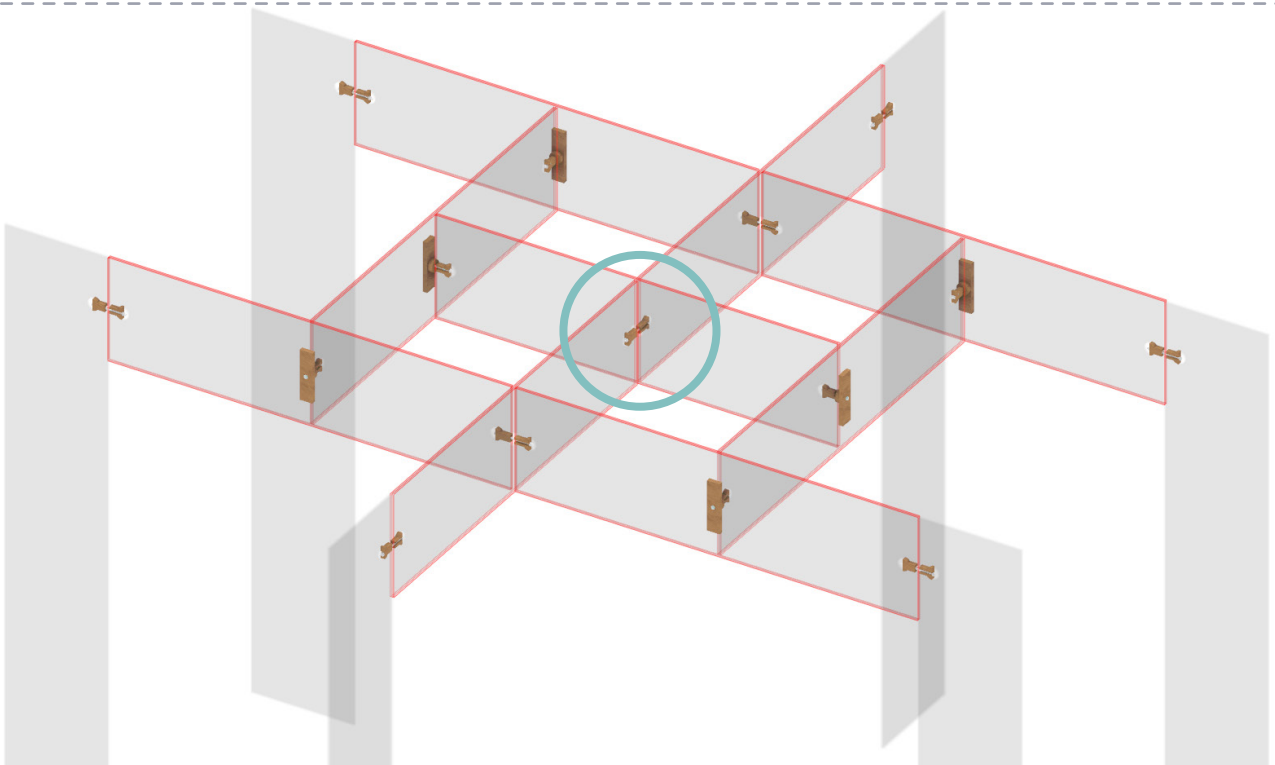


Figure 8.3.13, Pre-test prototype, location of point load in design. Source: Author's own.

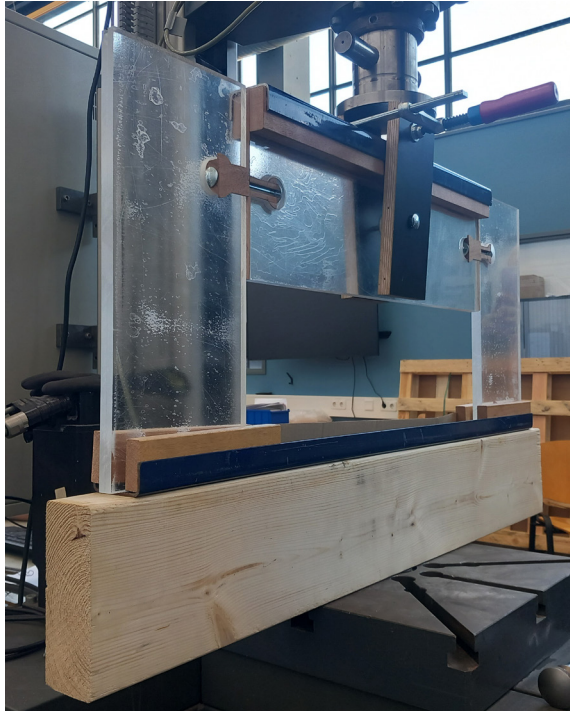


Figure 8.3.14 to 17, Pre-test prototype, Point load lab set ups. Source: Author's own.

- **Loading condition**

The loading was performed in stages:

1. First, the module was loaded up to the design load and held for 5 minutes.
2. Then, a second loading stage was applied, representing the expected load of medium-length modules from the simulation.
3. A third stage followed, based on the simulated load for large-length modules.
4. Finally, loading continued incrementally until visible deformation or failure occurred.



Stage 1:

Fmax:

285 N

dL at Fmax:

0.3 mm

Stage 2:

Fmax:

1032 N

dL at Fmax:

2.6 mm

Stage 3:

Fmax:

2484N

dL at Fmax:

8.3 mm

Stage 4: Ultimate

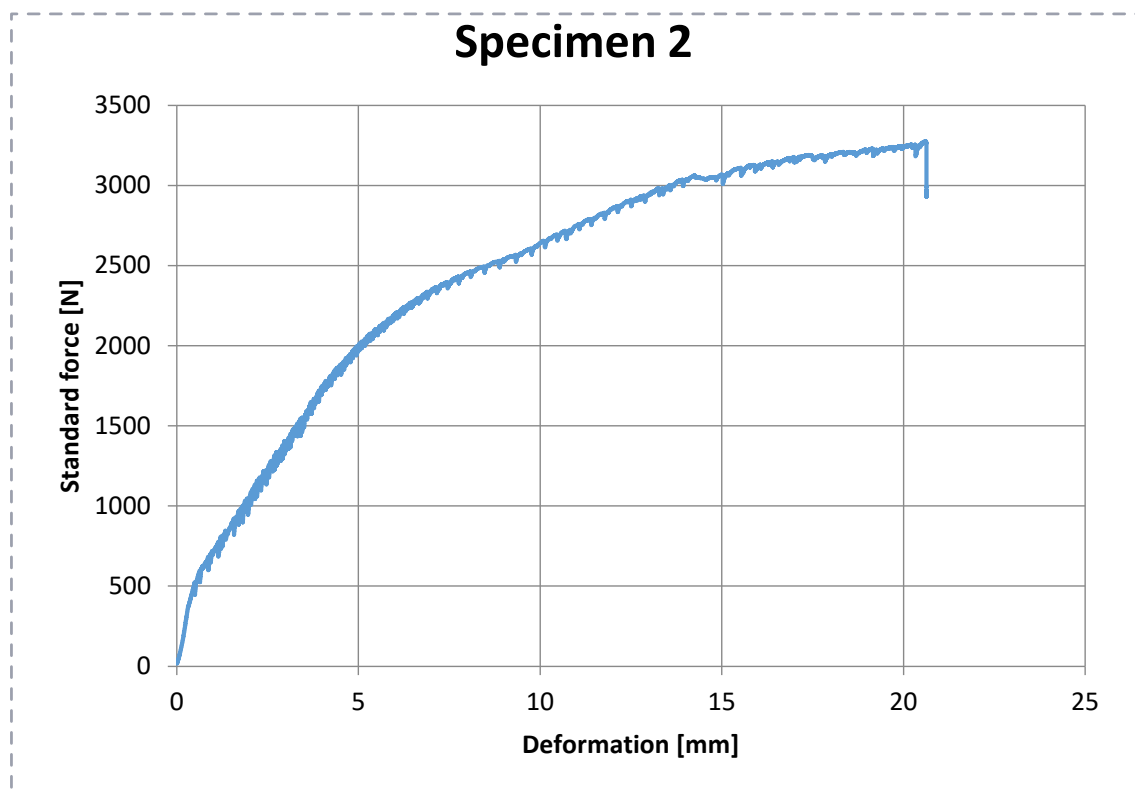
Fmax:

3050N

dL at Fmax:

20 mm

Figure 8.3.18, Pre-test prototype, Point load lab set ups. Source: Author's own.



- **Observations and Key Findings**

Point Load Behaviour:

In the second phase of the test, a point load was applied to the central hole of the middle panel, introducing a bending moment across the span.

While this setup was intended to evaluate the beam's bending resistance and the performance of the interlocking joints under localized load, a limitation emerged in the measurement process:

the testing machine recorded the displacement of the loading plate and Steel bolt used to load the cylinder, **which included deformation from the bent bolt itself, not just the system as a whole.**

As a result, the machine output did not accurately reflect the true displacement between the middle glass (plexiglass) panel and the fins. To overcome this issue, **the relative displacement was instead measured manually at the connection points.** The maximum recorded displacement was approximately 2.5 mm between fins and middle panel.

Importantly, even at double the design load, this displacement remained within acceptable structural limits. Given the span of the beam, the observed deflection corresponded to a span/250 limit, which is typically considered acceptable in serviceability design criteria for non-fragile systems. However, in future tests involving glass, stricter deflection limits may be necessary due to the brittle nature of the material.

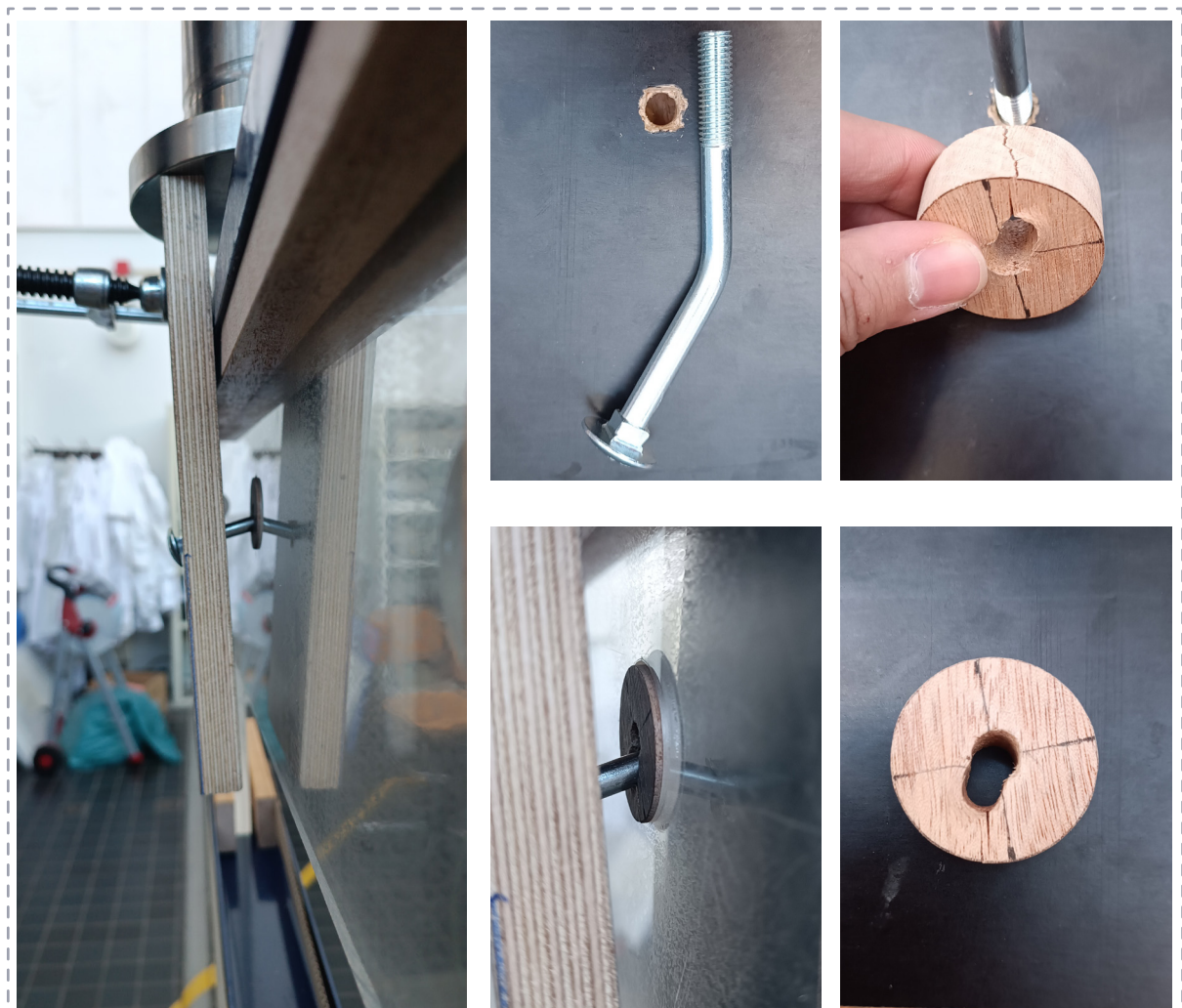


Figure 8.3.T9 to 23, Pre-test prototype, results after failure accrues. Source: Author's own.

Load Response:

Under uniform vertical loading, the maximum relative displacement observed between the central panel and the fins was approximately 2.5 mm. Most of this deformation appeared to result from localized crushing of the wood around the bolts, as well as plastic bending of the bolts themselves.

Right side:



Left side:

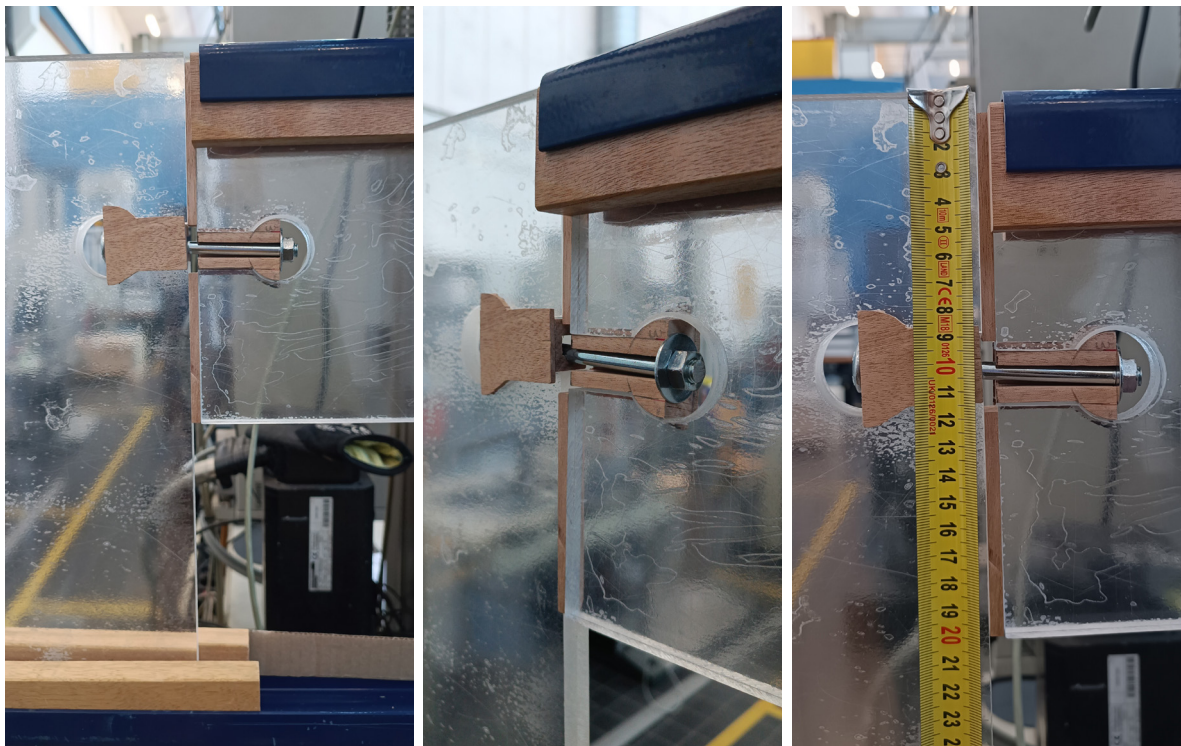


Figure 8.3.24 to 29, Pre-test prototype, results after failure accrues. Source: Author's own.

Asymmetric Deformation:

Notably, one side of the assembly experienced greater displacement and slight rotation, despite symmetrical loading. This is likely due to inconsistent pretension in the bolts, as the tightening process was done by hand without torque control. This underlines the need for torque-measured installation in future experiments.

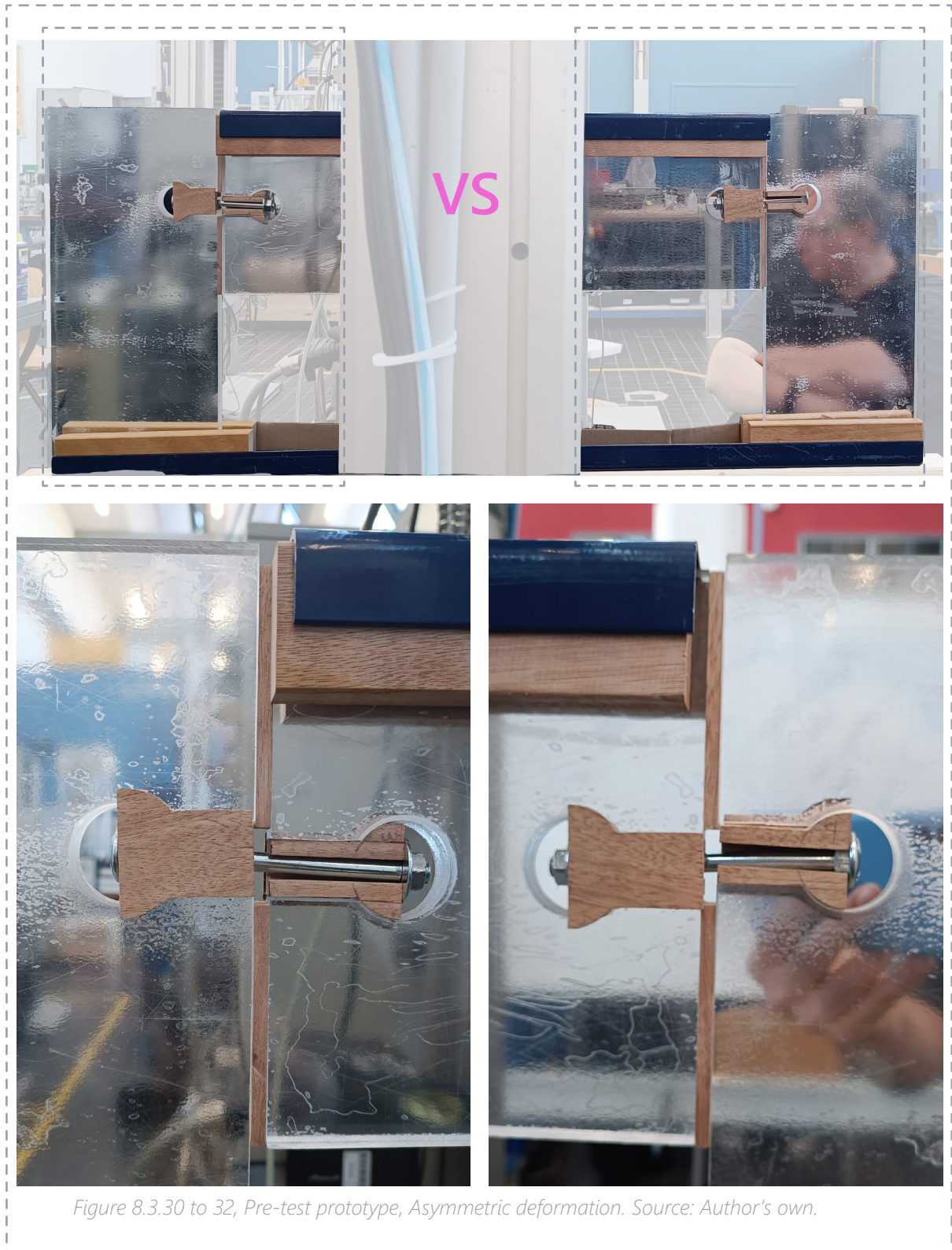


Figure 8.3.30 to 32, Pre-test prototype, Asymmetric deformation. Source: Author's own.

Hole Precision & Fit:

During assembly, it became clear that minor inaccuracies in hole diameter or alignment resulted in tight or uneven fits. As a result, the final prototypes were produced with CNC-cut wooden connectors, matched precisely to the waterjet-cut glass panels, thereby reducing manufacturing inaccuracies and improving overall assembly quality.

Wooden Connection Geometry:

The current shape of the meranti connectors required slight revision to ensure consistent fit and reduce the need for forceful assembly. The interlocking parts were not forgiving to minor misalignments, which may pose challenges during actual installation.



Figure 8.3.33 to 35, Pre-test prototype, Deformation in wooden components. Source: Author's own.

Bolt Length Adjustment:

Due to the small diameter of the drilled holes, standard M10 bolts did not fit properly—10 cm bolts were too short, and 12 cm bolts were too long. As a temporary solution, the 12 cm bolts were cut to the required length. However, for real-life application, this needs to be changed.

Bolt Deviation Under Point Load:

After applying a 3 kN point load, a slight deviation was observed in one bolt, likely due to uneven pretension. This highlights the importance of controlled and consistent bolt tightening to ensure symmetrical performance.



Figure 8.3.36, Pre-test prototype, Bolt deviation due to exceeding preload in joint in loading until failure scenario Source: Author's own.

3. Conclusions and Adjustments for Final Glass Testing

This preliminary test was instrumental in revealing both mechanical and practical aspects of the system that require refinement. The following changes are planned for the final tests:

- Larger bolt holes in the glass panels to account for fabrication tolerances , space needed for bolt fastening and reduce stress concentrations.
- Revised geometry of the timber connectors from circular grooves for bolts to rectangular cross-section for easier, more precise assembly with Carriage bolts.
- Torque-controlled bolt tightening to ensure uniform pretension and prevent asymmetric deformation.
- Revised configuration for applying the point load to prevent failure of the steel pin and to obtain more accurate results in identifying failure points and potential maximum local stress concentrations.
- Review of the assembly sequence, including whether temporary support or scaffolding is necessary during installation.
- For real-life application, the design should be adjusted to accommodate standard bolt sizes, either by increasing hole dimensions or selecting an alternative bolt type.

8.3.2. Main test 1

As introduced earlier (see Section 8.3. Prototyping & Experiment):

The aim of the experiment is to investigate how mechanical interlocking timber-glass connections perform under vertical loading. The focus is on understanding their load-bearing capacity, displacement behaviour, and short-term stability, while also checking how bolt pretension and friction affect the connection's overall performance. From preliminary test there was points to revise:

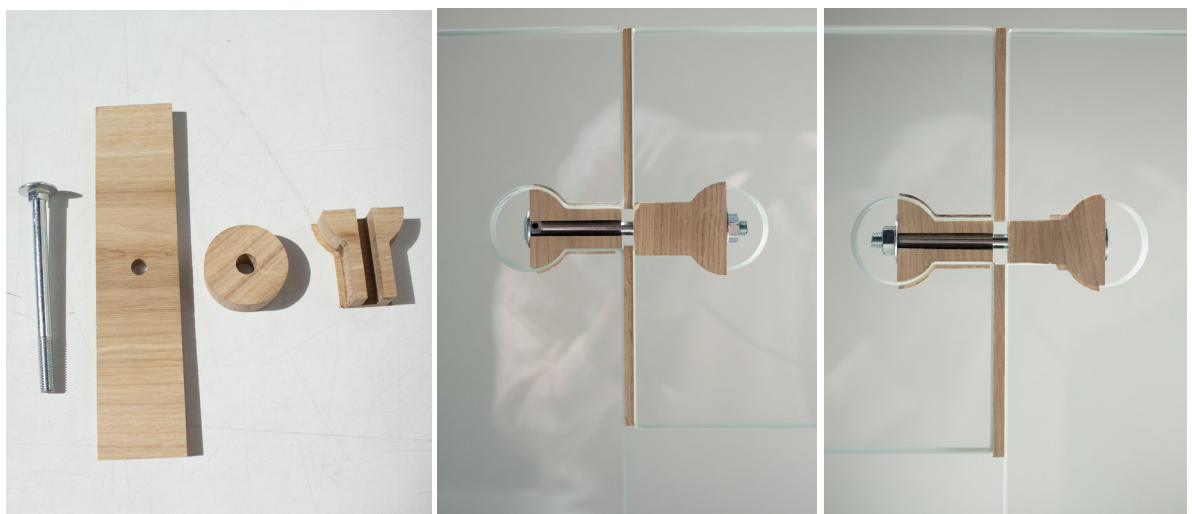


Figure 8.3.37 to 40, Glass test prototype, Set ups Source: Author's own.

Fabrication of the Prototype

The glass panels were ordered from Sedak (Germany), with the specification of three sets of heat-strengthened glass. Each panel had smooth ground edges with a small chamfer produced by tooling, and all edges were finished to the same quality standard. The glass had a thickness of 16 mm and included a 1.5 mm PVB interlayer to improve safety and post-breakage behavior.



Figure 8.3.41, Final Glass test prototype & Set ups Source: Author's own.

The wooden components were made from a Quarter sawn (Heart Piece) oak plank, sourced from Hornbach. This type was chosen for its high dimensional stability, particularly in terms of minimizing swelling or warping due to moisture changes. The pieces were CNC-cut to precise shapes and then sanded manually to achieve a perfect fit with the glass, ensuring tight tolerances for the interlocking joints.



Figure 8.3.42 to 46, Final Glass test prototype, Sedak sticker on glass, Oak used for CNC milling connector, Oak timber after CNC cut geometries came out. Source: Author's own.

For assembly, M8 galvanized steel bolts with a square neck, 8 mm diameter, and 120 mm length were used. The bolts were selected so that the shear and load transfer occurred along the unthreaded shank, improving structural reliability and reducing stress concentrations near the joint. Washers and nuts were added to allow for controlled pretension during tightening.

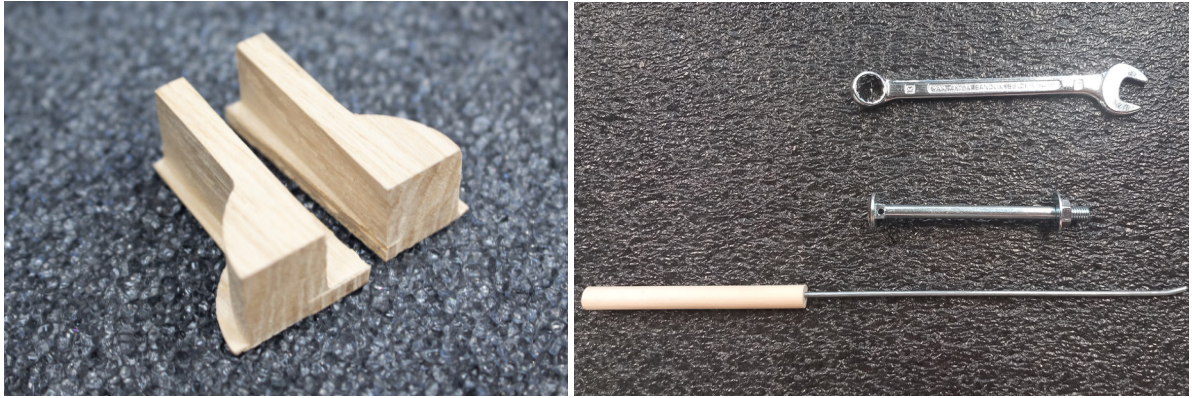


Figure 8.3.47 & 48, Bolt preloading setup using pin driver through neck hole to prevent torsional failure in wood. The image also shows failure in the wooden connector caused by torsional stress from bolt rotation. Source: Author's own.

As shown in the figure, during assembly, applying torque to the bolt caused it to rotate despite using a square-neck bolt. This unintended rotation led to stress concentrations and occasional breakage in the wooden connectors. To resolve this, a small hole was drilled through the neck of the bolt, allowing a pin driver to hold it in place during tightening. This simple modification successfully prevented bolt rotation and minimised additional stress on the wooden surface during assembly.

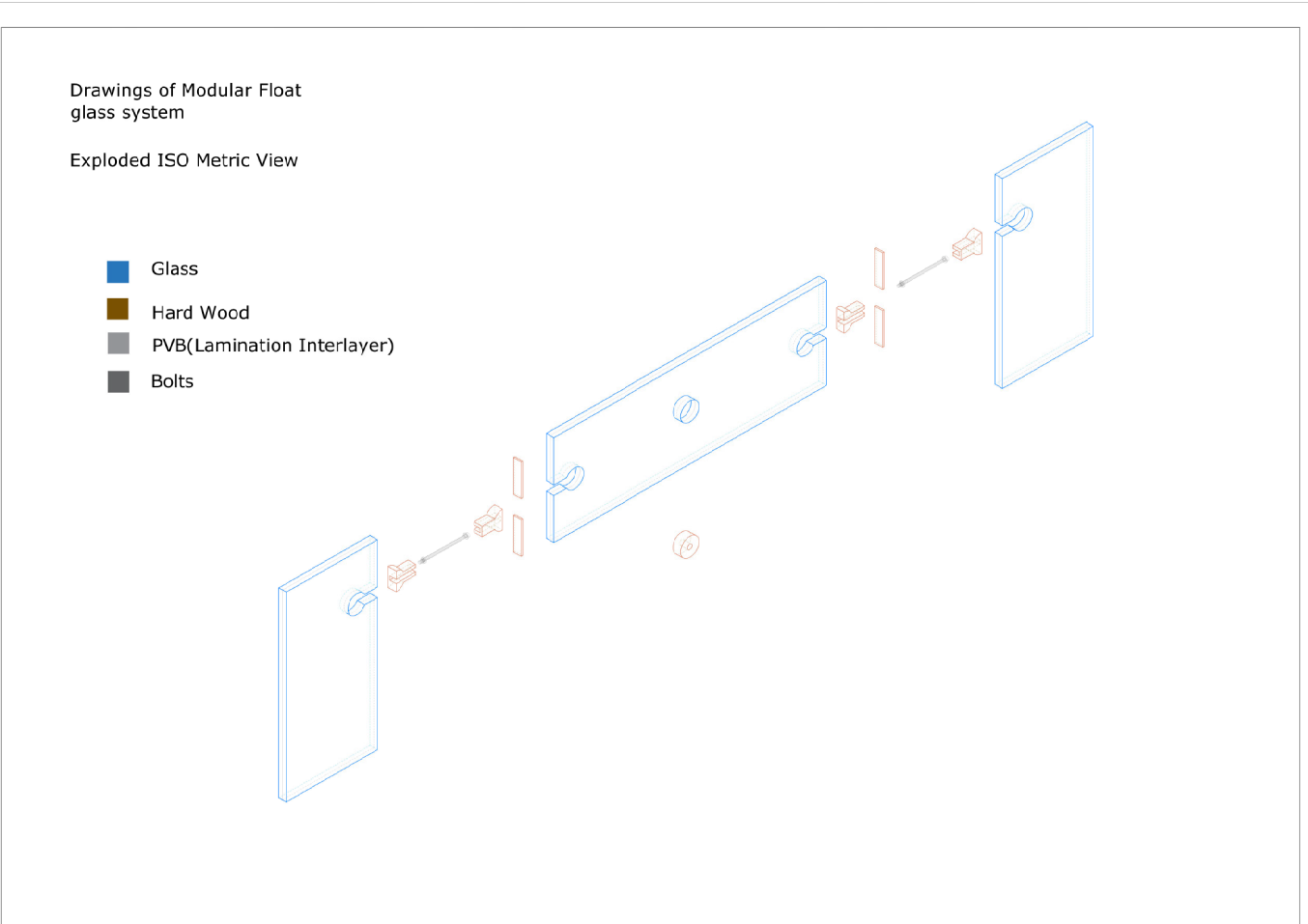
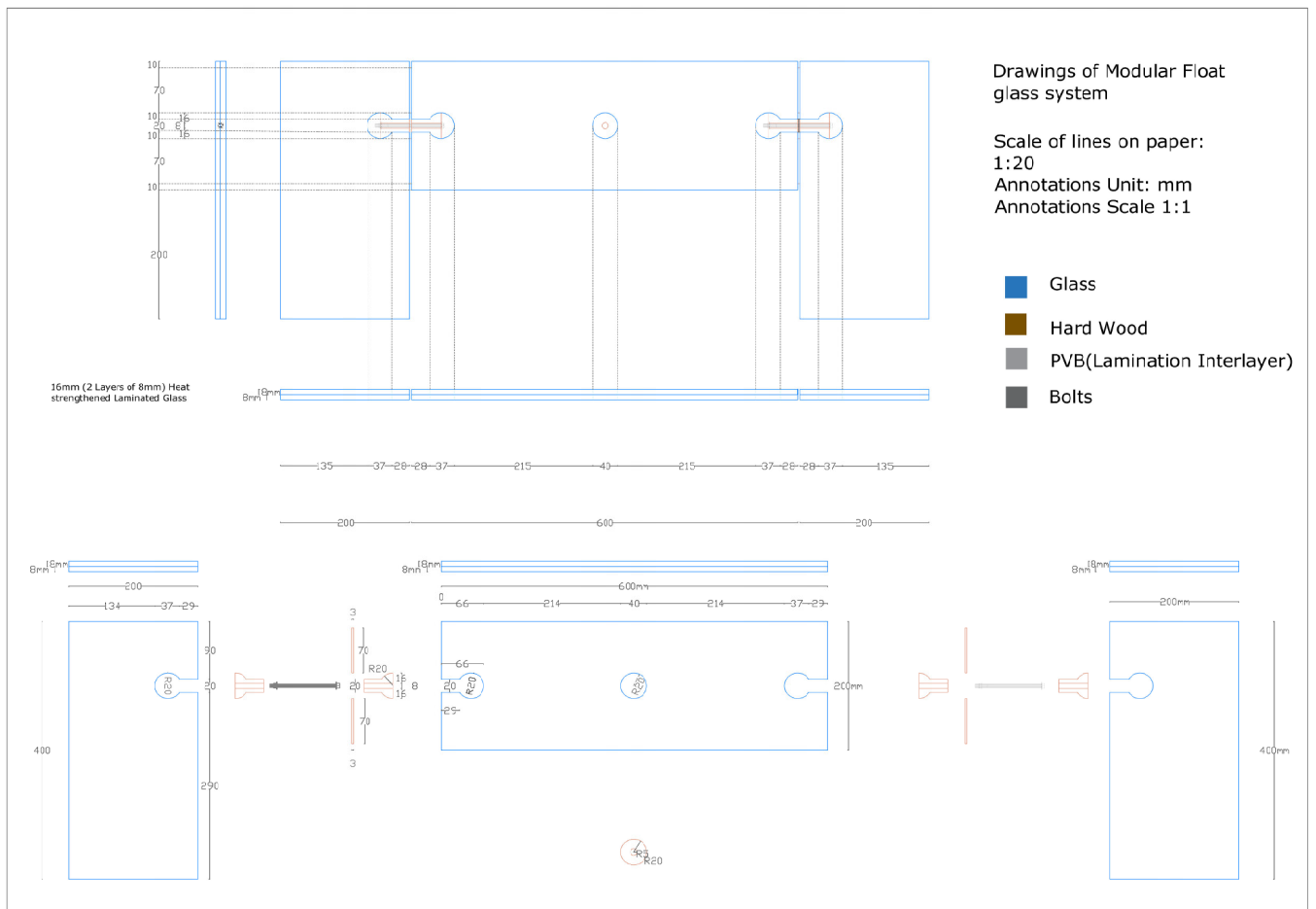


Figure 8.3.49, Natural imperfections in wood and some errors during fabrication. Source: Author's own.

Several practical challenges arose during the fabrication phase. The oak timber used had a thickness of approximately 19 mm, while the designed connector depth was 17.5 mm. This 1.5 mm flange at the back of the connectors was often removed by the laser during CNC cutting, rendering many samples unusable. Precision was also critical: although the joints fit perfectly when first assembled, slight moisture fluctuations caused the wood to swell by the next day. As a result, minor sanding was required to ensure proper fitting. While the material removed was negligible, it significantly affected the tolerances of the interlocking system.

In addition, the natural variability of wood posed further complications. Some samples were discarded due to knots, cracks, or inconsistent grain patterns, which led to uneven deformation or local weakness. These issues highlight the importance of accounting for natural imperfections when working with biological materials like hardwood.

Here is manufacturing Drawings:



Test Setup and Procedure Revised from pretest:

1. Larger bolt holes in the glass panels :

The hole size from 34mm diameter changed to 40mm diameter

2. Revised cross section of the timber connectors from circular grooves for bolts to rectangular :



Figure 8.3.50, rectangular groove to fit the square neck bolt better. Source: Author's own.

3. Revised configuration for applying the point load

In the previous test, the results were not fully accurate due to bending in the bolt, which prevented the experiment from continuing to the point of failure. To address this issue, a larger M12 bolt was used in the second setup, along with a threaded rivet to secure the bolt in position and help transfer the load more evenly around the hole. In addition, two wooden pieces were added on either side of the glass to clamp it more effectively. This modification reduced the gap that had previously existed on both sides of the bolt, which had caused the load to act at a distance and introduced a bending moment. With these adjustments, the bending effect on the bolt was significantly reduced, resulting in a more reliable setup and improved load-bearing capacity of the connection.



Figure 8.3.51, Revision in applying point load, bigger bolt M12, rivet, and wooden clamping surface. Source: Author's own.



Figure 8.3.52, Revision in applying point load, bigger bolt M12, rivet, and wooden clamping surface. Source: Author's own.

4. Torque-controlled bolt

Unfortunately, the hole was still too small to fit the head of the torque wrench and its socket attachment inside the connection. As a result, the torque could not be applied directly while the bolt was in place. To work around this, the torque was applied to an identical bolt outside the connection, and the resulting exposed length after tightening the nut was measured as a reference. Since all bolts used were of the same type and length, the remaining bolts were tightened manually until they matched this reference length, ensuring consistent pretension across all connections.

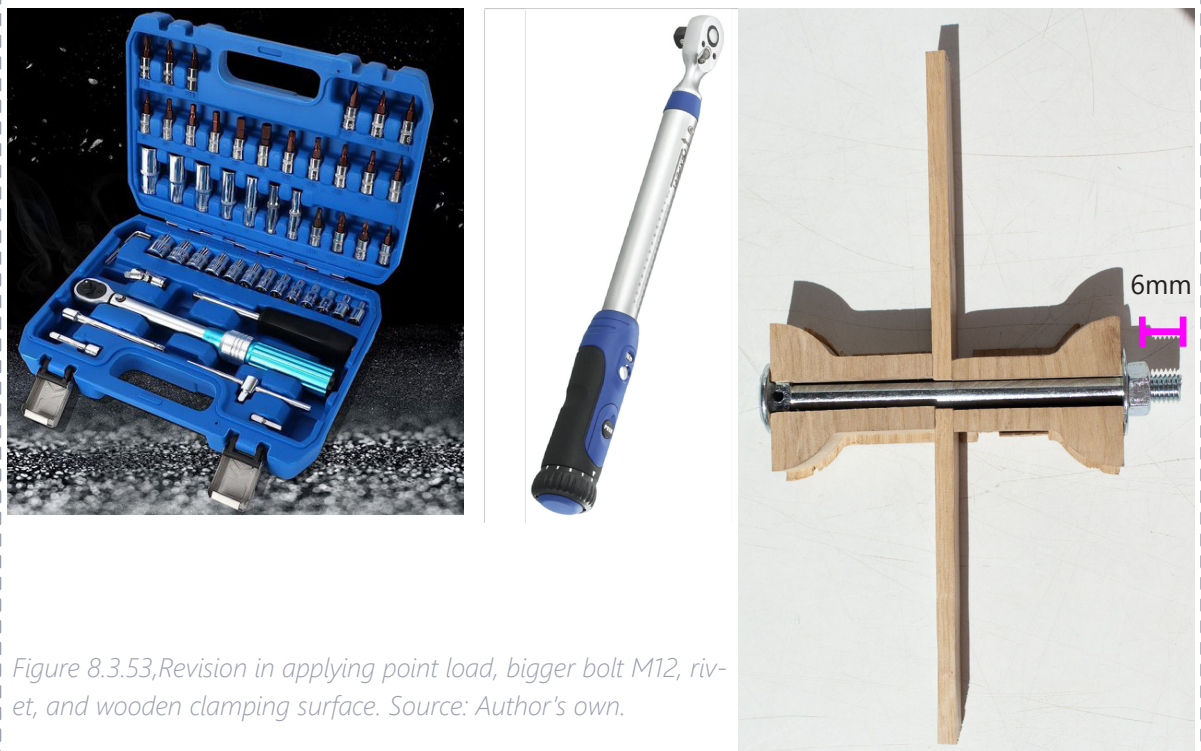


Figure 8.3.53, Revision in applying point load, bigger bolt M12, rivet, and wooden clamping surface. Source: Author's own.

- **Objective of glass test 1:**

- To verify that the connection system can safely support the expected design loads.

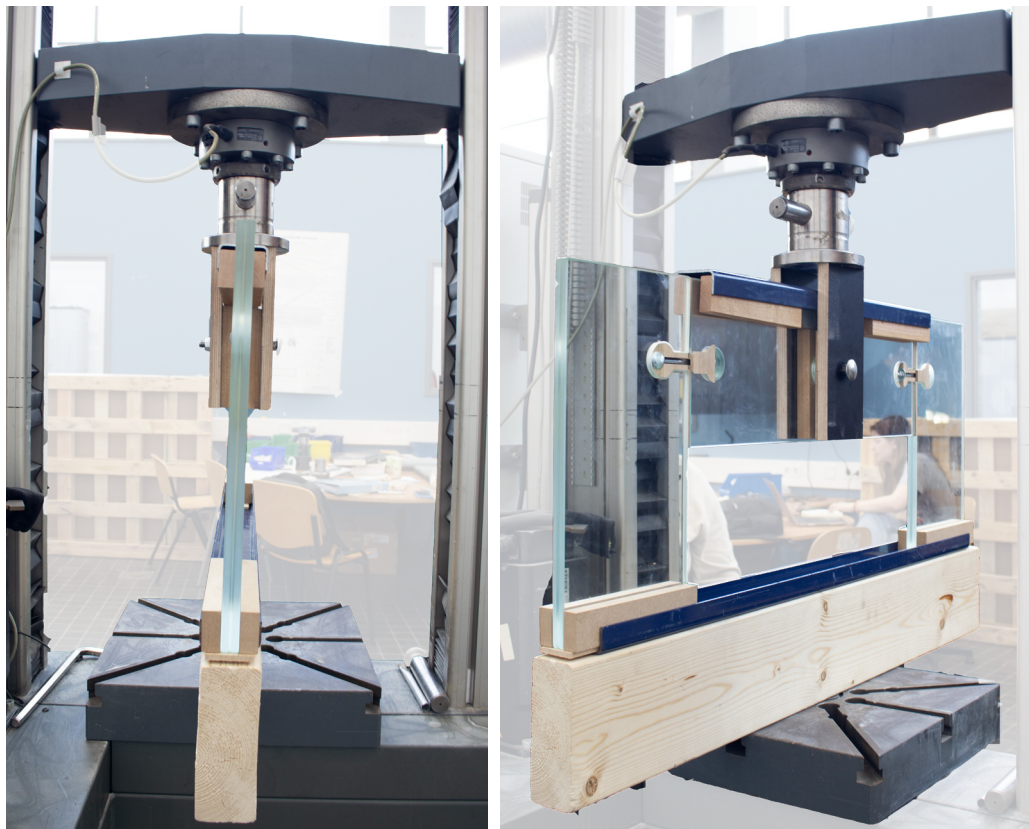


Figure 8.3.54 , 55, prototype in the position and under Loads. Source: Author's own.

- To determine the ultimate load capacity, defined as the maximum vertical force the system can sustain before failure (such as glass cracking, wood crushing, bolt yielding, or full separation of components).
- To determine whether the bolt pretension (tightening force) is sufficient to prevent slippage between the glass and wood under vertical load. This test also assesses whether friction alone provides adequate resistance to movement at the interface.
- **Measured Parameters:**
 - Load at which failure occurs.
 - Type and location of failure (e.g. glass fracture, bolt deformation, wood damage).
 - Load–displacement relationship (linear and non-linear response zones).

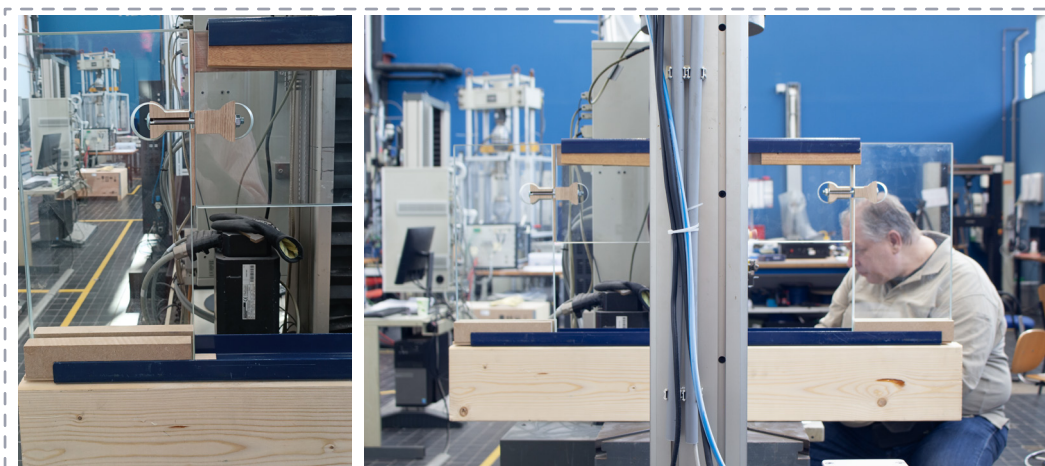


Figure 8.3.56 , 57, prototype in the position and under Loads. Source: Author's own.

- **Loading condition**

The loading was carried out in multiple stages.

Step1: The system was loaded up to the design load and held for five minutes to mimic short-term loading conditions on glass. After that, the test continued in seven steps:

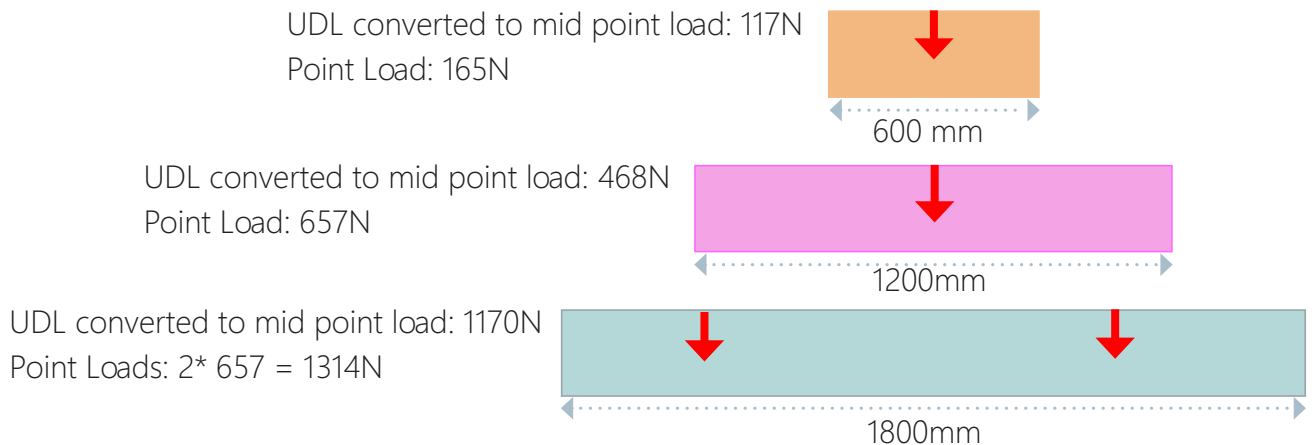
Step 2: Load applied corresponding to the medium-sized module

Step 3: Load applied based on the large module

Step 4: Load calculated to create the same bending stress as Step 2, but applied on the small module

Step 5: Load calculated to create the same bending stress as Step 3, but again applied on the small module

Step 6: Load applied in a way to alternate forces, pushing the system toward failure



In Steps 4 and 5, the goal was to replicate the bending stress experienced by longer modules (from Steps 2 and 3) within the shorter test module. To achieve this, the bending moment formulas for both cases were equated, allowing the calculation of higher concentrated loads needed to produce the same internal bending moment in the shorter span. Since a shorter beam requires a greater force to reach the same bending stress as a longer beam under lower loading, this method effectively translated the loading conditions of larger modules onto the small test specimen. This ensured that the connection's performance could be assessed under equivalent bending demands without changing the physical test setup. Which the resulted numbers for loads are:

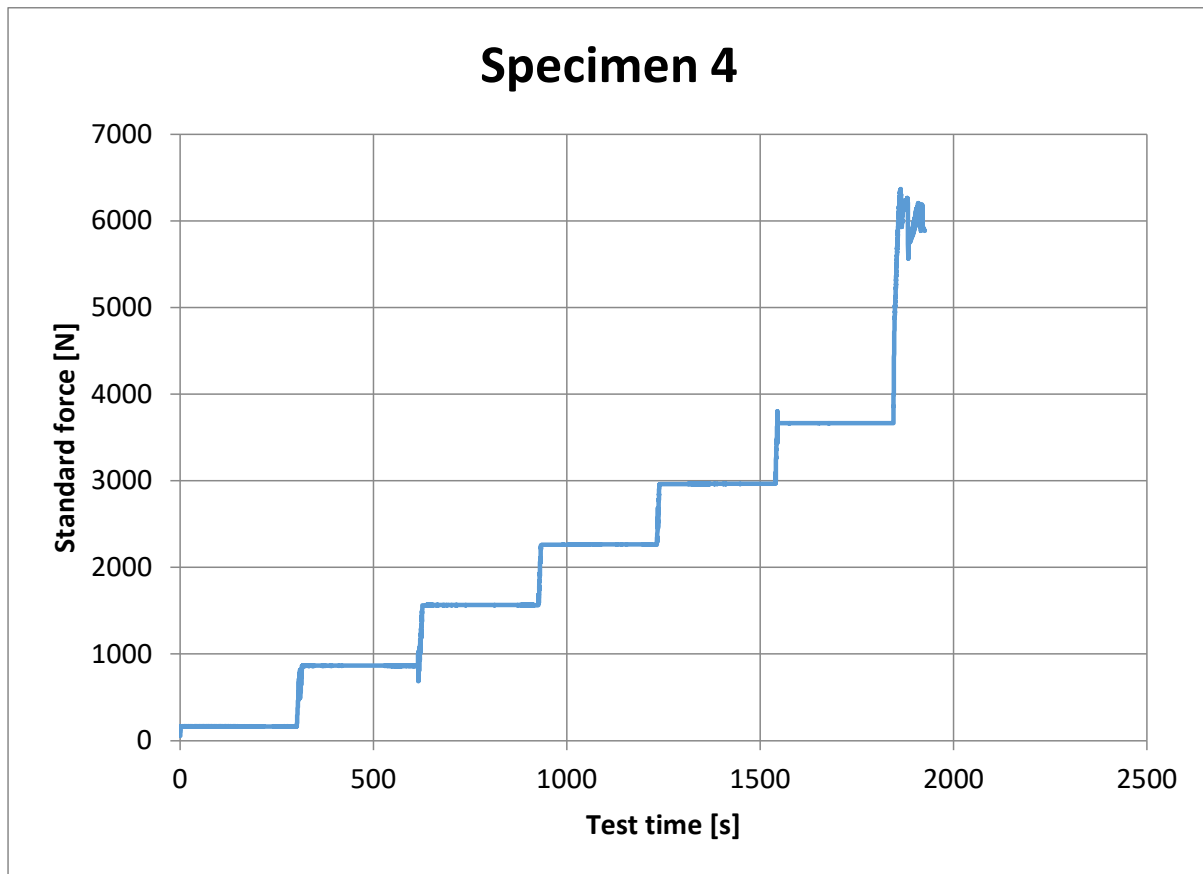
Step 1: 0.285KN

Step 2: 1.032KN

Step 3: 2,484KN

Step 4: 2,688KN

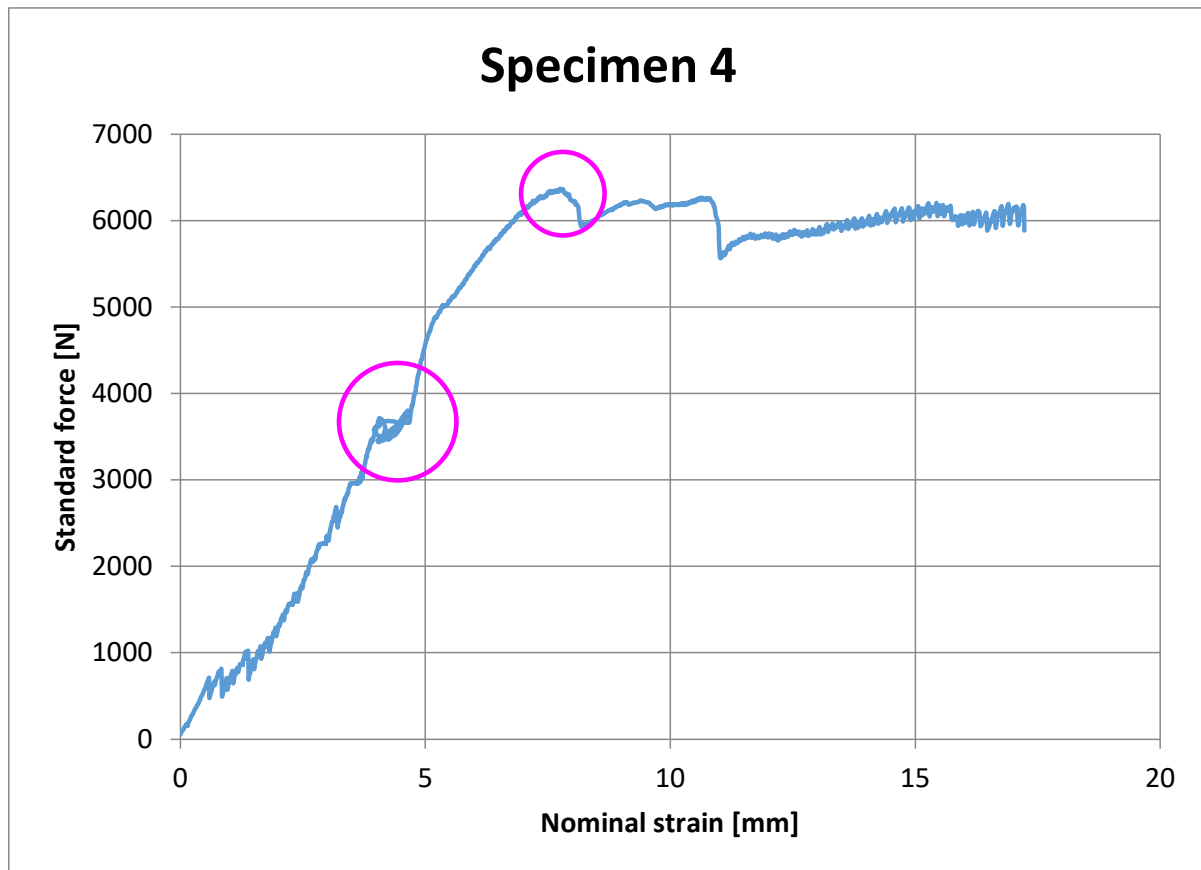
Step 5: 5,800 KN



At each stage of loading, the force was held for five minutes to replicate short-term load conditions in glass. The primary serviceability check—displacement within the span/300 limit—was relevant only for the first step, which corresponds to the design load for this module size. The subsequent steps applied higher loads representative of longer modules, not intended for this particular specimen. These additional tests aimed to assess whether the connection remained stable under other two variations loads, and whether the calculated preload for the bolts was sufficient in practice under extreme loading scenarios. Remarkably, the module sustained up to 2200 N—ten times its design load—while still remaining within serviceability limits.

- **Observations and Key Findings**

At this stage, the system performed successfully through all five loading steps, including the design load and the adjusted loads that mimicked the behavior of other module sizes. There were no signs of failure or excessive deformation during the test. The maximum load was held for approximately five minutes, after which the vertical displacement was recorded. After full unloading, even though the wooden connectors showed signs of breakage, the system remained stable. It was still possible to lift and move the assembly to another location without it falling apart. This indicates that up to a certain point, even if parts of the connection are damaged, the structure can maintain its form and continue transferring loads, which is a promising sign of robustness in the system. Below there are pictures of deflection in step 4, and it was still in allowable deflection limits.



Stage 1:

Fmax:

285 N

dL at Fmax:

0.2 mm

Stage 2:

Fmax:

1032 N

dL at Fmax:

1.7 mm

Stage 3:

Fmax:

2484N

dL at Fmax:

2.9 = 3 mm

Stage 4:

Fmax:

2688N

dL at Fmax:

3.3 mm

Stage 5:

Fmax:

584N

dL at Fmax:

6.6 mm

Stage 6: Ultimate

Fmax:

5900N

dL at Fmax:

17.2 mm

In the first highlighted part of the test, cracking sounds were heard, which initially led us to believe that the central cylindrical wooden piece may have cracked under load. However, inspection showed that both side connectors remained intact, and no visible damage was found in the middle. This suggests the sound likely came from settlement in the system, or internal adjustment within the wooden components, which is expected to some extent due to the non-uniform and anisotropic nature of wood.

The second highlighted part represents the nominal load that the system was able to resist—successfully enduring all five loading steps without failure. This confirms that the connection is not only sufficient for the designed loads but also shows promising performance for practical applications, with a degree of resilience and load redistribution even under partial damage or movement.

Displacement at step 4:



Images for step 6 after reaching to the ultimate point and failure in connectors



Figure 8.3.58 ,63, Deliberate overload applied to reveal ultimate failure characteristics of the joint. Source: Author's own.

One important observation during testing was that the wooden connector cracked in two areas: at the groove surface in contact with the bolt and through the middle of the slot. These failures were likely due to bolt bending, which caused uneven stress in the wood. As the middle section tore, it was pushed toward the laminated glass, and the bolt was close to making direct contact, which could have caused local stress concentrations and glass fracture at the slot corners. This highlights the need for better connector geometry and bolt restraint in future designs. for more detailed explanation read figure discription below.

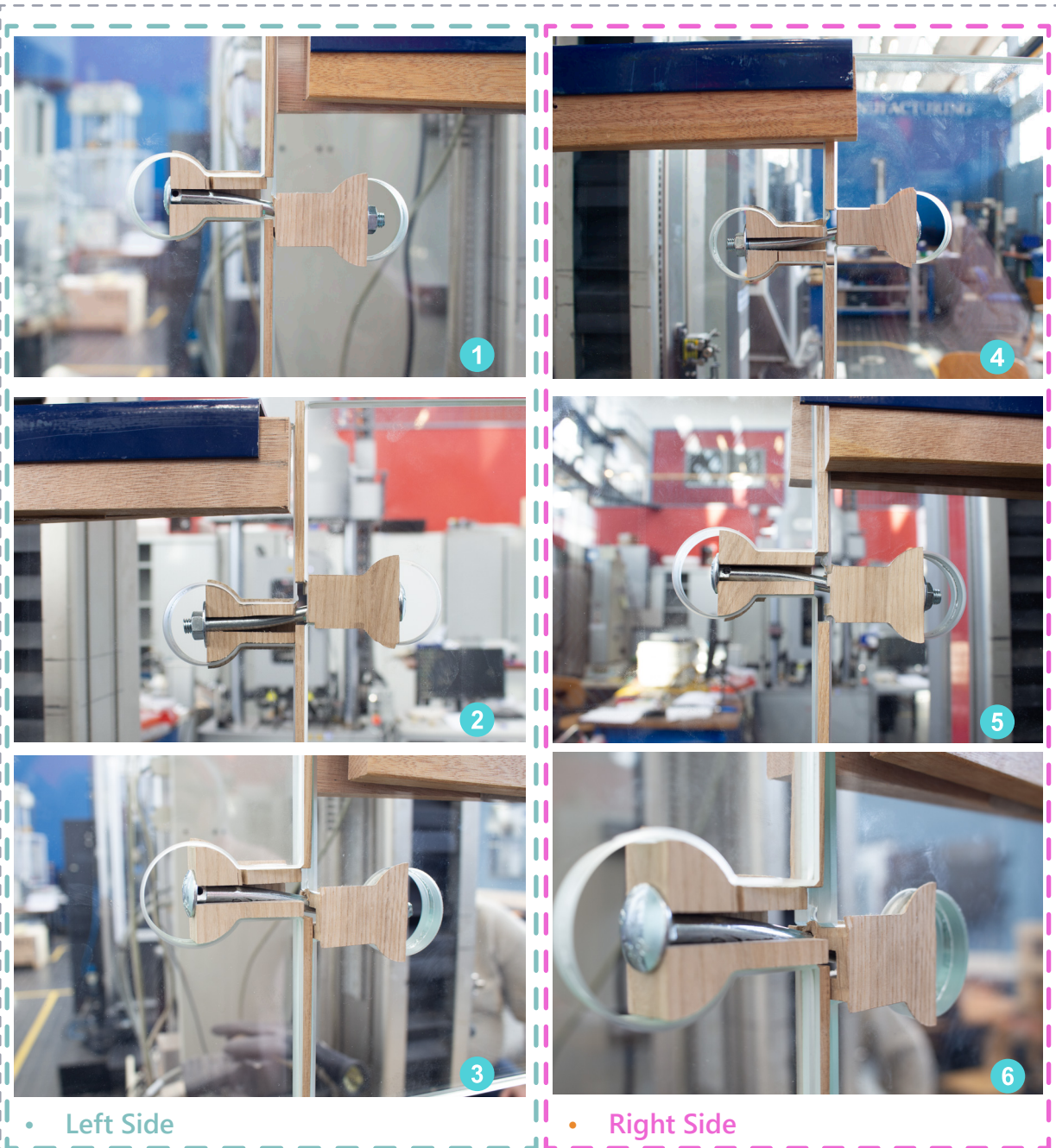


Figure 8.3.64 ,69,1)Front view of the left joint: visible cracking in the wooden connector of the side (fin) module. 2)Rear view of the left joint: no breakage observed, but minor bolt rotation occurred. 3)Perspective view: bolt visibly bent, wooden flanges crushed under pressure. 4)Front view of the right joint: failure occurred in the wooden connector of the middle module. 5)Back view of the right joint. 6)Perspective view of the right joint: wood tearing visible, with the lamination between the two glass panels due to compression. Source: Author's own.

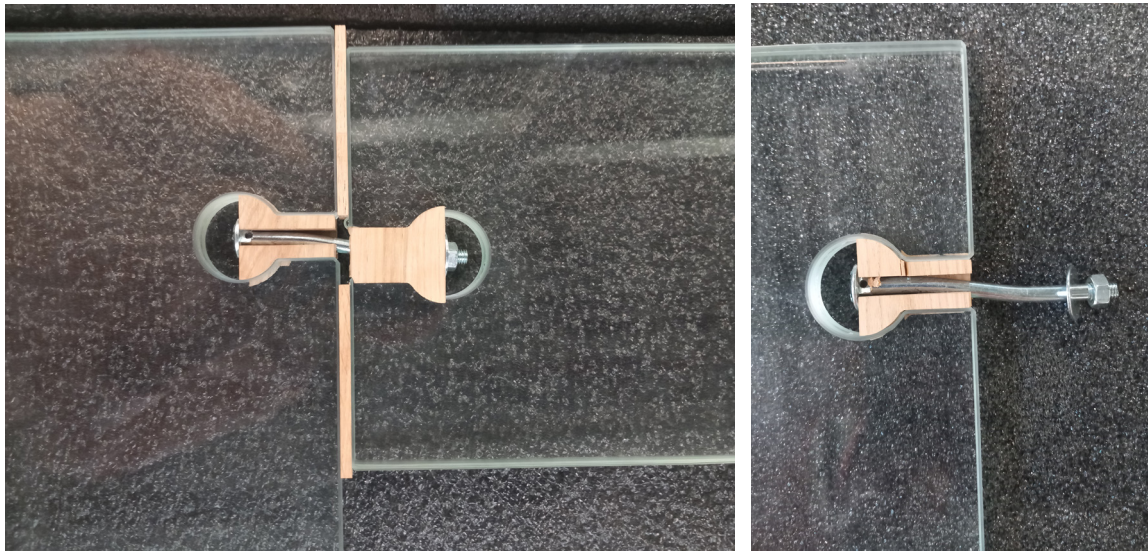


Figure 8.3.70, post failure, bending in bolt proving semi moment resistant behaviour of joint after exceeding the preload force Source: Author's own.

Conclusions based on results

- The overall results were favorable, and the design showed promising performance under the tested loading conditions.
- The accuracy of the experiment could be improved if each module had been tested with its own specific load, rather than applying loads from longer modules to the small one.
- Bolt and fastening improvements:
 1. A more efficient solution would involve bolts that can be accessed from the side elevation, rather than inserting tools through the glass holes.
 2. The standard torque wrench used had a large head, which didn't fit through the holes. A better option would be a torque tool with a ring spanner or open spanner head, allowing for easier and more precise preload application.



Figure 8.3.71 to 74, Bolt revision alternatives for sake of easy and controllable assembly, second alternative using special version of torque wrench with compatible head providing more access during fastening Source: Zipbolt.com

- During fastening, some wooden pieces cracked, mainly due to:
 1. The rotation of the square bolt head, which added stress and caused failure at sharp corners. This issue was solved by drilling a hole in the bolt and using a pin driver to hold it in place during tightening.
 2. Fast tightening also contributed to failure at critical points. The applied preload of 5.3 Nm was relatively high, so a slower tightening process would have reduced the risk.

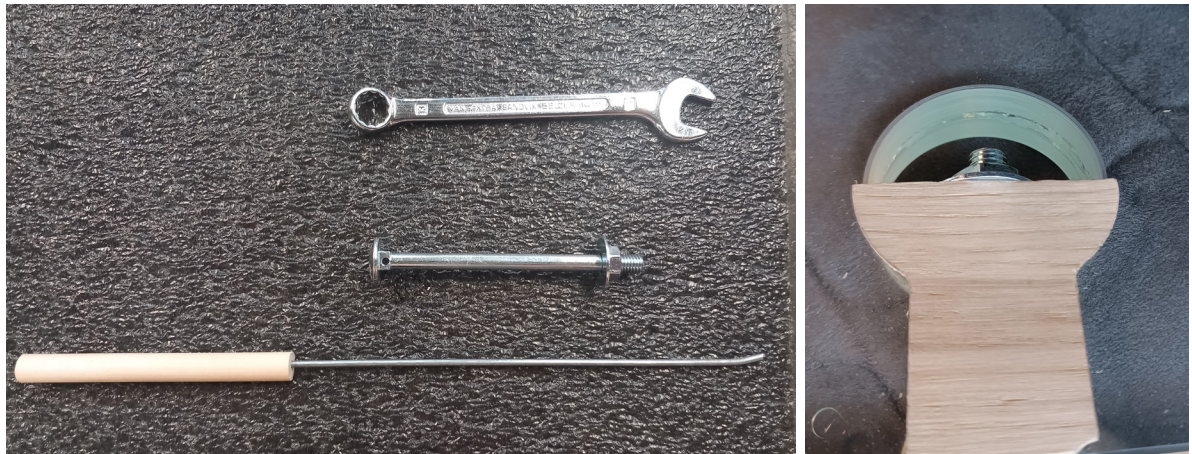



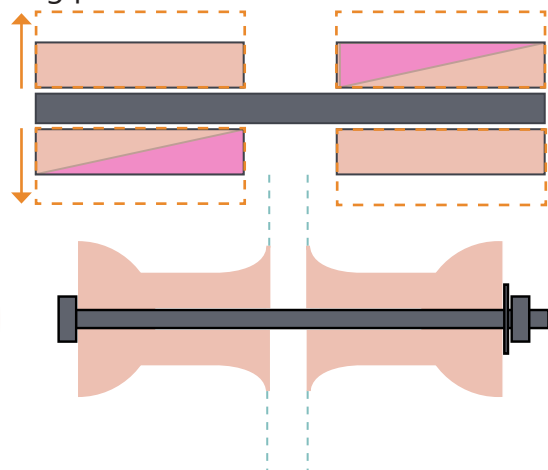
Figure 8.3.75 & 76, left, current bolt fastening and preload appliance tools, Right miss alignments in glass panels due to inaccurate lamination Source: Author's own.

- **Assembly and material behavior:**
 1. The wooden connectors had to be sanded twice, due to: Moisture and heat changes affecting the wood overnight, resulting in a looser fit.
 2. Lamination inaccuracies in the glass panels, where misalignments between layers or protruding PVB interlayer around the holes created uneven contact surfaces with the wooden parts.
- Due to the type and location of failure observed in the wooden connectors, it may be necessary to reconsider and redesign their shape by increasing material to the web of wooden connector or make it hybrids system of aluminum and wood, additionally add to the fillet radius in corners to better distribute stress and avoid splitting or tearing under load.
- Despite these challenges, the connection design remained stable, easy to handle even under partial damage, and shows strong potential for further refinement and practical application.

Increased web of connectors

 The parts of wooden connectors resisting maximum loads

Rounded corners



- Looking ahead, some adjustments to the connection design may be necessary to improve both safety and ease of assembly. This could involve using more material in critical areas or reinforcing zones that experienced high stress during testing. Small changes, such as rounding the edges of both the wood and glass components, could help prevent the wooden connector from being pushed into the glass interlayer and reduce the risk of stress concentration. Additionally, increasing the size of holes and grooves may allow for easier assembly while also enabling thicker wooden sections where needed. These refinements would help improve both mechanical performance and tolerance control during fabrication.
- Despite these challenges, the connection design remained stable, easy to handle even under partial damage, and shows strong potential for further refinement and practical application.

8.3.2. Main test 2

As introduced earlier (see Section 8.3.1, Main Test 1), the prototyping, fabrication process, loading conditions, and measurement parameters for both Test 1 and Test 2 were identical.

The objective of Test 2 was to examine the earlier hypothesis regarding the optimal fibre orientation of wood in this connector design. Theoretically, it was proposed that shear loads from the general loading direction should align with the longitudinal grain direction to maximise the shear strength of the wood, while the preload forces would act perpendicular to the grain (in the radial direction). In this test, the outcomes of Test 2 are presented and later compared with those from Test 1 to determine the most effective grain orientation for each stress axis in the connector components.



Figure 8.3.77, left, perpendicular to grain direction in loading position, Right parallel to grain direction in loading position, far right, if applied torque is done fast and with out system of pin driver, most likely the square neck of bolt will rotate and break the wood specially in this direction was fragile than then other one.
Source: Author's own.

For additional safety during this test, a layer of plastic foil was applied over the glass surface to minimise the risk of injury in case of breakage or shattering within the laboratory environment.



Figure 8.3.78 & 79, left, perpendicular to grain direction in loading position, Right parallel to grain direction in loading position. Source: Author's own.

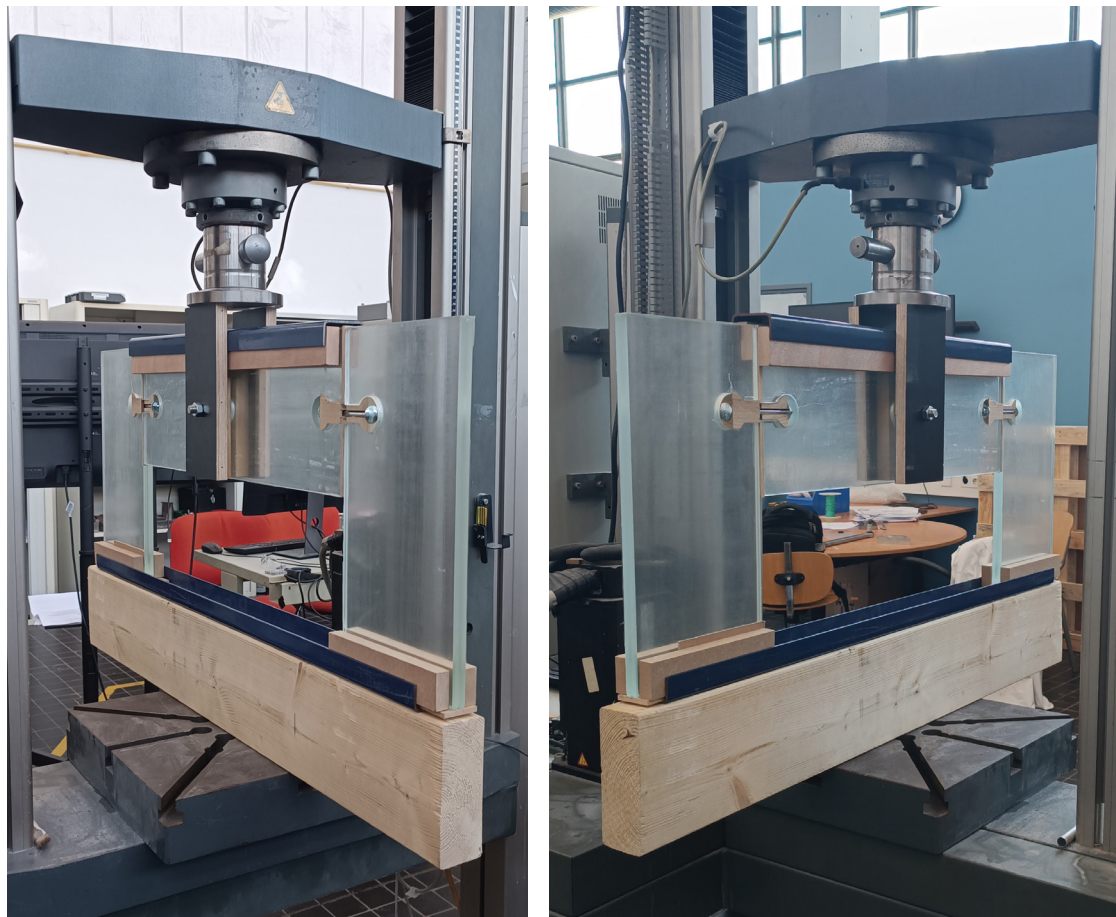
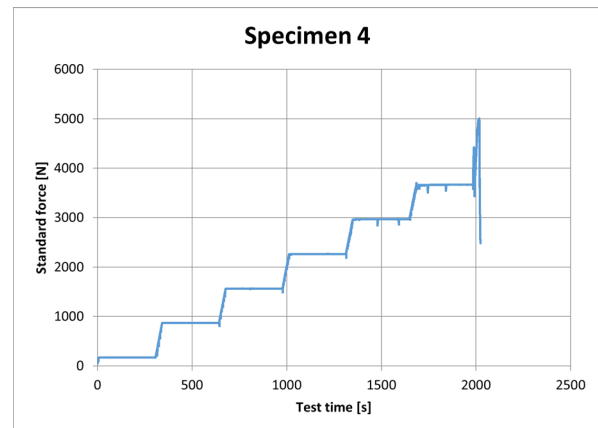


Figure 8.3.80 & 81, Prototype in the loading position and set ups. Source: Author's own.

Stage 1:
Fmax:
 285 N
dL at Fmax:
 1.1mm

Stage 2:
Fmax:
 1032 N
dL at Fmax:
 3.4 mm



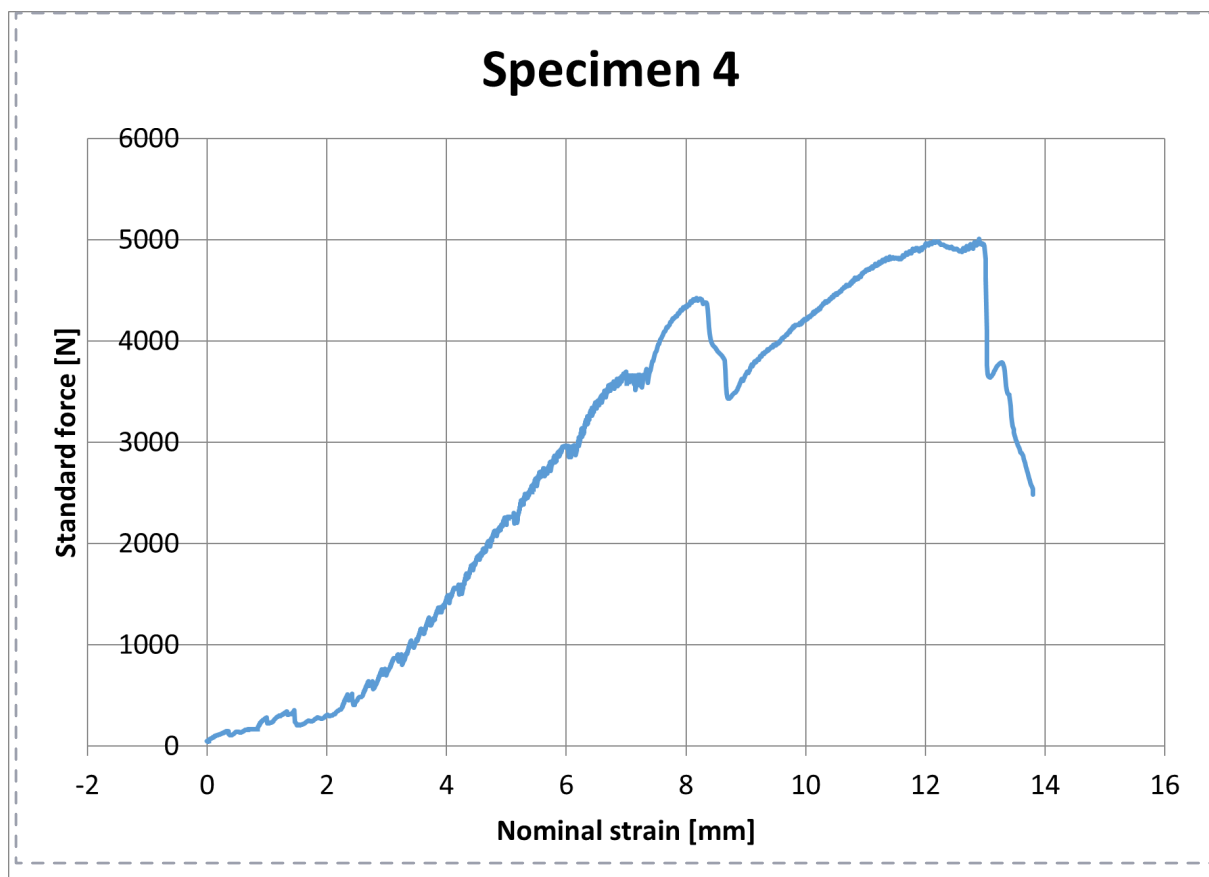
Stage 3:
Fmax:
 2484N
dL at Fmax:
 5.3 mm

Stage 4:
Fmax:
 2688N
dL at Fmax:
 5.6 mm

Stage 5:
Fmax:
 5800N. ✗
dL at Fmax:

Stage 6: Ultimate
Fmax:
 5009N
dL at Fmax:
 13 mm

A step-by-step comparison of the two configurations showed that the parallel-to-grain setup consistently resulted in lower displacement and higher load capacity, despite identical preload levels and matching test conditions.





1



2

1 & 2

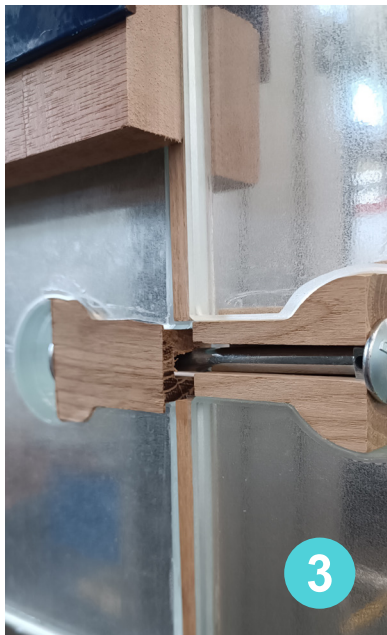
Stage 2:

Fmax:

1032 N

dL at Fmax:

3.4 mm



3



4

3 & 4

Stage 3:

Fmax:

2484N

dL at Fmax:

5.3 mm



5



6

5 & 6

Stage 4:

Fmax:

2688N

dL at Fmax:

5.6 mm

Figure 8.3.82 & 87, photos showing the displacement and deformation in the each step . Source: Author's own.



Figure 8.3.88 & 90, photos showing the displacement and deformation in Ultimate step .
Source: Author's own.

7 & 8

Stage 6: Ultimate

F_{max}:

5009N

dL at F_{max}:

13 mm

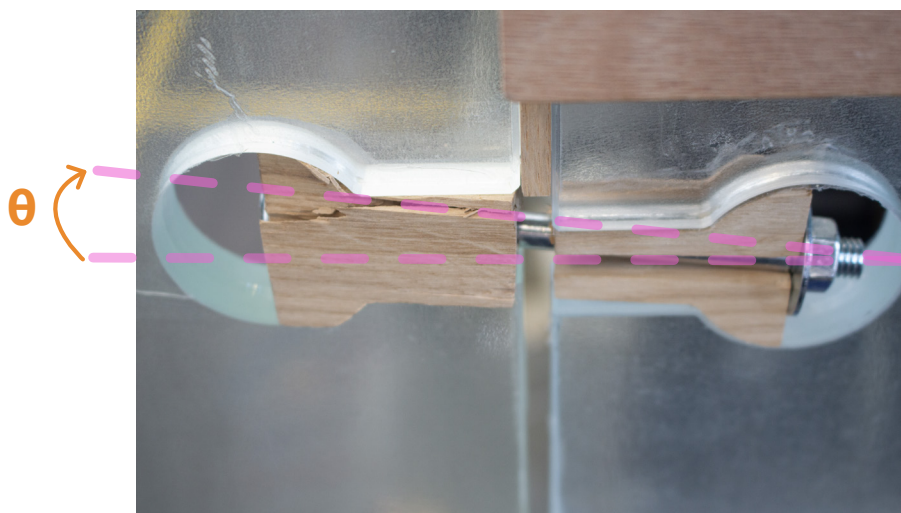
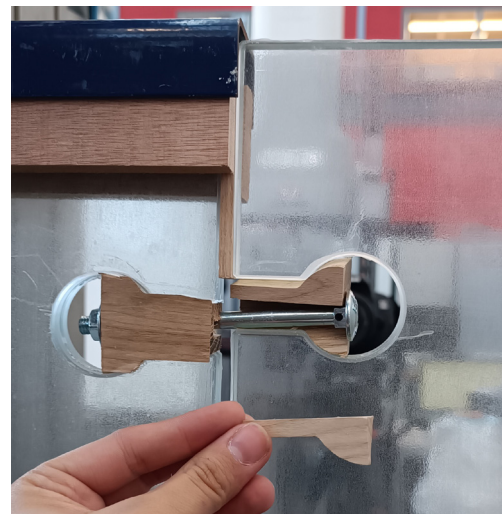


Figure 8.3.91, Rotation and slippage of bolt in Ultimate step . Source: Author's own.

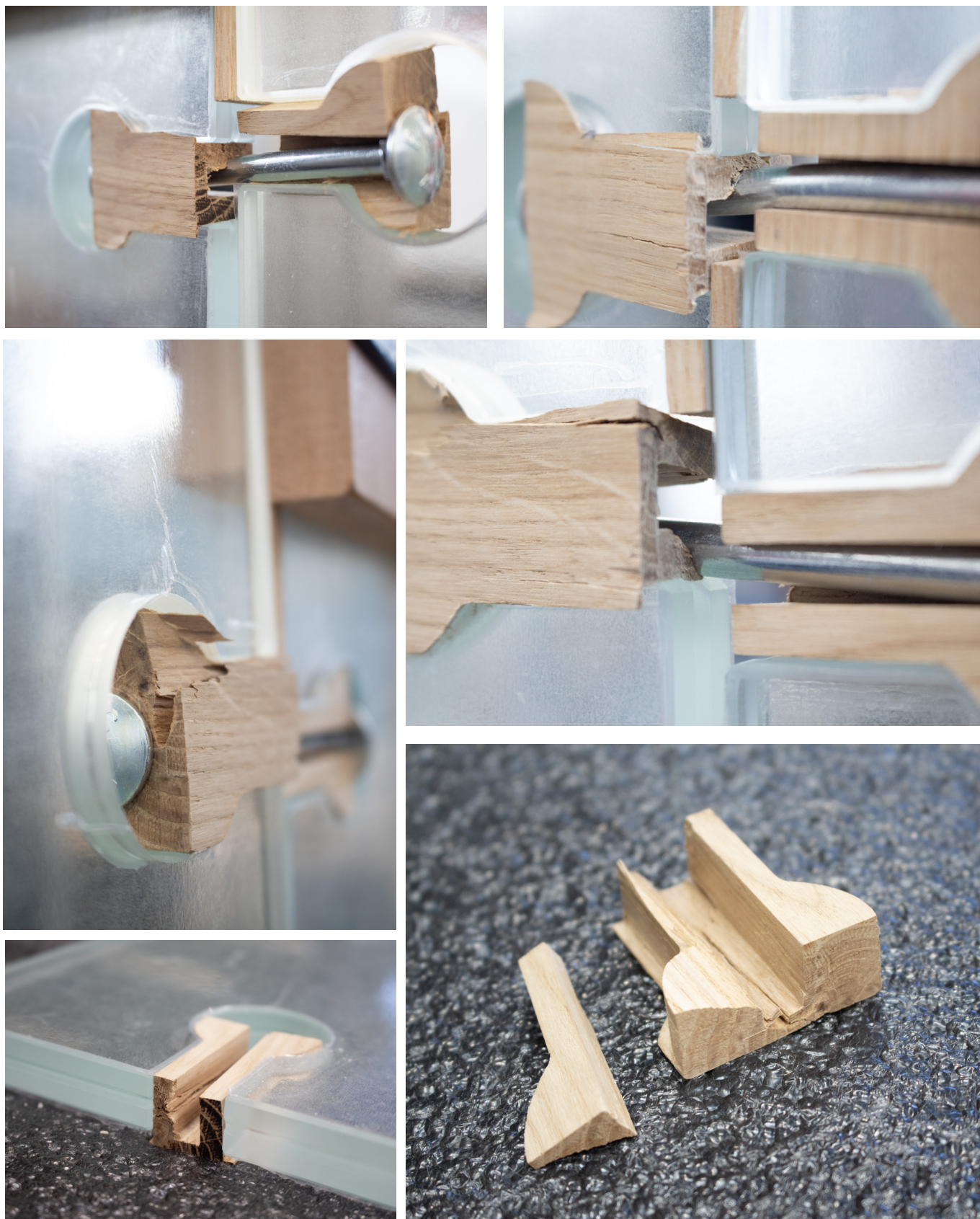
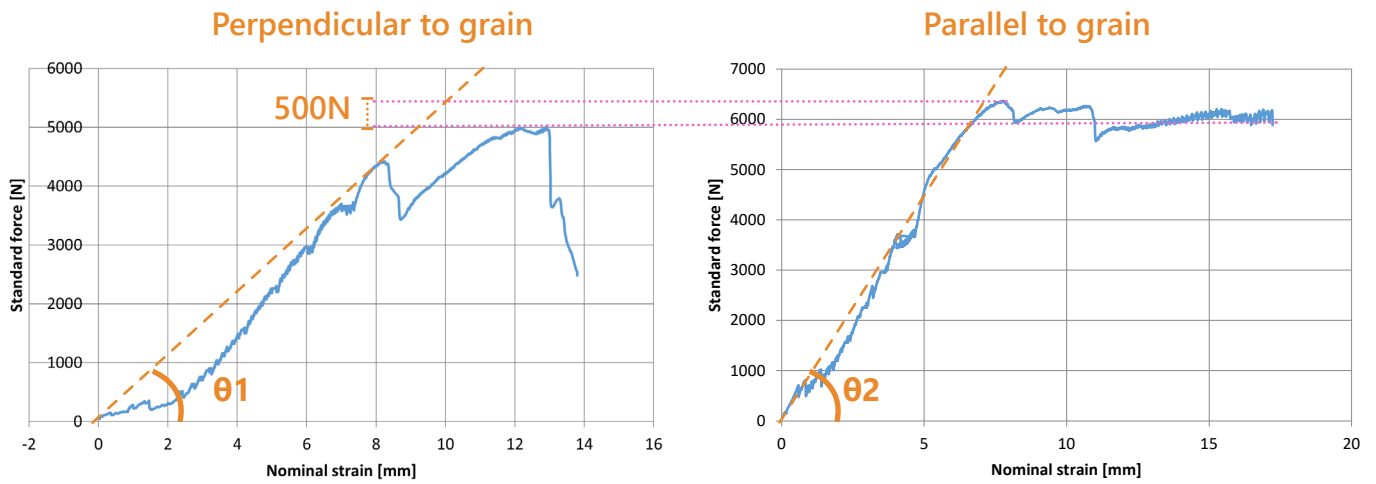


Figure 8.3.92 to 97, Deformation and failure accrued in wood connector Ultimate step . Source: Author's own.



- **Analysis and comparison**

- The slope of force / strain ratio curve in the parallel-to-grain configuration was steeper, indicating lower displacement and greater load-bearing capacity.
- Notably, this configuration sustained approximately 500 N more load than the perpendicular-to-grain option.

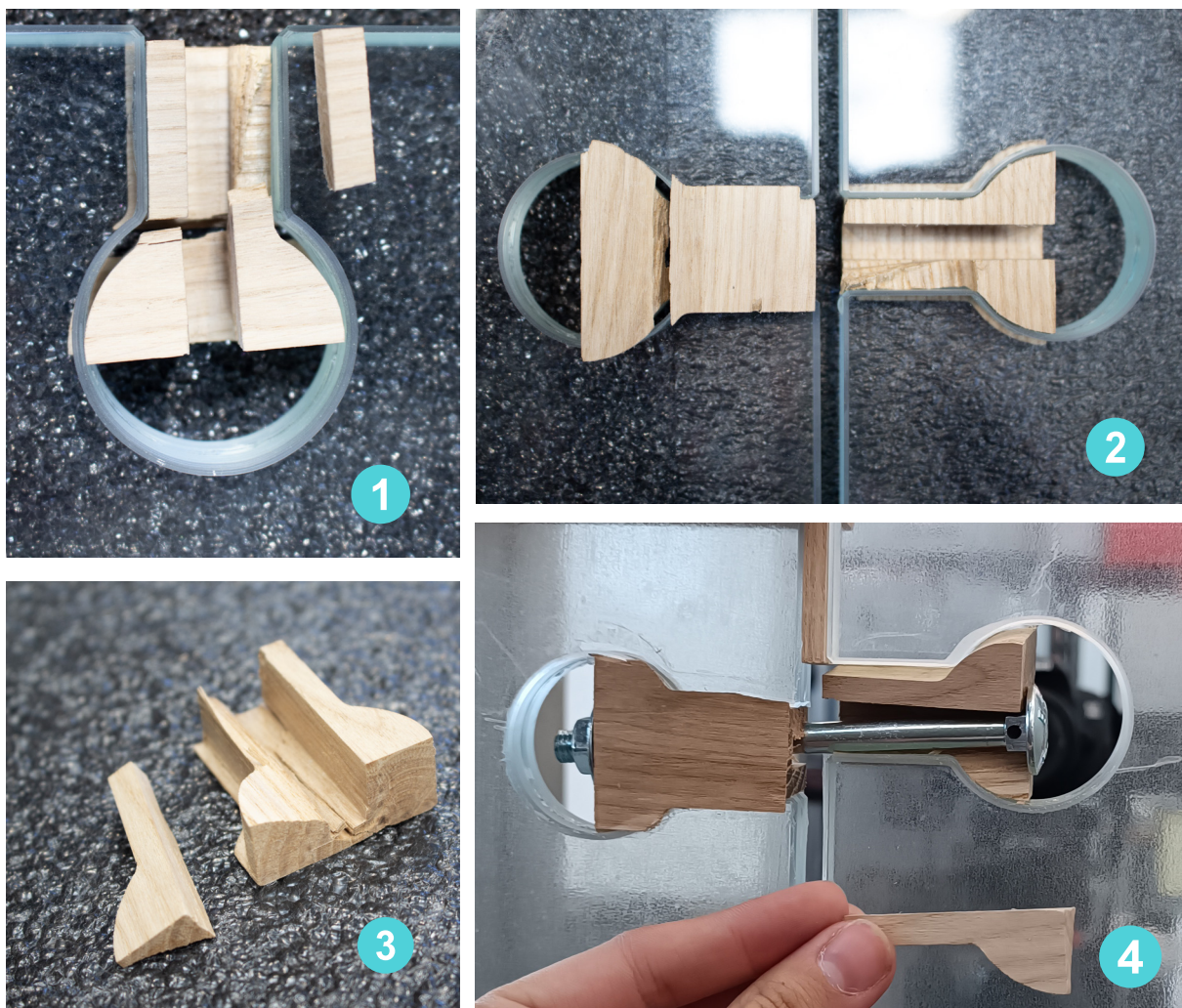
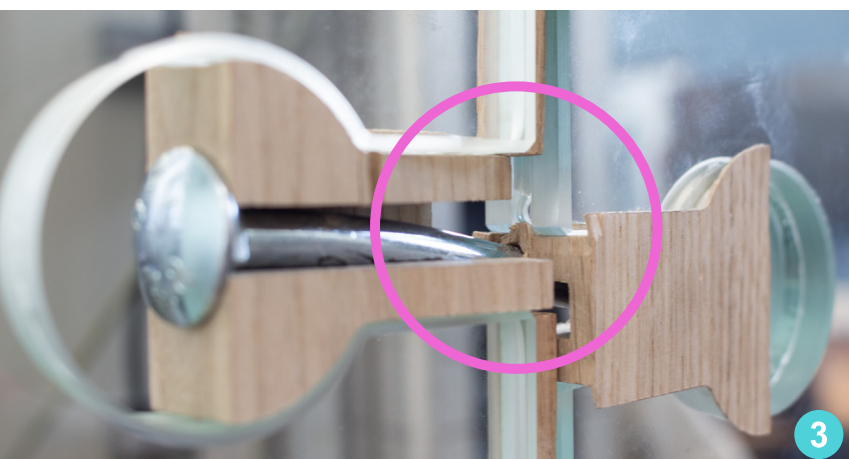
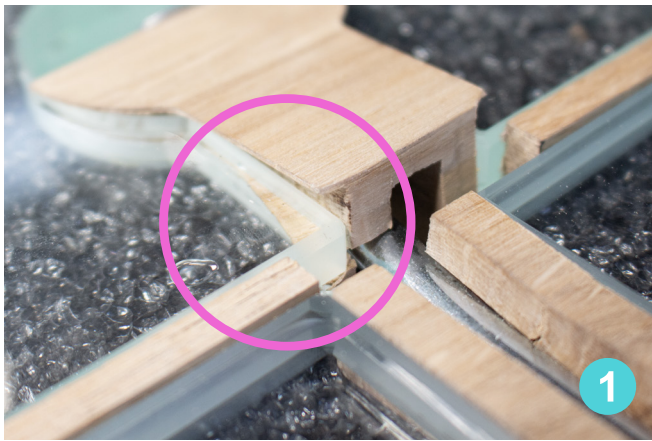


Figure 8.3.98 to 101, failure accrued in wood connector Ultimate step 1,2 parallel to grain from test 2 and 3,4 perpendicular to the grain from test 3 . Source: Author's own.

- Furthermore, the failure pattern confirmed its safety advantage: the parallel arrangement kept the connector stable and prevented the bolt from making contact with the glass—unlike the perpendicular case, where the connector shifted, increasing the risk of glass damage.
- In both tests, the wooden connectors were crushed due to excessive loading beyond their material strength or the preload capacity of the bolt. However, in the parallel-to-grain configuration, the crushed wood remained interlocked within the lamination of the glass, maintaining its position even after failure—this is highly favourable for a safe post-fracture



load state (PFLS). In contrast, the perpendicular-to-grain connector failed more abruptly, breaking into pieces and completely losing its grip on the joint.

Conclusion:

These observations confirm the earlier theoretical prediction: the parallel-to-grain orientation is the most reliable and structurally effective direction for the wooden connectors in this system.

Figure 8.3.102 to 106, failure accrued with in fibers of wooded connector in Ultimate step 1,2,3 parallel to grain from test 2 and 4,5 perpendicular to the grain from test 3 . Source: Author's own.

9. Final Products

9.1. Final Usecase proposals

- Walk way shade

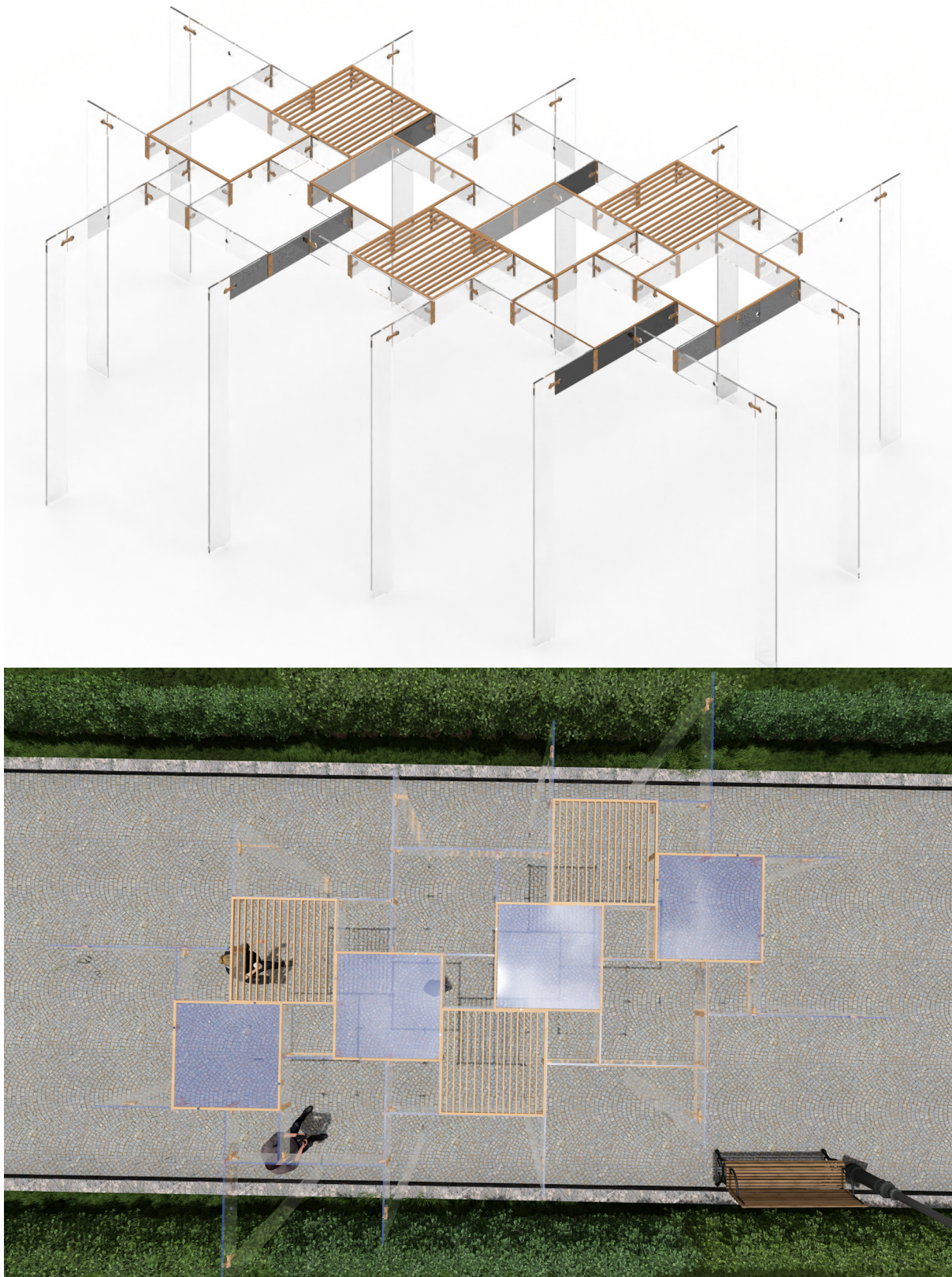


Figure 9.1.1& 2 Design use case sketches. Source: Author's own.

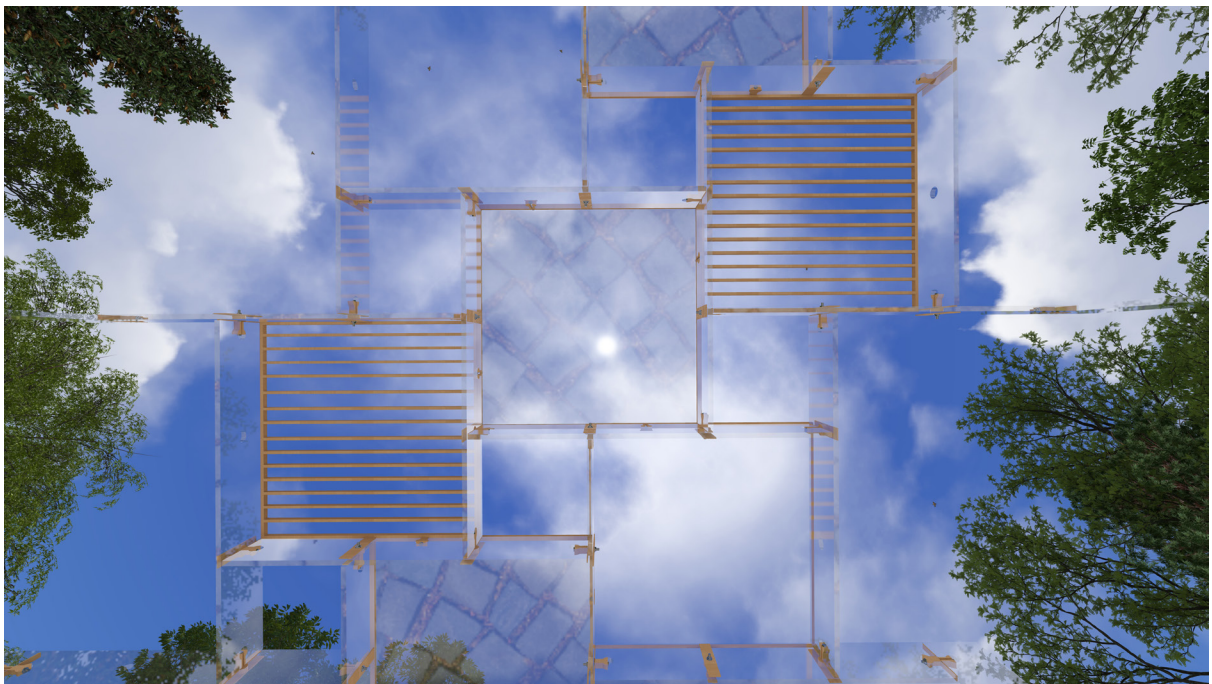


Figure 9.1.3& 4 Design use case sketches. Source: Author's own.

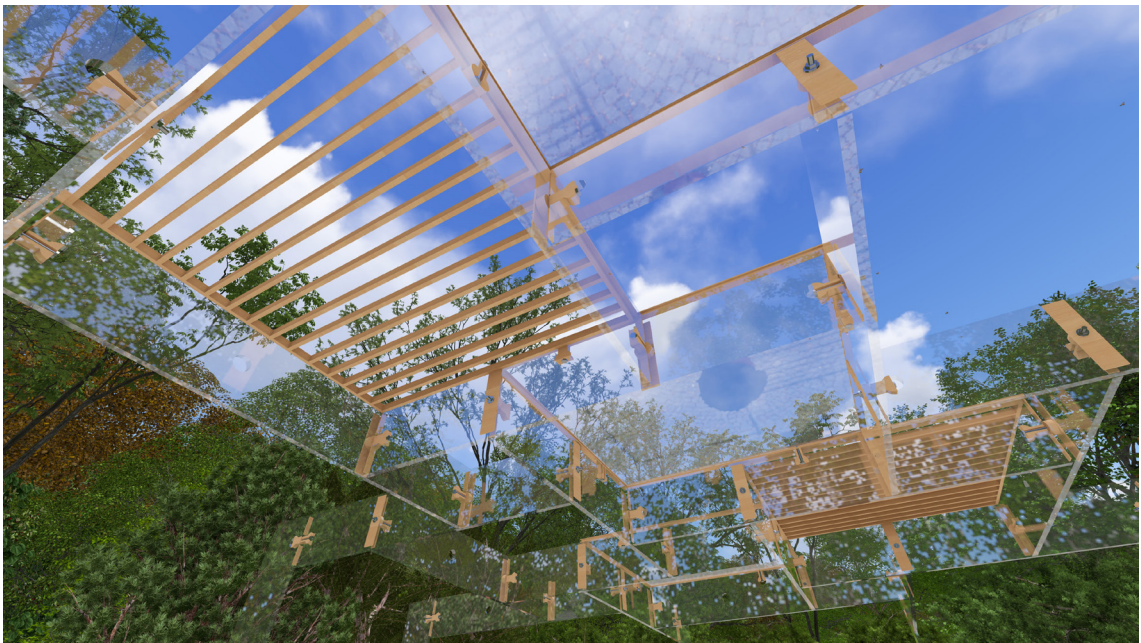
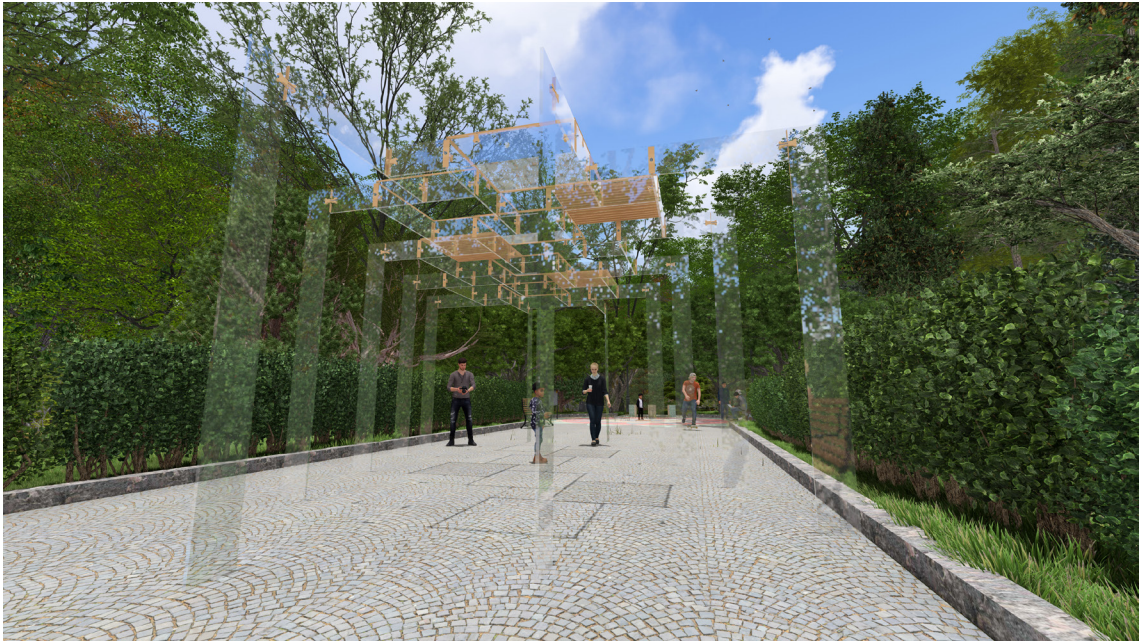


Figure 9.1.5to 7 Design use case sketches. Source: Author's own.

- Pergola

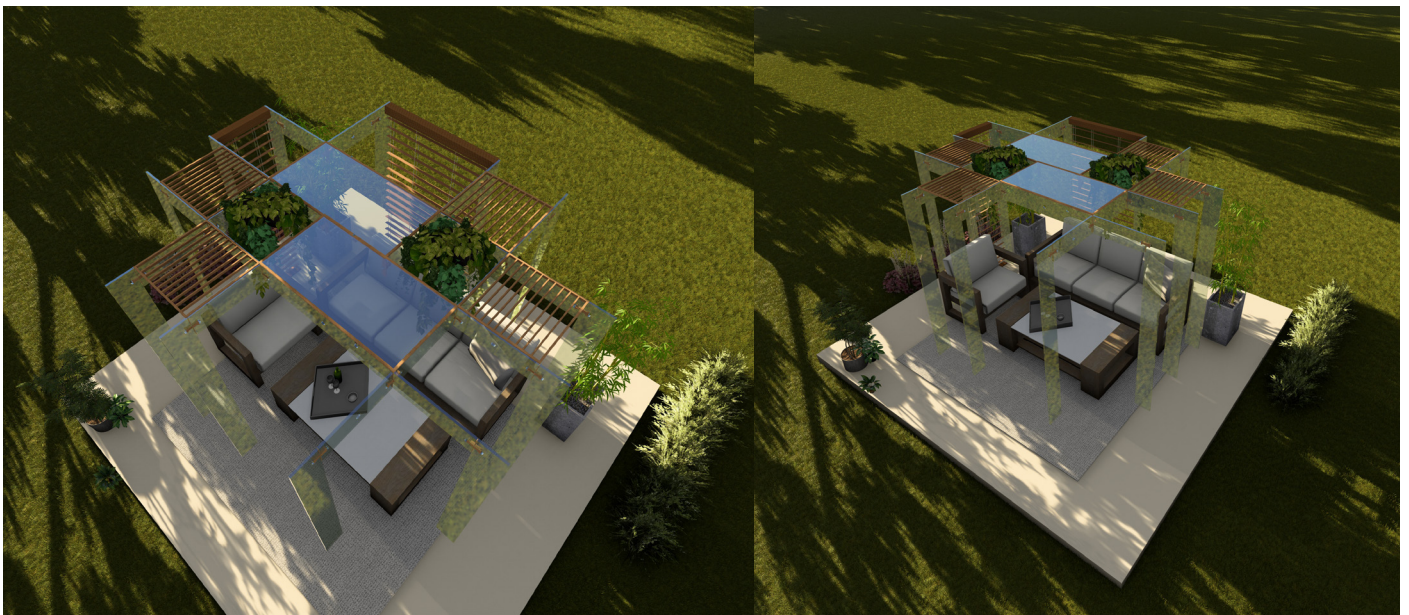


Figure 9.1.8 to 10 Design use case sketches. Source: Author's own.

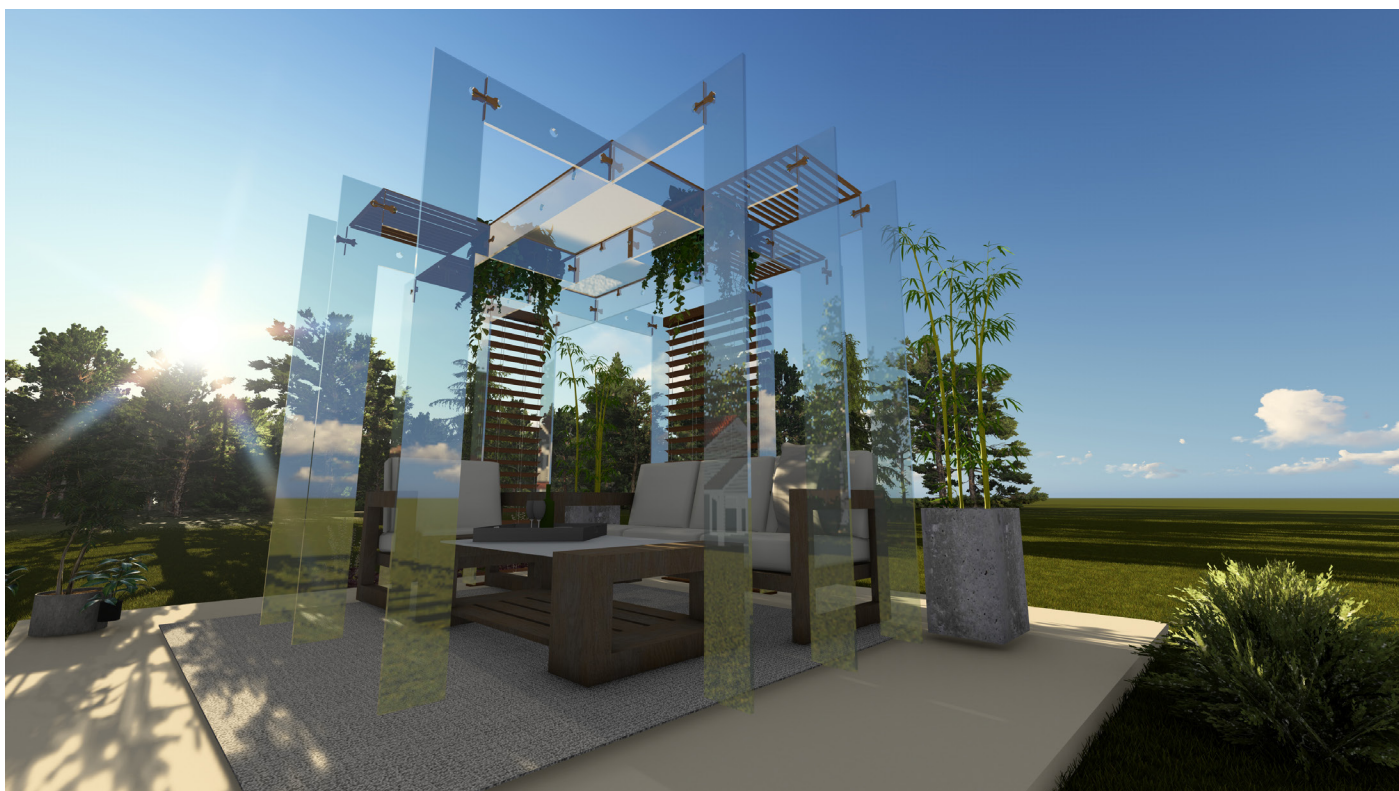
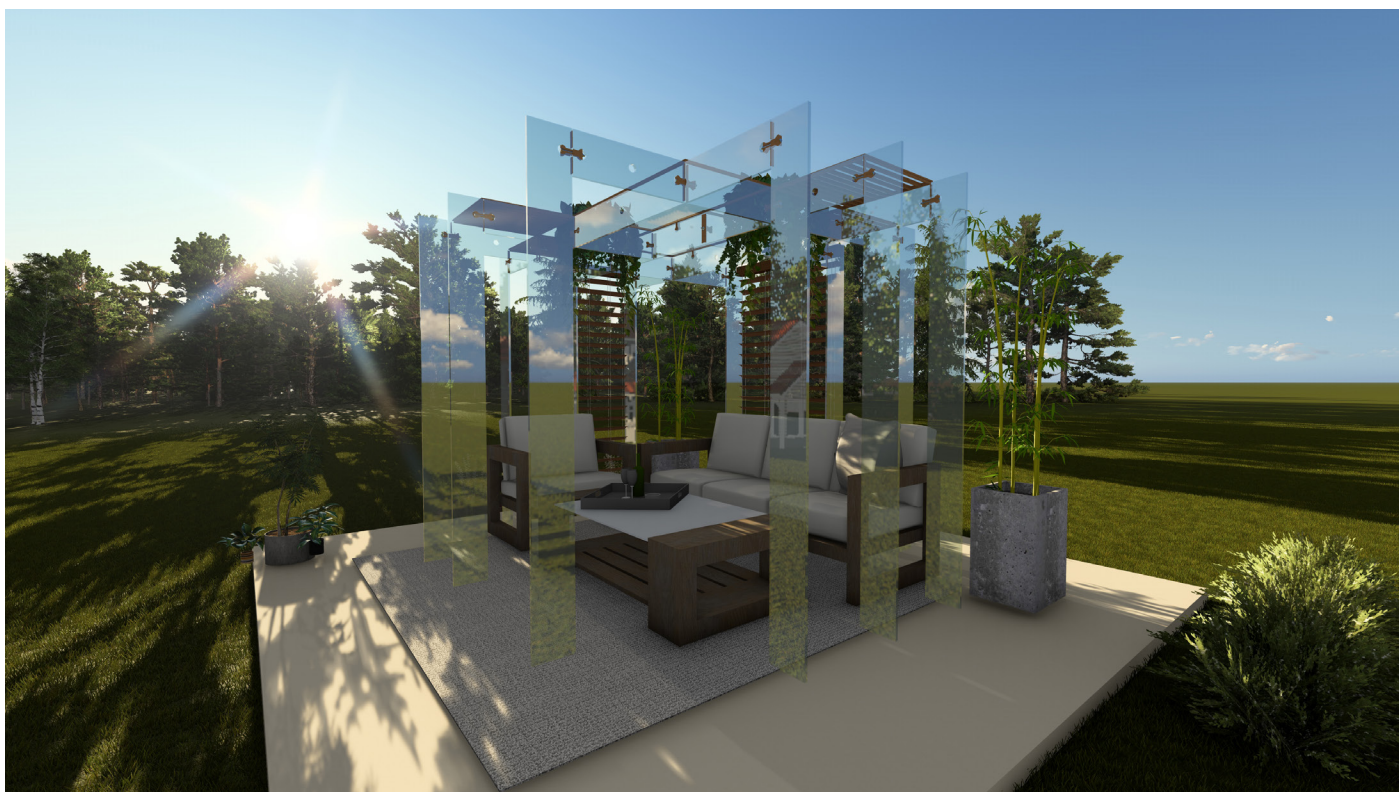


Figure 9.1.10 to 12 Design use case sketches. Source: Author's own.

- Pavilion

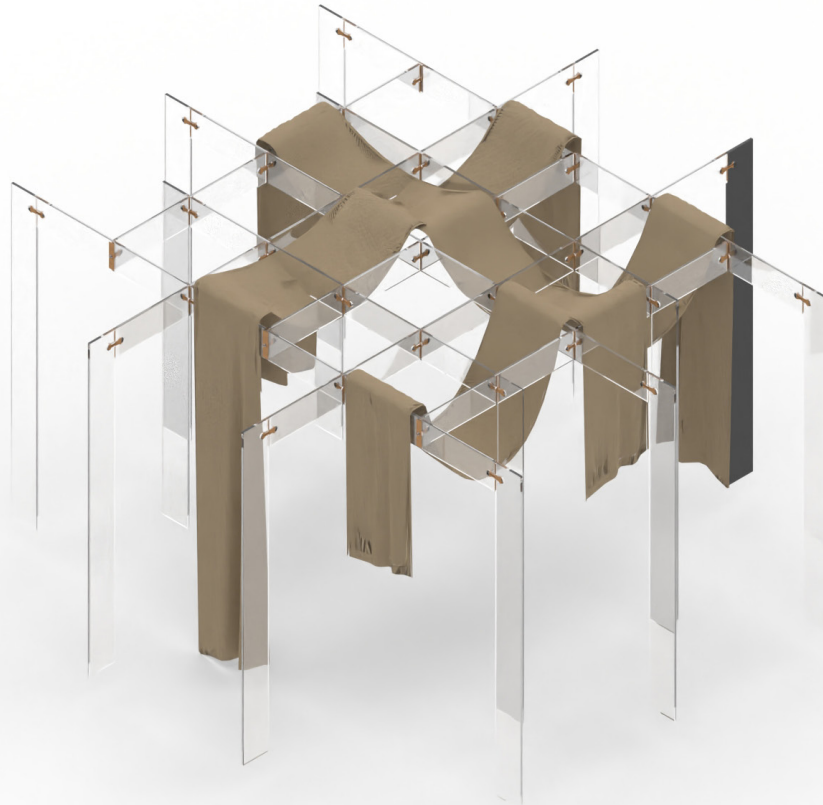
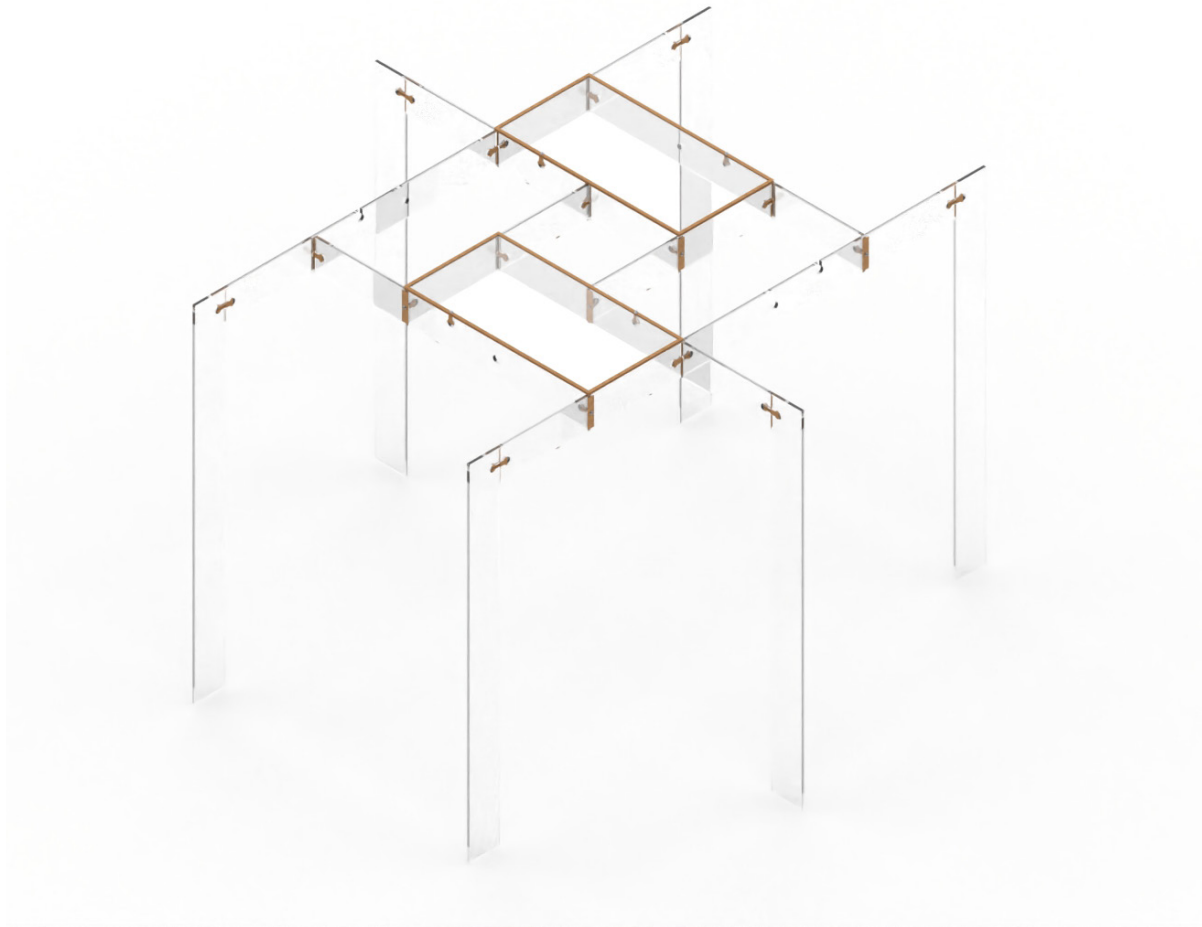


Figure 9.1.13 & 14 Design use case sketches. Source: Author's own.



Figure 9.1.15 &16 Design use case sketches. Source: Author's own.

- Pavilion 2



- Pavilion 3



Figure 9.1.17 & 18 Design use case sketches. Source: Author's own.



Figure 9.119 & 20 Design use case sketches. Source: Author's own.



Figure 9.1.20 & 21Design use case sketches. Source: Author's own.



Figure 9.1.22&23 Design use case sketches. Source: Author's own.

- Pavilion 4 / Walk way shade

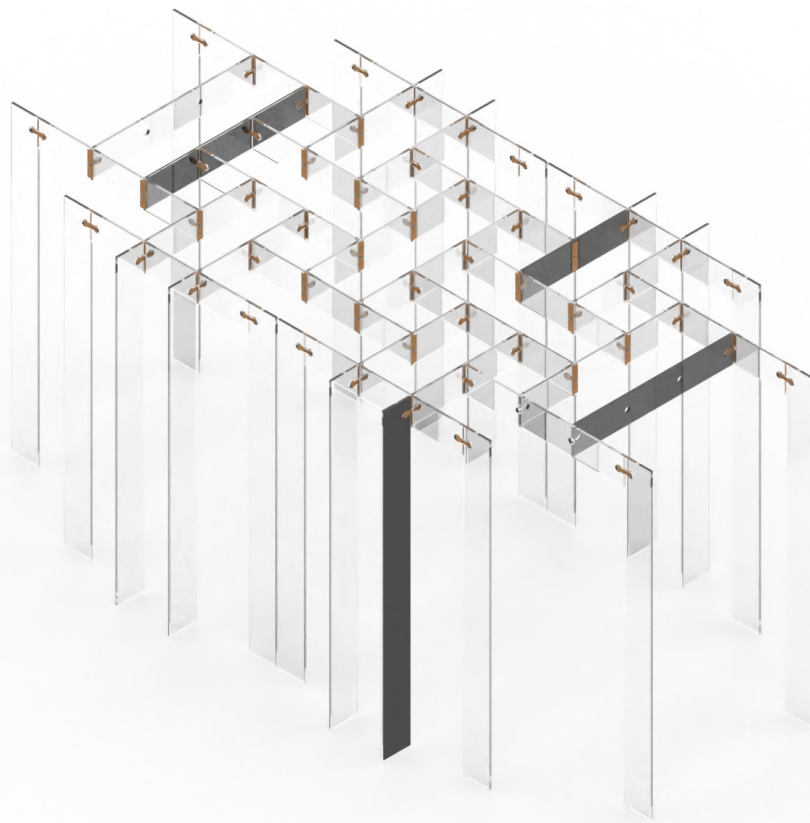


Figure 9.1.24 & 25 Design use case sketches. Source: Author's own.

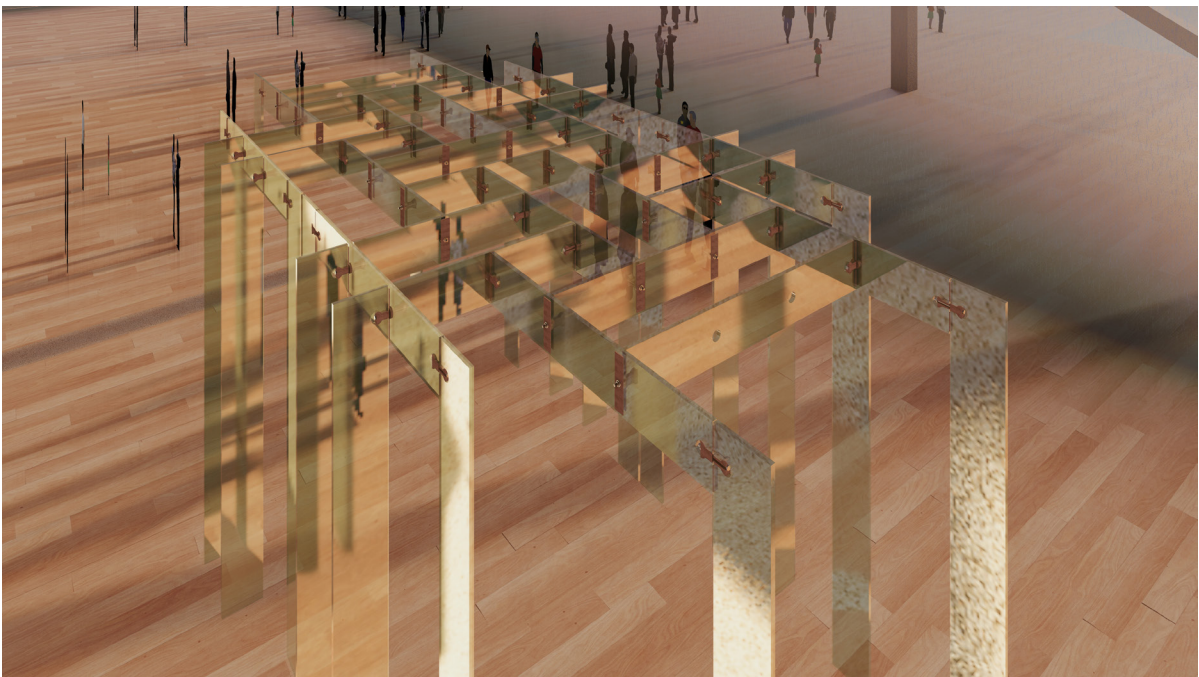


Figure 9.1.26to28 Design use case sketches. Source: Author's own.

- Patio glass reciprocal roof structure



Figure 9.1.29 & 30 Design use case sketches. Source: Author's own.

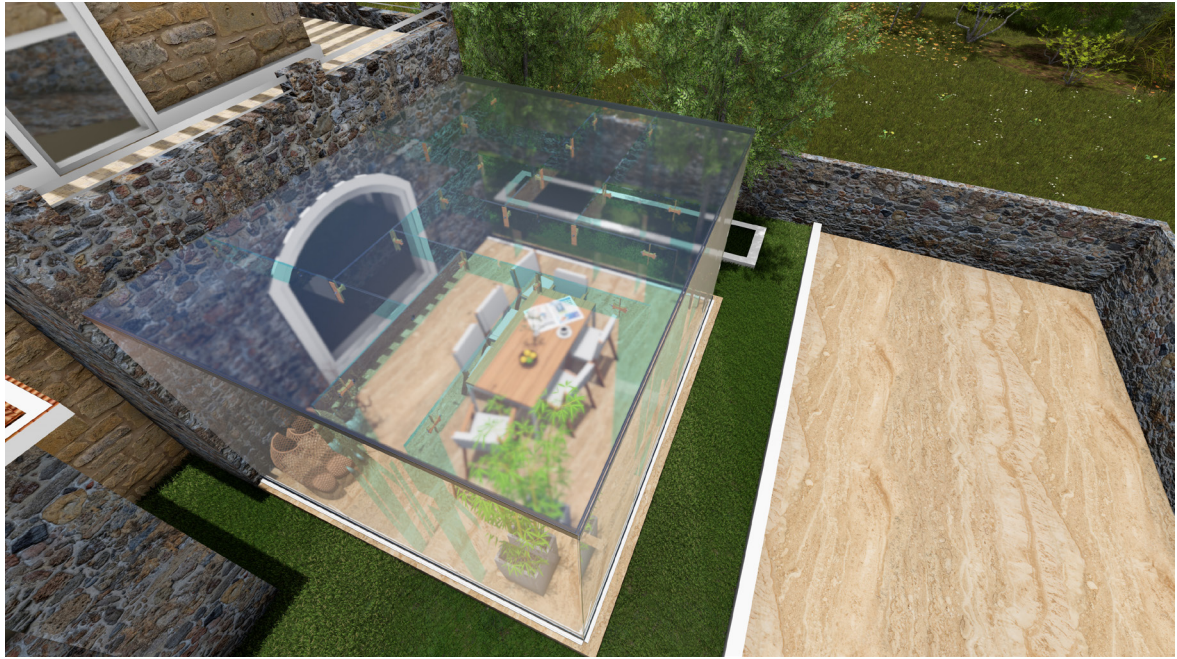


Figure 9.1.31to 33 Design use case sketches. Source: Author's own.

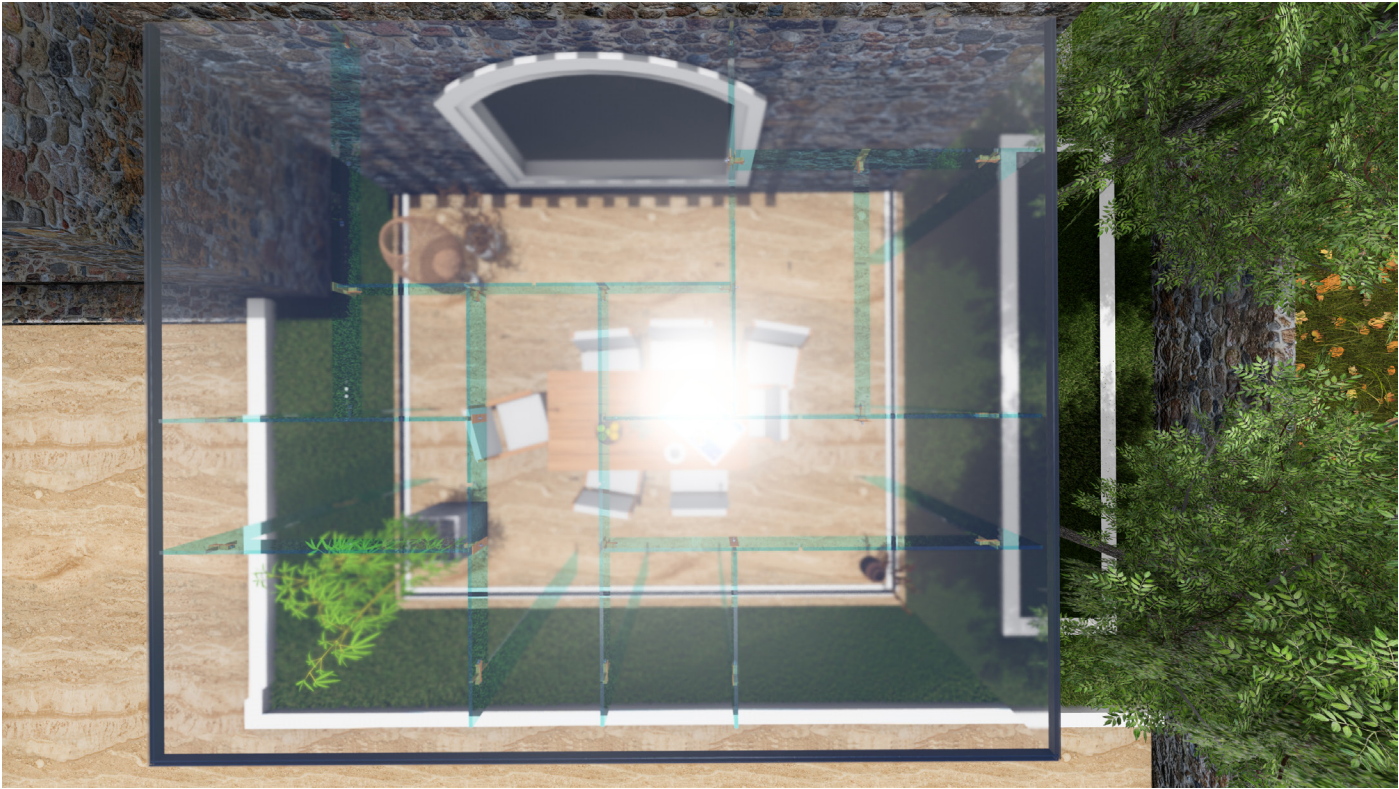


Figure 9.1.34 &35 Design use case sketches. Source: Author's own.

9.2. Assembly Sequence

The modules are first packed into crates at the factory and transported by truck to the construction site. Upon arrival, the crates are unloaded, and a temporary wooden scaffold—designed in a grid pattern—is assembled. Workers then pre-assemble the fins on the ground using their rigid clamp connections.

Using mobile scaffolds with wheels, the workers transport the fins to their intended positions. The modules are placed onto the scaffold and connected to the fins, progressing inward as each adjacent module is installed. Once all joints are secured, the scaffolds can be removed, and the structure—whether a pavilion, pergola, or walkway shade—is ready for use.

If relocation is needed, the process can be reversed. The scaffold is rebuilt, and the modules are disassembled starting from the centre outward. Finally, the fins are detached, all components are repacked into crates, and the scaffold is taken down for reuse at the new location.

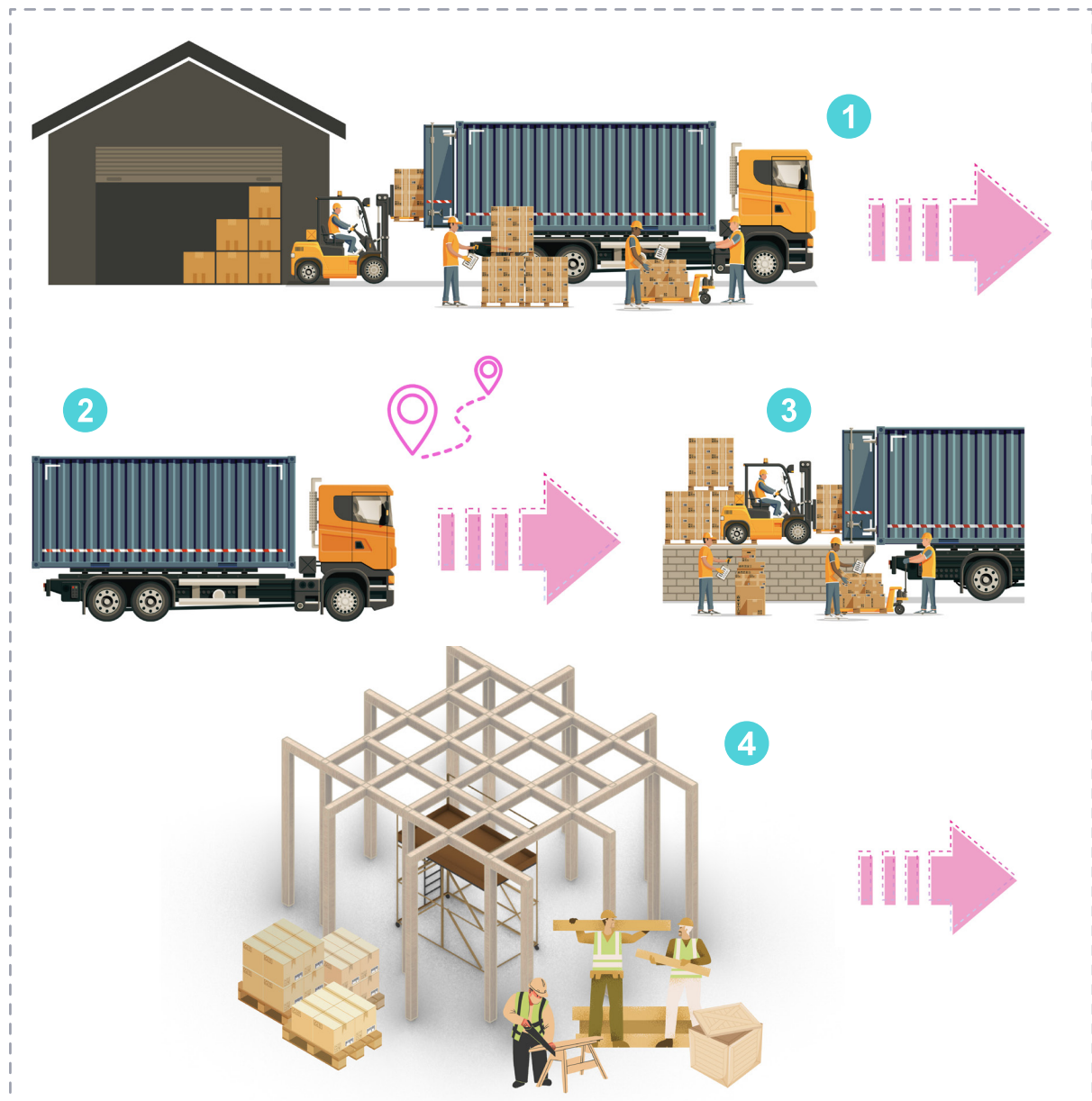


Figure 9.2.1 to 3, Step by Step Assembly sequence diagram. Source: Author's own.

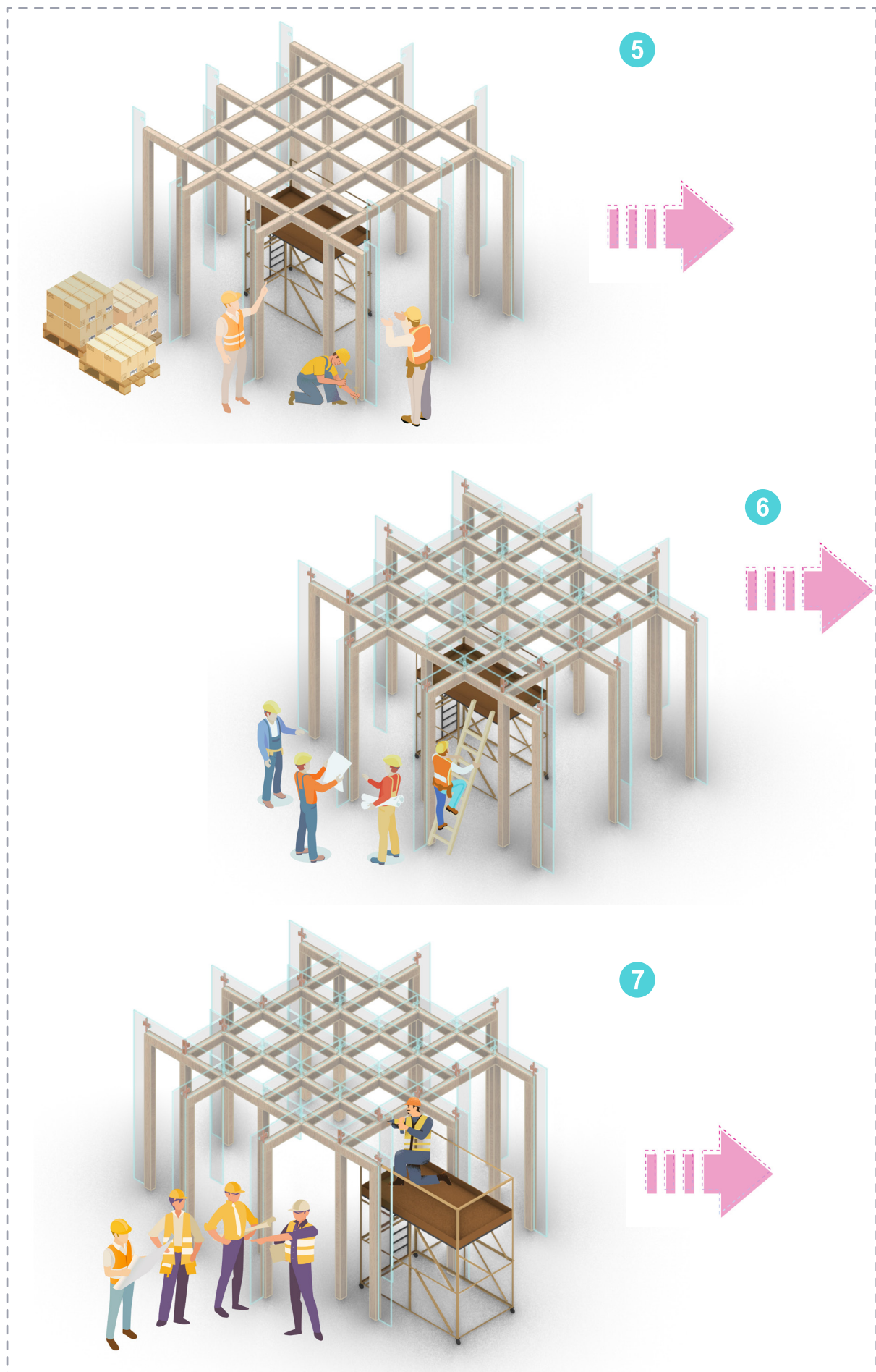


Figure 9.2.4 to 6, Step by Step Assembly sequence diagram. Source: Author's own.

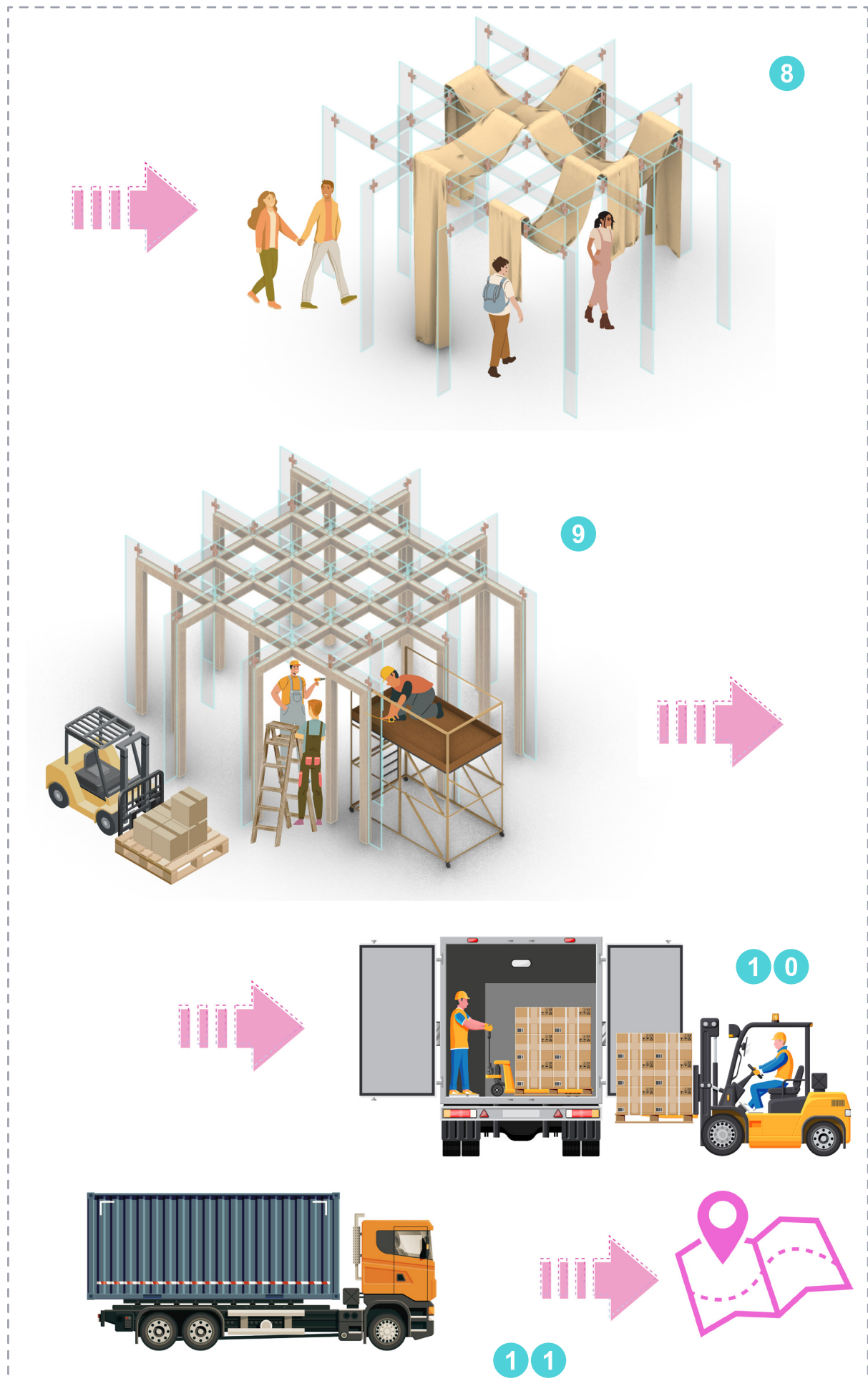


Figure 9.2.7 to 10, Step by Step Assembly sequence diagram. Source: Author's own.

- Line Joint Assembly process

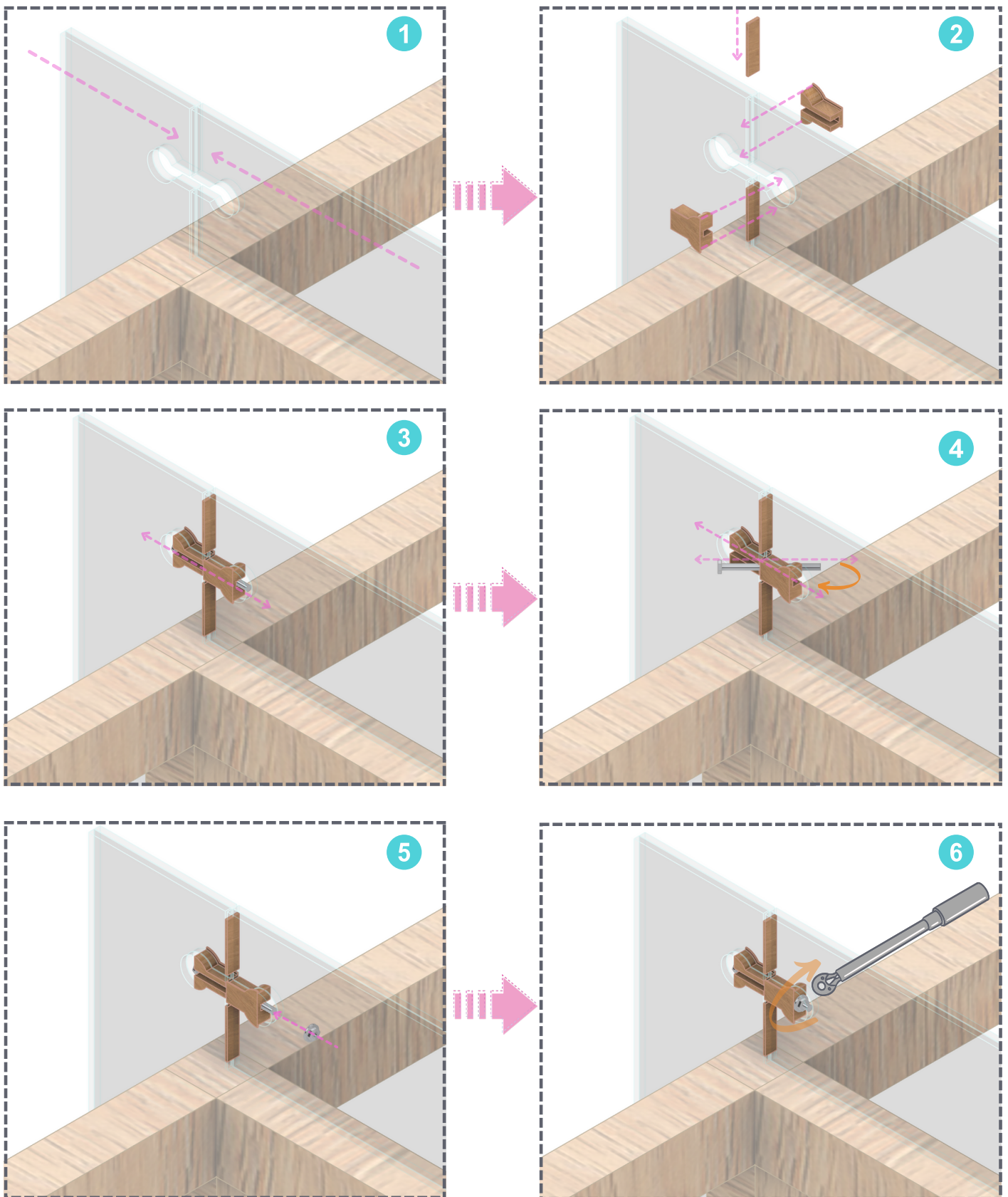


Figure 9.2.11 to 16, Step by Step Line Joint Assembly sequence diagram. Source: Author's own.

- T Joint Assembly process

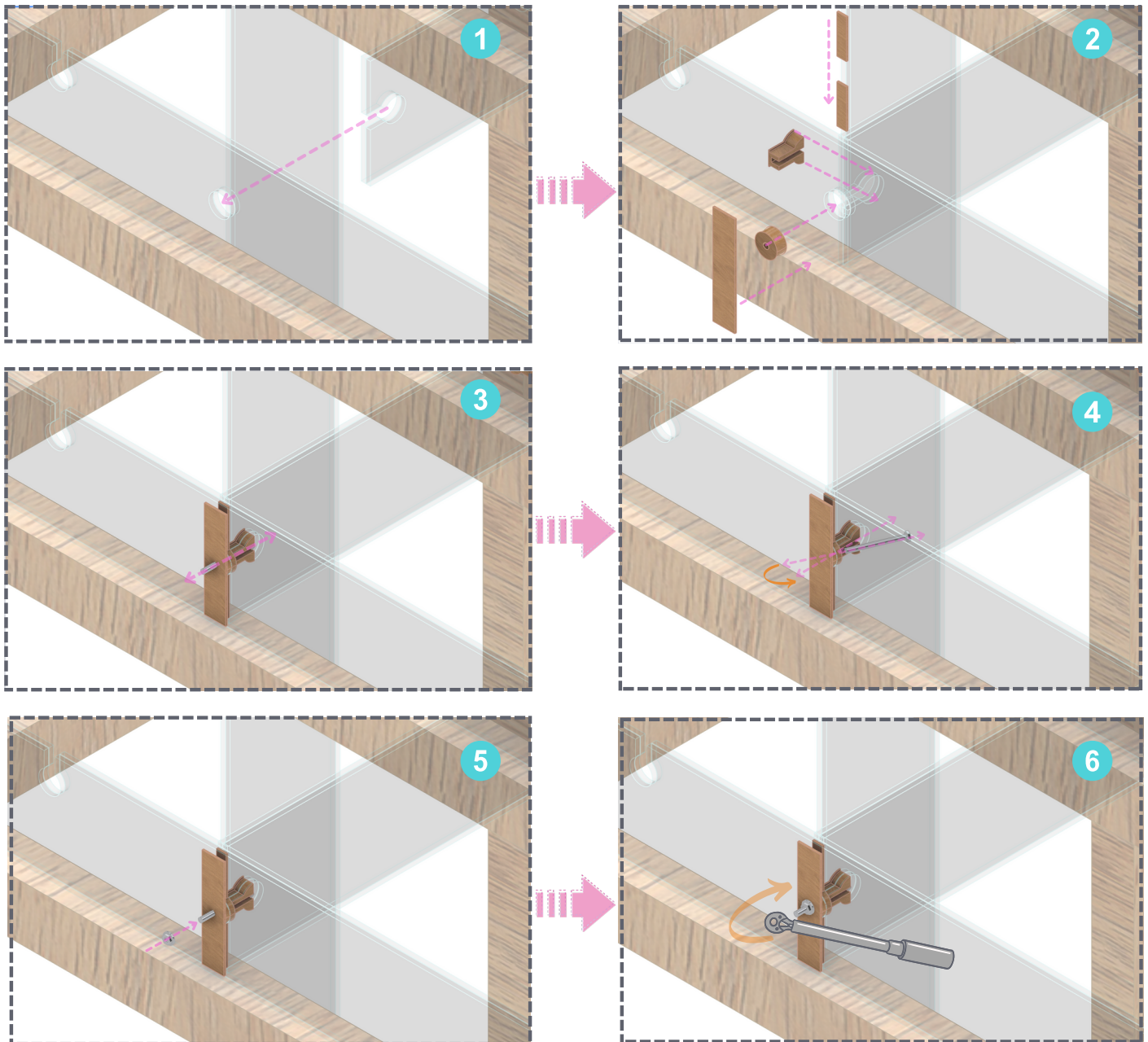


Figure 9.2.17 to 22, Step by Step T shape Joint Assembly sequence diagram. Source: Author's own.



Figure 9.2.23, Real world prototype of T shape connection . Source: Author's own.

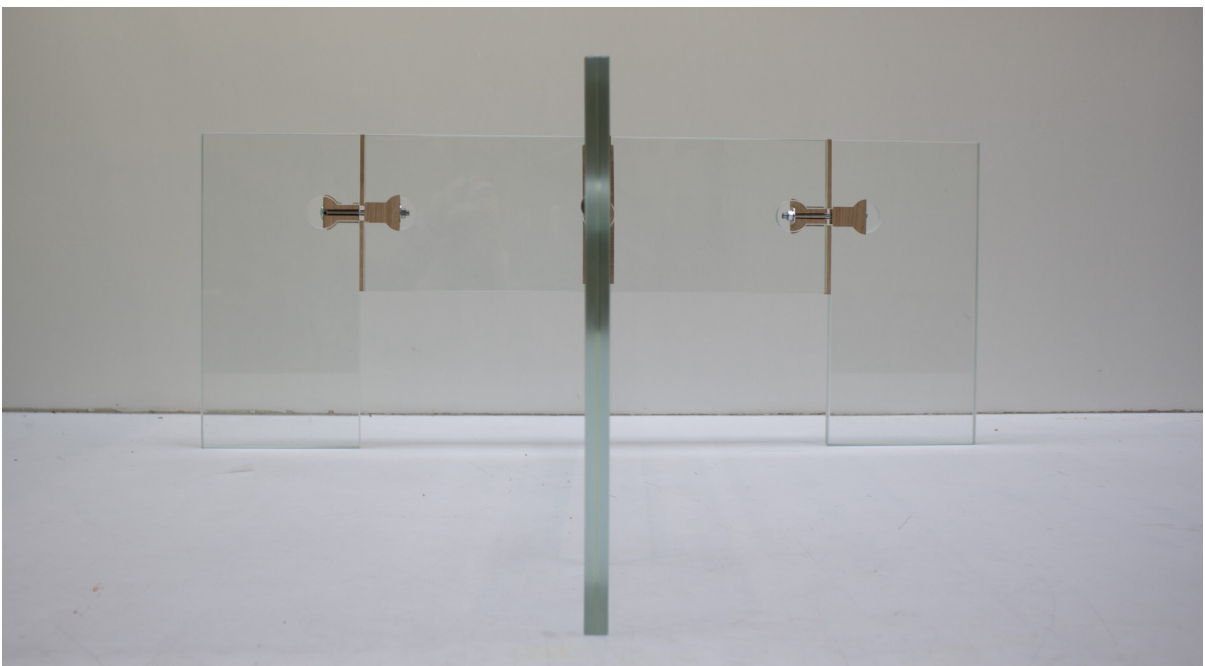


Figure 9.2.24 to 26, Real world prototype of T shape connection . Source: Author's own.

- Cross Joint Assembly process

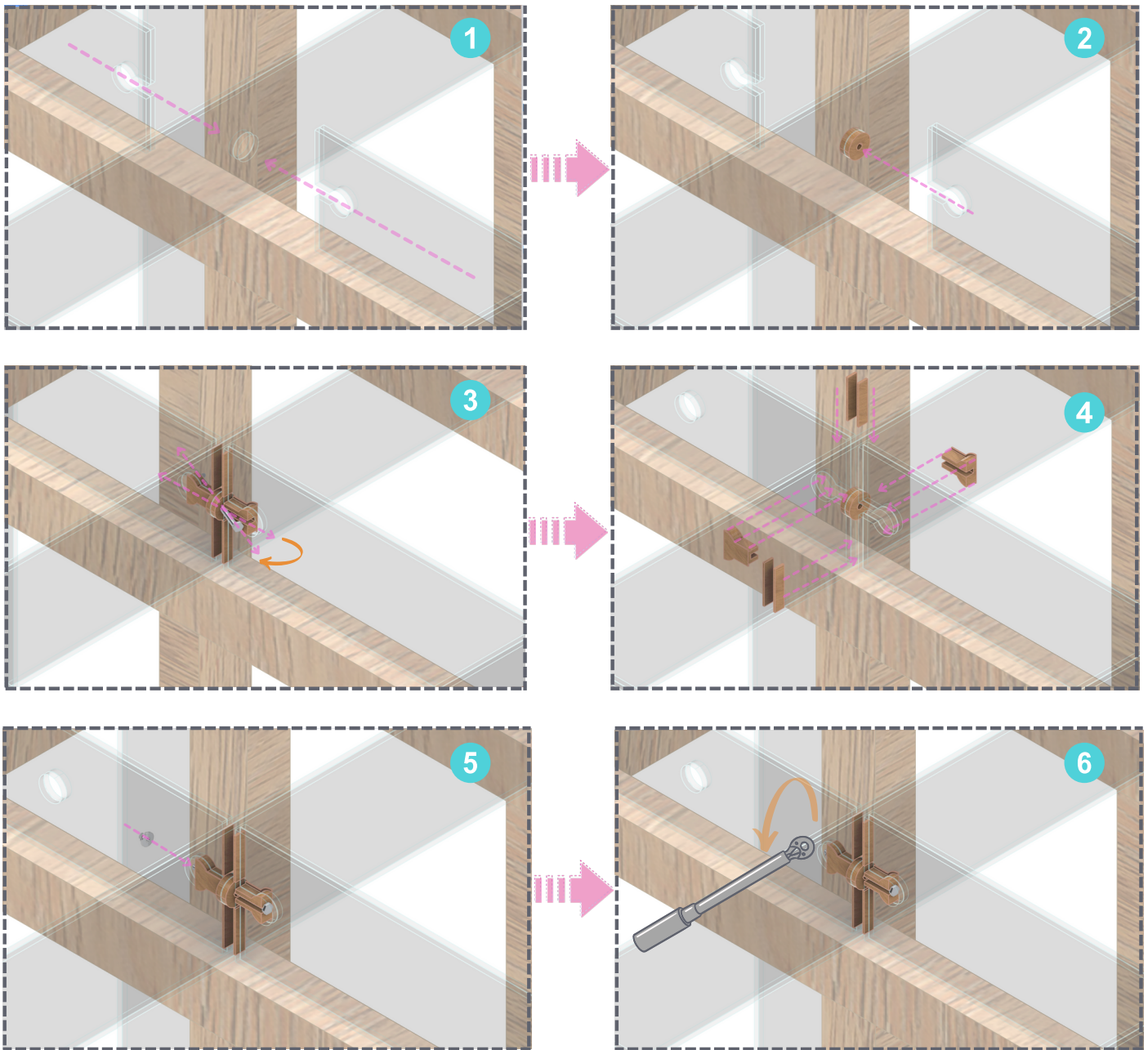


Figure 9.2.27 to 32, Step by Step Cross shape Joint Assembly sequence diagram. Source: Author's own.

9.3. End of life Scenarios

- Reusability and Adaptability of the Glass Modules

These glass modules serve as structural elements and are inherently reusable due to the absence of bonded or permanent connections. This allows them to be easily repurposed—for example, as façade fins—without altering the glass itself, which is heat-strengthened and cannot be cut or re-drilled post-production. While the modules remain unchanged, the connection type can be adapted to suit new project requirements. In their current form, the connectors safely resist moderate wind loads. With minor adjustments to the connector material or bolt design, the modules can be efficiently reused in a variety of applications such as reciprocal roof systems, pergolas, pavilions, or walkway shades. Their modular nature allows for flexible configurations, enabling different compositions and architectural expressions in each reuse.

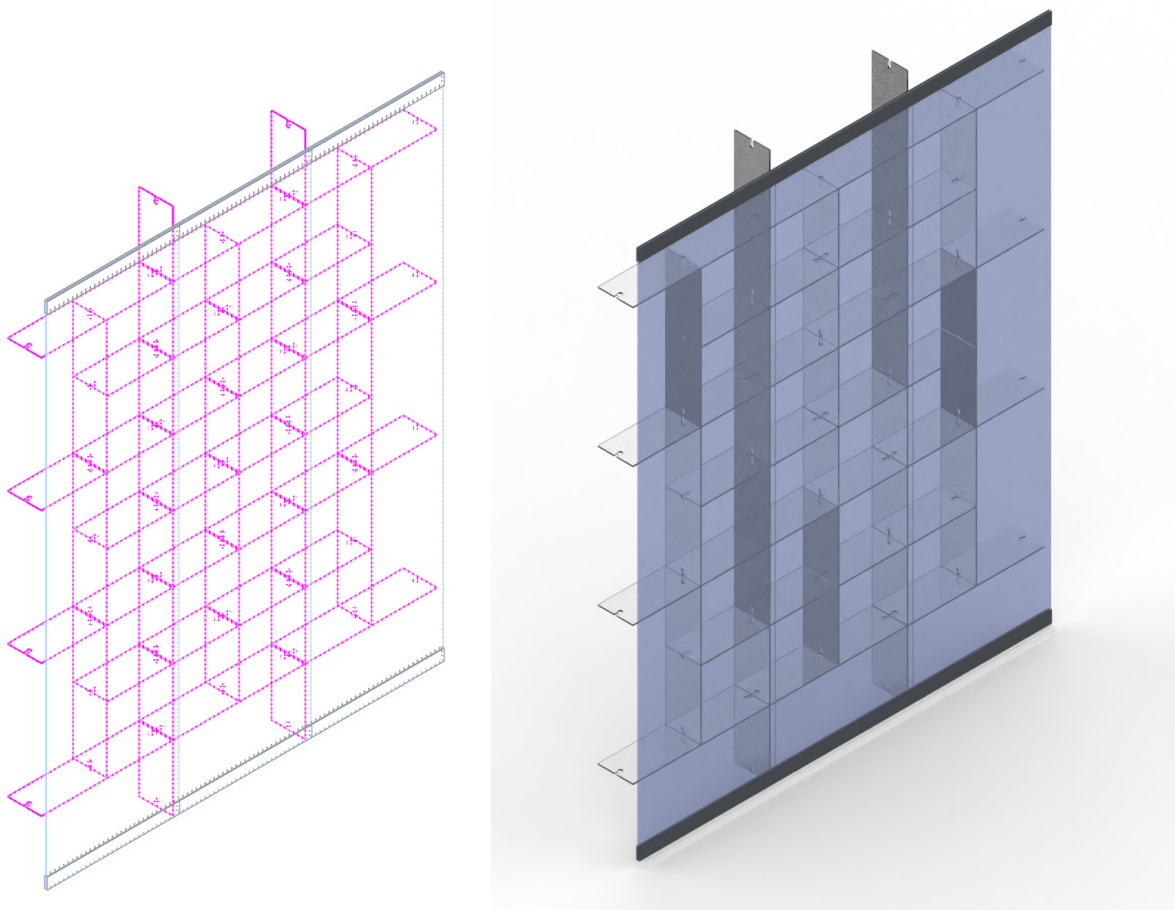


Figure 9.3.1&2, End of life scenario proposal sketch. Source: Author's own.

10. Reflection

This graduation project is positioned primarily within the structural domain of the Building Technology track, with a strong focus on the performance and detailing of structural glass and demountable connections. The research dives into material behaviour, load transfer, and component interaction, placing it firmly within the engineering side of the track. At the same time, the project touches on product design, particularly in the development of a connector system with precise geometry, assembly logic, and fabrication constraints. Computational tools such as Rhino, Grasshopper, ANSYS, and Karamba were integrated throughout the process to support both the design development and the structural validation of the system.

The research-through-design approach was used to explore and develop the concept. Starting with a research question and a clear problem statement, I investigated structural glass, its mechanical limitations, and the possibilities for dry, reusable connections. This led to the design of modular systems and connector variations inspired by woodworking and cabinet joints. Rather than being a linear process, the design and research evolved in loops: module shape influenced connection, and connection limitations led to adjustments in the modules and reciprocal system shaped by modules.

To validate the concept, I built prototypes and performed full-scale tests, starting with Plexi glass and wooden (Meranti) mock-ups and later testing with the final material: laminated, heat-strengthened glass and hard wood(oak) connectors. These tests revealed useful insights—such as bolt bending, wood cracking, and misalignment—which led to changes in bolt type, connector shape, and preload strategy. Structural analysis ran in parallel using Karamba (for system-level behaviour) and ANSYS (for detailed simulation of connections and modules). The final physical tests (two times) confirmed that the system could safely carry the design load and helped determine its ultimate load capacity. Notably, ANSYS results aligned well with physical testing, confirming the simulation's reliability for further development.

While the studio methodology follows a structured, step-by-step approach, my process followed the same logic in a loop-based way. Instead of moving strictly from theory to validation, I moved back and forth between testing, prototyping, and redesign. This allowed the research and design to continuously inform one another while remaining within the framework of the studio's methodological goals.

Research and design were tightly linked throughout the project. Insights from material studies and joinery systems guided early design decisions, while physical tests and simulations repeatedly raised new design questions. In this way, the development of the system was not based on abstract research alone but grounded in direct material feedback and assembly behaviour.

One ethical consideration in this project was the conscious selection of locally available hardwood and glass panels sourced from within Europe to reduce the embodied carbon associated with long-distance transportation. Among various candidate materials

for the connector, wood was chosen not only for its dimensional performance but also for being a natural, renewable, and sustainable option. Although stronger but high embodied carbon alternatives could have been used for higher loading conditions, the decision to work with hardwood was made to prioritize environmental responsibility and align the project with low-impact, sustainable design principles.

Additionally, considering a broader context, making the connector system affordable and widely available could increase its acceptance within the industry. Since glass panels are inherently luxurious and costly components, both contractors and clients would prefer failure to occur predictably in less expensive, easily replaceable parts. This makes wooden connectors particularly advantageous. Wood's lower stiffness relative to glass allows minor misalignments or inaccuracies during assembly to be accommodated without causing critical stress concentrations or breakages in the glass itself. This also significantly reduces the need for costly precision and permits simple on-site adjustments by workers. Consequently, this approach enhances safety, reduces overall project costs, and maintains the structural integrity of the critical glass components.

1. Societal Impact and Broader Relevance

This project was developed with the aim of making glass use more sustainable by addressing a major limitation in current construction: the lack of reusable glass connections. While glass is technically recyclable, its practical reuse is limited due to permanent fixing or bounding methods. The design proposed here reimagines glass as a modular element, capable of being assembled, disassembled, and reshaped—similar to LEGO pieces. This design-for-reuse logic has the potential to extend the lifespan of glass, reduce energy consumption associated with recycling, and minimize construction waste.

The intermediate material, oak, was selected for its dimensional stability, local availability, and relatively low environmental impact. As a result, the system demonstrates how three different materials—glass, wood, and steel bolts—can work together in a structurally and environmentally responsible way.

The broader societal impact of the project lies in its potential to influence the culture of building with glass. If adopted, modular glass systems could reduce material waste, extend the lifelong span of glass components for more than only one time use, and support circular construction strategies. The project also introduces a new architectural language that embraces reversibility and assembly as design features—not just technical constraints.

Not only does the project aim to extend the lifespan of glass components, but it also thoughtfully considers end-of-life scenarios for repurposing glass units, further prolonging their usability before recycling becomes necessary. Beyond their original modular design purpose, these glass modules are structural elements in their nature and could serve structural roles such as fins and beams in facade systems or even find new

life in permanent small-scale structures like greenhouses or furniture, such as bookshelves. Thus, this approach significantly broadens the sustainability potential of the materials used, reduces embodied carbon emissions, and ensures the project's environmental impact remains positive across multiple life cycles.

2. Limitations and Future Work

Overall, this project has successfully demonstrated a viable solution to the initial research problem, achieving strong results in line with the established design goals and assessment criteria. Therefore, I believe the project has effectively accomplished its intended objectives, while simultaneously opening new avenues for future exploration and development.

The practicality and simplicity of the modular system and its connections, combined with the realistic approach in their assessment and testing, enhance the likelihood of industry adoption and practical implementation.

While the system proved successful in the tested configurations, several limitations need to be acknowledged. The scope of the project is inherently broad; modular systems allow for countless geometric variations, and it is unrealistic to guarantee the performance of every potential configuration. In this study, four specific variations were structurally analysed and found to perform safely. Consequently, future users must individually verify the structural performance of their specific configurations, which is a common consideration rather than a limitation inherent to modular systems.

Due to testing constraints and available facilities at TU Delft, only the smallest module size and one of three connection categories could be tested. Full-scale testing for longer spans or other module types exceeded the scope of this master's thesis. However, structural simulations conducted with ANSYS covered all proposed connection types and span variations, effectively compensating for the limitations in physical testing and reinforcing the overall validity of the project's findings.

Furthermore, lateral loads were addressed in only one iteration at an average of 0.5 kN/m^2 . Although the system successfully resisted these loads, considerations for outdoor use, such as moisture resistance and thermal performance, remain important for future development. These factors should be addressed through additional number of connectors, modified bolt types, and slight geometric refinements.

Initially designed as a pure shear connection, testing revealed that the system behaves more like a moment-resisting joint, significantly impacting structural behaviour and detailing logic. Typically, moment connections are known for their complexity and higher implementation costs compared to shear connections. However, in this case, the developed joint remains relatively straightforward in terms of assembly and analysis but limited to bolt moment resistance after exceeding the clamp and friction force which could be less favourable.

The hardwood connectors performed adequately under moderate loading conditions; however, alternative materials may need consideration for applications involving larger spans or heavier loads. Several suitable alternatives were proposed within the report. Nevertheless, within the designed loading conditions, hardwood (specifically oak) remains the optimal choice due to its predictable failure behaviour and cost-effectiveness (wood crushes and glass is safe). Furthermore, the overall cost for materials and CNC milling with the required precision in wood is significantly lower—approximately 50 times less expensive—compared to aluminium. For each set of 4 connectors and one cylindrical component wood stands about 5 to 6 euros and aluminium is 350euros.

Bolt access and preload control posed practical challenges. More specialized tools could address these issues by enabling easier tightening without inducing extra stress in wooden components or glass, also, enable higher accuracy in applying deigned torque. Although such equipment was beyond the student's budget, practical recommendations have been provided in report.

Manufacturing challenges included maintaining tight tolerances and friction-based performance, which could be disrupted by changes in moisture, temperature, or glass alignment. This study emphasized that wooden components should be stored in controlled conditions (e.g., vacuum-sealed with silica packs) and standardized tolerances established through testing. However, the precision required for wooden connections remains lower than alternatives such as aluminium, making the design practical and cost-effective.

Despite these limitations, the system exhibited robust behaviour. Even after partial failures, such as connector cracking, the overall structure remained stable, functional, and replaceable This robustness indicates a reassuring level of redundancy and safety within a delicate material system. This condition was also tested in Karmba, assuming failure in one glass panel, but the structure was able to keep stability until replacement could occur.

3. Outlook and Next Steps

Moving forward, this project offers several promising avenues for further research and practical application, suitable for additional master's theses or PhD research within TU Delft or internationally. Proposed next steps include:

- Conducting further testing on the existing design:
 1. Exploring additional connection types and varying module sizes, potentially in collaboration with other faculties, such as civil engineering, to extend beyond current testing limitations.
 2. Evaluating alternative materials like aluminum for enhanced structural capacity. Preliminary investigations, including material preparation and CNC milling consultations was done by this author but it was not financially affordable to be done within this project (350 Euros)

- Investigating a wider variety of module shapes to broaden design possibilities. For instance, developing curved modules suitable for arch formations or modules designed specifically as connectors could significantly expand the system's versatility.
- Refining the design to accommodate longer spans, increased loading conditions, or more challenging outdoor environments by:
 - Introducing additional connection points (holes and connectors number) to improve the system's structural capacity.
 - Enlarging holes in glass modules, while carefully maintaining aesthetic standards, to help reduce local stress concentrations by increasing contact surface area.
 - Adopting stiffer connector materials such as aluminium or titanium, which better match the mechanical properties of glass and can support heavier loads than wood.
 - Implementing Minor refinements in wooden connectors to boost joint performance, such as:
 - Adding an extra wooden capping layer secured by screws to reduce bolt slip-page.
 - Utilizing larger bolts to enhance preloading capability, significantly increasing the joint's resistance (Higher Cr and Ct of joint).
 - Increasing the number of support points and fully utilizing available fin-to-beam joint positions to improve overall stability.
 - Replacing wooden strips used as intermediate spacers between glass panels with materials exhibiting higher friction coefficient, thereby enhancing the connection's load-bearing capacity.
- Adapting and developing the design for applications and use cases beyond modular structural glass systems, such as facade systems or furniture, to demonstrate the practical flexibility and potential broader appeal of the modular concept.
- Utilizing this project as a foundational case study to stimulate further exploration of modular systems or alternative connection types, such as pure shear joints. The novel nature of this research positions it as a potential cornerstone for future innovations in structural glass.
- Advancing parametric modeling using Grasshopper scripts integrated with Karamba for automated assessment of structural performance. By defining module lengths, connection types, and span limitations, the proposed system could automatically generate viable modular arrangements. This step has been taken partially by this author and proper reference paper in exact this scope has been provided supporting the feasibility of this ambitious goal.

10. Conclusion

This project successfully demonstrated the feasibility of a modular, dry-assembled glass-timber system designed for reuse. While simplifications were made—especially regarding testing scale and environmental conditions—the system was developed, tested, and validated to the extent possible within the timeframe. The concept opens new possibilities for adaptable, structurally expressive glass architecture, and lays the foundation for continued development toward practical application in circular building systems.

11 References

1. ArchDaily. (2016). Temporary Permanence Installation / Arup Associates. Retrieved from <https://www.archdaily.com/786564/urban-public-spatial-installation-arup-associates>
2. Arch2O. (2016). Temporary Permanence Installation | Arup Associates. Retrieved from <https://www.arch2o.com/temporary-permanence-installation-arup-associates/>
3. Bedon, C., & Santarsiero, M. (2018). Transparency in structural glass systems via mechanical, adhesive, and laminated connections: Existing research and developments. *Advanced Engineering Materials*, 20(1700815), 1-18. <https://doi.org/10.1002/adem.201700815>
4. Bedon, C., & Santarsiero, M. (2022). Transparency in structural glass systems via mechanical, adhesive, and laminated connections. *Journal of Structural Glass Systems*, 15(4), 123-140.
5. Brisogianni, T., & Oikonomopoulou, F. (2023). Glass up-casting: A review on the current challenges in glass recycling and a novel approach for recycling "as-is" glass waste into volumetric glass components. *Glass Structures & Engineering*, 8(1), 255-302. <https://doi.org/10.1007/s40940-022-00206-9>
6. Chong, H.-Y., Fan, S.-L., Sutrisna, M., & Hwang, B.-G. (2019). Incorporating sustainability in glass materials: The modular design approach. *Journal of Sustainable Construction Materials and Technologies*, 3(2), 85-95.
7. Dimas, M., Oikonomopoulou, F., & Bilow, M. (2022). An interlayer material study towards circular, dry-assembly, interlocking cast glass block structures. *Challenging Glass Conference Proceedings*, 8, Ghent University. <https://doi.org/10.47982/cgc.8.416>
8. Eversmann, P., & Ihde, A. (2018). Laminated glass connection details: Towards homogeneous material joints in glass. *Challenging Glass Conference Proceedings*, Delft University of Technology. <https://doi.org/10.7480/cgc.6.2158>

9. Goel, S. (2016). Optimal segmentation of glass shell structures. Challenging Glass 5: Conference on Architectural and Structural Applications of Glass, Ghent University. ISBN: 978-90-825-2680-6
10. Gugger, H., Boecker, L., & Hermann, G. (2020). Modular design principles in the built environment: A focus on glass systems. *Architectural Research Quarterly*, 24(1), 45-62.
11. Hänig, J., & Weller, B. (2022). Integrated connections for glass–plastic–composite panels: an experimental study under tensile loading at +23, +40, and +60 °C and different glass build-ups. *Glass Struct. Eng.*, 7(211), 211-229. <https://doi.org/10.1007/s40940-022-00174-0>
12. Hartwell, R., & Overend, M. (2019). Unlocking the reuse potential of glass façade systems. In *GPD Glass Performance Days Proceedings*. Retrieved from GPD Glass Performance Days 2019, Finland.
13. Kibert, C. J. (2016). *Sustainable construction: Green building design and delivery* (4th ed.). Wiley.
14. Krousti, A., Snijder, A., & Turrin, M. (2018). Kinematics of folded glass plate structures: Study of a deployable roof system. Challenging Glass 6, Delft University of Technology. <https://doi.org/10.7480/cgc.6.2117>
15. Lu, Y., Seyedahmadian, A., Chhadeh, P.A., Cregan, M., Bolhassani, M., Schneider, J., Yost, J.R., Brennan, G., & Akbarzadeh, M. (2022). Funicular glass bridge prototype: Design optimization, fabrication, and assembly challenges. *Glass Structures & Engineering*. <https://doi.org/10.1007/s40940-022-00177-x>
16. Lyon, A., & Garcia, R. (2011). Interlocking, Ribbing and Folding: Explorations in Parametric Constructions. *Nexus Network Journal*, 13(1), 221-234. <https://doi.org/10.1007/s00004-011-0051-y>
17. Marinitsch, S., Schranz, C., & Teich, M. (2016). Folded plate structures made of glass laminates: a proposal for the structural assessment. *Glass Structures & Engineering*, 1(2), 451–460. <https://doi.org/10.1007/s40940-015-0002-1>

18. Miotto, Bruscato Underléa; García Alvarado Rodrigo (2010). Pixel wall: digital exploration of a construction system of interlocking plates. SIGraDi 2010_Proceedings of the 14th Congress of the Iberoamerican Society of Digital Graphics, pp. 205-208, http://itc.scix.net/paper/sigradi2010_205
19. Oikonomopoulou, F., Bristogianni, T., & Overend, M. (2023). An interlayer material study towards circular, dry-assembly, interlocking cast glass block structures. *Architectural Engineering and Design Management*, 19(3), 56-78.
20. Overend, M., Nhamoinesu, S., & Watson, J. (2013). Structural performance of bolted connections and adhesively bonded joints in glass structures. *Journal of Structural Engineering*, 139(12), 04013015. [https://doi.org/10.1061/\(ASCE\)ST.1943-541X.0000748](https://doi.org/10.1061/(ASCE)ST.1943-541X.0000748)
21. Populous. (2015). Populous creates Eames-inspired installation for World Architecture Festival London. ArchDaily. Retrieved from <https://www.archdaily.com/769325/populous-creates-eames-inspired-installation-for-world-architecture-festival-london>
22. Rammig, L. M. (2022). Advancing Transparency: Connecting glass with heat – An experimental approach to the implementation of heat bonding into glass connection design for structural applications (Dissertation, Delft University of Technology). A+BE | Architecture and the Built Environment. <https://doi.org/10.7480/abe.2022.09>
23. Rammig, L. (2022). The pursuit of transparency. In *Rethinking Building Skins* (pp. 90-97). Elsevier. <https://doi.org/10.1016/B978-0-12-822477-9.00033-4>
24. Santarsiero, M. (2023). Laminated glass connection details towards homogeneous material joints in glass. *Structural Glass Systems Review*, 18(2), 45-90.
25. Stevels, W., Fildhuth, T., Wüest, T., Haller, M., & Schieber, R. (2022). Design Base for a Frameless Glass Structure Using Structural PVB Interlayers and Stainless-Steel Fittings. *Challenging Glass Conference Proceedings*, 8, 369. <https://doi.org/10.47982/cgc.8.369>
26. Trometer, S., & Krupna, M. (2006). Development and design of glass folded plate structures. *Journal of the International Association for Shell and Spatial Structures*,

47(3), 152. Retrieved from

27. Vasilchenko-Malishev, G., & Chesnokov, S. (2018). Zaryadye Park Glass Grid Shell Roof. In *Challenging Glass 6 – Conference on Architectural and Structural Applications of Glass* (Louter, Bos, Belis, Veer, & Nijse, Eds.), Delft University of Technology. DOI: 10.7480/cgc.6.2196.

28. Volakos, E., Davis, C., Teich, M., Lenk, P., & Overend, M. (2021). Structural performance of a novel liquid-laminated embedded connection for glass. *Glass Structures & Engineering*, 6(4), 487–510. <https://doi:10.1007/s40940-021-00162-w>.

29. Yost, J. R., Huisa Chacon, J., Lu, Y., Akbarzadeh, M., & Bolhassani, D. (2024). Experimental behavior of a prototype 3m-span modular glass pedestrian bridge. *Challenging Glass Conference Proceedings*, 9, TU Delft. <https://doi.org/10.47982/cgc.9.620>